Spinor-vector duality in smooth heterotic compactifications

by

Martin Hurtado Heredia

Supervisor: **Prof. Alon Faraggi**

A dissertation submitted in partial fulfillment
of the requirements for the degree of
Doctor of Philosophy
Mathematical Sciences

at the
University of Liverpool
August 2023

Spinor-vector duality in smooth heterotic compactifications

Martin Hurtado Heredia

Abstract

This thesis has as main motivation the possible extension of the spinor-vector duality, first observed in the free fermionic realization of $\mathbb{Z}_2 \times \mathbb{Z}_2$ heterotic orbifold models, to smooth compactifications of the heterotic string, i.e. Calabi-Yau manifolds with vector bundles. For this purpose, we use toric resolutions of the appropriate orbifolds as well as Gauged Linear Sigma Models (GLSMs) of these resolutions.
The project, which is still ongoing, is divided in different steps, of increasing difficulty, namely smooth compactifications to six, five and four dimensions. Interesting results are obtained for the $6D$ case, in which a fundamental anomaly cancellation condition constraints the duality to produce only "self-dual" models and for the $5D$ case in which the duality can be achieved but the gauge groups of the dual models are not the same. After that we turn our attention to the study of the $4D$ case, whose geometry, the resolution of the $T^6/\mathbb{Z}_2 \times \mathbb{Z}_2$ is significatively more involved. Motivated for a simplification of it we define a triangulation-independent formalism for that resolution. The last part of the thesis is devoted to the study of GLSMs in the $T^6/\mathbb{Z}_2 \times \mathbb{Z}_2$ and its resolution, including the implementation of a discrete torsion phase, whose understanding, (which is key for a full understanding of spinor-vector dualities) is generally unclear in the geometrical effective field theory .

Dedication

A La Papa

Declaration

I hereby declare that the material presented in this doctoral thesis is the result of my own research activity together with my collaborators. All references to other people's work are cited explicitly. All my work has been carried out in the String Phenomenology Group in the Department of Mathematical Sciences at the University of Liverpool during my PhD studies. The results presented in this thesis are based on the following publications:

- **Constraint on spinor-vector dualities in six dimensions**, A.E. Faraggi; Groot-Nibbelink, S.; Hurtado-Heredia, M.; Phys. Rev. D103 (2021) 126016. [1]
- **Uncovering a spinor-vector duality on a resolved orbifold**, A.E. Faraggi; Groot-Nibbelink, S.; Hurtado-Heredia, M.; Nucl. Phys. B969 (2021) 115473 [2]
- **Taming triangulation dependence of $T^6/Z_2 \times Z_2$ resolutions**, A.E. Faraggi; Groot-Nibbelink, S.; Hurtado-Heredia, M.; JHEP 01 (2022) 169 [3]
- **The fate of discrete torsion on resolved heterotic $Z_2 \times Z_2$ orbifolds using $(0, 2)$ GLSMs** , A.E. Faraggi; Groot-Nibbelink, S.; Hurtado-Heredia, M.; Nucl. Phys. B 988 (2023), 116111 [4]

Martin Hurtado Heredia
Madrid
August 14, 2023

Acknowledgements

First of all I want to thank my supervisor, Prof. Alon E. Faraggi for guiding me throughout my PhD. I am specially thankful to him for giving me the freedom to explore this exciting topic and for his great support in all the aspects of the PhD: pointing out research directions, providing theoretical background, being optimistic and proactive about the project, and favoring the interchange of ideas and collaboration with other researchers. He has definitely contributed to make the research work pretty enjoyable.
Secondly, I want to deeply thank our main collaborator, Stefan Groot Nibbelink. His great expertise in the areas explored, untiring work and patience to provide detailed explanations of key issues has been invaluable. His kindness and good humor has been also remarkable, ("Martin's 10 minutes" ;)) and it has been a real pleasure to work with him.
Then, I am also thankful to all the staff from the String Phenomenology Group of Liverpool: Thomas, Susha, Radu and Ed, who have created an exciting scenario to learn about the different aspects of String Theory, and have provided a cool atmosphere to work. As part of the String Group I want to thank specially to all the friends I have known within it. Thanks to Flavio and the great conversation and debates with him, to Viktor and his help at numerous times and efforts to make me an organised guy ahaha, and Bruno, Maxime and Ben for the overall good times we shared.
I would also like to thank to Andrei Constantin, Fabien Ruehle, Callum Brodie and Eric Sharpe for brief but useful discussions either face to face or via email, which has made some ideas to develop further.
Last but not least, I would like to thank the people who have always supported me, these PhD years included: Alex, Pablo, Cesar and Diego, and specially my brother and my mother who are and always will be a key part of everything I achieve.

Contents

List of Figures

List of Tables

Chapter 1

Introduction

1.1 String theory and string landscape

String theory provides a perturbatively consistent framework for the synthesis of gravity and the gauge interactions. Its internal consistency seems to mandate the existence of additional degrees of freedom beyond those observed in the Standard Models of particle physics and cosmology. The number of string theories in ten dimensions is relatively scarce, and includes five supersymmetric theories and eight that are not. Moreover, the supersymmetric versions, together with eleven dimensional supergravity, are believed to be different perturbative limits of a more fundamental theory, often dubbed M–theory.
The extra dimensions are compactified on an internal space such that they are hidden from contemporary experiments. As the choice of compactifications may be constrained, but is certainly not fixed, by string theory, there exists a plethora of string theory vacua in lower dimensions. These vacua can be studied either by using exact worldsheet constructions or effective field theory target space tools, that explore the low energy particle spectrum of string compactifications.

In our case we are interested in the **heterotic string**, for which examples of worldsheet constructions are free fermionic models [6, 7] and toroidal orbifold compactifications [8, 9]. These approaches are, in fact, closely related as particular fermionic formulations of the heterotic–string can be interpreted as $\mathbb{Z}_2 \times \mathbb{Z}_2$ toroidal orbifold compactifications [10, 50]. On the other side we have the study of Calabi–Yau compactifications with vector bundles [12], which utilises various effective field theory and cohomology methods. Using any of these approaches a strong effort has been made to construct low energy models which get surprisingly close to the Minimal Supersymmetric Standard Model (MSSM) : See refs. [13–15, 17–19] for free fermionic constructions, refs. [20–22, 24] for orbifold realisations and refs. [25–30, 32, 33, 36] for smooth compactifications, respectively.

1.2 Symmetries in the landscape

However, even though the space of low energy vacua of string theory is huge, there may exist symmetries that underlie the entire space of vacua in lower dimensions. The study of these dualities can be seen as an example of the "top–down" approach to string phenomenology, in which the aim is to explore the imprints and the constraints imposed by these dualities and

symmetries on the effective field theory representations of quantum gravity. (Note that this is a complementary approach to "bottom-up" logic of the current Swampland program [5], which asks about when an effective field theory model of quantum gravity have an ultraviolet complete embedding in string theory).
The initial motivation for this thesis was one of these symmetries, firstly observed in exact worldsheet constructions: the **spinor-vector duality** (SVD) [43, 44] which relates two models of the four dimensional fermionic $\mathbb{Z}_2 \times \mathbb{Z}_2$ string vacua by interchanging the total number of spinors plus antispinors states by vectorial states of the underlying gauge group.
It should be noted that the $\mathbb{Z}_2 \times \mathbb{Z}_2$ orbifold, in its fermionic incarnation as well as the bosonic, gave rise to a multitude of phenomenological three generation models with different unbroken $SO(10)$ subgroups (see *e.g.* [13, 14, 24, 81–84] and references therein). Spinor–vector duality plays a role in some of these constructions as well. Of particular note is the Z' model of ref. [85, 86] in which self–duality under the spinor–vector duality is instrumental to obtaining a three generation model with an extra $U(1)$ gauge symmetry, which is family universal and with the standard E_6 embedding of the Z' charges. It was argued in ref. [86] that existence of light sterile neutrinos mandates the existence of such an extra symmetry under which the sterile neutrinos are chiral and which remains unbroken down to low energy scales.
In this context a natural question to ask (which is the main topic of this thesis) is the following

"What is is the manifestation of SVD in the other side of the picture: i.e. the effective field theory limit?"

Part of the motivation for this lies in the parallelisms between SVD and another (celebrated) symmetry: the so-called "Mirror symmetry". Mirror symmetry was observed initially via the exact worldsheet CFT constructions [37, 38] and has profound implications for the geometrical spaces that are utilised in the effective field theory (type II theories compactified in Calabi-Yau threefolds) limits [39]. It should also be noted that mirror symmetry is related to T–duality [40]. In toroidal orbifold compactifications T–duality arises due to the exchange of the moduli of the internal six dimensional compactified manifold [41]. In this sense spinor-vector duality might be seen as an extension of mirror symmetry. Recall that in toroidal compactifications of the heterotic-string to four dimensions the moduli space is composed of the parameters of the metric and the anti-symmetric tensor field of the internal six dimensional compactified space; and the Wilson line moduli. While mirror symmetry corresponds to transformations of the internal moduli (i.e. it exchanges the complex structure moduli with the Kahler structure moduli that are parametrised in terms of the internal fields of the six dimensional compactified space) spinor-vector duality on the other hand can be shown to correspond to mappings of Wilson line moduli.
Whatever is the final relation between the two symmetries we expect Spinor–vector duality to have interesting imprints in the moduli space of heterotic string vacua and consequently stablish some connections between different compactifications over Calabi-Yau threefolds with vector bundles.
This thesis constitutes a first step for a broader understanding of SVD and consequently a better understanding of the whole space of dualities of string theory.

1.3 Outline of the thesis

- In **Chapter 2** we start giving the definition of SVD and recalling the minimal basic details of its origin in heterotic $\mathbb{Z}_2 \times \mathbb{Z}_2$ orbifold models. The aim of the chapter is not give a detailed explanation (we refer the reader to the existing literature) but providing a basic idea about the starting point of our "translation" (i.e. what is the duality that we want to translate to the smooth case).

- In the more extensive **Chapter 3** we give a more detailed recollection of the theoretical tools and concepts that we use to build our smooth compactifications. To do so we recall the details of toric resolutions of heterotic orbifolds. This chapter can be useful for those not familiar to resolutions of heterotic orbifolds as it outlines some of the most important concepts appearing in those constructions. We focus in line bundle resolutions and let the GLSM formalism description for the last chapter.

- **Chapter 4** is devoted to the study of SVD in the compactification to six dimensions. We will show that SVD is heavily constrained by a fundamental condition (i.e. the theory should be free of irreducible $SO(2N)$ anomalies) that impose that the duality can only be realized in the self-dual point.

- **Chapter 5** will study a case closely related to the previous case: the compactification to five dimensions (the manifold only differs by an addition of an extra circle S^1). By defining a Wilson line in this S^1 and switching on/off a generalised discrete torsion phase between it and the orbifold we can generate SVD. However, depending on this phase complementary parts of the twisted sector orbifold states are projected out, so that different blowup modes are available to generate the resolutions and consequently, not only the spectra of the dual pairs are different, but also the gauge groups are not identical making the duality less apparent.

- Although **Chapter 6** does not provide direct results for the SVD program, it is somewhat conceptually linked to it, because provides an useful geometrical study of the relevant geometry of SVD in four dimensions. This geometry (the resolution of the $T^6/\mathbb{Z}_2 \times \mathbb{Z}_2$) presents a huge dependence on the triangulation used to resolve the local singularities, making phenomenological studies less clear. By introducing a parametrisation to keep track of the triangulations used at all resolved singularities simultaneously, we can define a "triangulation-independent formalism" in which the physical consistency conditions of the model are simplified greatly. This allows a more general study of its moduli space, including the study of jumping spectra due to flop–transitions.

- Similar to the previous Chapter, **Chapter 7** is not specifically devoted to the implementation of SVD, but in some sense it has strong motivations and clear applications for its extension to $4D$. As we previously noted, the implementation of SVD to the smooth case requires a concrete understanding of discrete torsion in the effective theory limit. We kind of circumnavigated this issue in the $5D$ case, by mimicking the discrete torsion action in the orbifold case (and assigning "untwisted" and "twisted" states to the resolved $5D$ model). However, a formalism capable of providing a deep understanding of discrete torsion would be desirable. That is the reason why in Chapter 7 we study the $T^6/\mathbb{Z}_2 \times \mathbb{Z}_2$ resolution using the GLSM formalism. A main advantage of it relies in its capability of

describing the orbifold and blow-up regime using essentially the same set of equations. By appropriate superfield redefinitions we obtain GLSMs of models with/without discrete torsion between two orbifold twists. The needed discrete torsion (between the orbifold twist and the Wilson line) requires to build a slightly more complicated model (with more distinct bundle vectors) and it is not yet analyzed, but we expect the logic to be presumably similar.

- **Chapter 8** conclude the thesis by summarizing the main results and pointing out some possible extensions/outlook.

The following figure shows a pictorial representation of the conceptual structure of the thesis:

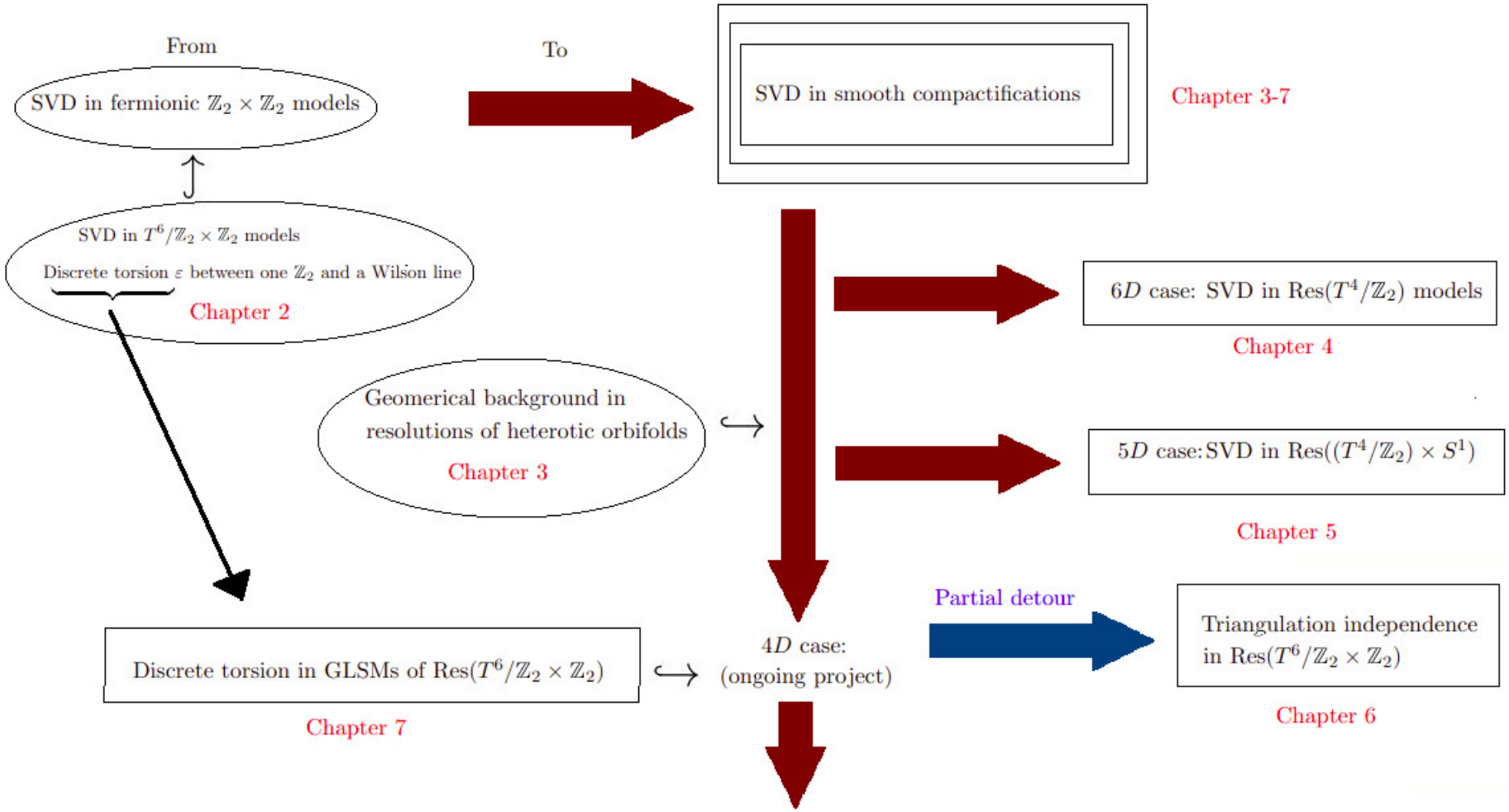

Figure 1.1: Conceptual structure of the thesis indicating the chapter devoted to each topic. Curved boxes indicate recollection of existing theory (i.e. background material), and straight ones indicate new results from this thesis. $A \hookrightarrow B$ indicates that A is needed for understanding of B

Chapter 2

A glance of spinor vector duality in free fermionic and orbifold models

In this chapter we give the basic definition of Spinor-vector duality (SVD) and study its origin in $\mathbb{Z}_2 \times \mathbb{Z}_2$ heterotic orbifold models (which are equivalent to free fermionic models (see for example [50]) for a dictionary of this equivalence). Even though the main focus of this thesis is smooth compactifications, it may be useful to give a basic idea of how SVD arises in the original formulations it was observed. However, before doing that, we start providing a very brief overview of the heterotic string and orbifold constructions.

2.1 Introduction to the heterotic string

In this thesis we build string models using different frameworks[1] of the same theory: the **heterotic string**, so it is useful to start giving a the basic details of it.
Recall that, in string theory, the left-moving and the right-moving excitations are completely decoupled so it is possible to construct a string theory whose left-moving excitations are treated as a bosonic string propagating in $d = 26$ dimensions, while the right-moving excitations are treated as a superstring in $d = 10$ dimensions. This is the fundamental idea behind the heterotic string, which provides an alternative method (to type I and type II theories) of constructing supersymmetric string theories in ten dimensions with $\mathcal{N} = 1$ supersymmetry.
There are two equivalent ways to construct the heterotic string: the **bosonic description** and the **fermionic description**. As the main bulk of this thesis is done in the framework of orbifold constructions, or more precisely, resolutions of them (via line bundles or described by GLSMs) we are going to focus in the bosonic one, as it is the natural formulation for these models. The other framework, the free fermionic, is obviously closer to the standard fermionic description, but it is still a different approach (While the standard fermionic description is built as a $10d$ theory, in the free fermionic formulation we can start directly from a $4d$ theory by interpreting all the world-sheet degrees of freedom required to cancel the conformal anomaly as free fermions propagating on the string world-sheet). As is not the main focus of this work we refer the reader to other references for further details of the free fermionic models

[1] We use four different frameworks: free fermion models, heterotic orbifolds, line bundle resolutions and GLSMs of orbifold resolutions. The two former are the ones in which SVD was observed and the two latter are the ones we use to see how SVD manifest in the effective limit (smooth compactifications).

[13–15, 17–19] and focus in the bosonic formulation (more suitable for orbifold theories) from now on. Most of the material of this section 2.1 is standard background in string theory. See for example [16, 34, 35] for nice reviews in these topics.

2.1.1 Bosonic formulation of the heterotic string

In the bosonic description of the heterotic string the mismatched 16 dimensions are considered to be compactified on an even, self-dual lattice. As there are two possible even self-dual lattices in 16 dimensions, we end with two types of the heterotic string (one with gauge group $SO(32)$ and another one with gauge group is $E_8 \times E_8'$). On this thesis we focus on the latter so we compactify on a $T_{E_8 \times E_8'}$, i.e. the root lattice of the group $E_8 \times E_8'$.
As usual, the string itself is described by maps $X^\mu(\tau, \sigma)$ that embed the two-dimensional worldsheet, equipped with coordinates (τ, σ), into the $10d$ target space M_{10}. Not all ten coordinates are independent. Therefore, in light cone coordinates, two components of the left and right movers are gauge fixed. We will denote the remaining physical degrees of freedom of the right moving superstring by X_R^i and Ψ_R^i (for $i = 1, \ldots, 8$). The coordinates X_R^i are worldsheet bosons and Ψ_R^i are worldsheet fermions. On the other side, the physical left moving degrees of freedom are denoted by $X_L^i, i = 1, \ldots, 8$, and $X_L^I, I = 1, \ldots, 16$, both worldsheet bosons. Since the coordinates X_L^I are compactified on the $T_{E_8 \times E_8'}$ we refer to them as gauge degrees of freedom.

Equations of motion

The equations of motion are obtained from the worldsheet action using the Hamilton principle. The result for the bosonic coordinates (for $i = 1, \ldots, 8$ and $I = 1, \ldots, 16$) together with the boundary conditions (with $\Lambda \in T_{E_8 \times E_8'}$) are:

$$\begin{aligned}
&\left(\frac{\partial^2}{\partial\tau^2} - \frac{\partial^2}{\partial\sigma^2}\right) X_L^i(\tau, \sigma) = 0, \quad X_L^i(\tau, \sigma + 2\pi) = X_L^i(\tau, \sigma) \\
&\left(\frac{\partial^2}{\partial\tau^2} - \frac{\partial^2}{\partial\sigma^2}\right) X_R^i(\tau, \sigma) = 0, \quad X_R^i(\tau, \sigma + 2\pi) = X_R^i(\tau, \sigma) \\
&\left(\frac{\partial^2}{\partial\tau^2} - \frac{\partial^2}{\partial\sigma^2}\right) X_L^I(\tau, \sigma) = 0, \quad X_L^I(\tau, \sigma + 2\pi) = X_L^I(\tau, \sigma) + 2\pi\Lambda^I.
\end{aligned} \tag{2.1}$$

Note that one end of the string corresponds to $\sigma = 0$ and the other to $\sigma = 2\pi$, so the equations state that both ends coincide. Therefore we are describing closed strings.

The general solution is given by mode expansion. For $i = 1, \ldots, 8$ we split the solution into right and left moving parts ($X = X_R + X_L$),

$$\begin{aligned}
X_R^i(\tau, \sigma) &= \frac{1}{2}x^i + \frac{1}{2}p^i(\tau - \sigma) + \frac{i}{2}\sum_{n\neq 0}\frac{\alpha_n^i}{n}e^{-in(\tau-\sigma)} \quad \text{(right mover)} \\
X_L^i(\tau, \sigma) &= \frac{1}{2}x^i + \frac{1}{2}p^i(\tau + \sigma) + \frac{i}{2}\sum_{n\neq 0}\frac{\tilde{\alpha}_n^i}{n}e^{-in(\tau+\sigma)} \quad \text{(left mover)} \\
X_L^I(\tau, \sigma) &= x_L^I + p^I(\tau + \sigma) + \frac{i}{2}\sum_{n\neq 0}\frac{\tilde{\alpha}_n^I}{n}e^{-in(\tau+\sigma)} \quad \text{(gauge d.o.f.)}
\end{aligned} \tag{2.2}$$

with the raising and lowering operators obeying: $\left(\alpha_n^i\right)^\dagger = \alpha_{-n}^i$, $\left(\tilde{\alpha}_n^i\right)^\dagger = \tilde{\alpha}_{-n}^i$ and $\left(\tilde{\alpha}_n^I\right)^\dagger = \tilde{\alpha}_{-n}^I$ so that X_R and X_L are real.
On the right moving sector we also have equations of motion for the fermionic coordinates, which are given by

$$\left(\frac{\partial}{\partial\tau} + \frac{\partial}{\partial\sigma}\right)\Psi_R^i(\tau,\sigma) = 0 \quad \text{for } i = 1,\ldots,8. \tag{2.3}$$

It turns out that Ψ_R^i can either have periodic or anti-periodic boundary conditions, called Ramond (R) and Neveu-Schwarz (NS) boundary conditions, respectively. They read

$$\Psi_R^i(\tau,\sigma+2\pi) = \pm\Psi_R^i(\tau,\sigma) \tag{2.4}$$

The general solution of the equation of motion is given by the mode expansions

$$\begin{aligned}\Psi_R^i(\tau,\sigma) &= \sum_{n\in\mathbb{Z}} d_n^i e^{-in(\tau-\sigma)} \quad \text{R}\\ \Psi_R^i(\tau,\sigma) &= \sum_{r\in\not{\exists}+\frac{1}{2}} b_r^i e^{-ir(\tau-\sigma)} \quad \text{NS}\end{aligned} \tag{2.5}$$

Right movers

In general, a quantized right mover is given by the bosonic oscillators α_n^i and the fermionic oscillators d_n^i and b_r^i acting on the right moving ground state $|0\rangle_R$.

We restrict ourselves to massless right movers. They are given by acting with either the NS-oscillators $b_{-1/2}^i$ or with the R-oscillators d_0^i on the right moving ground state (for $i = 1,\ldots,8$). Therefore, the corresponding states are denoted by NS or R, respectively. Now, it is useful to note that NS state transforms as an SO(8) vector and the R state as an SO(8) spinor. and consequently we can write the NS and R state as representations of SO(8) :

- The $SO(8)$ vector NS state can be represented by a weight vector

  $$q = (\underline{\pm 1,0,0,0)}) \quad \text{NS} \tag{2.6}$$

  (the underscore denotes that all permutations are included).

- The SO(8) spinor R state can be written as

  $$q = \left(\pm\frac{1}{2},\pm\frac{1}{2},\pm\frac{1}{2},\pm\frac{1}{2}\right) \quad \text{R} \tag{2.7}$$

  with an even number of plus signs. The first component of this spinor defines the four-dimensional chirality of the state,

  $$\begin{aligned}-\frac{1}{2} &\Leftrightarrow \text{ left-handed}\\ +\frac{1}{2} &\Leftrightarrow \text{ right-handed.}\end{aligned} \tag{2.8}$$

Both the NS and the R states $|q\rangle_R$ fulfill the same equation for massless right movers,

$$\frac{m_R^2}{4} = \frac{1}{2}q^2 - \frac{1}{2} = 0 \tag{2.9}$$

Left movers

We turn our attention now to the left movers. A quantized left mover is given by the oscillators $\tilde{\alpha}^i_{-n}$ and $\tilde{\alpha}^I_{-n}$ acting on the left moving ground state $|0\rangle_L$.

Since the sixteen gauge degrees of freedom X^I_L are compactified on a sixteen-torus $T_{\mathrm{E}_8\times\mathrm{E}'_8}$, the corresponding momenta p^I are quantized and correspond to the root vectors of the $\mathrm{E}_8\times\mathrm{E}'_8$ gauge group. Therefore, the momenta p^I can be seen as internal quantum numbers of the left moving ground state $|p\rangle_L$ that characterize the transformation properties of the ground state under the $\mathrm{E}_8\times\mathrm{E}'_8$ gauge group. The massless left movers fulfill the equation

$$\frac{m_L^2}{4} = \frac{1}{2}p^2 + \tilde{N} - 1 = 0 \tag{2.10}$$

where $p^2 = \sum_{I=1}^{16}\left(p^I\right)^2$, and $\tilde{N}$ is the number operator. It counts the number of oscillators $\tilde{\alpha}_{-n}$ acting on the ground state, i.e.

$$\begin{aligned}\tilde{N}\left(\tilde{\alpha}^i_{-n}|p\rangle_L\right) &= n\left(\tilde{\alpha}^i_{-n}|p\rangle_L\right)\\ \tilde{N}\left(\tilde{\alpha}^i_{-n}\tilde{\alpha}^j_{-m}|p\rangle_L\right) &= (n+m)\left(\tilde{\alpha}^i_{-n}\tilde{\alpha}^j_{-m}|p\rangle_L\right) \qquad \text{for } i\neq j.\end{aligned} \tag{2.11}$$

This yields the following massless left movers

$$\begin{aligned}&\tilde{\alpha}^i_{-1}|0\rangle_L \quad \mathrm{i}=1,\ldots,8\\ &\tilde{\alpha}^I_{-1}|0\rangle_L \quad \mathrm{I}=1,\ldots,16\\ &\left|p^I\right\rangle_L \quad \text{with } p^2=2.\end{aligned} \tag{2.12}$$

The ten-dimensional mass-squared operator is given by

$$m^2 = m_R^2 + m_L^2 \tag{2.13}$$

and the level-matching condition, which follows from modular invariance, requires

$$m_R^2 = m_L^2 \tag{2.14}$$

The $10D$ spectrum

To create all massless physical states we can tensor right and left movers together which yields:

- $|q\rangle_R\otimes\tilde{\alpha}^i_{-1}|0\rangle_L \rightarrow$ supergravity multiplet for ten-dimensional $\mathcal{N}=1$ supergravity ($i=1,\ldots,8$)
- $|q\rangle_R\otimes\tilde{\alpha}^I_{-1}|0\rangle_L \rightarrow$ 16 uncharged gauge bosons of $\mathrm{E}_8\times\mathrm{E}'_8$ and their superpartners ($I=1,\ldots,16$ correspond to the compactified dimensions)
- $|q\rangle_R\otimes\left|p^I\right\rangle_L \rightarrow$ 240 + 240 charged gauge bosons of $\mathrm{E}_8\times\mathrm{E}'_8$ and their superpartners (internal quantized momenta p^I with condition $p^2=2$ give 240 root vectors for each E_8)

$|q\rangle_R$ is either an NS or R state, leading to a space-time boson or fermion. In general, due to $\mathcal{N}=1$ supergravity, two states with the same left mover, but one with an NS right mover and the other with an R right mover, are SUSY partners.

To conclude, restricted to massless states, we can see that the previous construction of the heterotic string gives a ten-dimensional $\mathcal{N}=1$ supergravity theory with $\mathrm{E}_8\times\mathrm{E}'_8$ gauge group.

2.1.2 Orbifold compactification

Now, to make contact with the physical world and its four space-time dimensions, one has to compactify six spatial dimensions. Let us compactify the dimensions $i = 3, \ldots, 8$. Thus, our four-dimensional Minkowski space is given by the two (independent) uncompactified dimensions $\mu = 1, 2$ plus the two coordinates that were gauge fixed due to the light cone coordinates. However, if we choose our compactification space to be just the six-torus T^6, we end with a $\mathcal{N} = 4$ supersymmetric theory in four dimensions as one obtains four gravitini. This is so because the states coming from the supergravity multiplet in $10D$, i.e. $|q\rangle_R \otimes \tilde{\alpha}^i_{-1}|0\rangle_L$ would be in $4D$ for spinorial q:

$$| \underbrace{\pm\frac{1}{2}}_{\text{chirality}}, \underbrace{\pm\frac{1}{2}, \pm\frac{1}{2}, \pm\frac{1}{2}}_{\text{internal}}\rangle_R \otimes \tilde{\alpha}^\mu_{-1}|0\rangle_L \quad \text{(even \# of plus signs)}, \tag{2.15}$$

The first component of the right mover gives the chirality, because it corresponds to the two uncompactified dimensions. The three other components, which are correlated to the six compactified dimensions, can now be seen as internal quantum numbers. For these internal quantum numbers, there are four possibilities for each left- and right-handed state. Because one gravitino consists of both left- and righthanded parts, we have four gravitini.

The solution is compactifying on an orbifold, whose discrete symmetry projects out three gravitini, leaving $\mathcal{N} = 1$ supersymmetry unbroken.

We define our orbifold as T^6/P, where T^6 is the six-torus and P is the point group (which represents a discrete symmetry) whose elements are called twists.

Similarly to the choice of a Calabi-Yau threefold as a compactification space, the choice of P is also restricted by some phenomenological considerations: The holonomy group of the $6D$ space is SO(6) which is locally isomorphic to SU(4). If we additionally require to maintain $\mathcal{N} = 1$ SUSY, P must be a subgroup of SU(3). Since we can only mode out a symmetry that is a symmetry of the torus T^6, the elements of P are required to be automorphisms of the T^6 lattice and therefore the point group is discrete. Here we restrict ourselves to abelian groups only. Thus, there are two classes of point groups

- $\mathbb{Z}_N$: The cyclic group of order N, which consists of the elements

$$\mathbb{Z}_N = \left\{\theta^k \mid k = 0, \ldots, N-1\right\} \tag{2.16}$$

  and θ can be seen as a rotation by $2\pi/N$.

- $\mathbb{Z}_N \times \mathbb{Z}_M$: Each factor is given by a twist θ_1 and θ_2 of order N and M, respectively. Thus, the elements of the group are given by

$$\mathbb{Z}_N \times \mathbb{Z}_M = \left\{\theta_1^k \circ \theta_2^l \mid k = 0, \ldots, N-1 \text{ and } l = 0, \ldots, M-1\right\} \tag{2.17}$$

All admissible point groups have been classified in [8, 9, 134]. In our case as we are studying orbifold models related to free fermion ones, we are going to focus in $\mathbb{Z}_2 \times \mathbb{Z}_2$.
As we said previously, we defined our orbifold as T^6/P, but we can give the alternate definition $T^6/P = \mathbb{R}^6/S$, where we have introduced S, which is defined to be the point group P plus the

translations given by the lattice vectors e_α for $\alpha = 1, \ldots, 6$. By definition, the vectors e_α (with $|e_\alpha| = \sqrt{2}$) span the six-torus T^6. To summarize, the space group is defined as the set

$$S = \{(\theta, n_\alpha e_\alpha) \mid \theta \in P, n_\alpha \in \mathbb{Z}\} \tag{2.18}$$

where the sum over α from 1 to 6 is implied. The action of an element $g = (\theta, n_\alpha e_\alpha)$ of S on the six-dimensional space $\mathbb{R}^6$ is given by

$$gx = \theta x + n_\alpha e_\alpha \tag{2.19}$$

for $x \in \mathbb{R}^6$. Then, two points $x, y \in \mathbb{R}^6$ are identified, if they differ by the action of a space group element g

$$x \simeq y \quad \text{ if there is a } g \in S \text{ with } x = gy \tag{2.20}$$

and thereby the six-dimensional space $\mathbb{R}^6/S$ is defined.
The most important aspect of the geometry is going to be the set of fixed points. Fixed points are defined as points $X_f \in T^6$ that are invariant under the action of a nontrivial element of S,

$$X_f^i = \left(\theta^k X_f\right)^i + n_\alpha e_\alpha^i \tag{2.21}$$

for $i = 1, \ldots, 6$ and $k = 1, \ldots, N-1$. It is important to note that due to this equation a fixed point corresponds to a space group element $\left(\theta^k, n_\alpha e_\alpha\right)$.
Due to modular invariance, the gauge degrees of freedom are also going to transform according to the orbifold action. Concretely the action of the space group S must be embedded into the gauge degrees of freedom, $S \hookrightarrow G$. G is called the gauge twisting group. In general, G is a subgroup of the automorphisms of the $\mathrm{E}_8 \times \mathrm{E}_8'$ Lie algebra. Here, we restrict ourselves to the case of inner automorphisms, which can be realized as a shift V in the $\mathrm{E}_8 \times \mathrm{E}_8'$ root lattice.

The embedding of the space group into the gauge degrees of freedom $S \hookrightarrow G$ s given by $\left(\vartheta^k, n_\alpha e_\alpha\right) \mapsto (kV, n_\alpha W_\alpha)$ and $\left(\vartheta_1^k \circ \vartheta_2^l, n_\alpha e_\alpha\right) \mapsto (kV_1 + lV_2, n_\alpha W_\alpha)$ for the $\mathbb{Z}_N$ and $\mathbb{Z}_N \times \mathbb{Z}_M$ respectively.

Here we have introduced a very important element: the vectors W_α, which are the embeddings of the torus shifts e_α into the gauge degrees of freedom. They correspond to gauge transformations associated to non-contractible loops and are the so-called Wilson lines.

Accoding to this embedding we can see the action of an element of the gauge twisting group $\tilde{g}$ on X_L^I. For the $\mathbb{Z}_N$ case we have $\tilde{g} X_L^I = X_L^I + 2\pi \left(kV^I + n_\alpha W_\alpha^I\right)$. In our typical $\mathbb{Z}_2 \times \mathbb{Z}_2$ we would have $g_{i,j}$ with $i, j = 0, 1$ so we would have three different non trivial actions, corresponding to each twisted sector, for example $\tilde{g_{0,1}} X_L^I = X_L^I + 2\pi \left(lV_2^I + n_\alpha W_\alpha^I\right)$

The important idea is that points in the sixteen dimensions of the gauge degrees of freedom are identified, if they differ by the action of an element $\tilde{g}$ of the twisting group.

So to sum up taking into account the six dimensional internal space with the 16 gauge degrees of freedom our orbifold $\mathcal{O}$

$$\mathcal{O} = \mathbb{R}^6/S \otimes T_{\mathrm{E}_8 \times \mathrm{E}_8'}/G \tag{2.22}$$

defines a heterotic orbifold.
Further details (required for model building, e.g. calculation of the spectrum) will be developed in the sections in which each relevant orbifold appear (i.e 5.2 for $T^4/\mathbb{Z}_2$ and 7.3 for $T^6/\mathbb{Z}_2 \times \mathbb{Z}_2$).

Partition functions

To study the origin of spinor-vector duality we need to discuss a bit another result for heterotic orbifolds, i.e. the construction of partition functions. Recall that the one loop vacuum amplitude, also known as genus-one partition function, represents a fundamental quantity of the theory since it encodes the full perturbative spectrum. The modular invariant constraints (which have already imposed before making the gauge root lattice to be $E_8 \times E_8'$) are in fact derived from the calculation of the one-loop vacuum amplitude. The Feynman diagram, which describes a closed string propagating in time and returning to its initial state, is a donut-shaped surface, equivalent to a two-dimensional torus. A nice review of the discussion of partition functions for the heterotic orbifolds we are interested can be found in [135]. One of the main ideas is that the partition function of the $E_8 \times E_8'$ string can be written in terms of the $SO(2n)$ characters (O_{2n}, V_{2n}, S_{2n} and C_{2n}) which represents conjugacy classes of the $SO(2n)$ group (scalar, vectorial, spinorial and antispinorials). These characters are of the form:

$$O_{2n} = \frac{1}{2}\left(\frac{\theta_3^n}{\eta^n} + \frac{\theta_4^n}{\eta^n}\right), \quad V_{2n} = \frac{1}{2}\left(\frac{\theta_3^n}{\eta^n} - \frac{\theta_4^n}{\eta^n}\right), \quad S_{2n} = \frac{1}{2}\left(\frac{\theta_2^n}{\eta^n} + i^{-n}\frac{\theta_1^n}{\eta^n}\right), \quad C_{2n} = \frac{1}{2}\left(\frac{\theta_2^n}{\eta^n} - i^{-n}\frac{\theta_1^n}{\eta^n}\right), \tag{2.23}$$

where

$$\theta_3 \equiv Z_f \begin{pmatrix} 0 \\ 0 \end{pmatrix} \quad \theta_4 \equiv Z_f \begin{pmatrix} 0 \\ 1 \end{pmatrix} \quad \theta_2 \equiv Z_f \begin{pmatrix} 1 \\ 0 \end{pmatrix} \quad \theta_1 \equiv Z_f \begin{pmatrix} 1 \\ 1 \end{pmatrix}, \tag{2.24}$$

and Z_f is the partition function of a single worldsheet complex fermion, given in terms of theta functions. In $10D$ we would have

$$\mathcal{T}_{E_8\times E_8} = \left(\bar{V}_8 - \bar{S}_8\right)\left(O_{16} + S_{16}\right)\left(O_{16} + S_{16}\right) \tag{2.25}$$

However after compactifying in our six-torus we end with a partition function that is

$$Z_+ = \left(V_8 - S_8\right)\left(\sum_{m,n}\Lambda_{m,n}\right)^{\otimes 6}\left(\bar{O}_{16} + \bar{S}_{16}\right)\left(\bar{O}_{16} + \bar{S}_{16}\right). \tag{2.26}$$

where as usual, for each circle,

$$p^i_{\mathrm{L,R}} = \frac{m_i}{R_i} \pm \frac{n_i R_i}{\alpha'} \quad \text{and} \quad \Lambda_{m,n} = \frac{q^{\frac{\alpha'}{4}p^2_{\mathrm{L}}}\bar{q}^{\frac{\alpha'}{4}p^2_{\mathrm{R}}}}{|\eta|^2} \tag{2.27}$$

What we will see in the following section is that the introduction of the orbifold action is this partition function (2.26) will add an extra degree of freedom, the discrete torsion, which allow to choose a plus or minus signs between the orbits of the partition function. A consequence of some of these choices would be the spinor-vector duality.

2.2 Introduction to Spinor Vector duality

Once we have given the basic background of the heterotic models we are to use we can focus in the introduction of the spinor-vector duality.

2.2.1 Definition

We define spinor–vector duality (SVD) as a symmetry underlying the four dimensional fermionic $\mathbb{Z}_2 \times \mathbb{Z}_2$ string vacua which relates two models by interchanging the total number of spinors plus antispinors states by vectorial states of the underlying gauge group.

- More explicitly: for any vacuum 1, with $\#_1(S+\overline{S})$ and $\#_2(V)$ representations, there exist a dual vacuum 2 in which $\#_1 \leftrightarrow \#_2$, where S,$\overline{S}$ and V are the spinorial, anti-spinorial and vectorial representation of the underlying GUT group

2.2.2 Initial observation of SVD: counting number of models

SVD was originally observed in the context of the study of the fermionic $\mathbb{Z}_2 \times \mathbb{Z}_2$ orbifold. The duality was initially observed by simple counting [43], using the classification tools developed in [42, 43, 46] for the heterotic–string with unbroken $SO(10)$ GUT symmetry.
After that it was studied in detail for the $SO(12)$ or $SO(10)$ GUT groups in models with $\mathcal{N} = 2$ or $\mathcal{N} = 1$ spacetime supersymmetry, respectively [42–45]

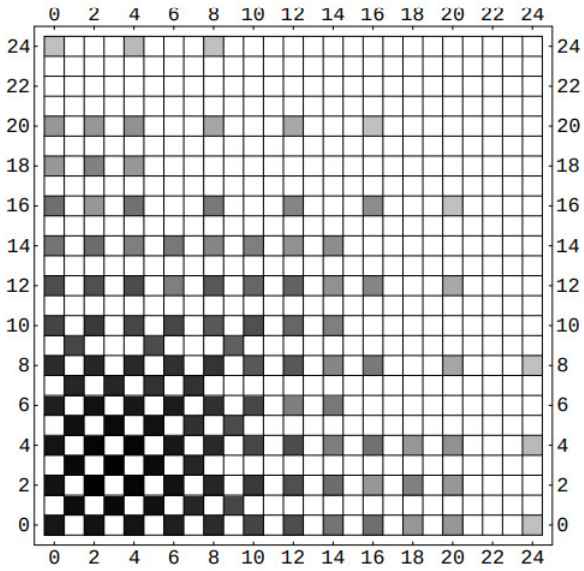

Figure 2.1: Density plot showing the spinor-vector duality in the space of fermionic $\mathbb{Z}_2 \times \mathbb{Z}_2$ heterotic-string models [43] The plot shows the number of vacua with a given number of $(16 + \overline{16})$ and 10 multiplets of $SO(10)$. It is invariant under exchange of rows and columns, reflecting the spinor-vector duality underlying the entire space of vacua. Models on the diagonal are self-dual under the exchange of rows and columns, i.e. $\#(16 + \overline{16}) = \#(10)$ without enhancement to E_6, which are self-dual by virtue of the enhanced symmetry. .

2.2.3 Further details of the duality

For further insight into SVD it is useful to study the behaviour of the representations of the underlying gauge goup.

Let us consider the $\mathcal{N}=1$ case, in which an $SO(10)\times U(1)$ symmetry is enhanced to E_6. In this case the string compactification possesses an (2,2) worldsheet supersymmetry. The representation of E_6 are the chiral 27 and anti–chiral $\overline{27}$, which decompose as

$$\begin{aligned} 27 &= 16_{+1/2}+10_{-1}+1_{+2} \\ \overline{27} &= \overline{16}_{-1/2}+10_{+1}+1_{-2} \end{aligned} \tag{2.28}$$

under $SO(10)\times U(1)$. If one now counts the sum of the number of all (16)– and ($\overline{16}$)–plets N_S and total number of (10)–plets N_V, it is obvious that in this case $N_S=N_V$. Thus, the point in the moduli space in which the symmetry is enhanced to E_6, is a self–dual point under the spinor–vector duality. This is similar to the case of T–duality on a circle, in which at the self–dual radius under T–duality the gauge symmetry is enhanced from $U(1)$ to $SU(2)$.

Away from the self–dual point the E_6 symmetry is broken to $SO(10)\times U(1)$ and the worldsheet supersymmetry is broken from $(2,2)$ to $(2,0)$. Another important fact, is that as the free fermionic heterotic–string vacua correspond to the $\mathbb{Z}_2\times\mathbb{Z}_2$ orbifolds, they contain three twisted sectors each preserving an $\mathcal{N}=2$ spacetime supersymmetry. The spinor–vector duality can then be realised in each twisted sector separately, *i.e.* it can be realised in models that possess $\mathcal{N}=2$, rather than $\mathcal{N}=1$, spacetime supersymmetry [44]. In the $\mathcal{N}=2$ vacua the enhanced symmetry at the self–dual point is E_7, which is broken to $SO(12)\times SU(2)$ away from the self–dual point, and the spinor–vector duality is realised in terms of the relevant representations of E_7 and $SO(12)\times SU(2)$ [44].
The origin of this breaking pattern both in the E_6 and E_7 (i.e. $\mathcal{N}=1$, and $\mathcal{N}=2$) cases, is the following

- In the bosonic description (i.e toroidal orbifold models) the E_6 or E_7 is broken by **discrete torsions** (which can be expressed as **Wilson lines**). The main difference is that in the vacua possessing $\mathcal{N}=2$ spacetime supersymmetry the mapping between the dual Wilson lines is continuous, whereas in those possessing $\mathcal{N}=1$ it is discrete, as the moduli which allowed the continuous interpolation in the $\mathcal{N}=2$ case are projected out [48]. We will briefly review this case in the next subsection.

- In the fermionic language the origin is in the exchange of generalised **GSO phases** in the one–loop partition function. For details we refer the reader to [45, 48].

2.3 The origin of SVD in $\mathbb{Z}_2\times\mathbb{Z}_2$ orbifold models

We present here the basic result of the orbifold case for the spinor-vector duality.

SVD arises as a result of switching on/off a discrete torsion between the orbifold twist and a Wilson line [47, 48].

To see how this result arises we come back to the study of the partition function of the heterotic $E_8\times E_8$ string compactified to four dimensions

Now we want to see how Z_+ is modified by the orbifold action: $\mathbb{Z}_2\times\mathbb{Z}_2' : g\times g'$ action.

- The first $\mathbb{Z}_2$ is freely acting. It couples a fermion number in the observable and hidden sectors with a $\mathbb{Z}_2$-shift in a compactified coordinate, and is given by $g : (-1)^{(F_1+F_2)}\delta$

where the fermion numbers $F_{1,2}$ act on the spinorial representations of the observable and hidden $SO(16)$ groups as $F_{1,2} : \left(\bar{O}_{16}^{1,2}, \bar{V}_{16}^{1,2}, \bar{S}_{16}^{1,2}, \bar{C}_{16}^{1,2}\right) \longrightarrow \left(\bar{O}_{16}^{1,2}, \bar{V}_{16}^{1,2}, -\bar{S}_{16}^{1,2}, -\bar{C}_{16}^{1,2}\right)$ and δ identifies points shifted by a Z_2 shift in the X_9 direction, i.e. $\delta X_9 = X_9 + \pi R_9$. The effect of the shift is to insert a factor of $(-1)^m$ into the lattice sum , i.e. $\delta : \Lambda^9_{m,n} \longrightarrow (-1)^m \Lambda^9_{m,n}$.

  - Alternatively, the first Z_2 action can be interpreted as a Wilson line in X_9 [48], $g : \left(0^7, 1 \mid 1, 0^7\right) \rightarrow E_8 \times E_8 \rightarrow SO(16) \times SO(16)$.

- The second $\mathbb{Z}_2$ acts as a twist on the internal coordinates: $g' : (x_4, x_5, x_6, x_7, x_8, x_9) \longrightarrow (-x_4, -x_5, -x_6, -x_7, +x_8, +x_9)$.

The effect of the second $\mathbb{Z}_2$ action (i.e the space twist) is to break $\mathcal{N} = 4 \rightarrow \mathcal{N} = 2$ spacetime supersymmetry and $E_8 \rightarrow E_7 \times SU(2)$ or, with the inclusion of the first $\mathbb{Z}_2$ (i.e. the Wilson line) $SO(16) \rightarrow SO(12) \times SO(4)$.
Now the resulting orbifold partition function is given by

$$Z = \left(\frac{Z_+}{Z_g \times Z_{g'}}\right) = \left[\frac{(1+g)}{2}\frac{(1+g')}{2}\right] Z_+ \tag{2.29}$$

it contains an untwisted sector and three twisted sectors. The winding modes in the sectors twisted by g and gg' are shifted by $1/2$, and therefore these sectors only produce massive states. The sector twisted by g gives rise to the massless twisted matter states. The partition function has two modular orbits and one discrete torsion $e = \pm 1$. Massless states are obtained for vanishing lattice modes. The terms in the sector g contributing to the massless spectrum take the form:

$$\begin{aligned}\Lambda_{p,q} \Bigg\{ \frac{1}{2}\left(\left|\frac{2\eta}{\theta_4}\right|^4 + \left|\frac{2\eta}{\theta_3}\right|^4\right)\left[P^+_\epsilon Q_s \bar{V}_{12}\bar{C}_4\bar{O}_{16} + P^-_\epsilon Q_s \bar{S}_{12}\bar{O}_4\bar{O}_{16}\right] + \\ \frac{1}{2}\left(\left|\frac{2\eta}{\theta_4}\right|^4 - \left|\frac{2\eta}{\theta_3}\right|^4\right)\left[P^+_\epsilon Q_s \bar{O}_{12}\bar{S}_4\bar{O}_{16}\right]\Bigg\} \quad + \text{ massive}\end{aligned} \tag{2.30}$$

where:

$$P^+_\epsilon = \left(\frac{1+\epsilon(-1)^m}{2}\right)\Lambda_{m,n}; \quad P^-_\epsilon = \left(\frac{1-\epsilon(-1)^m}{2}\right)\Lambda_{m,n} \tag{2.31}$$

Depending on the sign of $\epsilon = \pm$ it is seen from (2.31) that either the vectorial states, or the spinorial states, are massless. In the case with $\epsilon = +1$ we note from (2.32) that in this case massless momentum modes from the shifted lattice arise in P^+_ϵwhereas P^-_ϵonly produces massive modes. Therefore, in his case the vectorial character $\bar{V}_{12}$ in eq. produces massless states, whereas the spinorial character $\bar{S}_{12}$ generates massive states. In the case with $\epsilon = -1$ (2.33) shows that exactly the opposite occurs.

$$\epsilon = +1 \quad \Rightarrow \quad P^+_\epsilon = \quad \Lambda_{2m,n} \quad P_\epsilon - = \quad \Lambda_{2m+1,n} \tag{2.32}$$

$$\epsilon = -1 \quad \Rightarrow \quad P^+_\epsilon = \quad \Lambda_{2m+1,n} \quad P^-_\epsilon = \quad \Lambda_{2m,n} \tag{2.33}$$

Thus, the spinor-vector duality is generated by the exchange of the discrete torsion $\epsilon = +1 \rightarrow \epsilon = -1$ in the $\mathbb{Z}_2 \times \mathbb{Z}'_2$ partition function.
As we said in the previous subsection, the orbifold language is closer to our purposes (i.e. the

extension to the smooth case), and we can see already some relation with mirror symmetry. It can be observed a similar logic between the example we have just discussed and one of the simplest examples of mirror symmetry, i.e. in the $\mathbb{Z}_2 \times \mathbb{Z}$ orbifold model of [64], where the mirror symmetry map is induced by exchange of the discrete torsion between the two orbifold $\mathbb{Z}_2$ twists. In the mirror symmetry case the chirality of the fermion multiplets is changed, together with the exchange of the complex and Kähler moduli of the internal manifold. The total number of degrees of freedom is invariant under the mirror symmetry map. It is interesting to note that this is also the case in the case of the SVD. In this case there is a mismatch between the number of states in the vectorial, $12 \cdot 2 = 24$, and spinorial 32 , cases. It is noted from the second line in (2.30)that the vectorial case $\epsilon = +1$ is accompanied by 8 additional states, which are singlets of the $SO(12)$ GUT group. It is seen that the total number of degrees of freedom is preserved under the duality map, i.e. $12 \cdot 2 + 4 \cdot 2 = 32$

Chapter 3

Line bundle resolutions of heterotic orbifolds

3.0.1 Introduction: why resolved orbifolds

It is reasonable to assume that the idea of extending SVD to smooth compactifications may be better implemented if the models of both sides (orbifolds and smooth manifolds) are connected in such a way we have a complete control of the physical and geometrical changes we are doing while passing from one side to the other. This is the rationale behind choosing our smooth spaces to be Calabi-Yau manifolds defined as **resolutions of toroidal orbifolds** instead of other common choices as Complete Intersections Calabi-Yaus [95], elliptic fibrations [25] or hypersurfaces in four dimensional toric varieties, like the ones from the famous Kreuzer-Skarke database [103].
The strategy we will follow is to understand the element which generate the SVD in the orbifold side (which is the discrete torsion between the orbifold twist and Wilson line as we saw in the previous chapter) and try to guess how it works in the most similar (but smooth) model that we can define.
The orbifolds we start from are the $T^4/\mathbb{Z}_2$ in $6D$, the $(T^4/\mathbb{Z}_2)\times S^1$ in $5D$ and the $T^6/\mathbb{Z}_2\times\mathbb{Z}_2$ with Hodge numbers $(h^{1,1},h^{2,1})=(51,3)$ in $4D$ (see [99] for a classification of relevant orbifolds for free fermionic constructions). The resolution of the the first two ones is relatively simple (a $K3$ surface (or $K3\times S^1$)) while the last resolution is topologically non trivial and we will devote more time to study it.
Starting from the orbifold we are going to manipulate it in such a way we obtain a smooth manifold which inherits its geometrical structure (plus some extra structure, which is going to be new but controlled/known). This manipulation is going to be a well-defined geometrical and topological operation, the so-called resolution of singularities.
The resolved orbifolds we are dealing with in this thesis are studied by two different formalisms:

- In the simpler version we are introducing exceptional divisors and placing our gauge flux only inside of them (i.e. Abelian gauge flux). We refer to this as **line bundle resolutions** [32, 60, 61] and it will be the matter of this chapter. The general idea of the process has two main parts:
  - "Blow-up" the singularity by introducing an exceptional divisor which defines a line bundle. Physically this corresponds to give a non-vanishing vacuum expecta-

tion value (VEV) to a field. This results in a non-compact resolution of the local singularity.

– Glue the resolved pieces together to form a Calabi Yau manifold, which gives the final, compact resolution.

This will be the main formalism employed for the smooth models of Chapters 4, 5 and 6.

- In Chapter 7, we will use a more general formalism which allows to deal with orbifolds and (total and partial) resolutions of them (together with non geometrical regimes), the **Gauged Linear Sigma Models** (GLSMs) [112, 113]. In GLSMs we are interested in specifying a supersymmetric configuration of a two-dimensional SUSY field theory. Then by continuous variation of some of the parameters of the theory (the FI parameters and the complex parameters of the superpotential) we can go through topological changes from orbifold to resolved models and vice versa. Although it is conceptually more complex in some ways, its flexibility is better suited to study discrete torsion on both sides.

We will devote this chapter to the study of the basic topology, geometry and consistency conditions of line bundle resolutions (focusing on the $\text{Res}(T^6/(\mathbb{Z}_2 \times \mathbb{Z}_2))$) to offer a conceptual first approach to those not familiar to these techniques. This background material is basically a recollection/summary of [32, 60, 61, 63, 78] so we refer the reader to these papers for further details. The GLSM formalism will be studied in detail in Chapter 7.

3.1 Some useful concepts and definitions

We start giving a basic review of some concepts coming from Algebraic Geometry and related fields that will appear in the resolution formalism. As we said before, one of the key steps when we resolve a toroidal orbifold is to introduce a smooth submanifold of the resolved space, the so-called exceptional divisor. Hence, we first explain in some detail the concept of **divisor**. For intuition it is useful to think about them as the (linearly independent) pieces (submanifolds or more precisely hypersurfaces) inside our total Calabi Yau manifold. They (and their intersections) are going to encode most of the topological data which is going to constraint our resultant $4D$ theory.

Divisor On a complex n-fold $\mathcal{M}$, a divisor D is a locally finite linear combination of irreducible analytic hypersurfaces $\mathcal{Y}_i$ of $\mathcal{M}$:

$$D = \sum_i a_i \mathcal{Y}_i;\ a_i \in \mathbb{Z} \tag{3.1}$$

- An "analytic hypersurface" means that $\dim \mathcal{Y}_i = n - 1$ and that every $\mathcal{Y}_i$ is (locally at every point) given as the zero-set of a single holomorphic function.

- "Locally finite" means that for any $p \in \mathcal{M}$, there exists a neighborhood of p meeting only a finite number of the $\mathcal{Y}_i$'s appearing in D; if $\mathcal{M}$ is compact, this simply means that the defining sum for D is finite.

- A divisor is said to be "effective" if $a_i \geq 0$ for all i.

- Note that we are restricting ourselves to (what is called in Algebraic Geometry) Weyl divisors, so in our language: divisor ≡ Weyl divisor.

Vector bundle

In heterotic theory the gauge degrees of freedom are described geometrically by an holomorphic vector bundle. Let us give the technical definition.
A vector bundle $\mathcal{V}$ is a tuple (E, π, B, F, G) such that:

- E is a topological space called the total space.
- B is another topological space (a Calabi-Yau manifold in our case) called the base space.
- F is a vector space and it is called the fibre. When the dimension of F is 1 we have a **line bundle**, $\mathcal{L}$.
- $\pi : E \to M$ is a surjection called the projection. For any point $p \in B$ the inverse image $\pi^{-1}(p) = F_p \cong F$ is the fibre at p.
- A Lie group G called the structure group, which acts on F on the left. In heterotic compactifications we generally have that $G = SU(n)$. In our resolved models we will have different $U(1)$'s that can be embedded into some $S(U(1))^n$. See equation (3.61) and below.
- A set of open coverings $\{U_i\}$ of B with a diffeomorphism $\phi_i : U_i \times F \to \pi^{-1}(U_i)$ such that $\pi \circ \phi_i(p, f) = p$. The map ϕ_i is called the local trivialization since ϕ_i^{-1} maps $\pi^{-1}(U_i)$ onto the direct product $U_i \times F$.
- If we write $\phi_i(p, f) = \phi_{i,p}(f)$, the map $\phi_{i,p} : F \to F_p$ is a diffeomorphism. On $U_i \cap U_j \neq \emptyset$, we require that $t_{ij}(p) \equiv \phi_{i,p}^{-1} \circ \phi_{j,p} : F \to F$ be an element of G. Then ϕ_i and ϕ_j are related by a smooth map $t_{ij} : U_i \cap U_j \to G$ as:

$$\phi_j(p, f) = \phi_i(p, t_{ij}(p) f). \tag{3.2}$$

  The maps t_{ij} are called the transition functions.
- Depending on the vector bundle we can have a number of local sections $s_i : U_i \to E$ such that $\pi(s_i(p_i)) = p_i$ for all $p_i \in U_i$.

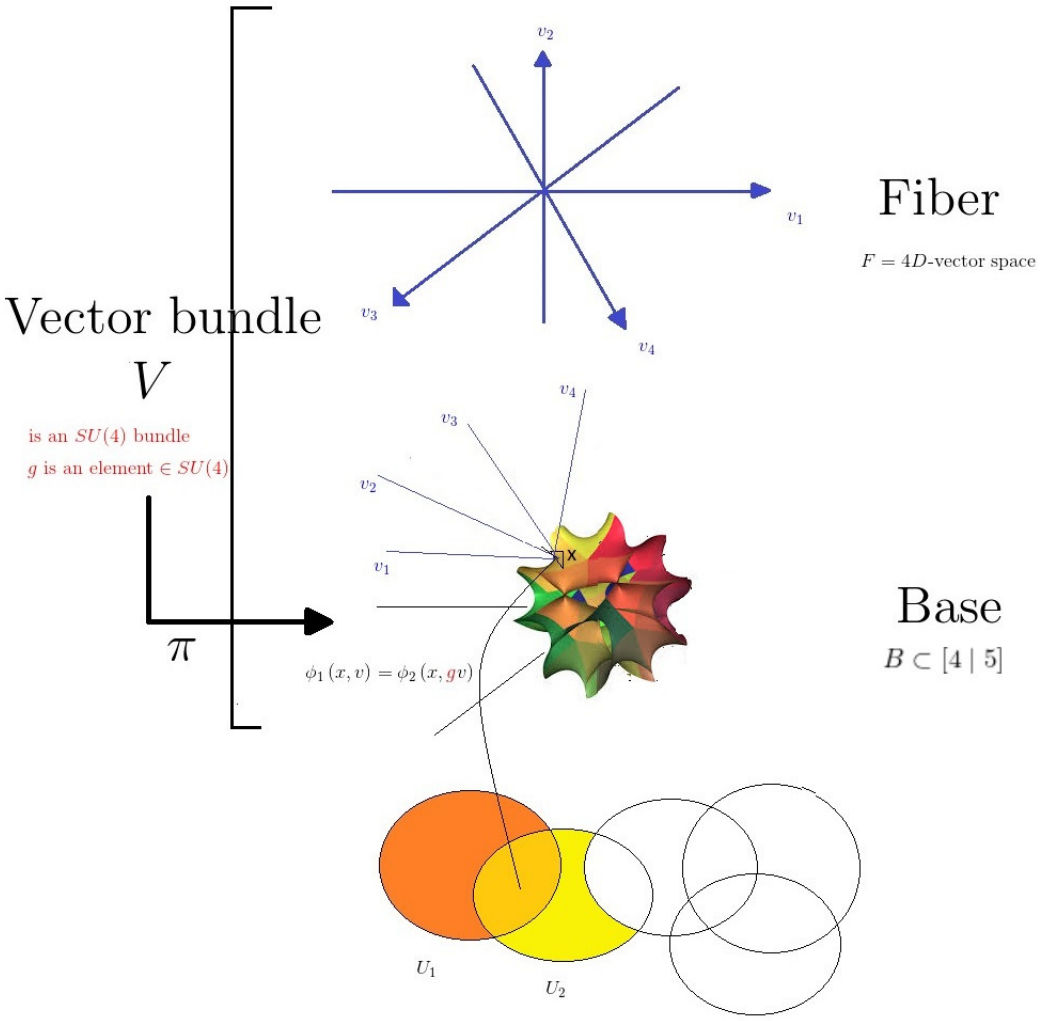

Figure 3.1: To illustrate the definition above we show an impresionistic representation of a $SU(4)$ vector bundfle over a CY threefold (in this case we represent a $2D$ slice of the quntic hypersurface in $\mathbb{P}^4$). The $SU(4)$ vector bundle is going to describe part of the gauge degrees of freedom of the original $E_8 \times E_8'$ leaving $SO(10) \times E_8'$ as the $4D$ gauge group

The construction of vector bundles is usually technically involved and implies techniques as monad bundles (based in short exact sequences[1] of line bundles [30]) or the use of spectral covers [23], among others. An advantage of the resolution formalism is that it allows the construction of vector bundles in a straightforward way as long as we only use Abelian gauge

[1]Recall that a short exact sequence is of the form: $0 \to A \xrightarrow{f} B \xrightarrow{g} C \to 0$ where A,B,C are vector bundles, the arrows are mappings between them, and they fulfil that $\text{im}(f) = \ker(g)$.

fluxes. That will imply that the flux is only located in the exceptional divisors, which define by the line bundle-divisor correspondence our bundle background.

Blowing-up and exceptional divisor

A process by which a point p in a complex n-dimensional space X is replaced by a compact complex $(n-1)$-dimensional space E in such a way that E is a complex subspace of the resulting blow-up, $\widetilde{X}_p$. In other words, the space E must admit a complex 1-dimensional fibration (i.e. line bundle) such that the n-dimensional total space of this fibration fits in the 'hole' left in X when p was removed. Note that p could have been a smooth or a singular point of X (in the case of orbifolds it would be singular); its replacement, E is going to be a special case of divisor, called the exceptional divisor of $\widetilde{X}_p$.

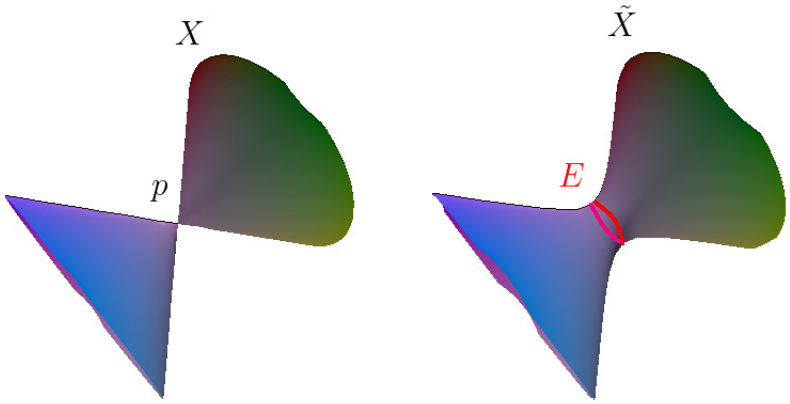

Figure 3.2: Simple illustration of the blow-up process for a conic singularity, which corresponds to $\mathbb{C}^2/\mathbb{Z}_2$. The exceptional divisor E is a $\mathbb{P}^1$ and the resolved space $\tilde{X}$ can be thought as a 1-dimensional fibration over E

Line bundle-divisor correspondence

We can assign a holomorphic line bundle $\mathcal{L}$ to a divisor. To do so let us choose an open cover $\{U_i\}$ of the base B and local trivializations

$$\phi_i : \mathcal{L}|_{U_i} \to U_i \times \mathbb{C}. \tag{3.3}$$

In terms of the trivializations ϕ_i, the holomorphic transition functions t_{ij} on the overlap of two open covers $U_i \cap U_j$ are given by $t_{ij} = \phi_i \circ \phi_j^{-1}$. Sections s_α of $\mathcal{L}$ associate points on the base B with points in the fiber $F \simeq \mathbb{C}$.

As divisors correspond to (a sum of) hypersurfaces $f_i = 0$ on open patches U_i with transition functions t_{ij} the identification is done by taking these transition functions to be the transition function of the associated line bundle. This implies that the degree of the f_i will be the first Chern class of the line bundle, which determines it uniquely.

Chern class

Chern classes are characteristic classes expressing topological invariants of complex vector

bundles. For a vector bundle $\mathcal{V}$ of rank n with curvature $F(\mathcal{V})$ its total Chern class is:

$$c(\mathcal{V}) = \det\left(1 + \frac{F(\mathcal{V})}{2\pi i}\right) = \mathbb{1} + c_1(\mathcal{V}) + c_2(\mathcal{V}) + ...c_n(\mathcal{V}) \tag{3.4}$$

where $c_i(\mathcal{V})$ is the i-th Chern class of the bundle. As we are generally dealing with vector bundles which are sum of line bundles it is interesting to remember the so-called splitting principle:

$$c(\mathcal{V}) = \prod_{i=1}^{n} c\left(\mathcal{L}_i\right) \tag{3.5}$$

- **For a line bundle** A complex line bundle $\mathcal{L}$ is completely determined by its first Chern class $c_1(\mathcal{L}) = F(\mathcal{L})/2\pi i$, which can be taken to be harmonic (1,1)-form. Because it is closed, locally its curvature can be written as $F(\mathcal{L}) = \mathrm{A}_i(\mathcal{L})$ in terms of a connection $A_i(\mathcal{L})$ in coordinate patch U_i. Between two coordinate patches U_i and U_j the connections

$$A_j(\mathcal{L}) = A_i(\mathcal{L}) + t_{ji}(\mathcal{L})^{-1} t_{ji}(\mathcal{L}) \tag{3.6}$$

  are related via the transition functions $t_{ji}(\mathcal{L})$.

Intersection number

The intersection numbers generalize the idea of the counting at how many points d two curves intersect, into higher dimensions. In particular, for a Calabi-Yau threefold we are interested in triple intersection numbers, which will be defined as:

$$\kappa_{ijk} = \int_X D_i D_j D_k \tag{3.7}$$

where D_α is any divisor of the Calabi-Yau. Note that there is no index α is excluded from the definition. Consequently one also can calculate self-intersections of divisors, which have a less straightforward geometric interpretation than "the number of times they intersect" . Roughly, self-intersections can be thought of as the intersection of a submanifold with its slightly perturbed copy and they can be fractional (for non-compact varieties) or negative (for exceptional divisors). A negative self-intersection then signals that a divisor cannot be moved. The fractional intersection numbers signal that by taking the local (non-compact) case we are neglecting contributions from the global gluing.

Toric variety

As the resolutions of toroidal orbifolds are going to be toric varieties and some important data of them (like the triangulation and the intersection numbers) can be read from some pictorial representation of the variety (the so-called toric diagram) it is helpful to introduce these definitions now.
An n-dimensional toric variety X has the form:

$$X = \left(\mathbb{C}^N - F\right) / \left(\mathbb{C}^*\right)^m \tag{3.8}$$

which contains the algebraic torus $\left(\mathbb{C}^*\right)^{N-m}$ which lends the variety its name. F is the so-called exclusion set and it is the subset that remains fixed under a continuous subgroup of $\left(\mathbb{C}^*\right)^m$ It must be subtracted for the variety to be well-defined.

Toric diagram

There is a convenient way to represent the properties of toric varieties including the properties of the divisors: the toric diagram. It is based in the concept of cone and fan. Define $M \cong \mathbb{Z}^N$ and $M_{\mathbb{R}} = M \otimes_{\mathbb{Z}} \mathbb{R}$. Then

- **Cone** A strongly convex rational polyhedral cone σ of dimension n, or cone for short, is spanned by a finite set of vectors $v_i \in M$,

$$\sigma = \left\{ \sum_{i=1}^{n} c_i v_i \mid c_i \in \mathbb{R}^+ \right\} \quad \Rightarrow \quad \sigma \subset M_{\mathrm{R}} \tag{3.9}$$

  such that $\sigma \cap (-\sigma) = \varnothing$. The cones of dimension one are called edges.

- **Fan** A fan Σ is a collection of cones such that each face of a cone in Σ is also a cone in σ and that the intersection of two cones in σ is a face of both cones. A fan is specified by its edges and its choice of the exclusion set.

To picture the toric diagram from this data we need to know the relation between the toric variety we have defined(3.9) and the vectors v_i. These vectors correspond to coordinates z_i of $\mathbb{C}^N$. The $(\mathbb{C}^*)^m$ actions relate the various coordinates and thus correspond to linear relations among the v_i. Finally, the exclusion set F contains those coordinates which correspond to vectors that do not belong to the same cone. The edges of the fan correspond to the divisors in X. We will see some examples of toric diagrams in the following subsections.

3.2 Resolution of $\mathbb{C}^n/\mathbb{Z}_n$ using toric geometry

We start from a $\mathbb{C}^n/\mathbb{Z}_n$ orbifold, which is defined as the complex space $\mathbb{C}^n$ with n local coordinates $\tilde{Z}_a$, on which the $\mathbb{Z}_n$ twist acts as:

$$\Theta(\tilde{Z}) = \theta \tilde{Z}, \quad \theta = e^{2\pi i \phi}, \quad \phi = \frac{1}{n}\,\mathrm{diag}(1, \ldots, 1) \tag{3.10}$$

This defines a space with a singularity and a deficit angle of $2\pi(1 - \frac{1}{n})$. We can avoid this singularity by defining a new set of n local coordinates Z_a in terms of the $n+1$ homogenous coordinates $z_1, \ldots, z_n, x \in \mathbb{C}$ in the following way

$$Z_1 = z_1 x^{\frac{1}{n}}, \quad \ldots \quad Z_n = z_n x^{\frac{1}{n}}, \tag{3.11}$$

As we are describing the n local coordinates using $n+1$ homogeneous coordinates, we must introduce a constraint which "kills" one degree of freedom, which is going to be the $\mathbb{C}^* = \mathbb{C} - 0$ "toric" action on the homogeneous coordinates. As we want our action to leave the local coordinates inert the $\mathbb{C}^*$ action is uniquely fixed to

$$\mathbb{C}^* : (z_1, \ldots, z_n, x) \sim \left(\lambda^{-1} z_1, \ldots, \lambda^{-1} z_n, \lambda^n x\right), \ \lambda \in \mathbb{C}^* \tag{3.12}$$

Consequently the resolution of $\mathbb{C}^n/\mathbb{Z}_n$ is defined by the toric variety:

$$\mathrm{Res}\,(\mathbb{C}^n/\mathbb{Z}_n) = \left(\mathbb{C}^{n+1} - F\right)/\mathbb{C}^*, \tag{3.13}$$

where the exclusion set F has been subtracted to ensure, that the resolution is not singular. As the $\mathbb{C}^*$ action should act non-trivially, we should exclude the origin, i.e. $F = \{z_1 = \ldots = z_n = x = 0\}$,

Now, it is useful to define a set of $n+1$ hypersurfaces of complex dimension $n-1$ (i.e. divisors). We have two types of divisors

- **Ordinary divisors** $D_i = \{z_i = 0\}$ which are non-compact. They are present in the original space.
- **Exceptional divisor** $E = \{x = 0\}$. This is the one that (according to our previous definition) is not present in the original space. It is obviously compact. Taking into account the rescaling of the toric action, we see that $E = \mathbb{CP}^{n-1}$ defined in terms of homogeneous coordinates. In agreement to the blow-up definition, this means that the singularity of the orbifold $\mathbb{C}^n/\mathbb{Z}_n$ has been "blown up" to a $\mathbb{CP}^{n-1}$.

Note that the resolution Res $(\mathbb{C}^n/\mathbb{Z}_n)$ itself can be thought of as a complex line bundle over $\mathbb{CP}^{n-1}$.

As we said before we can we can associate a complex line bundle to each of the divisors, which will be uniquely characterized by its holomorphic scalar transition functions. To determine these transition functions for the various divisors we write the defining equation of the divisor in each patch U_i.
This gives for the ordinary divisors D_i:

$$U_{j\neq i} : \frac{z_i}{z_j} = 0, \quad U_i : 1 = 0, \quad U_0 : x^{\frac{1}{n}} z_i = 0 \tag{3.14}$$

and for the exceptional divisor E:

$$U_j : \quad z_j^n x = 0, \quad U_0 : \quad 1 = 0. \tag{3.15}$$

Note that the inconsistent equations " $1 = 0$ " tell us that D_i does not live in U_i and E does not live in U_0.
From this we read off the transition functions for the associated line bundle of divisors D_i and E :

$$t_{kj}\left(D_i\right) = \frac{t_k}{t_j}, \quad t_{j0}\left(D_i\right) = x^{\frac{1}{n}} z_j, \qquad \text{and} \qquad t_{kj}(E) = \frac{z_j^n}{z_k^n}, \quad t_{j0}(E) = \frac{1}{z_j^n x} \tag{3.16}$$

It follows, that the transition functions of the line bundles, associated to the divisors, D_i and E, are all related to each other in every patch (so we drop the indices) according to:

$$t\left(D_1\right)^{-n} = \ldots = t\left(D_n\right)^{-n} = t(E) \tag{3.17}$$

As the divisors correspond to line bundles and they are totally characterized by the Chern class (i.e. we may write $D_i = c_1\left(D_i\right)$ and $E = c_1(E)$) we know by (3.17) that the divisors satisfy the following linear equivalence relations:

$$D_i \sim D_j, \quad nD_i + E \sim 0, \Leftrightarrow c(D_i) = c(D_j), \quad nc(D_i) + c(E) = 0, \tag{3.18}$$

On the other side the splitting principle (3.5) can be seen equivalently as the fact that the total Chern class $c(TX)$ of the tangent bundle of our manifold X is given as the product of

$1 + D$ over all compact and non-compact divisors D. For $X = \text{Res}(\mathbb{C}^n/\mathbb{Z}_n)$ this amounts to

$$c(TX) = (1 + E)\prod_{i=1}^{n}(1 + D_i) \tag{3.19}$$

from this equation and using the linear relations (3.18) we check that our space has a vanishing first Chern class as required for a Calabi-Yau space,

$$c_1(TX) = E + \sum_{i=1}^{n} D_i = 0 \tag{3.20}$$

We are also interested in the second Chern class which gives (using that $c_1(TX) = 0$)

$$c_2(TX) = E\sum_i D_i + \sum_{i<j} D_i D_j = \frac{n+1}{2} E D_1, \tag{3.21}$$

A key characteristic of any Calabi-Yau manifold, which define its Hodge numbers, are the holomorphic cycles within it, and the study of their intersections, the intersection numers we talked about in (3.7) .

The different holomorphic $(n-1)$-cycles are the D_i's and E and we can define any intersection numbers from them by integrating the appropriate $(n-i, n-i)$-form over the appropriate $(n-i)$ dimensional hypersurface. For example we can define the integral of any $(n-1, n-1)$-form, say, $D_2^{n-2}E$ over, for example, D_1, and denote it by $\int_{D_1} D_2^{n-2}E$.

As we said particular interesting case are the intersections of n different divisors are because they define zero dimensional surfaces, i.e. sets of points, what we called before triple intersection numbers. In general these numbers are read from the toric diagram when the divisors are all different (the intersection number of all divisors which form a cone together with the origin have intersection number 1) and we use some linear equivalence relations when we are dealing with self-intersections.

To build the toric diagram of $\text{Res}\,(\mathbb{C}^n/\mathbb{Z}_n)$ first give n vectors $v_1, \ldots, v_n$ that represent the n ordinary divisors $D_1, \ldots, D_n$. A possible basis is $v_1 = (1, 0, \ldots, 0)$, to $v_n = (0, \ldots, 0, 1)$. Then, exceptional divisor E is represented by the vector

$$w = \sum_i \phi_i v_i, \tag{3.22}$$

which in this basis (and recalling that ϕ_i is the one of the orbifold action (3.10) takes the form $w = (1, \ldots, 1)/n$. This basis $v_1, \ldots, v_n$ and w precisely dictate how to construct the local coordinates and it is a particularly simple example of what was explained in the definition of the toric diagram. We will have:

$$E \cdot \prod_{j\neq i} D_j = \int E D_2 \ldots D_n = 1 \tag{3.23}$$

as they form a cone with the origin (it can be checked for $\mathbb{C}^2/\mathbb{Z}_2$ and $\mathbb{C}^3/\mathbb{Z}_3$ s in figure 3.3). Then using the linear equivalences (3.18) we get that

$$E^n = (-n)^{n-1}\int D_2 \ldots D_n E = (-n)^{n-1} \tag{3.24}$$

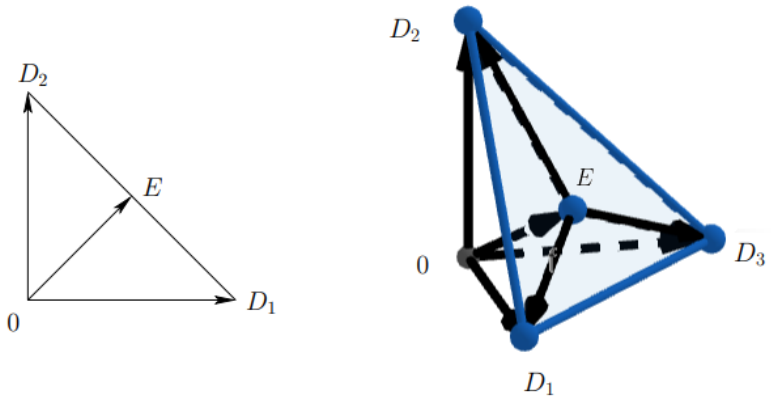

Figure 3.3: Toric diagrams of $\mathbb{C}^2/\mathbb{Z}_2$ and $\mathbb{C}^3/\mathbb{Z}_3$

Now we want to reconnect with the original heterotic orbifold theory and check that our construction is consistent with it. Our blowup models should satisfy the integrated version of the Bianchi identity

$$\mathrm{H} = \mathrm{tr}\,\mathcal{R}^2 - \mathrm{tr}\,(i\mathcal{F}_V)^2 \tag{3.25}$$

Here we have defined $i\mathcal{F}_V = i\mathcal{F}V^I H_I$ which is the embedding of the $U(1)$ gauge background in the SO(32) or $\mathrm{E}_8 \times \mathrm{E}_8$ gauge group. We can see the relation of this V^2 and the orbifold model defined by the gauge shift v by identifying the gauge background $\mathcal{F}_V$ with the orbifold action on the gauge degrees of freedom (up to vectors in the SO(32) or $\mathrm{E}_8 \times \mathrm{E}_8$ lattice, hence the $\equiv$ symbols)

$$v^I H_I \equiv \int_\gamma \mathcal{A}_V = -\frac{1}{n} V^I H_I \tag{3.26}$$

$$v^I H_I \equiv \int_{D_2 \ldots D_n} \mathcal{F}_V = -\frac{1}{n} V^I H_I \tag{3.27}$$

note the fractional nature of the orbifold gauge shift vector v is obtained by integrating over a non-compact curve. The integrated version Bianchi Identity is easily computed. For Res $\left(\mathbb{C}^2/\mathbb{Z}_2\right)$ we find

$$V^2 = -2\int \mathrm{tr}\,(\mathcal{F}_V)^2 = -2\int \mathrm{tr}\,\mathcal{R}^2 = 6, \tag{3.28}$$

when integrated over the whole resolution. For Res $\left(\mathbb{C}^3/\mathbb{Z}_3\right)$ we obtain

$$V^2 = \int_E \mathrm{tr}\,(\mathcal{F}_V)^2 = -3\int_{D_i} \mathrm{tr}\,(\mathcal{F}_V)^2 = -3\int_{D_i} \mathrm{tr}\,\mathcal{R}^2 = \int_E \mathrm{tr}\,\mathcal{R}^2 = 12 \tag{3.29}$$

Both conditions in two and three complex internal dimensions are compatible with the corresponding modular invariance conditions, $(2v)^3 = 2 \bmod 4$ and $(3v)^3 = 0 \bmod 6$, of the heterotic string, respectively.

[2] In later models, like Res$(T^6/(\mathbb{Z}_2 \times \mathbb{Z}_2))$ what we have is a set of $U(1)$'s located in the 48 different exceptional divisors and the embedding vectors V's (which should be $8+8$ dimensional vectors of integer of half-integer entries), which we informally call "*bundle vectors*", will be one of our main degrees of freedom for model building, (together with the choice of triangulation).

3.3 Orbifold resolutions with multiple exceptional divisors

The most important resolution we are going to study, the $\mathrm{Res}(T^6/(\mathbb{Z}_2 \times \mathbb{Z}_2))$, will need the introduction of several exceptional divisors so it is also enlightening to explain the more general case, i.e. considering non-compact orbifolds $\mathbb{C}^n/G$, where G is a finite group, Abelian for simplicity, and $n = 2, 3$. The action of an element $\theta \in G$ on the orbifold coordinates $\tilde{Z}_1, \ldots \tilde{Z}_n$ can he written as

$$\theta : \left(\tilde{Z}_1, \ldots, \tilde{Z}_n\right) \to \left(e^{2\pi i \phi_1(\theta)} \tilde{Z}_1, \ldots, e^{2\pi i \phi_n(\theta)} \tilde{Z}_n\right) \tag{3.30}$$

such that all $0 \leq \phi_i(\theta) < 1$.

We define the corresponding representative $[\theta]$ of the orbifold action to be the element that satisfies $\sum_i \phi_i(\theta) = 1$. Now, to each representative $[\theta]$ we associate an exceptional divisor E_θ. The total number of exceptional divisors is denoted as N. For even and odd ordered orbifolds the following holds: $N(\mathbb{Z}_{2k}) = N(\mathbb{Z}_{2k+1}) = k$ exceptional divisors. If we let $v_1, \ldots v_n$ define a basis for the toric diagram of the orbifold, then the vector

$$w_\theta = \sum_i \phi_i(\theta) v_i \tag{3.31}$$

identifies the exceptional divisor E_θ in the toric diagram of the resolution for each representative $[\theta]$. *This definition of exceptional divisors of the resolution is in one-to-one correspondence to the twisted sectors in orbifold string theory: Also there each representative* $[\theta]$ *corresponds to a distinct, e.g. first, second, etc., twisted sectors.* In particular, as is well-known the $\mathbb{C}^n/\mathbb{Z}_n$ orbifolds, with $n = 2, 3$, have only a single twisted sector, in agreements with the previous section where we only had a single exceptional divisor. As noted before, the set of vectors v_i and w_θ define the points in the toric diagram corresponding to the ordinary and exceptional divisors of the resolution, respectively.

Now we follow the same procedure than in the previous subsection. Each of the vectors, v_i and w_θ, correspond to a homogeneous coordinate, z_i and x_θ, of the resolution $\mathrm{Res}(\mathbb{C}^n/G)$, respectively. As in the previous section, the divisors are defined by setting the corresponding coordinate to zero:

$$D_i = \{z_i = 0\}, \quad E_\theta = \{x_\theta = 0\} \tag{3.32}$$

Similarly to (3.11) we introduce a set of n local coordinates Z_a defined in terms of $n + k$ homogeneous ones:

$$Z_j = \prod_{i=1}^{n} z_i^{(v_i)_j} \prod_{\theta=1}^{k} x_\theta^{(w_\theta)_j} \tag{3.33}$$

(where $(v_i)_j$ denotes the j th component of the vector v_i) and the corresponding $N = k$ toric actions $(\mathbb{C}^*)$ such that they leave the local coordinates invariant. We will also have n linear equivalence relations of the divisors:

$$\sum_i (v_i)_j D_i + \sum_\theta (w_\theta)_j E_\theta \sim 0. \tag{3.34}$$

The resolution of the $\mathbb{C}^n/G$ orbifold is also a toric variety defined as

$$\mathrm{Res}(\mathbb{C}^n/G) = \left(\mathbb{C}^{n+N} - F\right) / (\mathbb{C}^*)^N, \tag{3.35}$$

where exclusion set F is defined, such that in non of the coordinate patches singularities arise.

3.4 The geometry of Res($T^6/(\mathbb{Z}_2 \times \mathbb{Z}_2)$)

We will review the resolution of $T^6/(\mathbb{Z}_2 \times \mathbb{Z}_2)$ following the work of [32] as that is the manifold we are interested in for the $4D$ case, and the background geometry in Chapters 6 and 7. In fact Chapter 6 can be seen in some sense as the continuation of the cited paper.

3.4.1 The orbifold

The orbifold is defined as a six-torus:

$$T^6 = T^2 \times T^2 \times T^2 = \left\{ \sum_{p=1}^{6} x_p e_p;\ 0 \leq x_p < 1;\ e_p \equiv \text{orthonormal basis in } \mathbb{R}^6 \right\} = \\ = \mathbb{C}^3/\Gamma_{\text{fac}} = \mathbb{C}^3/\left\{ \sum_{p=1}^{6} n_p e_p;\ n_p \in \mathbb{Z} \right\} \tag{3.36}$$

modded out by a $\mathbb{Z}_2 \times \mathbb{Z}_2$ symmetry group, $\mathbb{Z}_2 \times \mathbb{Z}_2 \equiv \{\mathbb{1}, \theta_1, \theta_2, \theta_3\}$, whose twist elements θ_1, θ_2 and $\theta_3 = \theta_1\theta_2$ have the action:

$$\theta_i : (z_1, z_2, z_3) \mapsto (e^{2\pi i(\varphi_i)^1} z_1, e^{2\pi i(\varphi_i)^2} z_2, e^{2\pi i(\varphi_i)^3} z_3); \\ \varphi_1 = (0, \frac{1}{2}, -\frac{1}{2}), \varphi_2 = (-\frac{1}{2}, 0, \frac{1}{2}), \varphi_3 = \varphi_1 + \varphi_2 \tag{3.37}$$

To analyze the singularity structure it is useful to define the space group action over a point $z \in \mathbb{C}^3$ such that $\mathbb{Z}_2 \times \mathbb{Z}_2 : gz := z \mapsto \theta z + l$ with $\theta \equiv$ twist $\in \{1, \theta_1, \theta_2, \theta_3\}$ and $l \equiv$ shift $\in \Gamma_{\text{fac}}$ With singularity structure we refer to the fixed sets $\{z_f\}$ of this orbifold action, i.e. $\{z_f = gz_f\}$, for $\theta \neq 1$. These sets can be viewed quite easily either algebraically or geometrically: each $\theta_i, i = 1, 2, 3$ leaves invariant the corresponding two-tori T_i^2 (lying in the complex plane i), so we can naively think that as the three invariant sets are just only each T_i^2. However we must also think in the $l \in \Gamma_{\text{fac}}$. Taking this into account we see that there will be a copy of these T_i^2 with the same components in the z_i plane than the original but lying in the other $\mathbb{C}^2$ space such that it intersects the z_j and/or z_k complex planes in some point (z_j, z_k) such that it is remains the same when it is translated by the components l_j, l_k of the $l \in \Gamma_{\text{fac}}$, (which correspond for example in the θ_1-sector to each pair (•,•)).

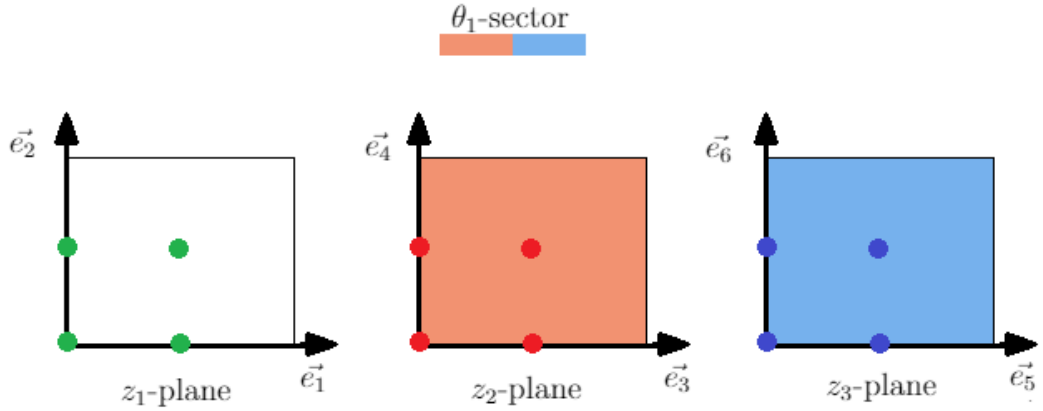

Figure 3.4: Fixed points

These would be also fixed two-tori (the naive case is the one such that $(z_j, z_k) = (0,0)$), so we will have $\underbrace{3}_{\theta_1,\theta_2,\theta_3} \times (\underbrace{4}_{each\ \bullet} \times \underbrace{4}_{each\ \bullet}) = 48$ fixed tori T^2. It is also easy to see that these 48 tori intersect at the points of $\mathbb{C}^3$ whose components are intersection points $\equiv$ ($\bullet$,$\bullet$,$\bullet$) in each combination $\leftrightarrow$ intersection points $=4_{\bullet} \times 4_{\bullet} \times 4_{\bullet} = 64$ intersection points.

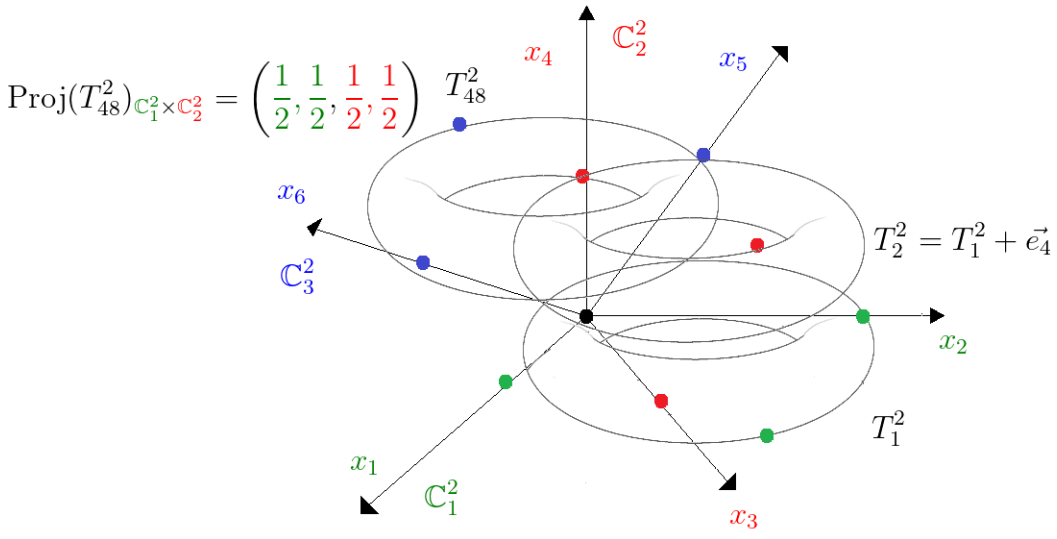

Figure 3.5: Inaccurate representation (just for some intuition) of some of the 48 fixed tori which are the ones sitting in each z_i plane $+l_j + l_k \in \Gamma_{fac}$

3.4.2 Local resolution: how to resolve the $\mathbb{C}^3/(\mathbb{Z}_2 \times \mathbb{Z}_2)$ singularities

The singular points of $T^6/(\mathbb{Z}_2 \times \mathbb{Z}_2)$ are of the form $\mathbb{C}^3/(\mathbb{Z}_2 \times \mathbb{Z}_2)$. We can see how to resolve them following the procedure of the previous subsection.

- A point in $\mathbb{C}^3/(\mathbb{Z}_2 \times \mathbb{Z}_2)$ is defined by $z = (z_1, z_2, z_3) \in \mathbb{C}^3$.
- Define the local coordinates according to (3.33)

$$Z_j = \prod_{i=1}^{3} z_i^{(v_i)_j} \prod_{\theta=1}^{3} x_\theta^{(w_\theta)_j} \tag{3.38}$$

  where v_i and x_θ represent the position of the ordinary divisor $D_i := \{z_i = 0\}$ and the exceptional divisor $E_\theta := \{x_\theta = 0\}$ in the toric diagram.

- Concretely we will have

$$v_1 = \begin{pmatrix} 2 \\ 0 \\ 0 \end{pmatrix}, v_2 = \begin{pmatrix} 0 \\ 2 \\ 0 \end{pmatrix}, v_3 = \begin{pmatrix} 0 \\ 0 \\ 2 \end{pmatrix} \tag{3.39}$$

  and as $w_k = (\tilde{\varphi_k})^j v_j$ where $(\tilde{\varphi_i})^j = (\varphi_i)^j \ mod\ 1$ (the φ's are the ones of the orbifold action) we will get

$$w_1 = \begin{pmatrix} 0 \\ 1 \\ 1 \end{pmatrix}; w_2 = \begin{pmatrix} 1 \\ 0 \\ 1 \end{pmatrix}; w_3 = \begin{pmatrix} 1 \\ 1 \\ 0 \end{pmatrix} \tag{3.40}$$

  – The basis of v_i has been chosen such that all the w_θ and v_i lie in the same plane (see section 4.3 in [62] about (non-compact) toric Calabi Yau varieties).

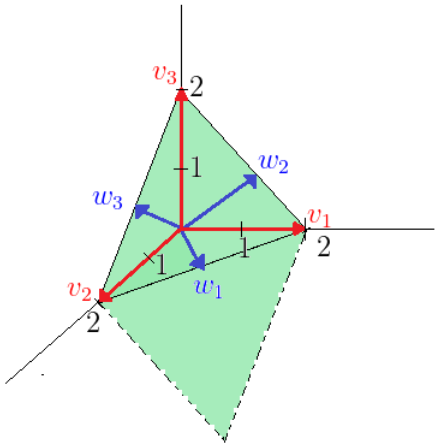

Figure 3.6

The projection of these vectors over the plane are the toric diagrams and each form of the joining the points such that no lines cross each other and no additional lines can be added would be a different triangulation.

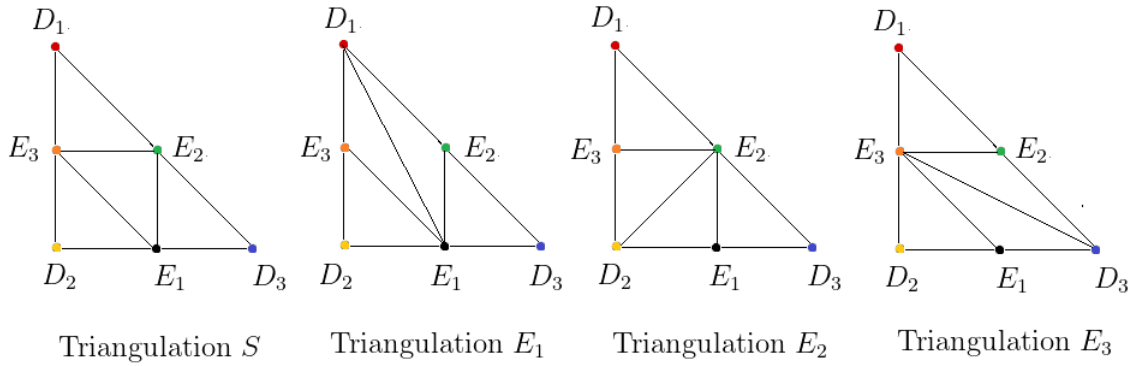

Figure 3.7: The 4 inequivalent triangulations of each $\mathbb{C}^3/(\mathbb{Z}_2 \times \mathbb{Z}_2)$ singularity

- The resolved space will have new homogeneous coordinates, z_1, z_2, z_3 not present in the singular space, associated to the exceptional divisors as seen in this illustration in lower dimension.

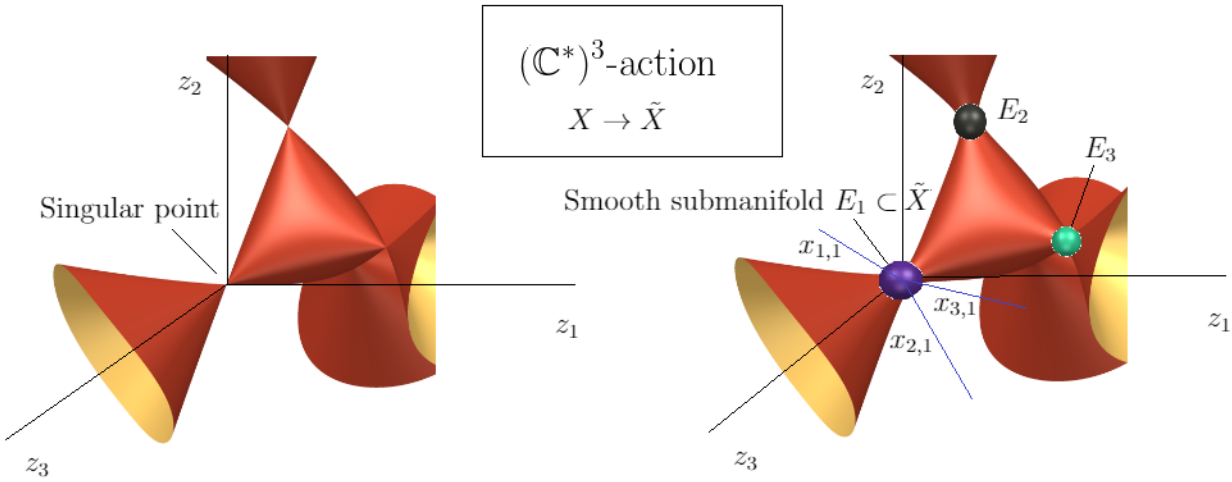

Figure 3.8: Illustration of the blow up in process in three of the singular point (obviously inaccurate because of the dimensionality)

- The concrete form of the local coordinates Z_j is (substituing the values of v_i and w_θ):

$$Z_j = Z_1 = z_1^2 x_2 x_3;\ Z_2 = z_3^2 x_1 x_3;\ Z_3 = z_3^2 x_1 x_2 \tag{3.41}$$

- Starting from the homogeneous coordinates $(z_1, z_2, z_3, x_1, x_2, x_3) \in \mathbb{C}^6$ and imposing three $\mathbb{C}^*$ actions one obtains a complex three-dimensional toric variety - the resolved $\mathbb{C}^3/\mathbb{Z}_2 \times \mathbb{Z}_2$

orbifold. At $x_k \neq 0$, one can use the $\mathbb{C}^*$ actions $\lambda_1 = \pm\sqrt{x_3}, \lambda_2 = \pm\sqrt{x_1}$ and $\lambda_3 = \pm\sqrt{x_2}$ to set the additional coordinates x_k to 1 , i.e. $(z_1, z_2, z_3, 1, 1, 1)$. Due to the possible choice of ± 1 in these $\mathbb{C}^*$ actions, a residual $\mathbb{Z}_2 \times \mathbb{Z}_2$ action remains. Hence, for $x_k \neq 0$ the resolution looks like the original $\mathbb{C}^3/\mathbb{Z}_2 \times \mathbb{Z}_2$ orbifold. We define exceptional divisors $E_k := \{x_k = 0\}$ which are hiding inside the orbifold singularity. As these divisors are smooth spaces, the $\mathbb{C}^3/\mathbb{Z}_2 \times \mathbb{Z}_2$ singularity has been resolved.

- As explained above the idea of toric resolution is to replace the orbifold action by a set of $\mathbb{C}^* = \mathbb{C} - \{0\}$ toric action such that one parameter $\lambda_i \in \mathbb{C}^*$ is needed for each θ_i-sector. The form of the toric action will be (in order to set the local coordinates invariant):

$$\mathbb{C}^* : (z_1, z_2, z_3, x_1, x_2, x_3) \sim (\lambda_1\lambda_3 z_1, \lambda_1\lambda_2 z_2, \lambda_2\lambda_3 z_3, \lambda_2^{-2} x_1, \lambda_3^{-2} x_2, \lambda_1^{-2} x_3) \tag{3.42}$$

- Consequently we can read the following linear equivalences between divisors from the form of the local coordinates

$$0 \sim 2D_1 + E_2 + E_3;\ 0 \sim 2D_2 + E_1 + E_3;\ 0 \sim 2D_3 + E_1 + E_2 \tag{3.43}$$

3.4.3 Global resolution: gluing the resolved singularities and forming a basis of divisors

Up to now we have explained the resolution of non-compact spaces. In the previous part we have described how to resolve each of the $\mathbb{C}^3/(\mathbb{Z}_2 \times \mathbb{Z}_2)$ singularities. However we do not have a compact Calabi-Yau threefold yet. To have it, we have to describe globally the resulting manifold and specify how the different (resolved) parts glue together. For the global description of our geometry we can follow a somewhat straightforward strategy for this concrete case : first, we describe the orbifold $T^6/\mathbb{Z}_2 \times \mathbb{Z}_2$ as a hypersurface in the $\mathcal{O}(2,2,2)$ bundle over $\left(\mathbb{CP}^{\mathbb{1}}\right)^3$, then we expand the equation of this hypersurface in terms of our local coordinates Z_j around each singularity and finally introduce the rescalings.
As each tori can be described as an elliptic curve we can let the hypersurface to take the following form:

$$y^2 = \prod_{i=1}^{3} P_i\left(U_i\right) \tag{3.44}$$

where each $P_i\left(U_i\right)$ is a homogeneous polynomial of degree four in terms of the coordinates $U_i = u_i, v_i$ of each of the three $\mathbb{CP}^1$. A concrete form of that polynomial is (see [32]):

$$P_i\left(U_i\right) = 4\prod_{\alpha=1}^{4} N_\alpha \cdot U_i \tag{3.45}$$

where the N_α are vectors given by $N_1 = (0,1), N_2 = (1, -\varepsilon_2), N_3 = (1, -\varepsilon_1)$ and $N_4 = (1, -\varepsilon_3)$. and correspond to the correspond to the four $\mathbb{Z}_2$-fixed points on the torus T^2 under the action $z_i \to -z_i$ on the torus coordinates.

The $\mathbb{C}^3/\mathbb{Z}_2 \times \mathbb{Z}_2$ singularities are located at the positions where all three polynomials P_i vanish simultaneously. For the $\mathbb{Z}_2 \times \mathbb{Z}_2$ singularity at $(0,0,0)$ we can expand the previous equation as

$$y^2 \simeq Z_1 Z_2 Z_3, \tag{3.46}$$

where $\simeq$ denotes equal up to a complex factor. In terms the homogeneous coordinates we have

$$y \simeq z_1 z_2 z_3 x_1 x_2 x_3 \tag{3.47}$$

by some homogeneous coordinates z_i, x_i for the neighborhood of the resolved singularity. Then we can obtain a similar description for all 64 $\mathbb{Z}_2 \times \mathbb{Z}_2$ fixed points simultaneously we write

$$\begin{aligned} &N_\alpha \cdot U_1 = z_{1,\alpha}^2 \prod_\gamma x_{2,\alpha\gamma} \prod_\beta x_{3,\alpha\beta}, \quad N_\beta \cdot U_2 = z_{2,\beta}^2 \prod_\gamma x_{1,\beta\gamma} \prod_\alpha x_{3,\alpha\beta}, \\ &N_\gamma \cdot U_3 = z_{3,\gamma}^2 \prod_\beta x_{1,\beta\gamma} \prod_\alpha x_{2,\alpha\gamma}, \quad y \simeq \prod_{i,\rho} z_{i,\rho} \prod_{i,\rho\sigma} x_{i,\rho\sigma} \end{aligned} \tag{3.48}$$

Note that we have 67 local coordinates $((3\cdot)u_i + (3\cdot)v_i + (1\cdot)y + (3\cdot 4\cdot)z_{i,\rho} + (3\cdot 4\cdot 4\cdot)x_{i,\rho\sigma})$ and only 13 equations. However our manifold is 3-dimensional so we need only 3 degrees of freedom. The other constraints come from our 51 $\mathbb{C}^*$ rescalings. They can be seen as 3 rescalings coming from the fact that the elliptic torus are defined over three $\mathbb{CP}^1$'s and the other 48 comes from the effect of those rescalings over the right hand side of equations (3.48)

Now we turn our attention to the other key ingredient to describe the properties of our manifold is to define a basis of linear independent divisors to form a homology basis of $(1,1)$-forms. For the coordinates used in the previous section is quite natural to define the following set $\{S_u\}$ of divisors. They are of different kind:

- 12 **ordinary divisors** $D_{1,\alpha} = \{z_{1,\alpha} = 0\}, D_{2,\beta} = \{z_{2,\beta} = 0\}, D_{3,\gamma} = \{z_{3,\gamma} = 0\}; \alpha, \beta, \gamma = 1, ..., 4$.
- 6 **"inherited" divisors** $R_i = \{u_i = 0\}, \tilde{R}_i = \{v_i = 0\}, i = 1, ..., 3$ which coming for setting the projective coordinates defining the tori, $u_i = 0, v_i = 0$ to 0.
- 48 **exceptional divisors** $E_{1,\beta\gamma} = \{x_{1,\beta\gamma} = 0\}, E_{2,\alpha\gamma} = \{x_{2,\alpha\gamma} = 0\}, E_{3,\alpha\beta} = \{x_{3,\alpha\beta} = 0\}; \alpha, \beta, \gamma = 1, ..., 4$ coming from the resolution.

As we said we are interested in forming a basis of linearly independent divisors. Using the equations (3.48) we get the following linear relations:

$$\begin{cases} 2D_{1,\alpha} \sim R_1 + \sum_\gamma E_{2,\alpha\gamma} - \sum_\beta E_{3,\alpha\beta} \\ 2D_{2,\beta} \sim R_2 + \sum_\gamma E_{1,\beta\gamma} - \sum_\alpha E_{3,\alpha\beta} \\ 2D_{1,\gamma} \sim R_3 + \sum_\beta E_{1,\beta\gamma} - \sum_\alpha E_{2,\alpha\gamma} \\ R_i \sim \tilde{R}_i \end{cases} \tag{3.49}$$

From the first three equations we see that the ordinary divisors can be expressed in terms of the exceptional and inherited ones, and that only three of the inherited divisors are independent. So, our basis of 51 divisors are $\{R_i, E_r\}$, $i = 1, ..., 3; , r = 1, ..., 48$. Although our basis comprises 51 divisors (which is going to be $h^{1,1}$ as we will check) in the practice we are going to use only the exceptional 48 to express our bundle as the gauge flux is going to be localized exclusively inside the exceptional divisors (abelian gauge fluxes).

The last key part of the topology is the intersection numbers. In our case we cannot read the intersection numbers directly from the toric diagram as we need to take into account the global structure of the resolution. To do that another tool is used: the auxiliary polyhedra, associated

to each toric diagram. It is build by assigning three s_i vectors (corresponding to the inherited divisors) defined such that they are perpendicular to the charges of the $\mathbb{C}^*$ scalings, namely $s_i + v_i/2 = 0$, so that

$$\mathrm{s}_1 = \begin{pmatrix} -1 \\ 0 \\ 0 \end{pmatrix}, \mathrm{s}_2 = \begin{pmatrix} 0 \\ -1 \\ 0 \end{pmatrix}, \mathrm{s}_3 = \begin{pmatrix} 0 \\ 0 \\ -1 \end{pmatrix} \tag{3.50}$$

By constructing the auxiliary polyedhra and using the linear equivalence relations we can get the set of triple intersection numbers of the resolution (see [32] for details). Note that they are going to be triangulation dependent in general (apart from $R_1R_2R_3, R_1E^2_{1,\beta\gamma}, R_2E^2_{2,\alpha\gamma}, R_3E^2_{3,\alpha\beta}$)

3.4.4 More details about the gauge background and consistency conditions

Recall that the basic idea of the resolution is to expand the gauge flux in terms of $(1,1)$ forms (i.e. divisors (via Poincare duality)):

$$\mathcal{F} \sim \sum_r D_r \sim \sum_r c_1(D_r) \tag{3.51}$$

As explained in previous subsections, our gauge background is going to be encoded in a set of "bundle vectors" which express how the $U(1)$'s coming from the blow-up modes (recall that we are using only are embedded into the $E_8 \times E_8$. abelian gauge fluxes which means that the flux is only inside the exceptional divisors E_r). As the gauge flux should be quantized, we have the following defining equation

$$\frac{1}{2\pi}\int_{C_i} \mathcal{F} = L_I H_I \Leftrightarrow \mathcal{F} = 2\pi c_1(D_r) V_r^I H_I \tag{3.52}$$

where C_i is any linear independent curve inside the manifold, i.e. any curve along each pair of divisor of the basis $\{D_r\}, r = 1, ..., 48$ intersect (e.g. $E_aR_b, E_aE_b...$), $\mathcal{F}$ is the gauge flux, L_I is a vector in the $E_8 \times E_8$ lattice and H_I are the Cartan generators of $E_8 \times E_8$ (and $I = 1, ..., 16$). For practical purposes (i.e. model building) the triangulation dependence is a great obstacle, that is the reason why we pursue the definition of a triangulation-independent one in Chapter 6. The main reason is that our bundlde vectors are subject to a number of physical consistency conditions which are going to be dependent on the intersection numbers and consequently on the triangulation chosen for each singularity. Without the tools of Chapter 6 the procedure to define a model would be:

- Choose a particular triangulation $T = \{S, E_1, E_2, E_3\}$ for each of the 64 singularities.
- The bundle vectors should satisfy:
  - **Flux quantization**: As the integrals of (X) are performed over all the curves of the resolution and some change depending on the triangulation, in principle they will be different. They yield linear relations on V_r's up to translations by $E_8 \times E_8$ roots

– Integrated **Bianchi identities**: The Green-Schwarz anomaly cancellation leads to constraints: The field strength H of the two-form field B is globally defined by

$$H = dB - \frac{\alpha'}{4}\left(\omega_{3,YM} - \omega_{3,L}\right), \tag{3.53}$$

where $\omega_{3,YM}$ and $\omega_{3,L}$ are the Yang-Mills and Lorentz Chern-Simons three-forms, respectively. Hence by acting on it with the exterior derivative one obtains a Bianchi identity. Integrating it over any closed 4-cycle S gives the condition in abscence of NS5 branes:

$$0 = \int_{\mathcal{S}} dH = \frac{\alpha'}{4}\int_{\mathcal{S}} \mathrm{TR}\left(\mathcal{R}^2\right) - \mathrm{TR}\left(\mathcal{F}^2\right) \tag{3.54}$$

This translates to the following the equation:

$$\kappa_{ijk} V_j \cdot V_k = -2c_{2i} \tag{3.55}$$

$$\kappa_{ijk} = \int_X D_i D_j D_k, \quad c_{2i} = \int_{D_i} c_2(X). \tag{3.56}$$

being X the whole resolution. This again yields linear realtions on V_r's up to translations by $E_8 \times E_8$ roots

– Impose the so-called Donaldson Uhlenbeck-Yau (DUY) equations. These equations are obtained by integrating the Hermitian YangMills (HYM) equations over the whole manifold. This results in the condition

$$\frac{1}{2}\int J \wedge J \wedge \frac{\mathcal{F}}{2\pi} = \mathrm{Vol}\left(D_i\right) V_i^I = 0, \tag{3.57}$$

for any divisor D_i which leads to the condition that the zero-vector can be obtained from a linear combination of the V_i^I with positive coefficients only.

- Calculate the 4D gauge group which is given by those roots p of $E_8 \times E_8$ that are uncharged under $\mathcal{F}$, i.e.

$$H_i(p) = V_i \cdot p = 0 \quad \forall i = 1, \ldots, h_{11}. \tag{3.58}$$

and the chiral part of the 4D matter spectrum by using the multiplicity operator,

$$\mathcal{N} = \frac{1}{6}\kappa_{ijk} H_i H_j H_k + \frac{1}{12} c_{2i} H_i, \tag{3.59}$$

evaluated on every root p

From the obtention of the $4D$ gauge group through the embedding $\{V_i\}$ we can get more information about the structure of our bundle. As in general heterotic compactifications the low energy gauge group G in the 4-dimensional theory is given by the commutant of the bundle structure group $H \subset E_8$ the same applies to our bundle background. In fact in previous works it was shown how to translate from our bundle description to other construction like vector bundles as a direct sum of line bundles. For example a typical example of a vector bundle $\mathcal{V}$ with structure group $\mathrm{S}\left(\mathrm{U}(1)^5\right)$ can be constructed on the CY X as a direct sum of line bundles

$$\mathcal{V} = \bigoplus_{a=1}^{5} \mathcal{O}_X\left(k_{(a)}^1, \ldots, k_{(a)}^{h_{11}}\right), \quad \sum_{a=1}^{5} k_{(a)}^i = 0 \tag{3.60}$$

labeled by the vectors $k_{(a)} = \left(k^1_{(a)}, \ldots, k^{h_{11}}_{(a)}\right) \in \mathbb{Z}^{h_{11}}$ with $a = 1, \ldots, 5$ and $i = 1, \ldots, h_{11}$.
In our formalism we can obtain a $SU(5)$ gauge group by choosing the V_i in the form

$$V_i = \left(a^5_i, b_i, c_i, d_i\right), \tag{3.61}$$

assuming that the parameters $a_i \neq 0, b_i, c_i, d_i$ are sufficiently generic as this will break the appropriate roots p. This parameterization can be related to the vectors k_i by comparing the charges of the states that appear in the branching (see [31] for details):

$$248 \to (24,1) + (1,24) + (10,5) + (\overline{10},\overline{5}) + (5,\overline{10}) + (\overline{5},10) \tag{3.62}$$

under $\mathrm{E}_8 \supset \mathrm{SU}(5) \times \mathrm{SU}(5)$. For illustration the translation will take the following form for $i = 1, ..., h^{1,1}$

$$\begin{pmatrix} a_i \\ b_i \\ c_i \\ d_i \end{pmatrix} = -\frac{1}{2} \begin{pmatrix} 1 & 1 & 1 & 1 \\ 1 & -1 & -1 & 1 \\ -1 & 1 & -1 & 1 \\ -1 & -1 & 1 & 1 \end{pmatrix} \begin{pmatrix} k^i_{(1)} \\ k^i_{(2)} \\ k^i_{(3)} \\ k^i_{(4)} \end{pmatrix} \tag{3.63}$$

In our case a $SU(4)$ vector bundle V (interesting for SVD purpose) can be expressed as a sum of line bundles, over the 48 divisors as

$$V = \bigoplus_{a=1}^{4} \mathcal{O}\left(k^a_1, .., k^a_{h_{11}}\right) = \underbrace{\mathcal{O}\left(k^1_1, .., k^1_{h_{48}}\right)}_{f_1} \oplus ... \oplus \underbrace{\mathcal{O}\left(k^4_1, .., k^4_{h_{48}}\right)}_{f_4} \tag{3.64}$$

The variable k_i is related to the divisor D_i in the sense that it is the first integrated Chern class of the bundle $\mathcal{V}$ over the dual curve to the divisor $\hat{D}_i$

$$\int_{\hat{\mathcal{C}}_i} c_1(V) = k_i \to c_1(V) = k_i D_i \to c_1(\mathcal{L}_a) = k^a_i D_i \tag{3.65}$$

when $\mathcal{L}_a$ is each of the line bundles.

3.4.5 Matching orbifold and resolution descriptions

Another important information encoded in our bundle vectors, more useful for our SVD purposes has to do with the *matching of orbifold and resolution descriptions*. This is specially important in order to know how the Wilson line information (needed for the discrete torsion potentially generating SVD) is encoded.
For the bosonic orbifold description of the heterotic string we know that the gauge degrees of freedom are described by real left moving coordinate fields

$$Y_L \in \frac{\mathbb{R}^{16}}{2\pi\Lambda_{E_8 \times E_8}} \tag{3.66}$$

We define the space group S which by its action:

$$\frac{\mathbb{R}^6}{S} = \frac{T^6}{\mathbb{Z}_2 \times \mathbb{Z}_2} \tag{3.67}$$

An element g of the group S acts on these gauge degrees of freedom as

$$Y_L \mapsto gL = Y_L + 2\pi V_g;\ V_g = k_S V_S + n_i W_i \begin{cases} k_S \in \{1, \theta_1, \theta_2, \theta_3\} \\ n_i \in \mathbb{Z}^6 \\ W_i \text{ is a discrete Wilson line} \end{cases} \tag{3.68}$$

V_g induces a gauge symmetry breaking localized at the g-fixed points. In the supergravity approximation this corresponds to the presence of the gauge background flux $\mathcal{F} = \mathcal{F}(V_r)$ and we can set:

$$V_g \cong \left(\int_C \mathcal{F}(V_r) \right) \Big|_{\text{each of the 64 fixed points}} \tag{3.69}$$

Again C is any linear independent curve inside the manifold, and V_r with $r = 1, ..., 48$ is some bundle vector and $\cong$ means up to some root of the $\Lambda_{E_8 \times E_8}$.
Taking all of this into account we can express the possible Wilson lines W_i in terms of our bundle vectors. Namely:

$$\begin{cases} V_{1,\beta\gamma} \cong V_{S1} + \sum_{i \neq 1,2} n^i_{1,\beta\gamma} W_i \\ V_{2,\alpha\gamma} \cong V_{S2} + \sum_{i \neq 3,4} n^i_{2,\alpha\gamma} W_i \\ V_{3,\alpha\beta} \cong V_{S3} + \sum_{i \neq 5,6} n^i_{3,\alpha\beta} W_i \end{cases} \Rightarrow \begin{cases} V_{S1} \cong V_{1,11} \\ V_{S2} \cong V_{2,11} \\ V_{S3} = V_{S1} + V_{S2} \cong V_{3,11} \\ W_1 \cong V_{2,31} - V_{2,11} \\ W_2 \cong V_{2,21} - V_{2,11} \\ W_3 \cong V_{3,13} - V_{3,11} \\ W_4 \cong V_{3,12} - V_{3,11} \\ W_5 \cong V_{1,13} - V_{1,11} \\ W_6 \cong V_{1,12} - V_{1,11} \end{cases} \tag{3.70}$$

The linear dependencies of the 48 V_r imply that:

$$\text{Information} \underbrace{(\text{48 bundle vectors})}_{\text{Resolution data}} \cong \text{Information} \underbrace{(\text{2 shifts and (up to) 6 Wilson lines})}_{\text{Orbifold data}} \tag{3.71}$$

3.5 Beyond line bundle models, GLSM consructions

Up to now all the resolutions of our toric orbifolds use line bundles for encoding the gauge background information. That will be enough to understand the resolved models of Chapters 4-6. In Chapter 7 we will use $(0, 2)$ Gauged Linear Sigma models (we need to go beyond the Standard embedding) for the $\text{Res}(T^6/(\mathbb{Z}_2 \times \mathbb{Z}_2))$. That model is new and as the geometry and field content of GLSMs is so closely related we will explain the basic details, including the geometry, there.
An important remark is that in general we will obtain something more complicated than a (sum

of) line bundles, which only arise when there are no fermionic super gauge transformations and no chiral superfields in the model. In general that is not the case and it is not clear to get a straightforward description of the bundle, which will be constructed from a complex of vector bundles, but that complex will not be a short exact sequence.
As we will see in Chapter 7, most of the key ingredients of the resolution like the set of exceptional divisors, triangulation dependence and so on will also appear in the model, but the continuous variation of some parameters (FI parameters and the complex parameters of the superpotential) will allow us to study both the orbifold and blow-up regimes.

Chapter 4

Constraint on Spinor–Vector Dualities in Six Dimensions

4.1 Introduction

We start the proper study of SVD by restricting ourselves to the six dimensional case. In this chapter we will show that spinor–vector dualities in six dimensions are constrained by a fundamental effective field theory consistency condition, namely that any six dimensional low energy theory must be free of irreducible $SO(2N)$ anomalies. Aspects of spinor–vector dualities are analysed in four six–dimensional free fermionic models which are distinguished by two generalised GSO phases. In addition, the constraint on the number of spinors and vectors is confirmed on generic spectra which may occur in K3 line bundle compactifications of the heterotic $E_8 \times E_8$ string.

Summary of the main finding

This chapter is a first step in the realisation of the spinor–vector duality in compactifications of the heterotic–string to six dimensions. Even though this case provides a particularly controlled setting, because supersymmetry requires the two dimensional complex manifold to be essentially unique, albeit, realised in various ways both as $T^4/\mathbb{Z}_K$ orbifolds or generic K3 geometries, it seems to have been omitted in the literature on the spinor–vector duality as far as we are aware. Our investigation of the spinor–vector duality makes use of both the string theory worldsheet tools as well as the effective field theory techniques. One central requirement on any effective field theory is that it is free of anomalies. Irreducible anomalies need to be absent entirely, while reducible anomalies may be compensated by some variant of the Green–Schwarz mechanism. If the effective field theory contains an $SO(2N)$ gauge group factor (immaterial of whether in the hidden or the observable sector), cancellation of its irreducible anomalies leads to a linear relation between the number of vectorial states and the sum of spinorial and conjugate spinorial representations constraining the possible realisations of any spinor–vector duality in six dimensions. Besides confirming this relation with many results in the literature, this relation is shown to be fulfilled in six dimensional models obtained from the free fermionic formulation with various choices of discrete generalised GSO phases. In addition, we confirm this result for any smooth K3 compactification with arbitrary line bundle gauge backgrounds.

Outline

The structure of the chapter is as follows: Section 4.2 study six dimensional effective theories and establishes a linear relation between the number of vectorial and the sum of spinorial and anti–spinorial representations. Section 4.3 considers a particular free fermionic construction of models in six dimensional target space. Even though, both gauge groups and spectra strongly depend on the choices of two generalised GSO phases, the constraint on the number of $SO(2N)$ vectors and spinors is always respected. Finally, Section 4.4 considers generic smooth K3 realisations with line bundle gauge backgrounds. Using the six dimensional multiplicity operator, generic formulae to count the total number of vectorial and the number of (conjugate) spinor representations are both expressed in terms of the instanton number in the observable E_8. As expected, also in all these cases the linear relation on the number of vectorial and spinorial states is respected.

4.2 Constraint on the number of spinorial and vectorial states

This section shows that in any six dimensional $\mathcal{N} = 1$ supersymmetric effective field theory with the numbers of vectors N_V and of spinors N_S (of either chirality) of some $SO(2N)$ gauge group are constrained by an anomaly condition to

$$N_V = 2^{N-5}\, N_S + 2N - 8 \ , \tag{4.1}$$

for $N \geq 3$. This result is derived under the assumption that the effective field theory in six dimensions possesses at least $\mathcal{N} = 1$ supersymmetry (i.e. $\mathcal{N} = 2$ supersymmetry in four dimensions) and the only $SO(2N)$ charged states in the spectrum are hyper multiplets in the vector and spinor representations and a gauge multiplet in the adjoint. In particular, the effective theory may contain other gauge interactions with matter in arbitrary representations. If a hyper multiplet in the vector or spinor representations is also charged under other gauge groups, then the dimension of these representations are contained in the numbers N_V and N_S. The validity of (4.1) can be checked for many six dimensional models in the literature. For example, all the perturbative and non–perturbative six dimensional orbifold and line bundle resolution models mentioned in [52] and [53] all fulfil this equation.

4.2.1 Irreducible $SO(2N)$ anomaly in six dimensions

To derive the equation (4.1), recall that gauge and gravitational anomalies in 6D are dictated by anomaly polynomials I_8 eight-forms [54, 55]. For charged fermions the anomaly polynomial takes the form:

$$I_{8|R} = \widehat{A}(R_2)\, \mathrm{ch}_R(F_2)\Big|_8 \ , \tag{4.2}$$

where the rooth–genus $\widehat{A}(R_2)$ as a function of the curvature two–form R_2 encodes gravitational anomalies and the Chern character

$$\mathrm{ch}_R(F_2) = \mathrm{tr}_R\Big[e^{i\frac{F_2}{2\pi}}\Big] \ , \tag{4.3}$$

depends on the field strength two–form F_2 of the gauge theory and on the representation R the fermions are in. Recall that anomalies can be divided into reducible and irreducible ones. The

former can be canceled by the Green-Schwarz mechanism([54,56]). The underlying idea is that, under certain conditions, the anomalies of a theory (a one-loop effect) may be cancelled by the anomalous variation of certain classical terms in the effective action (a tree-level effect) [49]. To explain this rather counterintuitive idea, it is useful to recall that in the context of effective theories (e.g. the low-energy supergravities of string theory), the low-energy effective action is usually said to be the action obtained by truncating the massive modes. However, according to its proper definition, the effective action is the action obtained by integrating out the massive modes. This would result in additional terms involving irrelevant higher-derivative operators. Since these terms have no a priori reason to respect the gauge symmetries of the theory, they can generally have anomalous variations. It may be then the case that these variations cancel the anomalies of the "naive" low-energy theory.
Concretely, this cancellation is possible if the anomaly polynomials I_{d+2} factorize as

$$I_{d+2} = \sum_{a=1}^{m} X_{k_a} X_{d+2-k_a}, \tag{4.4}$$

For example in $6D$ we have $I_8 \sim X_4 X_4$ where each of the factors, X_i are two polynomials constructed out of the same curvature invariants as I_{d+2}. The idea is to compensate the variation of the effective action by a counterterm having the form $S_{GS} = \int B_2 \wedge X_n$, where the integral is over the $n+2$ dimensions, B_2 is the rank-two Kalb-Ramond field, and X_n is an appropriate gauge invariant combination of the curvature forms. To see why this counterterm cancels the anomaly one can use Feyman diagrams: the relevant terms arise from chiral massless Weyl fermions at one loop order from $(d/2+1)$-sided polygon graphs where the external fields are gauge bosons or gravitons and fermions are running in the loop, and are one-loop exact. The anomaly graphs which are relevant here ($6D$) are thus given in terms of rectangle diagram (see figure) .

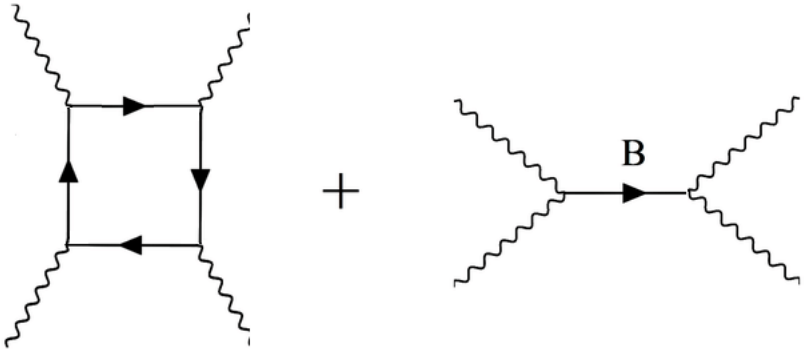

Figure 4.1: Anomalous diagram and the corresponding Green-Schwarz counterterm for anomalies in 6 dimensions.

However the irreducible anomalies cannot be canceled with these counterterms, hence for an effective theory to be consistent, all irreducible gauge and gravitational anomalies have to cancel among themselves. This goes in particular for irreducible $SO(2N)$ anomalies which is the sole focus of this section.

In six dimensions irreducible $SO(2N)$ anomalies, proportional to $\mathrm{tr}_V(iF_2)^4$ (where the trace is over the vector representation of $SO(2N)$), are possible and therefore their sum need to vanish. Derivations of relevant trace identities are recalled in Appendix 4.5. In light of the assumptions on the effective six dimensional supersymmetric theories under investigation, there are only three contributions to the irreducible $SO(2N)$ anomalies to be considered:

1. N_V Hyper multiplets in the vector representation:

$$I_{8|V} \supset N_V \, \frac{1}{4!} \mathrm{tr}_V \Big(i \frac{F_2}{2\pi} \Big)^4 \tag{4.5}$$

   This is obtained directly by expanding the Chern character to fourth order. Here, $\supset$ indicates that only irreducible $SO(2N)$ anomalies are considered, ignoring gravitational, other gauge and (mixed) reducible anomalies.

2. Gauge multiplet in the adjoint representation:

$$I_{8|Ad} \supset -\frac{1}{4!} \Big[(2N-8) \, \mathrm{tr}_V \Big(i \frac{F_2}{2\pi} \Big)^4 + 3 \, \Big(\mathrm{tr}_V \Big(i \frac{F_2}{2\pi} \Big)^2 \Big)^2 \Big] \supset -(2N-8) \, \frac{1}{4!} \mathrm{tr}_V \Big(i \frac{F_2}{2\pi} \Big)^4 \, . \tag{4.6}$$

   This result is derived in (4.35). The minus sign out front is due to the fact that the gauginos in six dimensions have the opposite chirality as the hyperinos.

3. N_S Hyper multiplets in the (conjugage) spinor representation:

$$I_{8|S} \supset N_S \, \frac{1}{4!} \, 2^{N-5} \Big[- \mathrm{tr}_V \Big(i \frac{F_2}{2\pi} \Big)^4 + \frac{3}{4} \, \Big(\mathrm{tr}_V \Big(i \frac{F_2}{2\pi} \Big)^2 \Big)^2 \Big] \supset -2^{N-5} \, N_S \, \frac{1}{4!} \mathrm{tr}_V \Big(i \frac{F_2}{2\pi} \Big)^4 \, . \tag{4.7}$$

   A derivation of this result can be found in (4.44).

The total irreducible $SO(2N)$ anomaly is the sum of these three contributions. It only vanishes if the sum of their pre–factors do, which is precisely condition (4.1).

4.3 Six Dimensional Free Fermionic Models

4.3.1 Generalities of free fermionic description

The six dimensional heterotic string is described in terms of 16 left–moving and 40 right–moving two dimensional real fermions in the free fermionic formulation in the light–cone gauge [6,7,57]. The string models are defined by specifying different phases picked up by fermions ($f_A, A = 1, \ldots, 56$) when transported along the non–trivial cycles of the vacuum–to–vacuum amplitude. Each model corresponds to a particular choice of fermion phases consistent with modular invariance that can be generated by a set of N_B basis vectors $B = \{v_a, a = 1, \ldots, N_B\}$, where each

$$v_a = \{\alpha_a(f_1), \ldots, \alpha_a(f_{56}))\} \ ,$$

dictates the transformation properties of each fermion

$$f_A \to -e^{i\pi\alpha_a(f_A)} \, f_A \ , \tag{4.8}$$

$A = 1, \ldots, 56$. It is important to emphasise that the free fermionic formalism is identical to the free bosonic formalism, *i.e.* to toroidal orbifold compactifications, which follows from the

equivalence of bosons and fermions in two dimensions. The two formulations are therefore describing the same physical object, albeit using different language and tools. While detailed dictionaries exist [50], translating a model from one representation to another can often be non–trivial. Each formalism carries its advantages and are in that respect complementary. In the free fermionic formalism all the moduli are taken a priori on equal footing and there is minimal structure, or not at all, to begin with. This has the advantage that some discrete torsions, for which some implicit choice has been made in orbifold constructions, are revealed at a very basic level in fermionic models. On the other hand, in the toroidal orbifold models there is a clearer distinction between the internal and the Wilson line moduli facilitating making contact with the smooth effective field theory limits in this approach.

The basis vectors generate a space Ξ which contains 2^{N_B} sectors that produce the string spectrum. Each sector arises as a combination of the basis vectors

$$\beta = \sum n_a v_a, \quad n_a = 0, 1 \ . \tag{4.9}$$

The spectrum is truncated by generalised GSO projections whose actions on a string state $|\text{state}\rangle_\beta$ are given by

$$e^{i\pi v_a \cdot F}|\text{state}\rangle_\beta = \delta_\beta \ c\begin{bmatrix}\beta\\ v_a\end{bmatrix}^* |\text{state}\rangle_\beta \ , \tag{4.10}$$

where $|\text{state}\rangle_\beta$ is a state with the vacuum defined by the worldsheet fermions that are periodic in the sector β with possibly fermionic oscillators acting on it, which are counted by F, the fermion number operator, and $\delta_\beta = \pm 1$ is the spacetime spin statistics index. Different choices for unfixed generalised GSO phases affect the states that remain massless in each of the sectors containing these basis vectors. In particular, some vectors act as projectors on some states, and do not merely fix some $U(1)$ charges of periodic fermions, when there is no overlap of periodic fermions between the basis vectors. Hence, different sets of projection coefficients $c\binom{\beta}{v_a} = \pm 1$ consistent with modular invariance give rise to different models. In summary: a model is defined uniquely by a set of basis vectors $v_a, a = 1, \ldots, N_B$ and a set of $2^{N_B(N_B-1)/2}$ independent projections coefficients $c\binom{v_a}{v_b}, a > b$.

4.3.2 Four free fermionic $T^4/\mathbb{Z}_2$ orbifold models

After this general outline of constructions of six dimensional target space model, the focus is now on a collection of basis vectors B which may be interpreted as $T^4/\mathbb{Z}_2$ orbifolds. To facilitate we divide the two dimensional free fermions in the light–cone gauge as follows: $\psi^{1,\ldots,4}, \chi^i, y^i, \omega^i$ (real left–moving fermions) and $\bar{y}^i, \bar{\omega}^i$ (real right–moving fermions) with $i = 3, \ldots, 6$ labeling the real torus directions and $\bar{\psi}^{1,\ldots,6}$, $\bar{\eta}^{2,3}$, $\bar{\phi}^{1,\ldots,8}$ (complex right–moving fermions). The models under investigation are generated by a basis B

$$B = \{v_1, v_2, \ldots, v_5\} \ ,$$

of $N_B = 5$ basis vectors defined as:

$$\begin{aligned}
v_1 = 1 &= \{\psi^{1,\ldots,4}, \chi^{3,\ldots,6}, y^{3,\ldots,6}, \omega^{3,\ldots,6} \,|\, \bar{y}^{3,\ldots,6}, \bar{\omega}^{3,\ldots,6}; \bar{\psi}^{1,\ldots,6}, \bar{\eta}^{2,3}, \bar{\phi}^{1,\ldots,8}\} \ , \\
v_2 = S &= \{\psi^{1,\ldots,4}, \chi^{3,\ldots,6}\} \ , \\
v_3 = z_1 &= \{\bar{\psi}^{1,\ldots,6}, \bar{\eta}^{2,3}\} \ , \\
v_4 = z_2 &= \{\bar{\phi}^{1,\ldots,8}\} \ , \\
v_5 = b_1 &= \{\psi^{1,\ldots,4}, y^{3,\ldots,6} \,|\, \bar{y}^{3,\ldots,6}; \bar{\psi}^{1,\ldots,6}\} \ .
\end{aligned} \tag{4.11}$$

The inclusion of the vector 1 in the additive group is mandated by the modular invariance constraints. The vector S is the spacetime supersymmetry generator. The basis vectors z_1 and z_2 identify the observable and hidden sectors, respectively. The vector b_1 corresponds to the $\mathbb{Z}_2$ twist in the corresponding $T^4/\mathbb{Z}_2$ toroidal orbifold model on the $SO(8)$ lattice. In addition, for later use we define the linear combination

$$e = 1 + S + z_1 + z_2 = \{y^{3,\ldots,6}, \omega^{3,\ldots,6} \,|\, \bar{y}^{3,\ldots,6}, \bar{\omega}^{3,\ldots,6}\} \,, \tag{4.12}$$

which e.g. induces a map between the periodic worldsheet fermions $\{y^{3,4,5,6}|\bar{y}^{3,4,5,6}\} \to \{\omega^{3,4,5,6}|\bar{\omega}^{3,4,5,6}\}$ when mapping b_1 to $b_1 + e$.

The matrix of one–loop generalised GSO phases is given by

$$c\begin{bmatrix}\alpha\\ \beta\end{bmatrix} = \begin{array}{c|ccccc} \beta|\alpha & 1 & S & z_1 & z_2 & b_1 \\ 1 & -1 & 1 & -1 & -1 & -1 \\ S & 1 & 1 & -1 & -1 & 1 \\ z_1 & -1 & -1 & 1 & \pm 1 & -1 \\ z_2 & -1 & -1 & \pm 1 & 1 & \pm 1 \\ b_1 & -1 & -1 & 1 & \pm 1 & -1 \end{array} \,. \tag{4.13}$$

Up to changes of internal chiralities, there is a twofold freedom in the choice of the generalised GSO phases: $c\left[\begin{smallmatrix}z_1\\ z_2\end{smallmatrix}\right] = c\left[\begin{smallmatrix}z_2\\ z_1\end{smallmatrix}\right] = \pm 1$ and $c\left[\begin{smallmatrix}b_1\\ z_2\end{smallmatrix}\right] = c\left[\begin{smallmatrix}z_2\\ b_1\end{smallmatrix}\right] = \pm 1$. These free generalised GSO phases can be translated to discrete torsion phases in the bosonic formalism.

4.3.3 Gauge groups

The gauge symmetry generated in the vacuum that contains the $\{1, S\}$ basis vectors is $SO(40)$. This gauge symmetry is broken by the basis vectors z_1 and z_2 to $SO(8) \times SO(16) \times SO(16)$. The generalised GSO phase $c\left[\begin{smallmatrix}z_1\\ z_2\end{smallmatrix}\right] = \pm 1$ enhances the gauge symmetry to $SO(8) \times E_8 \times E_8$ for $c\left[\begin{smallmatrix}z_1\\ z_2\end{smallmatrix}\right] = +1$, whereas with $c\left[\begin{smallmatrix}z_1\\ z_2\end{smallmatrix}\right] = -1$ the vector bosons arising from the sectors z_1 and z_2 are projected out and the gauge symmetry remains $SO(8) \times SO(16) \times SO(16)$. The inclusion of the final basis vector b_1 breaks $\mathcal{N} = 2$ six dimensional supersymmetry to $\mathcal{N} = 1$: The chirality of the gauginos and hyperinos are left– and right–handed corresponding to an even/odd number zero modes ψ_0^μ on their string vacuum states, respectively. Furthermore the basis vector b_1 reduces the gauge symmetry generated by the NS–sector alone to

$$SO(4)_{\bar{y}^{3,\ldots,6}} \times SO(4)_{\bar{\omega}^{3,\ldots,6}} \times SO(12)_{\bar{\psi}^{1,\ldots,6}} \times SO(4)_{\bar{\eta}^{2,3}} \times SO(16)_{\bar{\phi}^{1,\ldots,8}} \,, \tag{4.14}$$

where the subscripts indicate which worldsheet fermions generate the specified subgroup. As above if $c\left[\begin{smallmatrix}z_1\\ z_2\end{smallmatrix}\right] = -1$ no gauge enhancement occurs, while for $c\left[\begin{smallmatrix}z_1\\ z_2\end{smallmatrix}\right] = 1$ the gauge group enhancement depends on the other generalised GSO phase $c\left[\begin{smallmatrix}b_1\\ z_2\end{smallmatrix}\right]$. The resulting gauge groups for the choices of the two free generalised GSO phases are summarised in the top two rows of Table 4.2.

4.3.4 Hyper multiplet representations

The choices of the free GGSO phases $c\left[\begin{smallmatrix}z_1\\ z_2\end{smallmatrix}\right] = \pm 1$ and $c\left[\begin{smallmatrix}b_1\\ z_2\end{smallmatrix}\right] = \pm 1$ affect, in particular, the states that remain in the spectrum as massless hyper multiplets. To illustrate this focus for example on spinorial and vectorial representations under the $SO(12)$ GUT group. The spinorial

Gen. GSO		Sectors $b_1 \oplus (b_1+z_1)$			$(b_1+e)\oplus(b_1+e+z_1)$			$S+z_2$
$c\binom{z_1}{z_2}$	$c\binom{b_1}{z_2}$	$32_{\rm S}$	$12_{\rm V}$	$16_{\rm V}$	$32_{\rm S}$	$12_{\rm V}$	$16_{\rm V}$	$128_{\rm S}$
+	+	out	out	in	out	out	in	in
+	-	in	in	out	in	in	out	out
-	+	out	in	out	in	out	in	out
-	-	in	out	in	out	in	out	out

Table 4.1: The effect of the different choices of the generalised GSO phases $c\binom{z_1}{z_2}$ and $c\binom{b_1}{z_2}$ on the hyper spectrum of $SO(12)$ and $SO(16)$ spinors and vectors is displayed.

representations arise from the sectors b_1 and b_1+e, whereas the vectorial representations arise from the sectors b_1+z_1 and b_1+e+z_1. For example, the explicit generalised GSO projections in the b_1 and b_1+z_1 sectors are given by:

$$e^{i\pi z_2\cdot F_{b_1}}|b_1\rangle = \delta_{b_1}\; c\begin{bmatrix}b_1\\ z_2\end{bmatrix}|b_1\rangle \tag{4.15}$$

and $\mathrm{e}^{i\pi z_2\cdot F_{b_1+z_1}}\left(\{\bar\psi^{1,\ldots,6},\bar\phi^{1,\ldots,8}\}|b_1+z_1\rangle\right) = \delta_{b_1+z_1}c\binom{b_1+z_1}{z_2}\left(\{\bar\psi^{1,\ldots,6},\bar\phi^{1,\ldots,8}\}|b_1+z_1\rangle\right)$
$= \;-\; c\binom{b_1}{z_2}c\binom{z_2}{z_1}\left(\{\bar\psi^{1,\ldots,6},\bar\phi^{1,\ldots,8}\}|b_1+z_1\rangle\right)\;,$

respectively, where the { } brackets refer to the fermionic oscillators that act on the vacuum in the b_1+z_1 sector. As there is no overlap of periodic fermions between b_1 and z_2, it can be inferred from (4.10), that the z_2 basis vector either projects out the spinorial states from the sector b_1 altogether or keeps them all in. Given that $\bar\phi^{1,\ldots,8}$ are periodic in z_2, whereas $\bar\psi^{1,\ldots,6}$ are anti–periodic, the z_2 basis vector selects the vectorial states from the sector b_1+z_1. Similar projections operate in the sectors b_1+e and b_1+e+z_1 using the e–vector (4.12).

The spinorial and vectorial states for the different choices of $c\binom{b_1}{z_2}$ and $c\binom{z_1}{z_2}$ are displayed in Table 4.1. We omitted there the multiplicities that arise from oscillators of the internal fermions $\{\bar y,\bar\omega\}^{3,\ldots,6}$. Thus, we only list states that transform under the observable $SO(12)$ and hidden $SO(16)$ group factors. It is noted from this table that the spinor–vector duality is induced by the map

$$c\begin{bmatrix}b_1\\ z_2\end{bmatrix}\to -c\begin{bmatrix}b_1\\ z_2\end{bmatrix}\;. \tag{4.16}$$

The degeneracy with respect to the internal worldsheet fermions $\{y,\omega\,|\,\bar y,\bar\omega\}$ is identical in the spinorial sectors $b_1,\ b_1+e$ and the vectorial sectors $b_1+z_1,\ b_1+e+z_1$. Hence, the counting with respect to the internal fermions is identical for the spinorial and vectorial representations. The sector z_1 induces the so–called x–map of refs. [45, 58].

Table 4.2 summarises the complete massless spectrum in the four models that arise due to the four choices of the phases $c\binom{z_1}{z_2}$ and $c\binom{b_1}{z_2}$. The sector S gives rise to hyperinos in the $(1,1,12,4,1)$ representation of the gauge symmetry in (4.14) generated by the NS–sector alone. Since, when $c\binom{z_1}{z_2}=+1$ the z_1 sectors enhance the observable gauge symmetry to E_7, states

$\left(c\binom{z_1}{z_2},\ c\binom{b_1}{z_2}\right)$	$(+1,+1)$	$(+1,-1)$	$(-1,+1)$	$(-1,-1)$
Gauge Symmetry	$SO(4)\times SO(4)\times E_7\times SU(2)\times SO(16)$	$SO(4)\times SO(4)\times E_7\times SU(2)\times E_8$	$SO(4)\times SO(4)\times SO(12)\times SO(4)\times SO(16)$	$SO(4)\times SO(4)\times SO(12)\times SO(4)\times SO(16)$
Sector	Hyper Multiplet Representations			
S	$(4,4,1,1,1)$	$(4,4,1,1,1)$	$(4,4,1,1,1)$ $(1,1,12,4,1)$	$(4,4,1,1,1)$ $(1,1,12,4,1)$
$S\oplus(S+z_1)$	$(1,1,56,2,1)$	$(1,1,56,2,1)$		
$S+z_2$	$(1,1,1,1,128)$			
b_1				$(2_L,1,32,1,1)$ $(2_R,1,32,1,1)$
$b_1\oplus(b_1+z_1)$		$(2_L,1,56,1,1)$ $(2_R,1,56,1,1)$		
b_1+z_1	$(2_L,1,1,2_L,16)$ $(2_R,1,1,2_L,16)$	 $(2_L,4,1,2,1)$ $(2_R,4,1,2,1)$	$(2_L,1,12,2,1)$ $(2_R,1,12,2,1)$ $(2_L,4,1,2,1)$ $(2_R,4,1,2,1)$	$(2_L,1,1,2_L,16)$ $(2_R,1,1,2_L,16)$
b_1+e			$(1,2_L,\overline{32},1,1)$ $(1,2_R,\overline{32},1,1)$	
$(b_1+e)\oplus(b_1+e+z_1)$		$(1,2_L,56,1,1)$ $(1,2_R,56,1,1)$		
b_1+e+z_1	$(1,2_L,1,2_L,16)$ $(1,2_R,1,2_L,16)$	 $(4,2_L,1,2,1)$ $(4,2_R,1,2,1)$	$(1,2_L,1,2_R,16)$ $(1,2_R,1,2_R,16)$	$(1,2_L,12,2_L,1)$ $(1,2_R,12,2_L,1)$ $(4,2_L,1,2_R,1)$ $(4,2_R,1,2_R,1)$
$SO(12)$ $N_V=2N_S+4$	Self–dual by E_7 enhancement	Self–dual by E_7 enhancement	$N_V=12$ $N_S=4$	$N_V=12$ $N_S=4$
$SO(16)$ $N_V=8N_S+8$	$N_V=16$ $N_S=1$		$N_V=8$ $N_S=0$	$N_V=8$ $N_S=0$

Table 4.2: The six dimensional gauge group and massless matter depend the choices of the free generalised GSO phases: $c\binom{z_1}{z_2}$ and $c\binom{b_1}{z_2}$. Only the sectors are indicated that lead to non–vanishing hyperino states to form hyper multiplets in target space.

in $S + z_1$ expand this representation to $(1, 1, 56, 2, 1)$ as can be seen in the second and third column of Table 4.2.

4.3.5 Spinor–vector duality aspects

A curious map between the two models occurs in the sector z_2. Indeed, when in addition $c\binom{b_1}{z_2} = -1$, the left–moving oscillator acting on the vacuum in the physical states are $\psi^{1,\ldots,4}$, whereas when $c\binom{b_1}{z_2} = +1$ they are $\chi^{3,\ldots,6}$. Therefore, only in the case $c\binom{z_1}{z_2} = +1$, $c\binom{b_1}{z_2} = -1$ the symmetry is enhanced from $SO(16)$ to E_8. Nevertheless, the total number of massless degrees of freedom is maintained. This is a manifestation of the phenomenon discussed in [47, 48] that under such maps, induced by the changes of discrete torsions in the partition function, the organisation of the number of degrees of freedom under the spacetime group factors may change, but the total number of massless degrees of freedom is preserved.

In the case $c\binom{z_1}{z_2} = -1$ the gauge symmetry is not enhanced. The corresponding models in the final two columns exhibit the spinor–vector duality map, induced by the discrete change in (4.16). Albeit these two cases are, in fact, self–dual under spinor–vector duality, *i.e.* they contain an equal number of twisted spinorial and twisted vectorial representations of the $SO(12)$ GUT group, merely the $SO(12)$ chiralities of the spinorial states of these two models are opposite.

The final rows of Table 4.2 confirm condition (4.1) for these four six–dimensional free fermionic models. As can be inferred from this table, in all cases this condition is satisfied for both $SO(12)$ and $SO(16)$. The condition is automatically satisfied for E_7, as the $56 \to (32, 1) + (2, 12)$ is self–dual when branched to $SO(12)$ representations.

4.4 Smooth K3 Line Bundle Models

4.4.1 K3 Geometries

In four dimensions there is topologically just a single geometry that preserves supersymmetry, the so–called K3 surface. Particular geometrical descriptions of K3 can be obtained as orbifold resolutions [59]. In the discussion below such an interpretation is neither necessary nor implied. Depending on the set of independent divisors $\{D_\alpha\}$ labelled by α chosen the geometry may appear different. This work refers to divisors as two dimensional hyper surfaces as well as the associated two–forms interchangeably so that the context dictates how they should be interpreted. The intersection numbers

$$-\kappa_{\alpha\beta} = D_\alpha D_\beta = \int_{K3} D_\alpha D_\beta \ , \tag{4.17}$$

may be determined by integrating over the K3 as a whole. The Euler number of K3

$$\int_{K3} c_2 = -\frac{1}{2}\int_{K3} \mathrm{tr}\Big(\frac{\mathcal{R}_2}{2\pi}\Big)^2 = 24 \tag{4.18}$$

is given by the integral over its second Chern class c_2. Here $\mathcal{R}_2$ is the anti–Hermitian holomorphic curvature two–form.

4.4.2 K3 Line Bundles

The $U(1)$ gauge background encoded as an anti–Hermitian Abelian gauge field strength two–form can be expanded in terms of the divisors as: [60, 61]

$$\frac{\mathcal{F}_2}{2\pi} = D_\alpha \, \mathsf{H}_\alpha \ , \quad \mathsf{H}_\alpha = V_\alpha^I \, \mathsf{H}_I \ , \tag{4.19}$$

where the sums over the basis divisors labelled by α and over the Cartan generators labelled by I are implied. The Cartan generators H_I of $E_8 \times E_8$ are normalized such that $\mathrm{tr}\, \mathsf{H}_I \mathsf{H}_J = \delta_{IJ}$. The embedding of the line bundle background is therefore characterized by sixteen component line bundle (embedding) vectors $V_\alpha = (V_\alpha^I)$. (For translations to other characterizations see e.g. [36, 53].) Often it is convenient to split the line bundle vectors in contributions in the first and second E_8 as: $V_\alpha = (\vec{V}_\alpha)(\vec{V}'_\alpha)$ where $\vec{V}_\alpha$ and $\vec{V}'_\alpha$ both have 8 entries.

The fundamental consistency requirement of such backgrounds is determined from the integrated Bianchi identity $\mathrm{tr}(\mathcal{F}_2^2) - \mathrm{tr}(\mathcal{R}_2^2) = 0$. On K3 it can be cast in the form:

$$\tfrac{1}{2} \, \kappa_{\alpha\beta} \, V_\alpha^I V_\beta^I = 24 \ . \tag{4.20}$$

Using the splitting of the line bundle vectors in contributions in both E_8's this condition may be written as

$$c + c' = 24 \ , \qquad c = \tfrac{1}{2} \, \kappa_{\alpha\beta} \, \vec{V}'_\alpha \cdot \vec{V}'_\beta \ , \quad c' = \tfrac{1}{2} \, \kappa_{\alpha\beta} \, \vec{V}'_\alpha \cdot \vec{V}'_\beta \ , \tag{4.21}$$

introducing the instanton numbers c and c' in the first and second E_8. (If non–perturbative compactifications involving five–branes are considered the sum of the instanton numbers no longer need to add up to 24.)

In six dimensions the full charged spectrum can be determined using the multiplicity operator N given by [61]:

$$\mathsf{N} = -\int_{K3} \Big\{ \frac{1}{2} \Big(\frac{\mathcal{F}}{2\pi} \Big)^2 - \frac{1}{24} \, \mathrm{tr} \Big(\frac{\mathcal{R}}{2\pi} \Big)^2 \Big\} = \tfrac{1}{2} \, \kappa_{\alpha\beta} \, \mathsf{H}_\alpha \mathsf{H}_\beta - 2 \ . \tag{4.22}$$

This operator counts the number of fermions in a given representation and its sign determines the six dimensional chirality of the underlying fermionic states: It equals -2 on gaugino states, hence the multiplicity operator in six dimensions can be used to determine the gauge group unbroken by the line bundle background directly. The multiplicity operator N is positive on hyperinos as they have the opposite chirality in six dimensions as gauginos. Hence, if positive, it counts the number of hyper multiplets in a given representation of the gauge group.

4.4.3 Counting the Number of SO(10) Vector, Spinor and Singlet States

Consider line bundle vectors such that the first E_8 in the ten dimensional gauge group is generically broken to $SO(10)$:

$$V_\alpha = (\vec{V}_\alpha)(\vec{V}'_\alpha) \ , \qquad \vec{V}_\alpha = (V_\alpha^1, V_\alpha^2, V_\alpha^3, 0^5) \ . \tag{4.23}$$

Here it is assumed that the three entries, V_α^1, V_α^2 and V_α^3, of these bundle vectors are sufficiently general that the unbroken gauge group indeed contains an $SO(10)$ factor which is not enhanced to a larger (exceptional) gauge group. By evaluating the multiplicity operator on all of the weights of the first E_8 leads to Table 4.3.

E_8 Weight	SO(10) Repr.	Multiplicity
$\pm(0,0,0,\underline{\pm 1^2,0^3})(0^8)$	(45)	-2
$\pm(1,0,0,\underline{\pm 1,0^4})(0^8)$	(10)	$N_{(10)}^{\ 1} = \frac{1}{2}\,\kappa_{\alpha\beta}\,V_\alpha^1 V_\beta^1 - 2$
$\pm(0,1,0,\underline{\pm 1,0^4})(0^8)$		$N_{(10)}^{\ 2} = \frac{1}{2}\,\kappa_{\alpha\beta}\,V_\alpha^2 V_\beta^2 - 2$
$\pm(0,0,1,\underline{\pm 1,0^4})(0^8)$		$N_{(10)}^{\ 3} = \frac{1}{2}\,\kappa_{\alpha\beta}\,V_\alpha^3 V_\beta^3 - 2$
$\pm(\frac{1}{2},\frac{1}{2},\frac{1}{2},\underline{-\frac{1}{2}^e,\frac{1}{2}^{5-e}})(0^8)$	(16)	$N_{(16)} = \frac{1}{8}\,\kappa_{\alpha\beta}\,(V_\alpha^1+V_\alpha^2+V_\alpha^3)(V_\beta^1+V_\beta^2+V_\beta^3) - 2$
$\pm(-\frac{1}{2},\frac{1}{2},\frac{1}{2},\underline{-\frac{1}{2}^o,\frac{1}{2}^{5-o}})(0^8)$	$(\overline{16})$	$N_{(\overline{16})}^{\ 1} = \frac{1}{8}\,\kappa_{\alpha\beta}\,(-V_\alpha^1+V_\alpha^2+V_\alpha^3)(-V_\beta^1+V_\beta^2+V_\beta^3) - 2$
$\pm(\frac{1}{2},-\frac{1}{2},\frac{1}{2},\underline{-\frac{1}{2}^o,\frac{1}{2}^{5-o}})(0^8)$		$N_{(\overline{16})}^{\ 2} = \frac{1}{8}\,\kappa_{\alpha\beta}\,(\ \ V_\alpha^1-V_\alpha^2+V_\alpha^3)(\ \ V_\beta^1-V_\beta^2+V_\beta^3) - 2$
$\pm(\frac{1}{2},\frac{1}{2},-\frac{1}{2},\underline{-\frac{1}{2}^o,\frac{1}{2}^{5-o}})(0^8)$		$N_{(\overline{16})}^{\ 3} = \frac{1}{8}\,\kappa_{\alpha\beta}\,(\ \ V_\alpha^1+V_\alpha^2-V_\alpha^3)(\ \ V_\beta^1+V_\beta^2-V_\beta^3) - 2$
$\pm(0,1,\pm 1,0^5)(0^8)$	(1)	$N_{(1)}^{\pm 1} = \frac{1}{2}\,\kappa_{\alpha\beta}\,(V_\alpha^2 \pm V_\alpha^3)(V_\beta^2 \pm V_\beta^3) - 2$
$\pm(1,0,\pm 1,0^5)(0^8)$		$N_{(1)}^{\pm 2} = \frac{1}{2}\,\kappa_{\alpha\beta}\,(V_\alpha^1 \pm V_\alpha^3)(V_\beta^1 \pm V_\beta^3) - 2$
$\pm(1,\pm 1,0,0^5)(0^8)$		$N_{(1)}^{\pm 3} = \frac{1}{2}\,\kappa_{\alpha\beta}\,(V_\alpha^1 \pm V_\alpha^2)(V_\beta^1 \pm V_\beta^2) - 2$

Table 4.3: The SO(10) spectrum of gauge and hyper multiplet of a class of line bundle models. The hyper multiplet states are in the vector (10), spinor (16) or $(\overline{16})$ or singlet (1) representations of SO(10) arising from a single E_8 .

It follows from Table 4.3, that the total number N_V of (10)–plets only depends on the instanton number of the first E_8:

$$N_V = N_{(10)}^{1} + N_{(10)}^{2} + N_{(10)}^{3} = \tfrac{1}{2}\,\kappa_{\alpha\beta}\,\vec{V}_\alpha\cdot\vec{V}_\beta - 6 = c - 6\ . \tag{4.24}$$

Similarly, the total number N_S of (16)– and $(\overline{16})$–plets also only depends on c:

$$N_S = N_{(16)} + N_{(\overline{16})}^{1} + N_{(\overline{16})}^{2} + N_{(\overline{16})}^{3} = \tfrac{1}{2}\,\kappa_{\alpha\beta}\,\vec{V}_\alpha\cdot\vec{V}_\beta - 8 = c - 8 \tag{4.25}$$

Consequently, it is straightforward to verify, that (4.1) is fulfilled,

$$N_V - N_S = (c-6) - (c-8) = 2\ , \tag{4.26}$$

for $N = 5$. Notice that in this case, even for the total number of singlets $N_{(1)}$ coming from the fist E_8 one can obtain a similar result:

$$N_{(1)} = N_{(1)}^{+1} + N_{(1)}^{-1} + N_{(1)}^{+2} + N_{(1)}^{-2} + N_{(1)}^{+3} + N_{(1)}^{-3} = 2\,\kappa_{\alpha\beta}\,\vec{V}_\alpha\cdot\vec{V}_\beta - 12 = 4\,c - 12 \tag{4.27}$$

Hence the $SO(10)$ spectrum is completely fixed in terms of the instanton number c of the first E_8. These results hold in particular, if one assumes that the line bundle vectors only have non–zero entries in the first E_8, i.e. $\vec{V}'_\alpha = 0$, and hence $c = 24$:

$$N_V = 24 - 6 = 18\ ,\quad N_S = 24 - 8 = 16\ ,\quad N_V - N_S = 2\ ,\quad N_{(1)} = 4\cdot 24 - 12 = 84\ . \tag{4.28}$$

4.4.4 Counting the Number of SO(2N) Vectors and Spinors

This exercise can be generalised to line bundle vectors that have $1 \le n \le 8$ non–zero entries in the observable E_8, i.e. $\vec{V}_\alpha = (V_\alpha^1, \ldots, V_\alpha^n)$ and the rest in the second E_8. The resulting gauge group is $SO(2N)$ with $N = 8 - n$. The number of $SO(2N)$ vectors is given by:

$$N_V = \sum_{I=1}^{n}\Big(\tfrac{1}{2}\,\kappa_{\alpha\beta}\,\vec{V}_\alpha^I\vec{V}_\beta^I - 2\Big) = c - 2n\ . \tag{4.29}$$

The sum of the numbers of spinor and conjugate–spinor contribution can be computed as:

$$N_S = \sum_{\vec{S}}\Big(\tfrac{1}{2}\,\kappa_{\alpha\beta}\,(\vec{S}\cdot\vec{V}_\alpha)(\vec{S}\cdot\vec{V}_\beta) - 2\Big) = 2^{n-1}\Big(\tfrac{1}{2}\,\kappa_{\alpha\beta}\,\frac{\vec{V}_\alpha}{2}\cdot\frac{\vec{V}_\beta}{2} - 2\Big) = 2^{n-3}(c-8)\ , \tag{4.30}$$

since the set of spinor–configurations to be considered is $\big\{\vec{S} = (\underline{-\tfrac{1}{2}^{x}, \tfrac{1}{2}^{n-x}})$ for $x \le [n/2]\big\}$; 2^{n-1} in total. In the second step it is used that all the cross terms with different entries of the vectors $\vec{V}_\alpha$ and $\vec{V}_\beta$ cancel out, since all possible sign combinations are summed over, hence only "squares" $V_\alpha^I V_\beta^I$ remain. (This result can easily be verified directly for the cases $n = 1, 2$.) Notice that the expressions (4.29) and (4.30) provide lower bounds on the instanton number: $c \ge 2n$ or $c \ge 8$, which ever is the strongest, otherwise the number of vectors or spinor become negative (which is impossible).

The multiplicities of vectors (4.29) and spinors (4.30) satisfy the condition (4.1) of vanishing irreducible $SO(2N)$ anomalies. Indeed, inserting these expressions in this condition leads to:

$$N_V - 2^{N-5}\,N_S = c - 2n - 2^{N-5}\,2^{n-3}(c-8) = 8 - 2n = 2N - 8\ , \tag{4.31}$$

using that $n = 8 - N$.

4.5 SO(2N) Trace Identities

In order to make this paper self–contained this appendix derives a number of trace identities used in the anomaly analysis presented in Section 4.2. Most of the results presented here are known in the literature on anomalies, see e.g. [55, 65, 66] and textbooks like [67, 68].

4.5.1 Traces in the vector representation

In the vector representation, denoted by V, the Hermitian $SO(2N)$ gauge field strength two–form F_2 may be block diagonalized as:

$$iF_2 = \begin{pmatrix} 0 & F_2^1 & & & \\ -F_2^1 & 0 & & & \\ & & \ddots & & \\ & & & 0 & F_2^N \\ & & & -F_2^N & 0 \end{pmatrix} , \quad (iF_2)^2 = \begin{pmatrix} (F_2^1)^2 & & & & \\ & (F_2^1)^2 & & & \\ & & \ddots & & \\ & & & (F_2^N)^2 & \\ & & & & (F_2^N)^2 \end{pmatrix} , \tag{4.32}$$

for certain two–form eigenvalues F_2^I labeled by $I = 1, \ldots, N$. Taking the trace over the vector representation of the k–th power of this it follows immediately:

$$\mathrm{tr}_V (iF_2)^{2k} = 2 \sum_I (F_2^I)^{2k} , \tag{4.33}$$

for $k \geq 1$; $\mathrm{tr}_V(\mathbb{1}) = 2N$.

4.5.2 Traces in the adjoint representation

The adjoint $Ad = [V]_2$ of $SO(2N)$ is the two times anti–symmetrisation of the vector representation V. In general, the Chern character of a two times anti–symmetrised representation $[R]_2$ is related to the Chern character of the representation R via

$$\mathrm{ch}_{[R]_2}(F_2) = \frac{1}{2}\Big(\Big(\mathrm{ch}_R(F_2) \Big)^2 - \mathrm{ch}_R(2F_2) \Big) . \tag{4.34}$$

By expanding this relation to fourth order leads to the identity

$$\mathrm{tr}_{Ad}(iF_2)^4 = (2N-8)\,\mathrm{tr}_V(iF_2)^4 + 3\left(\mathrm{tr}_V(iF_2)^2\right)^2 . \tag{4.35}$$

4.5.3 Traces in the chiral spinor representations

To obtain trace identities for $SO(2N)$ spinor representations $S^\pm$ it is convenient to have an explicit basis for the spin–generators of $SO(2N)$. Like in the vector representation V, one may assume that the system is diagonalised and one is working on the Cartan of $SO(2N)$ generated by the following N matrices

$$\Sigma_1 = \tfrac{1}{2}\sigma_3 \otimes \mathbb{1}_2 \otimes \cdots \otimes \mathbb{1}_2 , \quad \ldots \quad \Sigma_N = \mathbb{1}_2 \otimes \cdots \otimes \mathbb{1}_2 \otimes \tfrac{1}{2}\sigma_3 . \tag{4.36}$$

obtained from N times tensor products of the Pauli matrices σ_i. The $SO(2N)$ chirality operator $\widetilde{\Gamma}$ can be used to define projections on positive and negative chiral subspaces of the spinor representation

$$P^{\pm} = \frac{\mathbb{1} \pm \widetilde{\Gamma}}{2} \ , \qquad \widetilde{\Gamma} = \sigma_3 \otimes \cdots \otimes \sigma_3 \ . \tag{4.37}$$

Expand the $SO(2N)$ gauge field strength in spinor representations in this Cartan basis can be expressed as

$$iF_2 = \sum F_2^I \, \Sigma_I \ , \quad (iF_2)^2 = \frac{1}{4} \sum_I (F_2^I)^2 + \sum_{J \neq I} F_2^I F_2^J \, \Sigma_I \Sigma_J \tag{4.38}$$

for $N \geq 3$. (For $N = 2$: $\Sigma_1 \Sigma_2 = \widetilde{\Gamma}/4$; for $N = 1$ the second term does not exists. These case are ignored.) The traces over positive or negative chiral spinor representations $S^{\pm}$ are given by

$$\mathrm{tr}_{S^{\pm}} (iF_2)^{2k} = \mathrm{tr}_S \Big[(iF_2)^{2k} \frac{\mathbb{1} \pm \widetilde{\Gamma}}{2} \Big] \ , \qquad \mathrm{tr}_{S^{\pm}} \mathbb{1} = \mathrm{tr}_S \Big[\frac{\mathbb{1} \pm \widetilde{\Gamma}}{2} \Big] = 2^{N-1} \ , \tag{4.39}$$

over $2^N \times 2^N$ spinor matrices.

The middle term of the square of (4.38),

$$(iF_2)^4 = \Big(\frac{1}{4} \sum_I (F_2^I)^2 \Big)^2 + 2 \Big(\frac{1}{4} \sum_I (F_2^I)^2 \Big) \sum_{J \neq I} F_2^I F_2^J \, \Sigma_I \Sigma_J + \Big(\sum_{J \neq I} F_2^I F_2^J \, \Sigma_I \Sigma_J \Big)^2 \ , \tag{4.40}$$

vanish as the Pauli matrices are traceless. To evaluate the trace of the final term, note that

$$\mathrm{tr}_S \Big(\Sigma_I \Sigma_J \, \Sigma_K \Sigma_L \, \frac{\mathbb{1} \pm \widetilde{\Gamma}}{2} \Big) = 2^{N-1} \, (\frac{1}{4})^2 \Big(\delta_{IK} \delta_{JL} + \delta_{IL} \delta_{JK} \Big) \ , \tag{4.41}$$

for $J \neq I$ and $K \neq L$. Thus,

$$\mathrm{tr}_S \Big[\Big(\sum_{J \neq I} F_2^I F_2^J \, \Sigma_I \Sigma_J \Big)^2 \, \frac{\mathbb{1} \pm \widetilde{\Gamma}}{2} \Big] = 2^{N-4} \sum_{J \neq I} (F_2^I)^2 (F_2^J)^2 = 2^{N-4} \Big(\sum_I (F_2^I)^2 \Big)^2 - \sum_I (F_2^I)^4 \ . \tag{4.42}$$

Putting all contributions together leads to

$$\mathrm{tr}_{S^{\pm}} (iF_2)^4 = 2^{N-5} \Big\{ \Big(\sum_I (F_2^I)^2 \Big)^2 + 2 \Big[\Big(\sum_I (F_2^I)^2 \Big)^2 - \sum_I (F_2^I)^4 \Big] \Big\} \ . \tag{4.43}$$

Expression this in terms of traces over the vector representation finally leads to the identity

$$\mathrm{tr}_{S^{\pm}} (iF_2)^4 = 2^{N-5} \Big\{ - \mathrm{tr}_V (iF_2)^4 + \frac{3}{4} \Big(\mathrm{tr}_V (iF_2)^2 \Big)^2 \Big\} \ . \tag{4.44}$$

This important result can also be found in [55].

Chapter 5

Uncovering a Spinor–Vector Duality on a Resolved Orbifold

5.1 Introduction

In this chapter we focus in the following logical step: i.e. compactifying our theory to five dimensions.

As a guideline for this exploration we start with orbifold models discussed in [48] on $T^4/\mathbb{Z}_2 \times S^1$ with a Wilson line on the additional circle. We then consider the resolution of this orbifold to a smooth K3$\times S^1$ realisation and investigate how this effects the spinor–vector duality. In particular, we show that this duality can still be realised, but in a more complicated guise.

Outline

Section 5.2 first recalls the description of the $T^4/\mathbb{Z}_2$ orbifold of the heterotic $E_8 \times E_8$ string, a similar analysis than the previous chapter, but this time focusing on the spectrum. After that an additional circle is considered with a Wilson line. The effect of switching on a generalised torsion between the orbifold action and the Wilson line concludes this section.

Section 5.3 describes some properties of the resolution of the $T^4/\mathbb{Z}_2$ orbifold. In particular line bundle gauge backgrounds are introduced and the multiplicity operator is given to compute the full massless spectrum in six dimensions.

The effect of the Wilson line is discussed next. The simplest case is the situation without the torsion phase switched on as the resulting five dimensional spectrum can just be analysed by field theory techniques. Since it is unclear how to switch on the generalised torsion phase between the orbifold twist and the Wilson line on the smooth side, an educated guess is made for its effects based on the results of the previous section on the orbifold theory with an additional circle. The effect of the Wilson line with torsion is that the twisted states which were used as blowup modes are kicked out and the resulting model seems to be inconsistent. This may be overcome by selecting other blowup modes which are kept by the Wilson line projection modified by the generalised torsion. Possible consequences of this for the spinor–vector duality conclude this section.

The conclusion Section 6.6 summarises the results obtained in the chapter and is completed by a short outlook on future directions.

5.2 Five Dimensional $T^4/\mathbb{Z}_2 \times S^1$ Model with Wilson Line

In this section a (very similar) orbifold model will be presented as studied in [48]. There the orbifold $T^4/\mathbb{Z}_2 \times T^2$ with a Wilson line on one of the $S^1 \subset T^2$ was considered. The resulting models exhibit a spinor–vector duality induced by switching on/off a generalised GSO phase between the orbifold twist and the Wilson line: For one choice of the discrete torsion, the zero modes of the untwisted torus in the $\mathcal{N} = 2$ twisted sector are attached to the spinorial characters of the GUT group, whereas for the other choice they are attached to the vectorial character.

Since the second circle was just a spectator in the discussion of the spinor–vector duality in [48], it is omitted here for clarity, so that the focus is on the five dimensional geometry $T^4/\mathbb{Z}_2 \times S^1$ with a Wilson line on the circle. To demonstrate the effect the possible torsion phase between the orbifold twist and the Wilson line, first the theory on the orbifold $T^4/\mathbb{Z}_2$ is recalled. For simplicity the orbifold standard embedding is chosen for the computation of the six dimensional massless states. After that the Wilson line projections without or with torsion are taken into account to determine the resulting five dimensional spectra.

5.2.1 Spectrum on $T^4/\mathbb{Z}_2$ in the Orbifold Standard Embedding

This section begins with an introduction to the heterotic $E_8 \times E_8$ string on the orbifold $T^4/\mathbb{Z}_2$ using the orbifold standard embedding. The material here is standard and may be found e.g. in [8, 9]; the notation used here follows [71]. The orbifold modular invariance condition

$$V^2 - v^2 \equiv 0 \ , \tag{5.1}$$

is trivially solved by taking the non–zero entries of the twist and the gauge embedding identical:

$$v = (\tfrac{1}{2}^2, 0^2) \ , \qquad V = (\tfrac{1}{2}^2, 0^6)(0^8) \tag{5.2}$$

The massless spectrum in six dimensions on the orbifold is determined by setting the left–moving mass

$$0 = M_R^2 = p_{\rm sh}^2 - \tfrac{1}{2} + \delta c \ , \qquad p_{\rm sh} = p + k\, v \ , \tag{5.3}$$

and right–moving mass

$$0 = M_L^2 = P_{\rm sh}^2 - 1 + \delta_c + \omega_i\, N_i + \overline{\omega}_i\, \overline{N}_i \ , \qquad P_{\rm sh} = P + k\, V \ , \tag{5.4}$$

to zero. Here $k = 0$ labels the untwisted sector and $k = 1$ the twisted sector. The momenta p and P are taken from the lattices:

$$p \in \Lambda_{SO(8)} \ , \qquad P \in \Lambda_{E_8 \times E_8} \ . \tag{5.5}$$

Furthermore, the following notation is introduced:

$$\delta c = \tfrac{1}{2} \sum_i \omega_i (1 - \omega_i) \ , \qquad \omega_i \equiv k\, v_i \ , \qquad \overline{\omega}_i \equiv -k\, v_i \ , \tag{5.6}$$

where $\equiv$ means equal up to integers, such that $0 < \omega_i, \overline{\omega}_i \leq 1$. Concretely, for the $\mathbb{Z}_2$ orbifold at hand, this reduces to: $\omega_i = \overline{\omega}_i = 1$, $\delta c = 0$ for $k = 0$ and $\omega_i = \overline{\omega}_i = \frac{1}{2}$, $\delta c = \frac{1}{4}$ for $k = 1$.

The gauge group in six dimensions is determined by

$$P^2 = 2 \ , \qquad V \cdot P \equiv 0 \ . \tag{5.7}$$

These come as bosons (gauge fields) with $p = \pm(0^2, \underline{1,0})$ and spinors (gauginos) with $p = (\underline{\frac{1}{2}, -\frac{1}{2}}, \overline{-\frac{1}{2}, \frac{1}{2}})$. Here the underline indicates that all possible permutations are to be considered as well. The untwisted charged matter is characterized by:

$$V \cdot P - v \cdot p \equiv 0 \ , \tag{5.8}$$

with $N_i = \overline{N}_i = 0$. In addition, there are uncharged untwisted matter with $P = 0$ and one $N_i, \overline{N}_i$ equal to 1 and the rest zero. These states come as bosons with $p = \pm(\underline{1,0},0^2)$ and spinors of the opposite chirality (hyperinos) $p = \pm(\frac{1}{2}^2, \pm\frac{1}{2}^2)$. The twisted matter comes in multiples of 16 due to the fact that there are 16 fixed points. The right-moving momentum is fixed to:

$$p_{\rm sh}^2 = \tfrac{1}{2} \ . \tag{5.9}$$

Hence, we can only have the bosonic states $p_{\rm sh} = (\underline{\frac{1}{2}, -\frac{1}{2}}, 0^2) = v + p$ with $p = (\underline{0, -1}, 0^2)$ and fermionic states $p_{\rm sh} = (0, 0, \pm\frac{1}{2}^2) = v + p$ with $p = (-\frac{1}{2}^2, \pm\frac{1}{2}^2)$. Their representation with respect to the gauge group are determined by

$$P_{\rm sh}^2 = \tfrac{3}{2} - \tfrac{1}{2} \sum_i (N_i + \overline{N}_i) \ . \tag{5.10}$$

The solutions of this mass equation are well–known [53, 72] and are summarized in Table 5.1 for later convenience.

5.2.2 Orbifold with Wilson line on an Additional Circle – No Torsion

Next, the model is compactified further down to five dimensions by a discrete $\mathbb{Z}_2$ Wilson line given by $W = (0^7, 1)(0^7, 1)$ on an additional circle S^1. In this subsection the option of adding a torsion phase between the orbifold action and the Wilson line is ignored; this will be considered in the next subsection. The projection conditions are determined by the requirement [71]:

$$e^{2\pi i (V_{h'} \cdot P_{\rm sh} - v_{h'} \cdot p_{\rm sh} + v_{h'} \cdot (N - \overline{N}))} \cdot e^{2\pi i \frac{1}{2} (V_{h'} \cdot V_h - v_{h'} \cdot v_h)} \stackrel{!}{=} 1 \ , \tag{5.11}$$

where $V_h = k\,V + n\,W$, $v_h = k\,v$, $P_{\rm sh} = P + V_h$ and $p_{\rm sh} = p + v_h$. The first factor can be understood in field theory while the second factor is the vacuum phase of the string. For the choice

$$v = (\tfrac{1}{2}^2, 0^2) \ , \quad V = (\tfrac{1}{2}^2, 0^6)(0^8) \ , \quad W = (0^7, 1)(0^7, 1) \ , \tag{5.12}$$

the vacuum phase is trivial: $\frac{1}{2}(V_{h'} \cdot V_h - v_{h'} \cdot v_h) \equiv 0$. The first phase in (5.11) leads to the orbifold projection:

$$V \cdot P - v \cdot p + (N_i - \overline{N}_i) v_i \equiv 0 \tag{5.13}$$

and the projection due to the Wilson line:

$$W \cdot P \equiv 0 \ . \tag{5.14}$$

$P_{\rm sh}$	$W \cdot P_{\rm sh} \equiv$	$SU(2) \times E_7 \times E_8'$	$SU(2)_1 \times SU(2)_2 \times SO(12) \times SO(16)'$
$\pm(1^2, 0^6)(0^8)$	0	$SU(2)$ gauge	$SU(2)_1$ gauge
$\pm(0^2, \underline{\pm 1^2, 0^4})(0^8)$	0	E_7 gauge	$SO(12)$ gauge
$(\underline{1, -1}, 0^6)(0^8)$	0		$SU(2)_2$ gauge
$(\underline{\frac{1}{2}, -\frac{1}{2}}, \underline{-\frac{1}{2}^o, \frac{1}{2}^{6-o}})(0^8)$	$\frac{1}{2}$		$(1, 2, 32)(1)$ gauge
$(0^8, 0^8)$	0	$4\,(1, 1)(1)$	$4\,(1, 1, 1)(1)$
$\pm(\underline{1, 0, \pm 1}, 0^5)(0^8)$	0	$(2, 56)(1)$	$(2, 2, 12)(1)$
$\pm(\frac{1}{2}^2, \underline{-\frac{1}{2}^e, \frac{1}{2}^{6-e}})(0^8)$	$\frac{1}{2}$		$(2, 1, 32)(1)$
$(\underline{\frac{1}{2}, -\frac{1}{2}}, \underline{\pm 1}, 0^5)(0^8)$	0	$16\,\frac{1}{2}(1, 56)(1)$	$16\,\frac{1}{2}(1, 2, 12)(1)$
$\pm(0^2, \underline{-\frac{1}{2}^e, \frac{1}{2}^{6-e}})(0^8)$	$\frac{1}{2}$		$16\,\frac{1}{2}(1, 1, 32)(1)$
$\pm(\frac{1}{2}^2, 0^6)(0^8)$	0	$32\,(2, 1)(1)$	$32\,(2, 1, 1)(1)$
$\pm(0^8)(\underline{\pm 1^2, 0^6})$	0	E_8 gauge	$SO(16)$ gauge
$\pm(0^8)(\underline{-\frac{1}{2}^e, \frac{1}{2}^{8-e}})$	$\frac{1}{2}$		$(1, 1, 1)(128)$ gauge

Table 5.1: This table gives the weights of the massless states on the $T^4/\mathbb{Z}_2$ orbifold. In addition, the eigenvalue $W \cdot P_{\rm sh}$ and the resulting branching of this spectrum due to the Wilson line W is indicated. (The underline indicates that all permutations are to be considered and o and e go over all odd and even numbers, respectively, such that the powers never go negative.) The matter multiplets are hyper multiplets or half–hyper multiplets (i.e. hyper multiplets with a reality condition imposed), the latter are indicated by the $\frac{1}{2}$ in front of the states.

Here we are using the fact that we are considering a general point in the moduli space, hence no winding mode states accidentally become massless. Consequently, the Wilson line reduces the gauge group to

$$SU(2)_1 \times SU(2)_2 \times SO(12) \times SO(16)' \tag{5.15}$$

with the spectrum in five dimensions:

$$(2,2,12)(1) + 16\,\tfrac{1}{2}(1,2,12)(1) + 32\,(2,1,1)(1) + 4(1,1,1)(1)\ . \tag{5.16}$$

Note, in particular, that this spectrum does not contain any spinorial representation of $SO(12)$.

5.2.3 Orbifold with Wilson line on an Additional Circle – With Torsion

In this subsection the same compactification on S^1 with the Wilson line (5.12) is investigated, but now the option of switching on a torsion phase between de orbifold action and the Wilson line is considered [71]:

$$T = (-1)^{\epsilon(kn'-k'n)}\ , \tag{5.17}$$

where $k = 0, 1$ labels the untwisted ($k = 0$) and the twisted ($k = 1$) sectors and $n = 0, 1$ the $\mathbb{Z}_2$ Wilson line sectors. The primed versions define the orbifold and Wilson line projections. The torsion phase is switched on and off for $\epsilon = 1$ and 0, respectively.[1] The projection conditions (5.11) are then modified to:

$$e^{2\pi i(V_{h'}\cdot P_{\rm sh} - v_{h'}\cdot p_{\rm sh} + v_{h'}\cdot(N-\overline{N}))}\cdot e^{2\pi i\frac{1}{2}(V_{h'}\cdot V_h - v_{h'}\cdot v_h)}\cdot e^{2\pi i\,\frac{1}{2}(kn'-k'n)} \stackrel{!}{=} 1\ , \tag{5.18}$$

Away from special points in moduli space, the winding modes with $n = 1$ will be massive and hence do not affect the massless spectrum and will therefore be ignored. Thus when the torsion phase is switched on it only modifies the Wilson line projection (5.14) to:

$$W \cdot P_{sh} \equiv \tfrac{1}{2}\,k\ \ : \tag{5.19}$$

Thus, for the untwisted states the projection is the same as without torsion, for the twisted states things change: The twisted states that were projected out before are kept with the torsion phase and vise versa. Thus, in particular, the gauge group remains the same

$$SU(2)_1 \times SU(2)_2 \times SO(12) \times SO(16)' \tag{5.20}$$

but the spectrum in five dimensions changes to:

$$(2,2,12)(1) + 16\,\tfrac{1}{2}(1,1,32)(1) + 4(1,1,1)(1)\ . \tag{5.21}$$

As compared to the spectrum (5.16) the 16 vectorial half–hyper multiplets $(1,1,12)(1)$ have been replaced by 16 spinorial half–hyper multiplets $(1,1,32)(1)$ and the 32 doublets $(2,1,1)(1)$ have been removed all together. Switching the torsion (5.17) on or off thus induces a spinor–vector duality between the two Wilson line models considered in these two subsections.

[1] Note that is a generalisation of discrete torsion considered in [64, 73], which is between two orbifold twists.

5.3 Line Bundle Resolutions of $T^4/\mathbb{Z}_2 \times S^1$ with Wilson Lines

5.3.1 Geometry of the $T^4/\mathbb{Z}_2$ Resolution

The techniques to determine resolutions of toroidal orbifolds have been well–studied [59,74,75]; here in particular the methods exploited in [76] are used. The resolution of the $T^4/\mathbb{Z}_2$ orbifold can be described with four inherited divisors R_1, R_1', R_2, R_2', eight ordinary divisors $D_{1,\alpha_3\alpha_4}$ and $D_{2,\alpha_1\alpha_2}$ and sixteen exceptional divisors E_α, where $\alpha = (\alpha_1, \alpha_2, \alpha_3, \alpha_4)$ with $\alpha_i = 0, 1$ labels the sixteen isolated $\mathbb{Z}_2$ singularities on the torus T^4. There are a number of linear relations among these divisors

$$R_1 \sim R_1' \sim 2\, D_{1,\alpha_3\alpha_4} + \sum_{\alpha_1,\alpha_2} E_\alpha \ , \qquad R_2 \sim R_2' \sim 2\, D_{2,\alpha_1\alpha_2} + \sum_{\alpha_3,\alpha_4} E_\alpha \ . \tag{5.22}$$

These relations show that ordinary divisors $D_{1,\alpha_3\alpha_4}$ and $D_{2,\alpha_1\alpha_2}$ and inherited divisors R_1' and R_2' may be replaced by inherited divisors R_1, R_2 and exceptional divisors E_α. The non–vanishing intersection numbers of the remaining divisors may be summarised as:

$$R_1 R_2 = 2 \ , \qquad E_\alpha E_\beta = -2\, \delta_{\alpha\beta} \ . \tag{5.23}$$

The total Chern class may be represented as

$$c = (1-R_1)(1-R_1')(1-R_2)(1-R_2') \prod_{\alpha_3,\alpha_4} (1+D_{1,\alpha_3\alpha_4}) \prod_{\alpha_1,\alpha_2} (1+D_{2,\alpha_1\alpha_2}) \prod_{\alpha} (1+E_\alpha) \ . \tag{5.24}$$

Expanding this to first and second order gives

$$c_1 = 0 \ , \qquad c_2 = 24 \ . \tag{5.25}$$

The first signifies that this resolution is a four dimensional K3 surface with Euler number 24 as the second Chern class c_2 indicates.

5.3.2 Line Bundles on the $T^4/\mathbb{Z}_2$ Resolution

For orbifold resolution models it is generically assumed that the gauge flux is located on the exceptional divisors only. Hence, the line bundle background encoded by an anti–Hermitian Abelian gauge field strength two–form $\mathcal{F}_2$ given by [32,60,61,77]:

$$\frac{\mathcal{F}_2}{2\pi} = \sum_\alpha E_\alpha\, \mathsf{H}_\alpha \ , \quad \mathsf{H}_\alpha = V_\alpha^I\, \mathsf{H}_I \ , \tag{5.26}$$

where the sum over the Cartan generators labelled by I is implied. The Cartan generators H_I of $E_8 \times E_8$ are normalized such that $\mathrm{tr}\, \mathsf{H}_I \mathsf{H}_J = \delta_{IJ}$. The embedding of the line bundle background is therefore characterized by sixteen component line bundle (embedding) vectors $V_\alpha = (V_\alpha^I)$. (For translations to other characterizations see e.g. [78].) Often it is convenient to split the line bundle vectors in contributions in the first and second E_8 as: $V_\alpha = (\vec{V}_\alpha)(\vec{V}_\alpha')$ where $\vec{V}_\alpha$ and $\vec{V}_\alpha'$ both have 8 entries.

The fundamental consistency requirement of such backgrounds is determined from the integrated Bianchi identity $\mathrm{tr}(\mathcal{F}_2^2) - \mathrm{tr}(\mathcal{R}_2^2) = 0$. On this resolution it can be cast in the form:

$$\sum_\alpha V_\alpha^2 = 24 \ . \tag{5.27}$$

Another consistency condition that is required in any smooth heterotic compactifaction is the stability of the vector bundle, which is guarantedd by imposing the DUY equation. In our case, as the compact space is four dimensional we have that:

$$\frac{1}{2}\int_{K3} J\wedge\frac{\mathcal{F}}{2\pi}=\mathrm{Vol}\,(D_i)\,V_i^I=0, \tag{5.28}$$

and as we said before (3.57), we need that the zero-vector can be obtained from a linear combination of the V_i^I with positive coefficients only.

On the other side, the six dimensional spectrum of the line bundle model can be computed using multiplicity operator [60]:

$$\mathsf{N}=-\int\Big\{\frac{1}{2}\Big(\frac{\mathcal{F}}{2\pi}\Big)^2-\frac{1}{24}\,\mathrm{tr}\Big(\frac{\mathcal{R}}{2\pi}\Big)^2\Big\}=\sum_\alpha \mathsf{H}_\alpha^2-2\ . \tag{5.29}$$

This operator counts the number of fermions in a given representation. The sign of this operator may be positive or negative and is determined by the six dimensional chirality of the underlying fermionic states: It equals -2 on gaugino states; the multiplicity operator directly identifies the gauge group unbroken by the line bundle background. The multiplicity operator N is positive on hyperinos as they have the opposite chirality as gauginos in six dimensions. Hence, if positive, it counts the number of hyper multiplets in a given representation of the gauge group.

5.3.3 Line Bundle Model with Vectorial Blowup Modes

Consider the resolution model with two set of line bundle vectors:

$$V_\alpha=(\tfrac{1}{2},-\tfrac{1}{2},1,0^5)(0^8)\ ,\ \alpha=1,..,8\quad V_\alpha=(-\tfrac{1}{2},\tfrac{1}{2},-1,0^5)(0^8)\ ,\ \alpha=9,..,16 \tag{5.30}$$

Here half of the bundle vectors have been chosen with negative sign respect to the others to allow the fulfilment of (5.28). As the multiplicity operator depends cuadratically on the bundle vectors we can treat all 16 vectors identically and simplify N as:

$$\mathsf{N}=16\,\mathsf{H}_V^2-2\ . \tag{5.31}$$

Using this operator the multiplicities of the $E_8\times E_8'$ roots can be computed. The resulting spectrum is given in Table 5.2. The assignment of untwisted and twisted states in this table is done by comparing with the untwisted states on the orbifold which can be understood as from field theoretical orbifolding of the $E_8\times E_8'$ ten-dimensional gauge multiplet. Since $T^4/\mathbb{Z}_2$ has 16 fixed points and all fixed points (and their blowups) are treated identically, multiples of 16 are required.

Matching with the Orbifold Spectrum

The above resolution model can be understood as a blowup of the orbifold standard embedding model. The techniques to understand the relations between the orbifold and resolutions spectra were discussed in e.g. [32, 77, 79, 80]. The choice of the line bundle vectors as (5.45) can be interpreted as using the identical blowup modes with this shifted momenta

$$P_{\mathrm{sh},\alpha}=V_\alpha=V+P\ ,\quad V=(\tfrac{1}{2},\tfrac{1}{2},0,0^5)(0^8)\quad\text{and}\quad P=(0,-1,1,0^5)(0^8) \tag{5.32}$$

weight	H_V^2	N	$SU(2) \times E_6 \times E_8'$	$SU(2) \times SO(10) \times SO(16)'$
$\pm(1,1,0,0^5)(0^8)$	0	-2_U	$SU(2)$ gauge	$SU(2)$ gauge
$\pm(0,0,0,\underline{\pm 1^2,0^3})(0,^8)$	0	-2_U	E_6 gauge	$SO(10)$ gauge
$\pm(\frac{1}{2},-\frac{1}{2},-\frac{1}{2},\underline{-\frac{1}{2}^e,\frac{1}{2}^{5-e}})(0^8)$				$(1,16)(1)$ gauge
$\pm(1,0,-1,0^5)(0^8)$	$\frac{1}{4}$	2_U	$(2,27)(1)$	$(2,1)(1)$
$\pm(0,-1,-1,0^5)(0^8)$				
$\pm(\underline{1,0,0,\pm 1,0^4})(0^8)$				$(2,10)(1)$
$\pm(\pm\frac{1}{2}^2,-\frac{1}{2},\underline{-\frac{1}{2}^o,\frac{1}{2}^{5-o}})(0^8)$				$(2,16)(1)$
$\pm(1,-1,0,0^5)(0^8)$	1	$14 = 16_T - 2_U$	$(1,27)(1)$	$(1,1)(1)$
$\pm(0,0,1,\underline{\pm 1,0^4})(0^8)$				$(1,10)(1)$
$\pm(\frac{1}{2},-\frac{1}{2},\frac{1}{2},\underline{-\frac{1}{2}^o,\frac{1}{2}^{5-o}})(0^8)$				$(1,16)(1)$
$\pm(1,0,1,0^5)(0,0^7)$	$\frac{9}{4}$	$34 = 32_T + 2_U$	$(2,1)(1)$	$(2,1)(1)$
$\pm(0,-1,1,0^5)(0,0^7)$				
$\pm(0^8)(\underline{\pm 1^2,0^6})$	0	-2_U	E_8 gauge	$SO(16)$ gauge
$\pm(0^8)(\underline{-\frac{1}{2}^e,\frac{1}{2}^{8-e}})$				$(1,1)(128)$ gauge

Table 5.2: The multiplicities of the $E_8 \times E_8$ roots are indicated for the resolution model generated by identical vectorial blowup modes at all sixteen exceptional divisors. The states with a positive or a negative multiplicity form hyper or vector multiplets. The subscripts U and T indicate how these numbers can be used to interpret the corresponding states as untwisted or twisted, respectively. The final column gives the spectrum branched by the Wilson line.

at all sixteen fixed points. These shifted momenta identify the sixteen blowup modes to lie inside the $(1,2,12)(1) \subset (1,56)(1)$ half–hyper multiplets given in Table 5.1. Switching on these blowup modes leads to the symmetry breaking:

$$SU(2) \times E_7 \times E_8' \to SU(2) \times E_6 \times E_8' \tag{5.33}$$

In this process precisely the roots $\pm(1,1,0,0^5)(0^8)$, $\pm(0,0,1,\underline{\pm 1,0^4})$ and $\pm(\frac{1}{2},\frac{1}{2},\frac{1}{2},\underline{-\frac{1}{2}^o,\frac{1}{2}^{5-o}})$ of the $(1,27)(1)$ are broken. This corresponds to the computation $14 = 16_T - 2_U$, which can be understood as the super–Higgs effect where certain twisted states are "eaten" to form massive vector multiples. These are states that arise from the sixteen half–hyper multiplets $(1,56)(1)$. Under the symmetry breaking this branches to

$$\tfrac{1}{2}(1,56)(1) \to (1,27)(1) + (1,1)(1) \ , \tag{5.34}$$

where the states $(1,1)(1)$ can be identified as the blowup modes (BLW). On the resolution they are reinterpreted as sixteen model dependent axions, which do not contribute to the multiplicity operator [79].

The remaining fourteen states $(1,27)(1)$ after the Higgsing undergo a field redefinition when moving from the hyper multiplets on the orbifold to the states on the resolution:

$$(1,27)(1)_{\rm RES} = {\rm BLW}^{-1} \cdot (1,27)(1)_{\rm ORB} \tag{5.35}$$

Here the subscripts RES and ORB indicate whether the states are part of the resolution or orbifold description, respectively. Indeed, the corresponding weights can be matched exactly via:

$$\begin{array}{rcl}
\pm(0,0,-1,\underline{\pm 1,0^4})(0^8) & = & \pm\big[-(\frac{1}{2},-\frac{1}{2},1,0^5)(0^8) \ + \ (\frac{1}{2},-\frac{1}{2},0,\underline{\pm 1,0^4})\big] \\
\pm(-\frac{1}{2},-\frac{1}{2},-\frac{1}{2},\underline{-\frac{1}{2}^o,\frac{1}{2}^{5-o}})(0^8) & = & \pm\big[-(\frac{1}{2},-\frac{1}{2},1,0^5)(0^8) \ + \ (0,0,\frac{1}{2},\underline{-\frac{1}{2}^o,\frac{1}{2}^{5-o}})\big] \\
\pm(-1,1,0,0^5)(0^8) & = & \pm\big[-(\frac{1}{2},-\frac{1}{2},1,0^5)(0^8) \ + \ (-\frac{1}{2},\frac{1}{2},1,0^5)\big]
\end{array} \tag{5.36}$$

A similar field redefinition relate the doublet states on the orbifold to those on the resolutions:

$$(2,1)(1)_{\rm RES} = {\rm BLW} \cdot (2,1)(1)_{\rm ORB} \ , \tag{5.37}$$

or in terms of the corresponding weights:

$$\begin{array}{rcl}
\pm(1,0,1,0^5)(0^8) & = & \pm\big[(\frac{1}{2},-\frac{1}{2},1,0^5)(0^8) + (\frac{1}{2}^2,0,0^5)\big] \\
\pm(0,-1,1,0^5)(0^8) & = & \pm\big[(\frac{1}{2},-\frac{1}{2},1,0^5)(0^8) + (-\frac{1}{2}^2,0,0^5)\big]
\end{array} \tag{5.38}$$

Hence, using these field redefinitions the descriptions on the orbifold and on the resolutions agree on the level of the weights showing that the matching between the orbifold and resolved descriptions is complete.

5.3.4 Wilson Line Projected Vectorial Blowup Model

Next the consequences of the Wilson line on the additional circle is investigated in the resolved geometry. There are two cases to be considered depending on whether a generalisation of the torsion phase (5.17) has been switched on or not. On smooth geometries it is less clear how to implement the string torsion phases as the description starts from an effective field theory description in ten dimensions rather than the full one–loop partition function of string theory. For this reason the Wilson line projection conditions are strongly inspired by the conditions arising in the orbifold theory.

No Torsion

The model is compactified further on a circle S^1 with a discrete Wilson line:

$$W = (0^7, 1)(0^7, 1) \tag{5.39}$$

and the torsion phase (5.17) is switched off: $\epsilon = 0$. The Wilson line projection condition on the resolution is assumed to take the form:

$$W \cdot P \equiv 0 \ , \tag{5.40}$$

where P are the weights listed in Table 5.2. This directly follows from the orbifold Wilson line projection (5.14), since the difference between the $P_{\rm sh}$ and P is at most given by V_α, but $W \cdot V_\alpha = 0$. The gauge group therefore becomes:

$$SU(2) \times SO(10) \times SO(16)' \tag{5.41}$$

and the 5D spectrum:

$$2\,(2,10)(1) + 36\,(2,1)(1) + 14\,(1,10)(1) + 14\,(1,1)(1) \ . \tag{5.42}$$

Notice the absence of any spinors of $SO(10)$ in this resolution model after the Wilson line projection has been implemented.

This spectrum can also be understood as the blowup of the five dimensional $T^4/\mathbb{Z}_2 \times S^1$ model with the same Wilson line W discussed in Subsection 5.2.2. The blowup using the blowup modes (5.32) leads to the gauge symmetry breaking:

$$SU(2)_1 \times SU(2)_2 \times SO(12) \times SO(16)' \to SU(2)_1 \times SO(10) \times SO(16)' \ . \tag{5.43}$$

The broken weights are $(\underline{1,-1},0,0^5)(0^8)$ associated to $SU(2)_2$ and $\pm(0,0,1,\underline{\pm 1},0^4)$ associated to $2\,(1,10)(1)$. The spectrum is branched as follows:

$$\begin{aligned}
(2,2,12)(1) &\to 4\,(2,1)(1) + 2\,(2,10)(1) \ , \\
16\,\tfrac{1}{2}(1,2,12)(1) &\to 16\,(1,10)(1) + 32\,(1,1)(1) \ , \\
32\,(2,1,1)(1) &\to 32\,(2,1)(1) \ .
\end{aligned} \tag{5.44}$$

The number of $(2,10)(1)$ immediately agree, so do the number of $(2,1)(1)$: $4+32=36$. Of the sixteen $(1,10)(1)$'s two are eaten to form massive $(1,10)(1)$ vector multiplets leaving fourteen states. Finally, sixteen of the 32 charged singlets $(1,1)(1)$ should be identified as blowup modes and hence appear as axions in the resolved theory. Furthermore, two singlets are eaten to make the $SU(2)_2$ weights heavy, leaving $32-16-2=14$ charged singlets in the spectrum.

With Torsion

The description of the Wilson line on the additional circle with no torsion is fully self–consistent as was discussed above. On the contrary, switching the torsion (5.17), i.e. $\epsilon = 1$, leads to a number of issues:

First of all, it is not clear how to precisely implement the Wilson line projection in this case on the resolution. On the orbifold the projection condition (5.19) with torsion distinguishes between untwisted and twisted states. While on generic smooth compactifications such a distinction is completely meaningless, for smooth models obtained as orbifold resolutions it is possible to make an assignment of "untwisted" and "twisted" states as indicated in Table 5.2 and Table 5.3 based on intuition from and matching with the underlying orbifold theory. Hence, it is natural to assume that the discrete torsion modifies the projection condition analogously to the orbifold case.

Secondly, the blowup modes (5.32) used to generate the blowup model are projected out by the Wilson line when the torsion is switched on as the projection condition is modified to (5.14), since the blowup modes are twisted states with $k = 1$. (Resolution models with bundle vectors that would be associated with massive or projected out twisted states have been known in the literature but are not well–understood.)

A closely related issue is that there are states missing for the super–Higgs mechanism to be able to operate. On the orbifold the Wilson line would project the gauge group to $SU(2) \times SO(12) \times SO(16)'$. The blowup procedure leads to further breaking $SO(12) \to SO(10)$ hence two (10)'s of $SO(10)$ should form massive multiplets with (10)–plets as hyper multiplets. (The $14 = 16_T - 2_H$ computation discussed below (5.33).) But these twisted (10)-plets are projected out by the Wilson line when the torsion is switched on.

5.3.5 Line Bundle Model with Spinorial Blowup Modes

The main issue with the resolution model discussed just above is that the blowup modes which are supposed to generate the blowup are projected out by the Wilson line when the torsion is switched on. On the level of the orbifold this projection kicks out twisted vectorial states, including the blowup modes (5.32), while keeping spinorial ones. As it is a choice which twisted states are used as blowup modes, it instructive to investigate spinorial blowup modes instead. A concrete choice is to consider the resolution model with line bundle vectors

$$V_\alpha = (0^2, \tfrac{1}{2}^6)(0^8),\ \alpha = 1,..,8 \quad V_\alpha = (0^2, -\tfrac{1}{2}^6)(0^8),\ \alpha = 9,..,16 \tag{5.45}$$

Since, again, the same (up to a minus sign) line bundle vector is chosen on all exceptional divisors, the multiplicity operator reduces to (5.31). The spectrum can be determined as before and is given in Table 5.3.

Matching with the Orbifold Spectrum

The above resolution model can also be understood as the blowup of the orbifold standard embedding model. In this case blowup modes all have shifted momenta

$$P_{\mathrm{sh},\alpha} = V_\alpha = V + P\ , \quad V = (\tfrac{1}{2}^2, 0^6)(0^8) \quad \text{and} \quad P = (-\tfrac{1}{2}^2, \tfrac{1}{2}^6)(0^8) \tag{5.46}$$

weight	H_V^2	N	$SU(2)_1 \times E_6 \times E_8'$	$SU(2)_1 \times SU(2)_2 \times SU(6) \times SO(16)'$
$\pm(1^2,0,0^5)(0^8)$	0	-2_U	$SU(2)_1$ gauge	$SU(2)_1$ gauge
$(0^2,\underline{1,-1,0^4})(0,^8)$	0	-2_U	E_6 gauge	$SU(6)$ gauge
$(\underline{1,-1},0^6)(0,^8)$				$SU(2)_2$ gauge
$(\frac{1}{2},\underline{-\frac{1}{2},-\frac{1}{2}^3,\frac{1}{2}^3})(0^8)$				$(1,2,20)(1)$ gauge
$\pm(\underline{\pm1,0,1,0^5})(0^8)$	$\frac{1}{4}$	2_U	$(2,27)(1)$	$(2,2,6)(1)$
$\pm(\frac{1}{2}^2,\underline{\frac{1}{2}^4,-\frac{1}{2}^2})(0^8)$				$(2,1,15)(1)$
$\pm(-\frac{1}{2}^2,\underline{\frac{1}{2}^4,-\frac{1}{2}^2})(0^8)$				
$\pm(0^2,\underline{1^2,0^4})(0^8)$	1	$14 = 16_T - 2_U$	$(1,27)(1)$	$(1,1,15)(1)$
$\pm(\underline{\frac{1}{2},-\frac{1}{2},\frac{1}{2}^5,-\frac{1}{2}})(0^8)$				$(1,2,6)(1)$
$\pm(\frac{1}{2}^2,\frac{1}{2}^6)(0^8)$	$\frac{9}{4}$	$34 = 32_T + 2_U$	$(2,1)(1)$	$(2,1,1)(1)$
$\pm(-\frac{1}{2}^2,\frac{1}{2}^6)(0^8)$				
$\pm(0^8)(\underline{\pm1^2,0^6})$	0	-2_U	E_8 gauge	$SO(16)$ gauge
$\pm(0^8)(\underline{-\frac{1}{2}^e,\frac{1}{2}^{8-e}})$				$(1,128)$ gauge

Table 5.3: The multiplicities of the $E_8 \times E_8$ roots are indicated for the resolution model generated by identical spinorial blowup modes at all sixteen exceptional divisors. The states with a positive or a negative multiplicity form hyper or vector multiplets. The subscripts U and T indicate how these numbers can be used to interpret the corresponding states as untwisted or twisted, respectively. The final column gives the spectrum branched by the Wilson line.

at all sixteen fixed points. They live on the (shifted) spinorial lattice of $SO(16)$ and part of the sixteen half–hyper multiplets $(1,56)(1)$. Switching on these blowup models lead to the symmetry breaking:

$$SU(2) \times E_7 \times E_8' \to SU(2) \times E_6 \times E_8' \tag{5.47}$$

In this process precisely the roots $\pm(0^2, \underline{1^2, 0^4})(0^8)$ and $\pm(\frac{1}{2}, -\frac{1}{2}, \underline{-\frac{1}{2}, \frac{1}{2}^5})$ of the $(1,27)(1)$ are broken. This, again, corresponds to the computation $14 = \overline{16_T - 2_U}$, which can be understood by the super-Higgs effect where certain twisted states are "eaten" to form massive vector multiplets. These are states that arise from the 16 half-hyper multiplets $(1,56)(1)$. Under the symmetry breaking this branches to

$$\tfrac{1}{2}(1,56)(1) \to (1,27)(1) + (1,1)(1) \tag{5.48}$$

As before, the states $(1,1)(1)$ are the blowup modes (BLW), which on the resolution are reinterpreted as 16 model dependent axions not contributing to the multiplicity operator.

The remaining 14 states $(1,27)(1)$ after the Higgsing undergo a field redefinition when moving from the hyper multiplets on the orbifold to the states on the resolution:

$$(1,27)(1)_{\text{RES}} = \text{BLW}^{-1} \cdot (1,27)(1)_{\text{ORB}} \tag{5.49}$$

Indeed, the corresponding weights can be matched exactly via:

$$\begin{aligned} \pm(0^2, \underline{1^2, 0^4})(0^8) &= \mp\big[-(0^2, \tfrac{1}{2}^6)(0^8) + (0^2, \underline{-\tfrac{1}{2}^2, \tfrac{1}{2}^4})\big] \\ \pm(\underline{\tfrac{1}{2}, -\tfrac{1}{2}}, \underline{-\tfrac{1}{2}, \tfrac{1}{2}^5})(0^8) &= \mp\big[-(0^2, \tfrac{1}{2}^6)(0^8) + (\underline{-\tfrac{1}{2}, \tfrac{1}{2}}, \underline{1, 0^5})\big] \end{aligned} \tag{5.50}$$

A similar field redefinition relate the doublet states on the orbifold to those on the resolutions:

$$(2,1)(1)_{\text{RES}} = \text{BLW}^{-1} \cdot (2,1)(1)_{\text{ORB}} \ , \tag{5.51}$$

or in terms of the corresponding weights:

$$\pm(\mp\tfrac{1}{2}^2, \tfrac{1}{2}^6)(0^8) = \mp\big[-(0^2, \tfrac{1}{2}^6)(0^8) + (\pm\tfrac{1}{2}^2, 0, 0^5)\big] \tag{5.52}$$

This analysis shows that the spectrum on this orbifold resolution with spinorial blowup modes is the same as for the previous choice of bundle vectors corresponding to vectorial blowup modes. This can be seen explicitly by comparing columns three and four of Table 5.2 and Table 5.3. The effect of the Wilson line is very different however:

5.3.6 Wilson line projected spinoral blowup model – With Torsion

Since the spinorial blowup modes were precisely considered to avoid the issue that the blowup modes are projected out by the Wilson line on the additional torus if torsion is switched on, the case with torsion is discussed below. (The spinorial blowup model without torsion suffers from similar issues as the vectorial blowup model with torsion and is ignored in the following.)

As stressed on resolution geometries one has to make an educated guess how torsion between the Wilson line and the orbifold twist is implemented based on intuition derived from the orbifold description. Concretely, the spinorial blowup model is further compactified on a circle S^1 with a discrete Wilson line:

$$W = (0^7, 1)(1, 0^7) \ . \tag{5.53}$$

The Wilson line projection condition in the presence of torsion on this resolution is assumed to be implemented as follows:

$$W \cdot P \equiv 0 \ . \tag{5.54}$$

The motivation for this from the orbifold description is, that for the twisted states, which feel the presence of the torsion phase, the relation between the $P_{\rm sh}$ and P involves V_α for which $W \cdot V_\alpha = \frac{1}{2}$ in this case. Hence, the effect of the torsion for the projection condition (5.11) is compensated by the fact that the blowup mode itself is spinorial. Consequently, the gauge group on the blowup is:

$$SU(2)_1 \times SU(2)_2 \times SU(6) \times SO(16)' \tag{5.55}$$

and the resulting five dimensional spectrum reads:

$$2\,(2,2,6)(1) + 14\,(1,1,15)(1) \ . \tag{5.56}$$

This is compatible with the orbifold spectrum with the Wilson line and the torsion phase. Indeed, the spinorial blowup models induce the symmetry breaking:

$$SO(12) \to SU(6) \ . \tag{5.57}$$

The broken generators are $\pm(0^2, \underline{1^2, 0^4})(0^8)$ correspond to two massive vector multiplets in the $(1,1,15)(1)$ representation. The charged orbifold spectrum branches as follows:

$$\begin{aligned} (2,2,12)(1) \quad &\to \quad 2\,(2,2,6)(1) \ , \\ \tfrac{1}{2}(1,1,32)(1) \quad &\to \quad (1,1,1)(1) + (1,1,15)(1) \ . \end{aligned} \tag{5.58}$$

The sixteen singlets $(1,1,1)(1)$ are the sixteen blowup modes and appear on the blowup as axions. Two of the $(1,1,15)(1)$ pair up with the broken generators to form the two massive vector multiplets. This leaves fourteen $(1,1,15)(1)$ in the massless charged spectrum.

5.3.7 Spinor–Vector Duality on Resolutions

In this final subsection some possible lessons for the realisation of spinor–vector dualities on orbifold resolutions and smooth geometries in general are discussed based on the results of the previous subsections.

Like in free fermionic models, also on orbifolds one expect spinor–vector dualities to be present and easily identifiable. Both descriptions have an underlying worldsheet structure and can be encoded in (one–loop) string partition functions in which additional torsion phases may be present. The dictionary between free fermionic and orbifold models developed in [50] may be used to relate these description in all fine print.

Moving from the orbifold point to smooth resolutions blowup modes have to be selected. These are twisted states which develop VEVs inducing the blowup of the orbifold singularities. Since the Wilson lines on (additional) cycles lead to projections of the twisted spectrum with or without torsion, the selected blowup modes may not be in the spectrum anymore, which leads to various complications. A prime one being that the choice of the torsion phase affects which blowup modes are available.

In the particular cases considered here of orbifold and resolution models of $T^4/\mathbb{Z}_2 \times S^1$ with a Wilson line, the spinor–vector duality mapping is summarised in Table 5.4. On the

Torsion Phase (ϵ)	Without ($\epsilon = 0$)	With ($\epsilon = 1$)
Orbifold		
Gauge Group	$SU(2)_1 \times SU(2)_2 \times SO(12) \times SO(16)'$	$SU(2)_1 \times SU(2)_2 \times SO(12) \times SO(16)'$
Spectrum	$(2,2,12)(1) + 16\,\frac{1}{2}(1,2,12)(1)$	$(2,2,12)(1) + 16\,\frac{1}{2}(1,1,32)(1)$
	$+32\,(2,1,1)(1) + 4(1,1,1)(1)$	$+4(1,1,1)(1)$
Blowup		
Modes $P_{\mathrm{sh},\alpha} = V_\alpha$	$(\frac{1}{2}, -\frac{1}{2}, 1, 0^5)(0^8)$	$(0^2, \frac{1}{2}^6)(0^8)$
Gauge Group	$SU(2) \times SO(10) \times SO(16)'$	$SU(2)_1 \times SU(2)_2 \times SU(6) \times SO(16)'$
Spectrum	$2\,(2,10)(1) + 36\,(2,1)(1)$	$2\,(2,2,6)(1) + 14\,(1,1,15)(1)$
	$+14\,(1,10)(1) + 14\,(1,1)(1)$	

Table 5.4: This table summarises how a spinor–vector duality is visible in orbifold and resolution models. Since the resolutions depend on the choice of blowup modes, their gauge groups and therefore their spectra make this duality less apparent.

orbifold the spinor–vector duality can clearly be seen: the model without torsion contains sixteen additional $SO(12)$ vector which are also $SU(2)$ doublets but no $SO(12)$ spinors, while the model with torsion has sixteen $SO(12)$ spinors but the $SO(12)$ vectors are absent. On the resulting resolutions using blowup modes indicated in the table the picture is far less transparent because the gauge groups in both cases are different. But the important characteristics of the spinor–vector duality can still be identified: In the resolution model without torsion in total eighteen vectors of $SO(10)$ are present while in the model with torsion there are eight vectors, (6)–plets, and fourteen anti–symmetric tensors, the (15)–plets, of $SU(6)$ present. These (15)–plets can only arise from the branching of the spinorial representation of $SO(12)$. Hence, the spectra on the resolutions still exhibit properties associated to the spinor–vector duality, albeit in some disguise.

5.4 Conclusion

Summary

The main aim of this chapter was to study the spinor–vector duality on five dimensional smooth geometries. Inspired by the models presented in [48] the orbifold $T^4/\mathbb{Z}_2$ with an additional circle with a Wilson line, is considered. This Wilson line distinguishes between integral and half–integral weights in the string spectrum. As to be expected from that depending on a generalized torsion phase between the orbifold twist and the Wilson line, the resulting five dimensional models indeed exhibit a spinor–vector duality.

Using standard resolution techniques the blowup of the orbifold $T^4/\mathbb{Z}_2$ was constructed.

Since, this orbifold by itself leads to a six dimensional model, the full massless spectrum on the resolution can be determined with the help of the multiplicity operator and was shown to match completely with the orbifold spectrum upon taking field redefinitions involving the blowup modes into account. After that the effect of the Wilson line on the additional circle was considered in the resolution setting. In the resolution model where the blowup modes are all vectorial, this resulted in a projection of the massless spectrum consistent with the expectations from the orbifold theory.

On smooth geometries the interpretation and implementation of the torsion phase between the orbifold twist and the Wilson line is obscured as there is no notion of the former. Since the smooth geometry in the present chapter was obtained as an orbifold resolution, the effect of the generalised torsion phase on the blowup could be conjectured to act as expected from the orbifold theory. But proceeding in this way led to an inconsistent spectrum. The reason for this could be traced to the fact that, because of the torsion phase the vectorial twisted states were projected out, but precisely those were used to generate the blowup. To overcome this problem, a second resolution model was considered, where spinorial twisted states were used as blowup modes instead. The effect of the Wilson line with the torsion phase switched on is to keep them in the orbifold theory and the resolution spectrum made sense again. However, because the spinorial blowup modes led to a further symmetry breaking, the gauge group of interest was no longer $SO(10)$ but rather $SU(5)$. Table 5.4 collects the uncovered details of the spinor–vector duality on the orbifold and its resolution.

To summarise, an example of the spinor–vector duality could be realised on a smooth resolution, but the picture of the duality is more subtle as the gauge groups of the dual models are not the same. The underlying reason was that the available blowup modes with the torsion phase switched on or off are complementary, so that different blowup modes are needed to be selected depending on the torsion choice. We expect this feature to be generic as long as the generalised torsion involves the orbifold twist, since the projection of the twisted states (the candidate blowup modes) then depends on the choice of the torsion phase. Of course, there may be other ways, that a spinor–vector duality can be induced on smooth compactifications.

Outlook

One complication encountered in this work was how to implement generalised torsion phases on smooth geometries. In particular, in effective supergravity compactifications it is not clear how the generalised GSO phases of string theory should be taken into account. It is interesting to note that certain forms of discrete torsion can be understood as a group action on the B–field [87–90]. This description might help to develop a deeper understanding of generalised GSO projections on smooth geometries.

In any case, and motivated for the need of having a discrete torsion we can understand and implement into our resolved models we will take our attention to GLSM in Chapter 7.

Chapter 6

Taming Triangulation Dependence of $T^6/\mathbb{Z}_2 \times \mathbb{Z}_2$ Resolutions

6.1 Introduction

Resolutions of certain toroidal orbifolds, like $T^6/\mathbb{Z}_2 \times \mathbb{Z}_2$, are far from unique, due to triangulation dependence of their resolved local singularities. This leads to an explosion of the number of topologically distinct smooth geometries associated to a single orbifold. By introducing a parameterisation to keep track of the triangulations used at all resolved singularities simultaneously, (self–)intersection numbers and integrated Chern classes can be determined for any triangulation configuration. Using this method the consistency conditions of line bundle models and the resulting chiral spectra can be worked out for any choice of triangulation. Moreover, by superimposing the Bianchi identities for all triangulation options much simpler though stronger conditions are uncovered. When these are satisfied, flop–transitions between all different triangulations are admissible. Various methods are exemplified by a number of concrete models on resolutions of the $T^6/\mathbb{Z}_2 \times \mathbb{Z}_2$ orbifold.

The analysis of the effective field theory limit of $\mathbb{Z}_2 \times \mathbb{Z}_2$ heterotic–string orbifolds and their resolutions is therefore well motivated from the phenomenological as well as the mathematical point of views. The analysis proceeds by the construction of toroidal $T^6/\mathbb{Z}_2 \times \mathbb{Z}_2$ heterotic–string orbifolds and resolving the orbifold singularities using these well–established methodologies. However, a problematic caveat is the enormous number of possibilities that this opens up [32,76,77]: The $T^6/\mathbb{Z}_2 \times \mathbb{Z}_2$ orbifold has 64 $\mathbb{C}^3/\mathbb{Z}_2 \times \mathbb{Z}_2$ singularities where $\mathbb{Z}_2$–fixed tori intersect, which all need to be resolved to obtain a smooth geometry. Each $\mathbb{C}^3/\mathbb{Z}_2 \times \mathbb{Z}_2$ singularity can be blown up in four topologically distinct ways encoded by four triangulations of the toric diagram of the resolved singularity. This results in a total of 4^{64} a priori distinct possibilities. While the symmetry structure of the $\mathbb{Z}_2 \times \mathbb{Z}_2$ orbifold can be used to reduce this number by some factor, it still leaves a huge number (of the order of 10^{33}) genuinely distinct choices. This is not a minor complication, as many physical properties of the resulting effective field theories are sensitively dependent on the triangulation chosen. These range from the spectra of massless states in the low energy effective theory to the structure and strength of interactions among them. The only way to overcome this complication was by side stepping it: one simply makes some choice for the triangulation of all these resolved singularities and analyses the resulting physics in that particular case. This led to some insights in the structure

of the theory in a somewhat larger part of the moduli space, but it seemed hopeless to extract any meaningful generic information about the properties of resolved $T^6/\mathbb{Z}_2 \times \mathbb{Z}_2$ orbifolds.

A way forward is therefore to develop a formalism which allows computations for any choice of the triangulation of the 64 resolved $\mathbb{Z}_2 \times \mathbb{Z}_2$ singularities. This is the task that we undertake in this chapter. Moreover, having established such a method opens up the possibility to study some properties of resolved $T^6/\mathbb{Z}_2 \times \mathbb{Z}_2$ orbifolds which are independent of triangulation choices or that hold in all possible triangulations simultaneously. To this end the chapter has been structured as follows:

Outline

Section 6.2 lays the foundation of this work by first recalling some basic facts of resolutions of the $T^6/\mathbb{Z}_2 \times \mathbb{Z}_2$ orbifold and line bundle backgrounds on them. After that notation is developed to parameterise the triangulation choice at each of the 64 resolved $\mathbb{Z}_2 \times \mathbb{Z}_2$ singularities, in terms of which the fundamental (self–)intersection numbers and the Chern classes are expressed. This allows to obtain relatively compact expressions for the volumes of curves, divisors and the manifold as a whole. Moreover, the flux quantisation conditions, the Bianchi identities and the multiplicity operator to determine the chiral spectrum can all be written down for any triangulation choice.

In Section 6.3 it is argued that the flux quantisation conditions are, in fact, triangulation independent: if satisfied in a particular choice of triangulation, it holds for all. In addition, having written down Bianchi identities for any possible choice of triangulation of all 64 resolved singularities, one may wonder what requirements are obtained if one insists that these conditions hold for all triangulation choices simultaneously. Surprisingly, it can be shown that the resulting conditions are much simpler than those in any particular triangulation.

The following two sections provide various examples of the general results of the preceding two. In Section 6.4 models are considered without any Wilson lines so that all 64 resolved singularities may be treated in the same way. In particular, it stresses that the flux quantisation conditions are essential: when violated, the difference between the local multiplicities is not integral. Finally, Section 6.5 revisits the so–called resolved Blaszczyk GUT model [24, 32]. A model inspired by this GUT model is considered, which is consistent for any possible choice of triangulation.

The chapter is completed with a summary and an outlook. The Appendix **??** provides some useful identities for second and third Chern classes for manifolds with vanishing first Chern class.

6.2 Resolutions of $T^6/\mathbb{Z}_2 \times \mathbb{Z}_2$

This section is devoted to develop some of the topological and geometrical properties of resolutions of the toroidal orbifold $T^6/\mathbb{Z}_2 \times \mathbb{Z}_2$. In fact, there are various $T^6/\mathbb{Z}_2 \times \mathbb{Z}_2$ orbifolds [50, 99, 118, 128]: here we focus exclusively on the orbifold with Hodge numbers (51,3). Techniques to determine resolutions of toroidal orbifolds have been well–studied [76]; here, in particular, the methods exploited in [32] are used. Also the resolutions of this orbifold have been considered before, however in the past one always had to make some assumptions which triangulation(s) to be considered, as the total number of choices (naively 4^{64}) is a daunting

number. This section provides a brief review of this literature, but the main purpose is to develop a formalism to treat all of these possible triangulations simultaneously.

6.2.1 The $T^6/\mathbb{Z}_2 \times \mathbb{Z}_2$ orbifold

The orbifold geometry will be taken to be factorisable of T^6 on the simplest rectangular lattice. The six torus coordinates are grouped into three complex ones on which two order–two orbifold reflections R_1, R_2 and their product $R_3 = R_1 R_2$ act. They are representations of $\mathbb{Z}_2 \times \mathbb{Z}_2$ with non–trivial elements

$$\mathrm{diag}(R_1) = (1,-1,-1)\ , \quad \mathrm{diag}(R_2) = (-1,1,-1)\ , \quad \mathrm{diag}(R_3) = \mathrm{diag}(R_1 R_2) = (-1,-1,1)\ . \tag{6.1}$$

Each reflection, R_1, R_2 and R_3, has $4{\cdot}4 = 16$ fixed points: $f^1_{\beta\gamma}$, $f^2_{\alpha\gamma}$ and $f^3_{\alpha\beta}$. These singularities are conveniently labeled by $\mu,\nu,\alpha,\beta,\gamma = 1,2,3,4 = 00,01,10,11$; i.e. interpreting them as binary multi–indices $\alpha = (\alpha_1,\alpha_2)$ is reserved for the first two–torus, $\beta = (\beta_3,\beta_4)$ for the second and $\gamma = (\gamma_5,\gamma_6)$ for the third, with the entries take the values $\alpha_1,\alpha_2,\beta_3,\beta_4,\gamma_5,\gamma_6 = 0,1$. The translation between both conventions read: $\alpha = 2\alpha_1 + \alpha_2 + 1$, $\beta = 2\beta_3 + \beta_4 + 1$ and $\gamma = 2\gamma_5 + \gamma_6 + 1$, respectively. (The (multi–)indices μ,ν are used to label the fixed points in any of the three two–tori in order to write compact expressions.)

Assuming that the tori have unit length, the fixed points may be represented as

$$f^1_{\beta\gamma} = \left(0, \tfrac{\beta_1+\beta_2\,i}{2}, \tfrac{\gamma_1+\gamma_2\,i}{2}\right)\ , \quad f^2_{\alpha\gamma} = \left(\tfrac{\alpha_1+\alpha_2\,i}{2}, 0, \tfrac{\gamma_1+\gamma_2\,i}{2}\right)\ , \quad f^3_{\alpha\beta} = \left(\tfrac{\alpha_1+\alpha_2\,i}{2}, \tfrac{\beta_1+\beta_2\,i}{2}, 0\right)\ . \tag{6.2}$$

The fixed set of each reflection has the topology of a torus orbifolded by the action of the other orbifold actions which leads to four fixed points on a fixed tori. Hence, in total the $T^6/\mathbb{Z}_2 \times \mathbb{Z}_2$ orbifold possesses 64 $\mathbb{C}^3/\mathbb{Z}_2 \times \mathbb{Z}_2$ singularities,

$$f_{\alpha\beta\gamma} = \left(\tfrac{\alpha_1+\alpha_2\,i}{2}, \tfrac{\beta_1+\beta_2\,i}{2}, \tfrac{\gamma_1+\gamma_2\,i}{2}\right)\ , \tag{6.3}$$

coming from every combination of the four fixed points in each of the three complex planes.

6.2.2 Geometry of the $T^6/\mathbb{Z}_2 \times \mathbb{Z}_2$ Resolutions

The geometry of the resulting resolved orbifolds are characterised by the set of four-cycles (divsors), which are obtained by setting one complex coordinate used in the resolution to zero. There are three classes of divisors [32, 76]: 6 inherited divisors $R_i := \{u_i = 0\}$ and $R'_i := \{v_i = 0\}$ that descend from each of the three torus of the orbifold (u_i and v_i, $i = 1,2,3$ are the coordinates of the elliptic curves describing the two–dimensional tori that make up T^6), 12 ordinary divisors $D_{1,\alpha} := \{z_{1,\alpha} = 0\}\,, D_{2,\beta} := \{z_{2,\beta} = 0\}$, and $D_{3,\gamma} := \{z_{3,\gamma} = 0\}$ ($z_{i,\mu}$ $i = 1,2,3$ are the coordinates of the covering space) and finally 48 exceptional divisors $E_{1,\beta\gamma} := \{x_{1,\beta\gamma} = 0\}\,, E_{2,\alpha\gamma} := \{x_{2,\alpha\gamma} = 0\}$, and $E_{3,\alpha\beta} := \{x_{3,\alpha\beta} = 0\}$ ($x_{i,\mu\nu}$ are extra coordinates used for the resolution) that appear in the blow–up process.

Not all these divisors are independent; there are a number of linear relations among them, namely:

$$\begin{aligned} &2D_{1,\alpha} \sim R_1 - \sum_\gamma E_{2,\alpha\gamma} - \sum_\beta E_{3,\alpha\beta}\ , \quad 2D_{2,\beta} \sim R_2 - \sum_\gamma E_{1,\beta\gamma} - \sum_\alpha E_{3,\alpha\beta} \\ &2D_{3,\gamma} \sim R_3 - \sum_\beta E_{1,\beta\gamma} - \sum_\alpha E_{2,\alpha\gamma}\ , \quad R'_i \sim R_i \end{aligned} \tag{6.4}$$

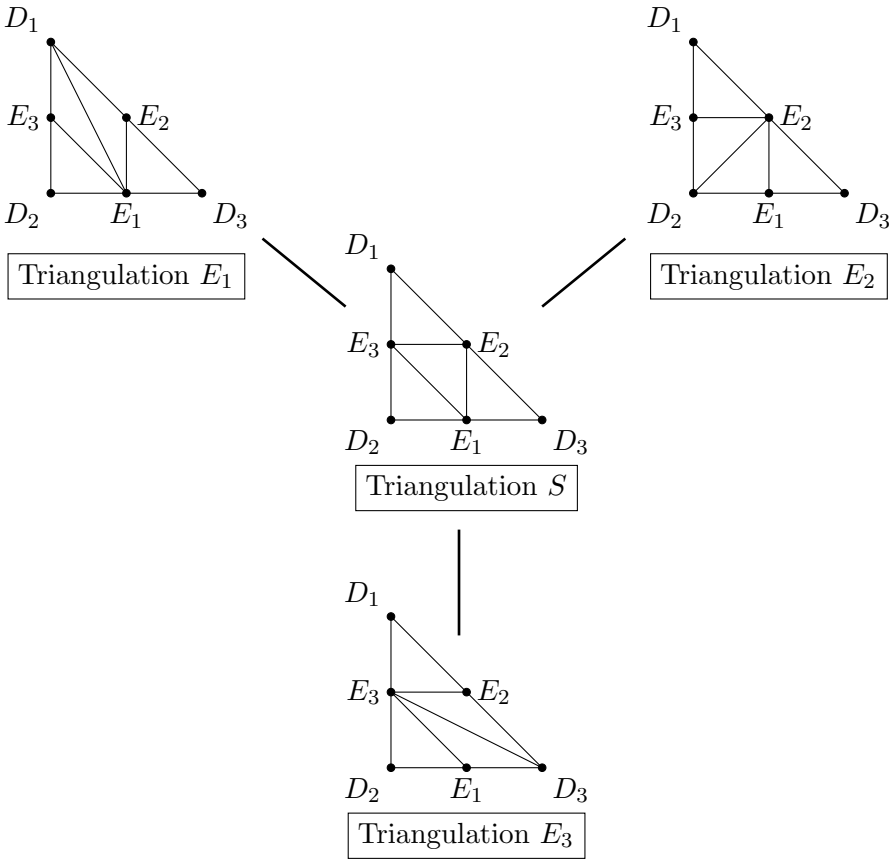

Figure 6.1: The four different triangulation, the E_1–, E_2–, E_3– and S–triangulation, of the projected toric diagram are given of the resolved $\mathbb{C}^3/\mathbb{Z}_2\times\mathbb{Z}_2$. The left–right–arrows indicate the possible flop–transition between different triangulations, which shows that any flop–transition always involves the S–triangulation.

Here $\sim$ means that these divisors interpreted as $(1,1)$–forms differ by exact forms. So in the end 3 R_i and 48 E_r provide via the Poincaré duality a basis of the real cohomology group, i.e. of the $(1,1)$–forms, on the resolved manifold.

6.2.3 Triangulation Dependence and Flop–Transitions

To complete the description of the geometry of a resolved orbifold, the intersection numbers of these divisors have to be specified. A major complication to specify the intersection numbers of the resolved $T^6/\mathbb{Z}_2\times\mathbb{Z}_2$ orbifold is that there is an indeterminacy, because of the triangulation dependence: each resolved $\mathbb{C}^3/\mathbb{Z}_2\times\mathbb{Z}_2$ admits four inequivalent resolutions encoded by four different triangulations of the toric diagram of the $\mathbb{C}^3/\mathbb{Z}_2\times\mathbb{Z}_2$ singularity. The local projected toric diagrams are given in figure 6.1. There are three triangulations, E_1, E_2 and E_3, where are all curves, that go through the interior of the projected toric diagram, connect to one of these exceptional divisors. For example in triangulation E_1 the curves E_1E_2, E_1E_3 and E_1D_1 all exist. In the final triangulation, dubbed the S–triangulation, all the exceptional divisors

Triangl.	$\delta^{E_1}_{\alpha\beta\gamma}$	$\delta^{E_2}_{\alpha\beta\gamma}$	$\delta^{E_3}_{\alpha\beta\gamma}$	$\delta^{S}_{\alpha\beta\gamma}$	$\Delta^1_{\alpha\beta\gamma}$	$\Delta^2_{\alpha\beta\gamma}$	$\Delta^3_{\alpha\beta\gamma}$	$1-\Delta^1_{\alpha\beta\gamma}$	$1-\Delta^2_{\alpha\beta\gamma}$	$1-\Delta^3_{\alpha\beta\gamma}$
E_1	1	0	0	0	-1	1	1	2	0	0
E_2	0	1	0	0	1	-1	1	0	2	0
E_3	0	0	1	0	1	1	-1	0	0	2
S	0	0	0	1	0	0	0	1	1	1

Table 6.1: The values of the step functions $\delta^T_{\alpha\beta\gamma}$ and their variations $\Delta^i_{\alpha\beta\gamma}$, defined in (6.5) and (6.7), resp., for the different triangulations are given.

intersect since the curves E_1E_2, E_2E_3 and E_3E_1 all exist.

The four triangulations of the projected toric diagram given in figure 6.1 are related to each other via flop–transitions. From this figure it can be inferred, that the E_1, E_2 and E_3–triangulations are all related via a single flop to the S–triangulation. For example, during the flop–transition from the E_1–triangulation to the S–triangulation, the curve E_1D_1 shrinks to zero size and disappears while the curve E_1E_2 appears. To go from one E–triangulation to another one always has to go through the S–triangulation. For example, for the transition from triangulation E_1 to E_2, first the curve E_1D_1 is replaced by the curve E_2E_3 to form the S–triangulation and after that the curve E_1E_3 is replaced by the curve E_2D_2 to arrive in the E_2–triangulation. This shows that the special role the S–triangulation plays in flop–transitions.

During a flop–transition some curve shrinks to zero size. This means that in this process the effective field theory approximation in the supergravity regime breaks down and stringy corrections could become important. Since, this work only makes use of effective field theory and geometrical methods, the flop–transitions themselves are beyond our description. But the geometries and the spectra on both sides of flops can be determined.

6.2.4 Parameterising Triangulations

Given that there are four triangulation for each $\mathbb{C}^3/\mathbb{Z}_2\times\mathbb{Z}_2$ and 64 $\mathbb{Z}_2\times\mathbb{Z}_2$ singularities, this gives a naively total number of 4^{64} possibilities (up to some permutation symmetries) [32]. As important topological data such as the intersection numbers of the divisors varies for each triangulation, it is particularly useful to develop some formalism to study spectra and the consistency conditions (such as Bianchi identities) for all triangulation choices simultaneously. Next, a formalism will be laid out that is capable of doing just that.

Define the following four functions:

$$\delta^T_{\alpha\beta\gamma}=\begin{cases}1 & \text{if triangulation } T \text{ is used,}\\ 0 & \text{if other triangulation is used,}\end{cases} \tag{6.5}$$

of (α,β,γ) for the four possible triangulations $T=S$, E_1, E_2 and E_3. Since at any of the 64 singularity resolutions one of the four triangulations has to be used, it follows that

$$\delta^{E_1}_{\alpha\beta\gamma}+\delta^{E_2}_{\alpha\beta\gamma}+\delta^{E_3}_{\alpha\beta\gamma}+\delta^{S}_{\alpha\beta\gamma}=1\ . \tag{6.6}$$

Thus, say, $\delta^S_{\alpha\beta\gamma}$ is a function of the others. The following combinations of the remaining three independent functions prove particularly useful:

$$\begin{aligned}\Delta^1_{\alpha\beta\gamma} &= -\delta^{E_1}_{\alpha\beta\gamma} + \delta^{E_2}_{\alpha\beta\gamma} + \delta^{E_3}_{\alpha\beta\gamma} \ , \\ \Delta^2_{\alpha\beta\gamma} &= \delta^{E_1}_{\alpha\beta\gamma} - \delta^{E_2}_{\alpha\beta\gamma} + \delta^{E_3}_{\alpha\beta\gamma} \ , \\ \Delta^3_{\alpha\beta\gamma} &= \delta^{E_1}_{\alpha\beta\gamma} + \delta^{E_2}_{\alpha\beta\gamma} - \delta^{E_3}_{\alpha\beta\gamma} \ .\end{aligned} \tag{6.7}$$

For example, this means that $\Delta^1_{\alpha\beta\gamma}$ equals -1 if singularity $f_{\alpha\beta\gamma}$ is resolved using triangulation E_1, 1 if E_2 and E_3 and 0 if S. The values that these functions take can be easily read off from the Table 6.1. It follows immediately that

$$1 - \Delta^1_{\alpha\beta\gamma} - \Delta^2_{\alpha\beta\gamma} - \Delta^3_{\alpha\beta\gamma} = \delta^S_{\alpha\beta\gamma} \ , \qquad 1 - \Delta^i_{\alpha\beta\gamma} = 2\,\delta^{E_i}_{\alpha\beta\gamma} + \delta^S_{\alpha\beta\gamma} \ . \tag{6.8a}$$

and

$$\Delta^2_{\alpha\beta\gamma} + \Delta^3_{\alpha\beta\gamma} = 2\,\delta^{E_1}_{\alpha\beta\gamma} \ , \qquad \Delta^1_{\alpha\beta\gamma} + \Delta^3_{\alpha\beta\gamma} = 2\,\delta^{E_2}_{\alpha\beta\gamma} \ , \qquad \Delta^1_{\alpha\beta\gamma} + \Delta^2_{\alpha\beta\gamma} = 2\,\delta^{E_3}_{\alpha\beta\gamma} \ . \tag{6.8b}$$

6.2.5 Triangulation Dependence of (Self–)Intersections and Chern Classes

The fundamental (self–)intersection numbers of the basis of divisors read:

$$\begin{aligned}&R_1E^2_{1,\beta\gamma} = R_2E^2_{2,\alpha\gamma} = R_3E^2_{3,\alpha\beta} = -2 \ , && R_1R_2R_3 = 2 \ , \\ &E_{1,\beta\gamma}E^2_{2,\alpha\gamma} = E_{1,\beta\gamma}E^2_{3,\beta\gamma} = -1 + \Delta^1_{\alpha\beta\gamma} \ , && E^3_{1,\beta\gamma} = \sum_\alpha \left(1 + \Delta^1_{\alpha\beta\gamma}\right) \ , \\ &E_{2,\alpha\gamma}E^2_{1,\beta\gamma} = E_{2,\alpha\gamma}E^2_{3,\beta\gamma} = -1 + \Delta^2_{\alpha\beta\gamma} \ , && E^3_{2,\alpha\gamma} = \sum_\beta \left(1 + \Delta^2_{\alpha\beta\gamma}\right) \ , \\ &E_{3,\alpha\beta}E^2_{1,\beta\gamma} = E_{3,\alpha\beta}E^2_{2,\alpha\gamma} = -1 + \Delta^3_{\alpha\beta\gamma} \ , && E^3_{3,\alpha\beta} = \sum_\gamma \left(1 + \Delta^3_{\alpha\beta\gamma}\right) \ , \\ &E_{1,\beta\gamma}E_{2,\alpha\gamma}E_{3,\beta\gamma} = 1 - \Delta^1_{\alpha\beta\gamma} - \Delta^2_{\alpha\beta\gamma} - \Delta^3_{\alpha\beta\gamma} \ .\end{aligned} \tag{6.9}$$

and all others are always zero. These (self–)intersection numbers can be partially inferred from the results in ref. [32] as follows: as observed in that paper the (partially self–)intersection numbers involving the ordinary divisors R_i are triangulation independent. The (partial self–)intersection numbers involving all three labels α, β and γ are fully local, i.e. defined only at the resolution of the single singularity $f_{\alpha\beta\gamma}$. Thus the intersection numbers for these (partial self–)intersections can be directly read off from Table 4 of ref. [32]. (Using the functions $\Delta^i_{\alpha\beta\gamma}$ precisely the local intersection numbers of the four different triangulations of that table are reproduced.) This leaves the cubic self–intersection numbers $E^3_{1,\beta\gamma}$, $E^3_{2,\alpha\gamma}$ and $E^3_{3,\alpha\beta}$. But these can be determined using the linear equivalence relations (6.4). For example, since the divisors $D_{1,\alpha}$, $D_{3,\gamma}$ and $E_{2,\alpha\gamma}$ lie on a straight line in the toric diagram, their intersection vanishes: $D_{1,\alpha}E_{2,\alpha\gamma}D_{3,\gamma} = 0$. Inserting the linear equivalence relations then leads to the identity

$$E^3_{2,\alpha\gamma} = -\sum_\beta \left\{E_{1,\beta\gamma}E^2_{2,\alpha\gamma} + E_{3,\alpha\beta}E^2_{2,\alpha\gamma} + E_{1,\beta\gamma}E_{2,\alpha\gamma}E_{3,\alpha\beta}\right\} = \sum_\beta \left(1 + \Delta^2_{\alpha\beta\gamma}\right) \ . \tag{6.10}$$

This expresses $E^3_{2,\alpha\gamma}$ in fully local (partial self–)intersection numbers just determined. Inserting those leads to the final expression in this equation. The other two cubic self–intersections are computed in an analogous fashion.

With the fundamental (self–)intersection numbers fixed for any choice of triangulation of all of the 64 resolved $\mathbb{Z}_2 \times \mathbb{Z}_2$ singularities, all kind of other quantities can be computed. For example, the second Chern classes integrated over the basis of divisors can be determined to be given by

$$\begin{aligned} &c_2R_1 = c_2R_2 = c_2R_3 = 24 \ , \quad c_2E_{1,\beta\gamma} = \sum_\alpha \big(1 - 2\Delta^1_{\alpha\beta\gamma}\big) \ , \\ &c_2E_{2,\alpha\gamma} = \sum_\beta \big(1 - 2\Delta^2_{\alpha\beta\gamma}\big) \ , \quad c_2E_{3,\alpha\beta} = \sum_\gamma \big(1 - 2\Delta^3_{\alpha\beta\gamma}\big) \ . \end{aligned} \tag{6.11}$$

The third Chern class can be evaluated as

$$c_3 = \frac{1}{3}\sum_u (-)^u S^3_u \ , \tag{6.12}$$

using (**??**) given that the first Chern class vanishes. Since the inherited torus divisors R_i, R'_i have vanishing triple self–intersections, this expression reduces to a sum over all ordinary and exceptional divisors

$$c_3 = \frac{1}{3}\sum_\alpha D^3_{1,\alpha} + \frac{1}{3}\sum_\beta D^3_{2,\beta} + \frac{1}{3}\sum_\gamma D^3_{3,\gamma} + \frac{1}{3}\sum_{\beta.\gamma} E^3_{1,\beta\gamma} + \frac{1}{3}\sum_{\alpha,\gamma} E^3_{2,\alpha\gamma} + \frac{1}{3}\sum_{\alpha,\beta} E^3_{3,\alpha\beta} \ . \tag{6.13}$$

The first term can be written as

$$\sum_\alpha D^3_{1,\alpha} = -\frac{1}{8}\sum_{\alpha,\gamma} E^3_{2,\alpha\gamma} - \frac{1}{8}\sum_{\alpha,\beta} E^3_{3,\alpha\beta} - \frac{3}{8}\sum_{\alpha,\beta,\gamma}\Big(E^2_{2,\alpha\gamma}E_{3,\alpha\beta} + E_{2,\alpha\gamma}E^2_{3,\alpha\beta}\Big) \ , \tag{6.14}$$

using that there are no non–vanishing intersections of R_1 with $E_{2,\alpha\gamma}$ or $E_{3,\alpha\beta}$. Adding similar expressions involving $D_{2,\beta}$ and $D_{3,\gamma}$, one can show that

$$\begin{aligned} c_3 = -\frac{1}{8}\sum_{\alpha,\beta,\gamma}\Big\{E_{1,\beta\gamma}\big(E^2_{2,\alpha\gamma} + E^2_{3,\alpha\beta}\big) + E_{2,\alpha\gamma}\big(E^2_{1,\beta\gamma} + E^2_{3,\alpha\beta}\big) + E_{3,\alpha\beta}\big(E^2_{1,\beta\gamma} + E^2_{2,\alpha\gamma}\big)\Big\} \\ + \frac{1}{4}\sum_{\beta.\gamma} E^3_{1,\beta\gamma} + \frac{1}{4}\sum_{\alpha,\gamma} E^3_{2,\alpha\gamma} + \frac{1}{4}\sum_{\alpha,\beta} E^3_{3,\alpha\beta} \ . \end{aligned} \tag{6.15}$$

Finally, inserting the triangulation dependent intersection numbers (6.9), gives

$$c_3 = \frac{1}{4}\sum_{i,\alpha,\beta,\gamma}\Big(1 + \Delta^i_{\alpha\beta\gamma}\Big) - \frac{1}{4}\sum_{i,\alpha,\beta,\gamma}\Big(-1 + \Delta^i_{\alpha\beta\gamma}\Big) = 96 \ . \tag{6.16}$$

Note, in particular, that all the triangulation dependence in the form of the functions $\Delta^i_{\alpha\beta\gamma}$ drops out and the final result equals the well–known Euler number 96.

6.2.6 Line Bundle Backgrounds

The line bundle backgrounds considered in this chapter only have flux supported on the exceptional cycles:

$$\frac{\mathcal{F}}{2\pi} = \sum_{i,\mu,\nu} E_{i,\mu\nu}\, \mathsf{H}_{i,\mu\nu} \ , \qquad \mathsf{H}_{i,\mu\nu} = \sum_{I} \mathcal{V}^{I}_{i,\mu\nu}\, \mathsf{H}_{I} \ . \tag{6.17}$$

Here the Cartan generators H_I are anti–Hermitian and therefore so is the field strength $\mathcal{F}$. The entries of the line bundle vectors $\mathcal{V}_{i,\mu\nu}$ are subject to flux quantisation conditions which are triangulation dependent:

$$\int_C \frac{\mathcal{F}}{2\pi} = L^I\, \mathsf{H}_I \ , \qquad L \cong 0 \ , \tag{6.18}$$

where $\cong$ means equal up to $E_8 \times E_8$ lattice vectors, for any C inside the resolved orbifold. The resulting conditions for any choice of triangulation are listed in Table 6.2.

Flux quantisation conditions for arbitrary triangulations			
$R_1 E_{1,\beta\gamma}$	$2\,\mathcal{V}_{1,\beta\gamma} \cong 0$	$D_{1,\alpha} E_{1,\beta\gamma}$	$\big(\mathcal{V}_{1,\beta\gamma} - \mathcal{V}_{2,\alpha\gamma} - \mathcal{V}_{3,\alpha\beta}\big)\delta^{E_1}_{\alpha\beta\gamma} \cong 0$
$R_2 E_{2,\alpha\gamma}$	$2\,\mathcal{V}_{2,\alpha\gamma} \cong 0$	$D_{2,\beta} E_{2,\alpha\gamma}$	$\big(\mathcal{V}_{2,\alpha\gamma} - \mathcal{V}_{1,\beta\gamma} - \mathcal{V}_{3,\alpha\beta}\big)\delta^{E_2}_{\alpha\beta\gamma} \cong 0$
$R_3 E_{3,\alpha\beta}$	$2\,\mathcal{V}_{3,\alpha\beta} \cong 0$	$D_{3,\gamma} E_{3,\alpha\beta}$	$\big(\mathcal{V}_{3,\alpha\beta} - \mathcal{V}_{1,\beta\gamma} - \mathcal{V}_{2,\alpha\gamma}\big)\delta^{E_3}_{\alpha\beta\gamma} \cong 0$
$R_1 D_{2,\beta}$	$-\sum_{\gamma} \mathcal{V}_{1,\beta\gamma} \cong 0$	$D_{1,\alpha} E_{2,\alpha\gamma}$	$-\sum_{\beta} \Big\{\mathcal{V}_{3,\alpha\beta} + \big(\mathcal{V}_{1,\beta\gamma} - \mathcal{V}_{2,\alpha\gamma} - \mathcal{V}_{3,\alpha\beta}\big)\delta^{E_1}_{\alpha\beta\gamma}\Big\} \cong 0$
$R_1 D_{3,\gamma}$	$-\sum_{\beta} \mathcal{V}_{1,\beta\gamma} \cong 0$	$D_{1,\alpha} E_{3,\alpha\beta}$	$-\sum_{\gamma} \Big\{\mathcal{V}_{2,\alpha\gamma} + \big(\mathcal{V}_{1,\beta\gamma} - \mathcal{V}_{2,\alpha\gamma} - \mathcal{V}_{3,\alpha\beta}\big)\delta^{E_1}_{\alpha\beta\gamma}\Big\} \cong 0$
$R_2 D_{1,\alpha}$	$-\sum_{\gamma} \mathcal{V}_{2,\alpha\gamma} \cong 0$	$D_{2,\beta} E_{1,\beta\gamma}$	$-\sum_{\alpha} \Big\{\mathcal{V}_{3,\alpha\beta} + \big(\mathcal{V}_{2,\alpha\gamma} - \mathcal{V}_{1,\beta\gamma} - \mathcal{V}_{3,\alpha\beta}\big)\delta^{E_2}_{\alpha\beta\gamma}\Big\} \cong 0$
$R_2 D_{3,\gamma}$	$-\sum_{\alpha} \mathcal{V}_{2,\alpha\gamma} \cong 0$	$D_{2,\beta} E_{3,\alpha\beta}$	$-\sum_{\gamma} \Big\{\mathcal{V}_{1,\beta\gamma} + \big(\mathcal{V}_{2,\alpha\gamma} - \mathcal{V}_{1,\beta\gamma} - \mathcal{V}_{3,\alpha\beta}\big)\delta^{E_2}_{\alpha\beta\gamma}\Big\} \cong 0$
$R_3 D_{1,\alpha}$	$-\sum_{\beta} \mathcal{V}_{3,\alpha\beta} \cong 0$	$D_{3,\gamma} E_{1,\beta\gamma}$	$-\sum_{\alpha} \Big\{\mathcal{V}_{2,\alpha\gamma} + \big(\mathcal{V}_{3,\alpha\beta} - \mathcal{V}_{1,\beta\gamma} - \mathcal{V}_{2,\alpha\gamma}\big)\delta^{E_3}_{\alpha\beta\gamma}\Big\} \cong 0$
$R_3 D_{2,\beta}$	$-\sum_{\alpha} \mathcal{V}_{3,\alpha\beta} \cong 0$	$D_{3,\gamma} E_{2,\alpha\gamma}$	$-\sum_{\beta} \Big\{\mathcal{V}_{1,\beta\gamma} + \big(\mathcal{V}_{3,\alpha\beta} - \mathcal{V}_{1,\beta\gamma} - \mathcal{V}_{2,\alpha\gamma}\big)\delta^{E_3}_{\alpha\beta\gamma}\Big\} \cong 0$
$E_{1,\beta\gamma} E_{2,\alpha\gamma}$	$2\,\mathcal{V}_{2,\alpha\gamma}\,\delta^{E_1}_{\alpha\beta\gamma} + 2\,\mathcal{V}_{1,\beta\gamma}\,\delta^{E_2}_{\alpha\beta\gamma} + \big(\mathcal{V}_{1,\beta\gamma} + \mathcal{V}_{2,\alpha\gamma} - \mathcal{V}_{3,\alpha\beta}\big)\delta^{S}_{\alpha\beta\gamma} \cong 0$		
$E_{1,\beta\gamma} E_{3,\alpha\beta}$	$2\,\mathcal{V}_{3,\alpha\beta}\,\delta^{E_1}_{\alpha\beta\gamma} + 2\,\mathcal{V}_{1,\beta\gamma}\,\delta^{E_3}_{\alpha\beta\gamma} + \big(\mathcal{V}_{1,\beta\gamma} + \mathcal{V}_{3,\alpha\beta} - \mathcal{V}_{2,\alpha\gamma}\big)\delta^{S}_{\alpha\beta\gamma} \cong 0$		
$E_{2,\alpha\gamma} E_{3,\alpha\beta}$	$2\,\mathcal{V}_{3,\alpha\beta}\,\delta^{E_2}_{\alpha\beta\gamma} + 2\,\mathcal{V}_{2,\alpha\gamma}\,\delta^{E_3}_{\alpha\beta\gamma} + \big(\mathcal{V}_{2,\alpha\gamma} + \mathcal{V}_{3,\alpha\beta} - \mathcal{V}_{1,\beta\gamma}\big)\delta^{S}_{\alpha\beta\gamma} \cong 0$		

Table 6.2: The flux quantisation conditions on the line bundle vectors $\mathcal{V}_{i,\mu\nu}$ the resolved orbifold X using arbitrary triangulation at the 64 $\mathbb{C}^3/\mathbb{Z}_2\times\mathbb{Z}_2$ resolutions.

6.2.7 General Bianchi Identities

Consistency of the effective field theory description demands that the integrated Bianchi identity

$$\int_D \Big\{ \mathrm{tr}\mathcal{F}^2 - \mathrm{tr}\mathcal{R}^2 \Big\} = 0 \tag{6.19}$$

over any divisor D vanishes. Here $\mathcal{R}$ denotes the anti–Hermitian curvature two–form. (When non–perturbative contributions of heterotic five–branes are taken into account this condition can be weakened somewhat [100].) By considering the basis of divisors spanned by the ordinary divisors R_i and the exceptional divisors $E_{1,\beta\gamma}$, $E_{2,\alpha\gamma}$ and $E_{3,\alpha\beta}$ the complete set of integrated Bianchi identities is obtained.

The three Bianchi identities on the three ordinary divisors, R_1, R_2 and R_3 are the ones one expects on K3 surfaces:

$$\sum_{\beta,\gamma} \mathcal{V}^2_{1,\beta\gamma} = 24 \ , \quad \sum_{\alpha,\gamma} \mathcal{V}^2_{2,\alpha\gamma} = 24 \ , \quad \sum_{\alpha,\beta} \mathcal{V}^2_{3,\alpha\beta} = 24 \ , \tag{6.20a}$$

and do not depend on the triangulations chosen. In contrast the Bianchi identities on the exceptional divisors are very sensitive to the triangulations used in the local resolutions. The sixteen Bianchi identities on $E_{1,\beta\gamma}$ take the form

$$\begin{aligned}\sum_{\alpha} \Big[&(1+\Delta^1_{\alpha\beta\gamma})\mathcal{V}^2_{1,\beta\gamma} + (-1+\Delta^1_{\alpha\beta\gamma})(\mathcal{V}^2_{2,\alpha\gamma}+\mathcal{V}^2_{3,\alpha\beta}) + 2(1-\Delta^1_{\alpha\beta\gamma}-\Delta^2_{\alpha\beta\gamma}-\Delta^3_{\alpha\beta\gamma})\mathcal{V}_{2,\alpha\gamma}\cdot\mathcal{V}_{3,\alpha\beta} \\ &+2(-1+\Delta^2_{\alpha\beta\gamma})\mathcal{V}_{1,\beta\gamma}\cdot\mathcal{V}_{2,\alpha\gamma} + 2(-1+\Delta^3_{\alpha\beta\gamma})\mathcal{V}_{1,\beta\gamma}\cdot\mathcal{V}_{3,\alpha\beta}\Big] = \sum_{\alpha}\Big[-2+4\,\Delta^1_{\alpha\beta\gamma}\Big] \ . \end{aligned} \tag{6.20b}$$

The sixteen Bianchi identities on $E_{2,\alpha\gamma}$ take the form

$$\begin{aligned}\sum_{\beta} \Big[&(1+\Delta^2_{\alpha\beta\gamma})\mathcal{V}^2_{2,\alpha\gamma} + (-1+\Delta^2_{\alpha\beta\gamma})(\mathcal{V}^2_{1,\beta\gamma}+\mathcal{V}^2_{3,\alpha\gamma}) + 2(1-\Delta^1_{\alpha\beta\gamma}-\Delta^2_{\alpha\beta\gamma}-\Delta^3_{\alpha\beta\gamma})\mathcal{V}_{1,\beta\gamma}\cdot\mathcal{V}_{3,\alpha\beta} \\ &+2(-1+\Delta^1_{\alpha\beta\gamma})\mathcal{V}_{2,\alpha\gamma}\cdot\mathcal{V}_{1,\beta\gamma} + 2(-1+\Delta^3_{\alpha\beta\gamma})\mathcal{V}_{2,\alpha\gamma}\cdot\mathcal{V}_{2,\alpha\gamma}\Big] = \sum_{\beta}\Big[-2+4\,\Delta^2_{\alpha\beta\gamma}\Big] \ . \end{aligned} \tag{6.20c}$$

And finally, the sixteen Bianchi identities on $E_{3,\alpha\beta}$ take the form

$$\begin{aligned}\sum_{\gamma} \Big[&(1+\Delta^3_{\alpha\beta\gamma})\mathcal{V}^2_{3,\alpha\beta} + (-1+\Delta^3_{\alpha\beta\gamma})(\mathcal{V}^2_{1,\beta\gamma}+\mathcal{V}^2_{2,\alpha\gamma}) + 2(1-\Delta^1_{\alpha\beta\gamma}-\Delta^2_{\alpha\beta\gamma}-\Delta^3_{\alpha\beta\gamma})\mathcal{V}_{1,\beta\gamma}\cdot\mathcal{V}_{2,\alpha\gamma} \\ &+2(-1+\Delta^1_{\alpha\beta\gamma})\mathcal{V}_{3,\alpha\beta}\cdot\mathcal{V}_{1,\beta\gamma} + 2(-1+\Delta^2_{\alpha\beta\gamma})\mathcal{V}_{3,\alpha\beta}\cdot\mathcal{V}_{2,\alpha\gamma}\Big] = \sum_{\gamma}\Big[-2+4\,\Delta^3_{\alpha\beta\gamma}\Big] \ . \end{aligned} \tag{6.20d}$$

6.2.8 Multiplicity Operators

A convenient tool to compute the chiral spectrum on a resolution with a line bundle background is the multiplicity operator N. It reads [60, 61]:

$$\mathsf{N} = \int_X \Big\{ \frac{1}{6}\Big(\frac{\mathcal{F}}{2\pi}\Big)^2 - \frac{1}{24}\Big(\frac{\mathcal{R}}{2\pi}\Big)^2 \Big\}\frac{\mathcal{F}}{2\pi} \tag{6.21}$$

and may be thought of as a representation dependent index. Hence, on all states it should be integral provided that the fundamental consistency conditions, flux quantisation and the integrated Bianchi identities, are fulfilled.

On the $T^6/\mathbb{Z}_2\times\mathbb{Z}_2$ resolutions the multiplicity operator can be evaluated to be equal to:

$$\begin{aligned}\mathsf{N}=\sum_{\alpha,\beta,\gamma}\Big[\;&\mathsf{H}_{1,\beta\gamma}\Big\{\tfrac{1}{3}(\mathsf{H}^2_{1,\beta\gamma}-\tfrac{1}{4})-\big(1-\Delta^1_{\alpha\beta\gamma}\big)\Big(\tfrac{1}{6}(\mathsf{H}^2_{1,\beta\gamma}-1)+\tfrac{1}{2}(\mathsf{H}_{2,\alpha\gamma}-\mathsf{H}_{3,\alpha\beta})^2\Big)\Big\}\\&+\mathsf{H}_{2,\alpha\gamma}\Big\{\tfrac{1}{3}(\mathsf{H}^2_{2,\alpha\gamma}-\tfrac{1}{4})-\big(1-\Delta^2_{\alpha\beta\gamma}\big)\Big(\tfrac{1}{6}(\mathsf{H}^2_{2,\alpha\gamma}-1)+\tfrac{1}{2}(\mathsf{H}_{1,\beta\gamma}-\mathsf{H}_{3,\alpha\beta})^2\Big)\Big\}\\&+\mathsf{H}_{3,\alpha\beta}\Big\{\tfrac{1}{3}(\mathsf{H}^2_{3,\alpha\beta}-\tfrac{1}{4})-\big(1-\Delta^3_{\alpha\beta\gamma}\big)\Big(\tfrac{1}{6}(\mathsf{H}^2_{3,\alpha\beta}-1)+\tfrac{1}{2}(\mathsf{H}_{1,\beta\gamma}-\mathsf{H}_{2,\alpha\gamma})^2\Big)\Big\}\\&-2\mathsf{H}_{1,\beta\gamma}\mathsf{H}_{2,\alpha\gamma}\mathsf{H}_{3,\alpha\beta}\;\Big]\,.\end{aligned}\tag{6.22}$$

The triangulation dependance is isolated to the second terms on the first three lines of this expression. From Table 6.1 it may be inferred that only the terms in the first line are switched on (with a multiplicative factor of 2) if triangulation E_1 is chosen, the second for E_2 and the third for E_3; all three are switched on (with a factor 1) for triangulation S.

Using the constraint (6.6) another representation of this operator can be obtained

$$\mathsf{N}=\sum_{\alpha,\beta,\gamma}\Big[\delta^{E_1}_{\alpha\beta\gamma}\,\mathsf{N}^{E_1}_{\alpha\beta\gamma}+\delta^{E_2}_{\alpha\beta\gamma}\,\mathsf{N}^{E_2}_{\alpha\beta\gamma}+\delta^{E_3}_{\alpha\beta\gamma}\,\mathsf{N}^{E_3}_{\alpha\beta\gamma}+\delta^{S}_{\alpha\beta\gamma}\,\mathsf{N}^{S}_{\alpha\beta\gamma}\Big]\,,\tag{6.23}$$

where

$$\mathsf{N}^{E_1}_{\alpha\beta\gamma}=\tfrac{1}{4}\,\mathsf{H}_{1,\beta\gamma}+\tfrac{1}{12}\,\mathsf{H}_{2,\alpha\gamma}\big(4\mathsf{H}^2_{2,\alpha\gamma}-1\big)+\tfrac{1}{12}\,\mathsf{H}_{3,\alpha\beta}\big(4\mathsf{H}^2_{3,\alpha\beta}-1\big)-\mathsf{H}_{1,\beta\gamma}\big(\mathsf{H}^2_{2,\alpha\gamma}+\mathsf{H}^2_{3,\alpha\beta}\big)\,,\tag{6.24a}$$

$$\mathsf{N}^{E_2}_{\alpha\beta\gamma}=\tfrac{1}{4}\,\mathsf{H}_{2,\alpha\gamma}+\tfrac{1}{12}\,\mathsf{H}_{1,\beta\gamma}\big(4\mathsf{H}^2_{1,\beta\gamma}-1\big)+\tfrac{1}{12}\,\mathsf{H}_{3,\alpha\beta}\big(4\mathsf{H}^2_{3,\alpha\beta}-1\big)-\mathsf{H}_{2,\alpha\gamma}\big(\mathsf{H}^2_{1,\beta\gamma}+\mathsf{H}^2_{3,\alpha\beta}\big)\,,\tag{6.24b}$$

$$\mathsf{N}^{E_3}_{\alpha\beta\gamma}=\tfrac{1}{4}\,\mathsf{H}_{3,\alpha\beta}+\tfrac{1}{12}\,\mathsf{H}_{1,\alpha\beta}\big(4\mathsf{H}^2_{1,\alpha\beta}-1\big)+\tfrac{1}{12}\,\mathsf{H}_{2,\alpha\gamma}\big(4\mathsf{H}^2_{2,\alpha\gamma}-1\big)-\mathsf{H}_{3,\alpha\beta}\big(\mathsf{H}^2_{1,\beta\gamma}+\mathsf{H}^2_{2,\alpha\gamma}\big)\,,\tag{6.24c}$$

$$\begin{aligned}\mathsf{N}^{S}_{\alpha\beta\gamma}=\;&\tfrac{1}{12}\,\mathsf{H}_{1,\beta\gamma}\big(2\mathsf{H}^2_{1,\beta\gamma}+1\big)+\tfrac{1}{12}\,\mathsf{H}_{2,\alpha\gamma}\big(2\mathsf{H}^2_{2,\alpha\gamma}+1\big)+\tfrac{1}{12}\,\mathsf{H}_{3,\alpha\beta}\big(2\mathsf{H}^2_{3,\alpha\beta}+1\big)+\mathsf{H}_{1,\beta\gamma}\mathsf{H}_{2,\alpha\gamma}\mathsf{H}_{3,\alpha\beta}\\&-\tfrac{1}{2}\,\mathsf{H}_{1,\beta\gamma}\big(\mathsf{H}^2_{2,\alpha\gamma}+\mathsf{H}^2_{3,\alpha\beta}\big)-\tfrac{1}{2}\,\mathsf{H}_{2,\alpha\gamma}\big(\mathsf{H}^2_{1,\beta\gamma}+\mathsf{H}^2_{3,\alpha\beta}\big)-\tfrac{1}{2}\,\mathsf{H}_{3,\alpha\beta}\big(\mathsf{H}^2_{1,\beta\gamma}+\mathsf{H}^2_{2,\alpha\gamma}\big)\,.\end{aligned}\tag{6.24d}$$

These operators can be thought of as the local resolution multiplicities at the resolved singularity (α,β,γ) using one of the four triangulations. In particular, when taking the same triangulation at all fixed points, the expressions (56) and (58) of ref. [32] are obtained from (6.23). In general, (6.23) implies that the spectrum in any triangulation can be determined from the local resolution operators (6.24) times the functions that indicate which triangulation has been used at each of the 64 $\mathbb{C}^3/\mathbb{Z}_2\times\mathbb{Z}_2$ resolved singularities. It should be emphasised that these local multiplicity operators $\mathsf{N}^T_{\alpha\beta\gamma}$ for a given triangulation T are not necessarily all integral; only their combination in (6.23) in general is.

6.2.9 Jumping Spectra due to Flop–Transitions

For a flop–transition to be possible it is necessary that all fundamental consistency conditions, like flux quantisation and the Bianchi identities, have to hold for both triangulation choices before and after the flop. Note that this implies, that if at some resolved singularity $f_{\alpha\beta\gamma}$ some of these fundamental consistency conditions are not fulfilled for triangulation S, then no flop–transitions can occur and resolution is frozen in one of the three triangulations E_1, E_2 or E_3. Moreover, if at all resolved $\mathbb{Z}_2 \times \mathbb{Z}_2$ singularities triangulation S is not admissible, no flop–transition is possible at all!

Assuming that at a resolved singularity $f_{\alpha\beta\gamma}$ a flop–transition can occur between triangulations S to E_i, the difference multiplicity

$$\Delta \mathsf{N}^i_{\alpha\beta\gamma} = \mathsf{N}^{E_i}_{\alpha\beta\gamma} - \mathsf{N}^S_{\alpha\beta\gamma} \tag{6.25}$$

measures the jump in the spectra when the flop–transition goes from triangulation S to E_i; $-\Delta \mathsf{N}^i_{\alpha\beta\gamma}$ the spectra jump in the opposite direction. This difference multiplicity operator has to be integral because the multiplicity operator (6.22) before and after the flop–transition is integral by an index theorem (since the fundamental consistency conditions are assumed to be fulfilled) and this operator is simply the difference of the spectra in the two cases.

6.2.10 Volumes and the DUY equations

Using the (self–)intersections (6.9) various volumes can be computed using the Kähler form

$$J = \sum_i a_i R_i - \sum_r b_r E_r \ , \tag{6.26}$$

involving the Kähler parameters a_i and b_r. The volumes of a curve C, a divisor D and the orbifold resolution X are given by

$$\mathrm{Vol}(C) = \int_C J \ , \qquad \mathrm{Vol}(D) = \int_D \frac{1}{2}\, J^2 \ , \qquad \mathrm{Vol}(X) = \int_X \frac{1}{3!}\, J^3 \ , \tag{6.27}$$

respectively. The resulting expressions for any choice of triangulation are given in Table 6.3.

The volumes of the divisors are constrained by the DUY equations [101,102]. The one–loop corrections to these equations are given by [77,93]

$$\int \frac{1}{2} J^2 \, \frac{\mathcal{F}}{2\pi} = \frac{e^{2\phi}}{16\pi} \int \Big\{ \mathrm{tr}\Big(\frac{\mathcal{F}'}{2\pi}\Big)^2 - \frac{1}{2}\mathrm{tr}\Big(\frac{\mathcal{R}}{2\pi}\Big)^2 \Big\} \frac{\mathcal{F}'}{2\pi} + (' \to '') \ , \tag{6.28}$$

where $\mathcal{F}'$ and $\mathcal{F}''$ denote the Abelian gauge fluxes in the first and second factor of the $E_8 \times E_8$ group, respectively, so that $\mathcal{F} = \mathcal{F}' + \mathcal{F}''$. This equation thus links the Kähler moduli a_i, b_r and the dilaton ϕ in general.

If the gauge background is embedded in just a single, say first E_8, or if one considers the heterotic $SO(32)$ theory instead, this equation may be rewritten as

$$\int \frac{1}{2} J^2 \, \frac{\mathcal{F}}{2\pi} = \frac{e^{2\phi}}{32\pi} \int \mathrm{tr}\Big(\frac{\mathcal{R}}{2\pi}\Big)^2 \frac{\mathcal{F}}{2\pi} = -\frac{e^{2\phi}}{16\pi} \int c_2 \frac{\mathcal{F}}{2\pi} \ , \tag{6.29}$$

Curves			
R_1R_2	$2\,a_3$	$D_{1,\alpha}E_{1,\beta\gamma}$	$\big(b_{1,\beta\gamma}-b_{2,\alpha\gamma}-b_{3,\alpha\beta}\big)\delta^{E_1}_{\alpha\beta\gamma}$
$R_1E_{1,\beta\gamma}$	$2\,b_{1,\beta\gamma}$	$D_{1,\alpha}E_{2,\alpha\gamma}$	$a_2-\sum\limits_{\beta}\Big\{b_{3,\alpha\beta}+\big(b_{1,\beta\gamma}-b_{2,\alpha\gamma}-b_{3,\alpha\beta}\big)\delta^{E_1}_{\alpha\beta\gamma}\Big\}$
$R_1D_{2,\beta}$	$a_3-\sum\limits_{\gamma}b_{1,\beta\gamma}$	$E_{1,\beta\gamma}E_{2,\alpha\gamma}$	$2\,b_{2,\alpha\gamma}\,\delta^{E_1}_{\alpha\beta\gamma}+2\,b_{1,\beta\gamma}\,\delta^{E_2}_{\alpha\beta\gamma}+\big(b_{1,\beta\gamma}+b_{2,\alpha\gamma}-b_{3,\alpha\beta}\big)\delta^{S}_{\alpha\beta\gamma}$

Divisors	
R_1	$2\,a_2a_3-\sum\limits_{\beta,\gamma}b^2_{1,\beta\gamma}$
$D_{1,\alpha}$	$a_2a_3-\sum\limits_{\gamma}a_2b_{2,\alpha\gamma}-\sum\limits_{\beta}a_3b_{3,\alpha\beta}+\sum\limits_{\beta,\gamma}\big(1-\delta^{E_1}_{\alpha\beta\gamma}\big)b_{2,\alpha\gamma}b_{3,\alpha\beta}$ $+\sum\limits_{\beta,\gamma}\delta^{E_1}_{\alpha\beta\gamma}\Big\{b_{1,\beta\gamma}\big(b_{2,\alpha\gamma}+b_{3,\alpha\beta}\big)-\frac{1}{2}\big(b^2_{1,\beta\gamma}+b^2_{2,\alpha\gamma}+b^2_{3,\alpha\beta}\big)\Big\}$
$E_{1,\beta\gamma}$	$2\,a_1b_{1,\beta\gamma}+\sum\limits_{\alpha}\Big\{\frac{1}{2}\big(1+\Delta^1_{\alpha\beta\gamma}\big)b^2_{1,\beta\gamma}+\big(1-\Delta^1_{\alpha\beta\gamma}-\Delta^2_{\alpha\beta\gamma}-\Delta^3_{\alpha\beta\gamma}\big)b_{2,\alpha\gamma}b_{3,\alpha\beta}$ $-\frac{1}{2}\big(1-\Delta^1_{\alpha\beta\gamma}\big)\big(b^2_{2,\alpha\gamma}+b^2_{3,\alpha\beta}\big)-\big(1-\Delta^2_{\alpha\beta\gamma}\big)b_{1,\beta\gamma}b_{2,\alpha\gamma}-\big(1-\Delta^3_{\alpha\beta\gamma}\big)b_{1,\beta\gamma}b_{3,\alpha\beta}\Big\}$

Full manifold	
X	$2\,a_1a_2a_3-\sum\limits_{\beta,\gamma}a_1b^2_{1,\beta\gamma}-\sum\limits_{\alpha,\gamma}a_2b^2_{2,\alpha\gamma}-\sum\limits_{\alpha,\beta}a_3b^2_{3,\alpha\beta}-\sum\limits_{\alpha,\beta,\gamma}\Big\{\frac{1}{2}\big(\Delta^1_{\alpha\beta\gamma}-1\big)b_{1,\beta\gamma}\big(b^2_{2,\alpha\gamma}+b^2_{3,\alpha\beta}\big)$ $+\frac{1}{2}\big(\Delta^2_{\alpha\beta\gamma}-1\big)b_{2,\alpha\gamma}\big(b^2_{1,\beta\gamma}+b^2_{3,\alpha\beta}\big)+\frac{1}{2}\big(\Delta^3_{\alpha\beta\gamma}-1\big)b_{3,\alpha\beta}\big(b^2_{1,\beta\gamma}+b^2_{2,\alpha\gamma}\big)+\frac{1}{6}\big(1+\Delta^1_{\alpha\beta\gamma}\big)b^3_{1,\beta\gamma}$ $+\frac{1}{6}\big(1+\Delta^2_{\alpha\beta\gamma}\big)b^3_{2,\alpha\gamma}+\frac{1}{6}\big(1+\Delta^3_{\alpha\beta\gamma}\big)b^3_{3,\alpha\gamma}+\big(1-\Delta^1_{\alpha\beta\gamma}-\Delta^2_{\alpha\beta\gamma}-\Delta^3_{\alpha\beta\gamma}\big)b_{1,\beta\gamma}b_{2,\alpha\gamma}b_{3,\alpha\beta}\Big\}$

Table 6.3: Volume of a collection of possibly existing curves, divisors and the resolved orbifold X as a whole using arbitrary triangulation at the 64 $\mathbb{C}^3/\mathbb{Z}_2\times\mathbb{Z}_2$ resolutions. Similar expression of the other curves and divisors can be obtained by permutations.

as $\mathcal{F}=\mathcal{F}'$ and $\mathcal{F}''=0$ using the integrate Bianchi identities (6.19). Inserting the expansion for the gauge flux in terms of the exceptional divisors E_r and using the integrated second Chern classes (6.11), leads to

$$\sum_{\beta,\gamma}\Big\{\mathrm{Vol}(E_{1,\beta\gamma})-\frac{e^{2\phi}}{16\pi}\sum_{\alpha}(1-2\Delta^1_{\alpha\beta\gamma})\Big\}\mathcal{V}^I_{1,\beta\gamma}+\sum_{\alpha,\gamma}\Big\{\mathrm{Vol}(E_{2,\alpha\gamma})-\frac{e^{2\phi}}{16\pi}\sum_{\beta}(1-2\Delta^2_{\alpha\beta\gamma})\Big\}\mathcal{V}^I_{2,\alpha\gamma}+$$
$$+\sum_{\alpha,\beta}\Big\{\mathrm{Vol}(E_{3,\alpha\beta})-\frac{e^{2\phi}}{16\pi}\sum_{\gamma}(1-2\Delta^3_{\alpha\beta\gamma})\Big\}\mathcal{V}^I_{3,\alpha\beta}=0\ . \tag{6.30}$$

If the gauge background lie in both E_8 factors simultaneously, then the $\mathrm{tr}\mathcal{R}^2$ term can be eliminated using the Bianchi identities (6.19) instead. Moreover, since both E_8 factors are

independent, the DUY equation may be split into two equations; one for each E_8 factor:

$$\begin{aligned}\int \frac{1}{2}J^2\,\frac{\mathcal{F}'}{2\pi} &= \frac{e^{2\phi}}{32\pi}\int\Big\{\mathrm{tr}\Big(\frac{\mathcal{F}'}{2\pi}\Big)^2-\mathrm{tr}\Big(\frac{\mathcal{F}''}{2\pi}\Big)^2\Big\}\frac{\mathcal{F}'}{2\pi}\ ,\\ \int \frac{1}{2}J^2\,\frac{\mathcal{F}''}{2\pi} &= -\frac{e^{2\phi}}{32\pi}\int\Big\{\mathrm{tr}\Big(\frac{\mathcal{F}'}{2\pi}\Big)^2-\mathrm{tr}\Big(\frac{\mathcal{F}''}{2\pi}\Big)^2\Big\}\frac{\mathcal{F}''}{2\pi}\ .\end{aligned} \tag{6.31}$$

Notice the relative sign difference between the otherwise very similar expressions in both E_8's. Evaluating these expressions further by inserting the intersection numbers (6.9) leads to rather lengthy and not very illuminating expressions. For this reason we refrain from stating them here.

6.3 Triangulation Independence

The results obtained in the previous section hold for any particular choice of the triangulation of each of the 64 resolved $\mathbb{C}^3/\mathbb{Z}_2\times\mathbb{Z}_2$ singularities. The aim of this section is to obtain results that hold for all choices of triangulation simultaneously: such results can be uncovered by superimposing the conditions for all the different choices of triangulation. It should be emphasised that we do not wish to imply that it is necessary that such results apply in all triangulations from the supergravity perspective. But surprisingly, superimposing consistency conditions leads to a huge reduction of the complexity of these equations. However, if all consistency conditions are satisfied in any triangulation, then arbitrary flop–transitions are admissible which opens up the possibility to study the resulting transitions in the massless spectra.

6.3.1 Flux Quantisation

Even though the flux quantisation conditions might seem to be dependent on the choice of the triangulations at the local singularities, in fact, they are all equivalent to

$$2\,\mathcal{V}_{i,\mu\nu}\cong 0\ ,\quad \sum_\rho \mathcal{V}_{i,\rho\nu}\cong 0\ ,\quad \sum_\rho \mathcal{V}_{i,\mu\rho}\cong 0\ ,\quad \mathcal{V}_{1,\beta\gamma}+\mathcal{V}_{2,\alpha\gamma}+\mathcal{V}_{3,\alpha\beta}\cong 0 \tag{6.32}$$

independently of the local triangulations chosen. To see this, notice first of all that the first three relations derived from curves that exist for any triangulation, see Table 6.2. Now, if triangulation E_1 has been chosen at the resolution of $f_{\alpha\beta\gamma}$, one has to impose the condition associated to curve $D_{1,\alpha}E_{1,\beta\gamma}$, if triangulation E_2 the condition associated to curve $D_{2,\beta}E_{2,\alpha,\gamma}$ and if triangulation E_3 the condition associated to curve $D_{3,\gamma}E_{3,\alpha\beta}$, respectively, while if triangulation S is used all the resulting three conditions have to be superimposed. However, all three of them are equivalent to the last condition in (6.32) using the first condition in this line which basically says that the signs of the bundle vectors in the flux quantisation conditions are irrelevant modulo 2. In other words, if the flux quantisation is satisfied for a single triangulation choice at all the 64 resolved $\mathbb{C}^3/\mathbb{Z}_2\times\mathbb{Z}_2$ singularities, the fluxes are properly quantised for any triangulation choice.

6.3.2 Reduction of Bianchi Identities

To determine the set of equations which guarantee that for any choice of triangulation of the 64 $\mathbb{C}^3/\mathbb{Z}_2 \times \mathbb{Z}_2$ resolutions, the Bianchi identities are solved, we can treat the triangulation dependent functions, $\Delta^1_{\alpha\beta\gamma}$, $\Delta^2_{\alpha\beta\gamma}$ and $\Delta^3_{\alpha\beta\gamma}$, as arbitrary functions. Hence, to solve the Bianchi identities for all choices, the coefficients in front of these functions need to cancel among themselves as well as the remaining contributions which do not multiply any of them. This leads to four set of equations for each set of sixteen Bianchi identities on each of the exceptional cycles. For the sixteen Bianchi identities on $E_{1,\beta\gamma}$ they read:

$$\sum_\alpha \Big[\mathcal{V}^2_{2,\alpha\gamma} + \mathcal{V}^2_{3,\alpha\beta} - \mathcal{V}^2_{1,\beta\gamma} + 2\,\mathcal{V}_{1,\beta\gamma}\cdot\mathcal{V}_{2,\alpha\gamma} + 2\,\mathcal{V}_{1,\beta\gamma}\cdot\mathcal{V}_{3,\alpha\beta} - 2\,\mathcal{V}_{2,\alpha\gamma}\cdot\mathcal{V}_{3,\alpha\beta}\Big] = -8\ ,$$

$$\mathcal{V}^2_{1,\beta\gamma} + \mathcal{V}^2_{2,\alpha\gamma} + \mathcal{V}^2_{3,\alpha\beta} - 2\,\mathcal{V}_{2,\alpha\gamma}\cdot\mathcal{V}_{3,\alpha\beta} = 4\ ,\quad \mathcal{V}_{1,\beta\gamma}\cdot\mathcal{V}_{2,\alpha\gamma} = \mathcal{V}_{1,\beta\gamma}\cdot\mathcal{V}_{3,\alpha\beta} = \mathcal{V}_{2,\alpha\gamma}\cdot\mathcal{V}_{3,\alpha\beta}\ . \tag{6.33}$$

For the sixteen Bianchi identities on $E_{2,\alpha\gamma}$ they read:

$$\sum_\beta \Big[\mathcal{V}^2_{1,\beta\gamma} + \mathcal{V}^2_{3,\alpha\beta} - \mathcal{V}^2_{2,\alpha\gamma} + 2\,\mathcal{V}_{2,\alpha\gamma}\cdot\mathcal{V}_{1,\beta\gamma} + 2\,\mathcal{V}_{2,\alpha\gamma}\cdot\mathcal{V}_{3,\alpha\beta} - 2\,\mathcal{V}_{1,\beta\gamma}\cdot\mathcal{V}_{3,\alpha\beta}\Big] = -8\ ,$$

$$\mathcal{V}^2_{1,\beta\gamma} + \mathcal{V}^2_{2,\alpha\gamma} + \mathcal{V}^2_{3,\alpha\beta} - 2\,\mathcal{V}_{1,\beta\gamma}\cdot\mathcal{V}_{3,\alpha\beta} = 4\ ,\quad \mathcal{V}_{1,\beta\gamma}\cdot\mathcal{V}_{2,\alpha\gamma} = \mathcal{V}_{1,\beta\gamma}\cdot\mathcal{V}_{3,\alpha\beta} = \mathcal{V}_{2,\alpha\gamma}\cdot\mathcal{V}_{3,\alpha\beta}\ . \tag{6.34}$$

And, finally, for the sixteen Bianchi identities on $E_{3,\alpha\beta}$ they read:

$$\sum_\gamma \Big[\mathcal{V}^2_{1,\beta\gamma} + \mathcal{V}^2_{2,\alpha\gamma} - \mathcal{V}^2_{3,\alpha\beta} + 2\,\mathcal{V}_{3,\alpha\beta}\cdot\mathcal{V}_{1,\beta\gamma} + 2\,\mathcal{V}_{3,\alpha\beta}\cdot\mathcal{V}_{2,\alpha\gamma} - 2\,\mathcal{V}_{1,\beta\gamma}\cdot\mathcal{V}_{2,\alpha\gamma}\Big] = -8\ ,$$

$$\mathcal{V}^2_{1,\beta\gamma} + \mathcal{V}^2_{2,\alpha\gamma} + \mathcal{V}^2_{3,\alpha\beta} - 2\,\mathcal{V}_{1,\beta\gamma}\cdot\mathcal{V}_{2,\alpha\gamma} = 4\ ,\quad \mathcal{V}_{1,\beta\gamma}\cdot\mathcal{V}_{2,\alpha\gamma} = \mathcal{V}_{1,\beta\gamma}\cdot\mathcal{V}_{3,\alpha\beta} = \mathcal{V}_{2,\alpha\gamma}\cdot\mathcal{V}_{3,\alpha\beta}\ . \tag{6.35}$$

Note that every time the top equations have a sum over one of the fixed point labels, while the lower three do not. Fortunately, many of these equations are redundant. The lower three relations for all three exceptional divisors have the same content: for any choice of (α,β,γ) the three inner products are constraint to:

$$\mathcal{V}_{1,\beta\gamma}\cdot\mathcal{V}_{2,\alpha\gamma} = \mathcal{V}_{1,\beta\gamma}\cdot\mathcal{V}_{3,\alpha\beta} = \mathcal{V}_{2,\alpha\gamma}\cdot\mathcal{V}_{3,\alpha\beta} = \tfrac{1}{2}\big(\mathcal{V}^2_{1,\beta\gamma} + \mathcal{V}^2_{2,\alpha\gamma} + \mathcal{V}^2_{3,\alpha\beta}\big) - 2\ . \tag{6.36}$$

Inserting these in the top equations with the sums results in $3\cdot 16$ equations

$$\sum_\alpha \Big[\mathcal{V}^2_{2,\alpha\gamma} + \mathcal{V}^2_{3,\alpha\beta}\Big] = 12\ ,\quad \sum_\beta \Big[\mathcal{V}^2_{1,\beta\gamma} + \mathcal{V}^2_{3,\alpha\beta}\Big] = 12\ ,\quad \sum_\alpha \Big[\mathcal{V}^2_{1,\beta\gamma} + \mathcal{V}^2_{2,\alpha\gamma}\Big] = 12\ . \tag{6.37}$$

If these equations are satisfied, then also the three Bianchi identities on the inherited divisors are automatically satisfied. Indeed, if one sums each of these sets of equations over the other two labels and then add two and subtract a third, the inherited Bianchi identities are recovered. But in fact these equations can be reduced even further by a similar procedure: Sum over one of the two free labels in these equations. One of the two terms is then precisely of the form of one of the inherited Bianchi identities equal to 24. Inserting that and rewriting leads to three sets of $2\cdot 4 = 8$ (hence 24 in total) even simpler equations:

$$\sum_\beta \mathcal{V}^2_{1,\beta\gamma} = \sum_\gamma \mathcal{V}^2_{1,\beta\gamma} = 6\ ,\quad \sum_\alpha \mathcal{V}^2_{2,\alpha\gamma} = \sum_\gamma \mathcal{V}^2_{2,\alpha\gamma} = 6\ ,\quad \sum_\alpha \mathcal{V}^2_{3,\alpha\beta} = \sum_\beta \mathcal{V}^2_{3,\alpha\beta} = 6\ . \tag{6.38}$$

Hence, if the equations (6.36) and (6.38) are simultaneously satisfied, then a solution is obtained of the 51 Bianchi identities that holds in any triangulation. In fact, in each of the three sets of 8 equations there is one linear dependence, since summing over the free indices in both (four) equations in each set, leads to the same equation.

6.3.3 Blowup Modes Without Oscillator Excitations

Assuming that all line bundle vectors can be associated to twisted states without oscillators, then they all square to:

$$\mathcal{V}_{a,\mu\nu}^2 = \tfrac{3}{2} \qquad \Rightarrow \qquad \mathcal{V}_{a,\mu\nu} \cdot \mathcal{V}_{b,\rho\sigma} = \tfrac{1}{4} \; ; \tag{6.39}$$

the equation after the implication sign follows upon using (6.36), with $\nu = \sigma$ for $a = 1$ and $b = 2$, $\mu = \sigma$ for $a = 1$ and $b = 3$, $\mu = \rho$ for $a = 2$ and $b = 3$, respectively. Since this solves all equations (6.36) and (6.38), such choices solve all Bianchi identities in any triangulation simultaneously.

6.3.4 Consequences of Triangulation Independence for the Multiplicity Operator

Contrary to the fundamental consistency conditions, the multiplicity operator does not simplify in any particular way, when line bundle resolutions models are considered that are admissible in any choice of triangulation of the 64 $\mathbb{Z}_2 \times \mathbb{Z}_2$ resolved singularities. However, it can be brought in a specific form. Since the S–triangulation plays a special role in flop–transitions as any flop involves the S–triangulation, the S–triangulation can be taken to be the reference triangulation at all the 64 $\mathbb{Z}_2 \times \mathbb{Z}_2$ resolved singularities. Using this the total multiplicity operator N can be written as

$$\mathsf{N} = \mathsf{N}^S + \sum_{\alpha,\beta,\gamma} \left[\delta^{E_1}_{\alpha\beta\gamma} \, \Delta\mathsf{N}^1_{\alpha\beta\gamma} + \delta^{E_2}_{\alpha\beta\gamma} \, \Delta\mathsf{N}^2_{\alpha\beta\gamma} + \delta^{E_3}_{\alpha\beta\gamma} \, \Delta\mathsf{N}^3_{\alpha\beta\gamma} \right] , \qquad \mathsf{N}^S = \sum_{\alpha,\beta,\gamma} \mathsf{N}^S_{\alpha\beta\gamma} \tag{6.40}$$

and $\Delta\mathsf{N}^i_{\alpha\beta\gamma}$ defined in (6.25). Both N^S and $\Delta\mathsf{N}^i_{\alpha\beta\gamma}$ are always integer: N^S is the multiplicity operator when at all 64 resolved singularities triangulation S is taken, hence it has to be integral on all chiral states in the spectrum; for the triangulation difference multiplicities $\Delta\mathsf{N}^i_{\alpha\beta\gamma}$ it was already established in Subsection 6.2.9 that they are always integral. This means that in the most general case one can define $3 \cdot 4^3 + 1 = 193$ multiplicity operators ($\Delta\mathsf{N}^i_{\alpha\beta\gamma}$ for $i = 1, 2, 3$, $\alpha, \beta, \gamma = 1, 2, 3, 4$ and N^S) that all have to be integral on any $E_8 \times E_8$ root.

6.4 Models Without Wilson Lines

This section is devoted to a number of simple line bundle models to illustrate the main ideas about dealing with the triangulation dependence. The focus is on demonstrating that the approach to parameterise all triangulations in the way discussed in the preceding sections always lead to sensible, e.g. integral spectra for any triangulation chosen provided that the consistency conditions have been solved for all triangulations simultaneously. However, these models should not be considered as fully realistic models. In particular, the consequences of the DUY equations will be mostly ignored.

Model	Twists / Gauge Shift Embeddings		
I	$v_1 = (0,0,\frac{1}{2},-\frac{1}{2})$,	$v_2 = (0,-\frac{1}{2},0,\frac{1}{2})$,	$v_3 = (0,\frac{1}{2},-\frac{1}{2},0)$.
$I.a$	$V_1 = (0,\frac{1}{2},-\frac{1}{2},0^5)(0^8)$	$V_2 = (-\frac{1}{2},0,\frac{1}{2},0^5)(0^8)$	$V_3 = (\frac{1}{2},-\frac{1}{2},0,0^5)(0^8)$
$I.b$	$V_1 = (0,\frac{1}{2},-\frac{1}{2},0^5)(1,0^7)$	$V_2 = (-\frac{1}{2},0,\frac{1}{2},0^5)(-1,0^7)$	$V_3 = (\frac{1}{2},-\frac{1}{2},0,0^5)(0,0^7)$
II	$v_1 = (0,0,\frac{1}{2},\frac{1}{2})$,	$v_2 = (0,\frac{1}{2},0,\frac{1}{2})$,	$v_3 = (0,-\frac{1}{2},-\frac{1}{2},1)$,
$II.a$	$V_1 = (0,\frac{1}{2},\frac{1}{2},0^5)(0^8)$	$V_2 = (\frac{1}{2},0,\frac{1}{2},0^5)(0^8)$	$V_3 = (-\frac{1}{2},-\frac{1}{2},1,0^5)(0^8)$
$II.b$	$V_1 = (0,\frac{1}{2},\frac{1}{2},0^5)(1,0^7)$	$V_2 = (\frac{1}{2},0,\frac{1}{2},0^5)(-1,0^7)$	$V_3 = (-\frac{1}{2},-\frac{1}{2},1,0^5)(0,0^7)$

Table 6.4: This table gives two different choices of the orbifold twist vectors v_a and two associated inequivalent gauge shift embeddings V_a for each choice.

6.4.1 $T^6/\mathbb{Z}_2 \times \mathbb{Z}_2$ Orbifold Models

From the orbifold perspective these are models without Wilson lines, this means that such orbifold models are characterised by just two gauge shifts V_a. They satisfy

$$V_a \cdot V_b - v_a \cdot v_b \equiv 0 \ , \tag{6.41}$$

for $a, b = 1, 2$. Here v_a denote the two independent four–component geometrical $\mathbb{Z}_2$ orbifold twists and V_a the sixteen–component shift embedding on the gauge lattice taken to be either the weight lattice of $E_8 \times E_8$ or $Spin(32)/\mathbb{Z}_2$. Furthermore, it is often convenient to introduce $v_3 \cong v_1 + v_2$ and $V_3 \cong V_1 + V_2$.

The geometrical twists v_1 and v_2 are conventionally chosen such as to preserve $\mathcal{N} = 1$ target space supersymmetry. On the level of the orbifold theory there are various equivalent choices for them. The most commonly used choice $I.$ is

$$v_1 = (0,0,\tfrac{1}{2},-\tfrac{1}{2}) \ , \qquad v_2 = (0,-\tfrac{1}{2},0,\tfrac{1}{2}) \ , \qquad v_3 = v_1 + v_2 = (0,-\tfrac{1}{2},\tfrac{1}{2},0) \cong (0,\tfrac{1}{2},-\tfrac{1}{2},0) \ . \tag{6.42a}$$

The first entry of these vectors corresponds to the four–dimensional Minkowski space in light–cone gauge; the other three components to the twist actions on the three two–torus that make up the T^6. The final expression for v_3 obtained by adding a lattice vector $(0,1,-1,0)$ making a permutation symmetry between the entries of v_1, v_2 and v_3 manifest. Note that with this form of v_3

$$v_a \cdot v_b = -\tfrac{1}{4} + \tfrac{3}{4}\,\delta_{ab} \ . \tag{6.42b}$$

A second choice $II.$ is given by

$$v_1 = (0,0,\tfrac{1}{2},\tfrac{1}{2}) \ , \qquad v_2 = (0,\tfrac{1}{2},0,\tfrac{1}{2}) \ , \qquad v_3 = v_1 + v_2 = (0,\tfrac{1}{2},\tfrac{1}{2},1) \cong (0,-\tfrac{1}{2},-\tfrac{1}{2},1) \ , \tag{6.43a}$$

where the latter form of v_3 in this case is obtained by adding $(0,-1,-1,0)$. With this form of v_3 the vectors v_a satisfy

$$v_a \cdot v_b = \tfrac{1}{4}\big(1 + \delta_{ab}\big) + \delta_{a3}\,\delta_{b3} \ . \tag{6.43b}$$

On the level of the orbifold theory both choices are equivalent. For both these forms there are two inequivalent choices for the gauge embedding, denoted by a and b. This leads to four possible gauge shift embeddings referred to as $I.a$, $I.b$, $II.a$ and $II.b$ in Table 6.4. On the level of the orbifold only the choices a or b lead to physically different models; as is shown below on the level of the resolution the choice of twist $I.$ or $II.$ is of significance as only one of the two choices can be associated to a line bundle model.

6.4.2 Models with Three Independent Line Bundles

First some general facts about associated blowup models are given. In this section the line bundle vectors are taken to be independent of the labels α, β, γ, i.e.:

$$\mathcal{V}_{1,\beta\gamma} = \mathcal{V}_1 \ , \quad \mathcal{V}_{2,\alpha\gamma} = \mathcal{V}_2 \ , \quad \mathcal{V}_{3,\alpha\beta} = \mathcal{V}_3 \ . \tag{6.44}$$

Consequently the triangulation independent flux quantisation conditions (6.32) reduce to

$$2\,\mathcal{V}_1 \cong 2\,\mathcal{V}_2 \cong 2\,\mathcal{V}_3 \cong \mathcal{V}_1 + \mathcal{V}_2 + \mathcal{V}_3 \cong 0 \ . \tag{6.45}$$

Such bundle vectors, $\mathcal{V}_1, \mathcal{V}_2$ and $\mathcal{V}_3$, can be obtained from the orbifold gauge shift vectors V_1, V_2 and V_3, by adding appropriate lattice vectors $L_{1,\beta\gamma}, L_{2,\alpha\gamma}$ and $L_{3,\alpha\beta}$. In this section they are chosen such that the bundle vectors $\mathcal{V}_1, \mathcal{V}_2$ and $\mathcal{V}_3$ can be associated with twisted states without oscillators satisfying the conditions (6.39).

The number N_T of times, that triangulation $T = E_1,\ E_2,\ E_3,\ S$ has been chosen at the 64 resolved $\mathbb{C}^3/\mathbb{Z}_2 \times \mathbb{Z}_2$ singularities, can be determined by summing the functions $\delta^T_{\alpha\beta\gamma}$ over all of them, e.g.:

$$N_T = \sum_{\alpha,\beta,\gamma} \delta^T_{\alpha\beta\gamma} \ , \tag{6.46}$$

hence, in particularly, for $i = 1, 2, 3$:

$$\sum_{\alpha,\beta,\gamma} \left(1 - \Delta^i_{\alpha\beta\gamma}\right) = 2\,N_{E_i} + N_S \ , \qquad N_E + N_S = 64 \ , \qquad N_E = N_{E_1} + N_{E_2} + N_{E_3} \ . \tag{6.47}$$

Then, if also the Cartan operators are abbreviated as

$$\mathsf{H}_1 = \mathsf{H}_{1,\beta\gamma} \ , \qquad \mathsf{H}_2 = \mathsf{H}_{2,\alpha\gamma} \ , \qquad \mathsf{H}_3 = \mathsf{H}_{3,\alpha\beta} \ , \tag{6.48}$$

the multiplicity operator (6.23) simplifies to

$$\mathsf{N} = N_{E_1}\,\mathsf{N}^1 + N_{E_2}\,\mathsf{N}^2 + N_{E_3}\,\mathsf{N}^3 + N_S\,\mathsf{N}^S \ , \tag{6.49}$$

expressed in terms of four multiplicity operators for each of the four triangulations

$$\mathsf{N}^1 = \tfrac{1}{4}\,\mathsf{H}_1 + \tfrac{1}{12}\,\mathsf{H}_2\big(4\mathsf{H}_2^2 - 1\big) + \tfrac{1}{12}\,\mathsf{H}_3\big(4\mathsf{H}_3^2 - 1\big) - \mathsf{H}_1\big(\mathsf{H}_2^2 + \mathsf{H}_3^2\big) \ , \tag{6.50a}$$

$$\mathsf{N}^2 = \tfrac{1}{4}\,\mathsf{H}_2 + \tfrac{1}{12}\,\mathsf{H}_1\big(4\mathsf{H}_1^2 - 1\big) + \tfrac{1}{12}\,\mathsf{H}_3\big(4\mathsf{H}_3^2 - 1\big) - \mathsf{H}_2\big(\mathsf{H}_1^2 + \mathsf{H}_3^2\big) \ , \tag{6.50b}$$

$$\mathsf{N}^3 = \tfrac{1}{4}\,\mathsf{H}_3 + \tfrac{1}{12}\,\mathsf{H}_1\big(4\mathsf{H}_1^2 - 1\big) + \tfrac{1}{12}\,\mathsf{H}_2\big(4\mathsf{H}_2^2 - 1\big) - \mathsf{H}_3\big(\mathsf{H}_1^2 + \mathsf{H}_2^2\big) \ , \tag{6.50c}$$

$$\begin{aligned}\mathsf{N}^S = {} & \tfrac{1}{12}\,\mathsf{H}_1\big(2\mathsf{H}_1^2 + 1\big) + \tfrac{1}{12}\,\mathsf{H}_2\big(2\mathsf{H}_2^2 + 1\big) + \tfrac{1}{12}\,\mathsf{H}_3\big(2\mathsf{H}_3^2 + 1\big) + \mathsf{H}_1\mathsf{H}_2\mathsf{H}_3 \\ & - \tfrac{1}{2}\,\mathsf{H}_1\big(\mathsf{H}_2^2 + \mathsf{H}_3^2\big) - \tfrac{1}{2}\,\mathsf{H}_2\big(\mathsf{H}_1^2 + \mathsf{H}_3^2\big) - \tfrac{1}{2}\,\mathsf{H}_3\big(\mathsf{H}_1^2 + \mathsf{H}_2^2\big) \ .\end{aligned} \tag{6.50d}$$

Since N_{E_1}, N_{E_2}, N_{E_3} and N_S are arbitrary non–negative integers subject to (6.47), it follows that if we substitute one of them away in (6.49), the resulting expression has to be integral on all $E_8 \times E_8$ weights for any choice of the remaining numbers. In particular, taking the triangulation S again as reference, i.e. solving N_S from (6.47) and substituting this in (6.49), gives

$$\mathsf{N} = N_{E_1}\,\Delta\mathsf{N}^1 + N_{E_2}\,\Delta\mathsf{N}^2 + N_{E_3}\,\Delta\mathsf{N}^3 + 64\,\mathsf{N}^S\ , \qquad \Delta\mathsf{N}^i = \mathsf{N}^i - \mathsf{N}^S\ , \tag{6.51}$$

for $i = 1, 2, 3$. In line with the general observation in Section 6.3.4, this expression should always be integral. Hence, in particular, the operators $\Delta\mathsf{N}^i$ have to be integral on any state.

6.4.3 $SO(10) \times SO(12)$ Line Bundle Models

Starting from the orbifold gauge embeddings $II.b$ of the classification in Table 6.4 a set of three line bundle vectors can be obtained

$$\mathcal{V}_1 = V_1 + L_1 = (0, \tfrac{1}{2}, \tfrac{1}{2}, 0^5)(1, 0, 0^6)\ , \qquad L_1 = (0^8)(0^8) \tag{6.52a}$$

$$\mathcal{V}_2 = V_2 + L_2 = (\tfrac{1}{2}, 0, \tfrac{1}{2}, 0^5)(0, 1, 0^6)\ , \qquad L_2 = (0^8)(-1, 1, 0^6)\ , \tag{6.52b}$$

$$\mathcal{V}_3 = V_3 + L_3 = (-\tfrac{1}{2}, -\tfrac{1}{2}, 1, 0^5)(0, 0, 0^6)\ , \qquad L_3 = (0^8)(0^8)\ . \tag{6.52c}$$

The bundle vectors satisfy the flux quantisation (6.45) for arbitrary triangulations. Note that, these bundle vectors cannot be obtained from orbifold model $I.b$. Thus equivalent choices on the orbifold level might lead to inequivalent choices from the smooth resolved perspective. The unbroken non–Abelian gauge group is $SO(10) \times SO(12)$.

The line bundle charges H_i, the triangulation multiplicities N^i, N^S and the triangulation difference multiplicities $\Delta\mathsf{N}^i$ of all the $E_8 \times E_8$ roots are given in Table 6.5. The triangulation multiplicities, and N^S in particular, are not integrally quantised. This might seem problematic, but it is not: triangulation S can be taken to be the reference triangulation at all 64 resolved singularities. Hence, if triangulation S is chosen at all resolved singularities, the spectrum is 64 times the triangulation multiplicity N^S and all states come in multiples of 16. Now, if at a certain resolved singularities one of the exceptional triangulations is used then the spectrum always changes by an integral amount as the triangulation difference multiplicities $\Delta\mathsf{N}^i$ are integral, see Table 6.5. Indeed, using this table the full spectrum in any triangulation can be determined to be:

$$\begin{aligned} &16\big\{(\mathbf{10})(\mathbf{1})_{0,0,\text{-}2;0} + (\mathbf{16})(\mathbf{1})_{\text{-}1,\text{-}1,1;0} + (\mathbf{1})(\mathbf{12})_{0;2,0} + (\mathbf{1})(\mathbf{12})_{0;0,2} + (\mathbf{1})(\mathbf{1})_{\text{-}2,0,\text{-}2;0} + (\mathbf{1})(\mathbf{1})_{0,\text{-}2,\text{-}2;0}\big\} + \\ &\quad 48\,(\mathbf{1})(\mathbf{1})_{\text{-}2,\text{-}2,0;0} + N_{E_3}\,(\mathbf{1})(\mathbf{1})_{2,2,0;0} + N_{E_2}\,(\mathbf{1})(\mathbf{1})_{\text{-}2,0,2;0} + N_{E_1}\,(\mathbf{1})(\mathbf{1})_{0,\text{-}2,2;0} + \\ &\quad 32\,(\mathbf{1})(\mathbf{1})_{0;\text{-}2,\text{-}2} + N_{E_3}\,(\mathbf{1})(\mathbf{1})_{0;2,2} + N_{E_1}\,(\mathbf{1})(\mathbf{1})_{0;\text{-}2,2} + N_{E_2}\,(\mathbf{1})(\mathbf{1})_{0;2,\text{-}2}\ . \end{aligned} \tag{6.53}$$

The five $U(1)$ charges given here are two times the first three weight entries of the observable E_8 and the first two of the hidden E_8. They can be used to distinguish otherwise vector–like states. When triangulation S is chosen at all fixed points, e.g. $N_{E_1} = N_{E_2} = N_{E_3} = 0$, the spectrum does not contain any vector–like pairs. For most other choices vector–like pairs do arise, but they presumably acquire a mass at some stage in the effective field theory description.

weight	H_1	H_2	H_3	N^1	N^2	N^3	N^S	$\Delta\mathsf{N}^1$	$\Delta\mathsf{N}^2$	$\Delta\mathsf{N}^3$	repr.
$(1,0,0,\underline{\pm1,0^4})(0^8)$	0	$\frac{1}{2}$	$-\frac{1}{2}$	0	0	0	0	0	0	0	$(\mathbf{10})(\mathbf{1})$
$(0,1,0,\underline{\pm1,0^4})(0^8)$	$\frac{1}{2}$	0	$-\frac{1}{2}$	0	0	0	0	0	0	0	$(\mathbf{10})(\mathbf{1})$
$(0,0,1,\underline{\pm1,0^4})(0^8)$	$\frac{1}{2}$	$\frac{1}{2}$	1	$-\frac{1}{4}$	$-\frac{1}{4}$	$-\frac{1}{4}$	$-\frac{1}{4}$	0	0	0	$(\mathbf{10})(\mathbf{1})$
$(\frac{1}{2},\frac{1}{2},\frac{1}{2},\underline{-\frac{1}{2}^e,\frac{1}{2}^{5-e}})(0^8)$	$\frac{1}{2}$	$\frac{1}{2}$	0	0	0	0	0	0	0	0	$(\mathbf{16})(\mathbf{1})$
$(-\frac{1}{2},\frac{1}{2},\frac{1}{2},\underline{-\frac{1}{2}^o,\frac{1}{2}^{5-o}})(0^8)$	$\frac{1}{2}$	0	$\frac{1}{2}$	0	0	0	0	0	0	0	$(\overline{\mathbf{16}})(\mathbf{1})$
$(\frac{1}{2},-\frac{1}{2},\frac{1}{2},\underline{-\frac{1}{2}^o,\frac{1}{2}^{5-o}})(0^8)$	0	$\frac{1}{2}$	$\frac{1}{2}$	0	0	0	0	0	0	0	$(\overline{\mathbf{16}})(\mathbf{1})$
$(\frac{1}{2},\frac{1}{2},-\frac{1}{2},\underline{-\frac{1}{2}^o,\frac{1}{2}^{5-o}})(0^8)$	0	0	-1	$-\frac{1}{4}$	$-\frac{1}{4}$	$-\frac{1}{4}$	$-\frac{1}{4}$	0	0	0	$(\overline{\mathbf{16}})(\mathbf{1})$
$(1,1,0,0^5)(0^8)$	$\frac{1}{2}$	$\frac{1}{2}$	-1	$-\frac{3}{4}$	$-\frac{3}{4}$	$\frac{1}{4}$	$-\frac{3}{4}$	0	0	1	$(\mathbf{1})(\mathbf{1})$
$(1,0,1,0^5)(0^8)$	$\frac{1}{2}$	1	$\frac{1}{2}$	$-\frac{1}{4}$	$-\frac{1}{4}$	$-\frac{1}{4}$	$-\frac{1}{4}$	0	0	0	$(\mathbf{1})(\mathbf{1})$
$(0,1,1,0^5)(0^8)$	1	$\frac{1}{2}$	$\frac{1}{2}$	$-\frac{1}{4}$	$-\frac{1}{4}$	$-\frac{1}{4}$	$-\frac{1}{4}$	0	0	0	$(\mathbf{1})(\mathbf{1})$
$(1,-1,0,0^5)(0^8)$	$-\frac{1}{2}$	$\frac{1}{2}$	0	0	0	0	0	0	0	0	$(\mathbf{1})(\mathbf{1})$
$(1,0,-1,0^5)(0^8)$	$-\frac{1}{2}$	0	$-\frac{3}{2}$	0	-1	0	0	0	-1	0	$(\mathbf{1})(\mathbf{1})$
$(0,1,-1,0^5)(0^8)$	0	$-\frac{1}{2}$	$-\frac{3}{2}$	-1	0	0	0	-1	0	0	$(\mathbf{1})(\mathbf{1})$
$(0^8)(1,0,\underline{\pm1,0^5})$	1	0	0	$\frac{1}{4}$	$\frac{1}{4}$	$\frac{1}{4}$	$\frac{1}{4}$	0	0	0	$(\mathbf{1})(\mathbf{12})$
$(0^8)(0,1,\underline{\pm1,0^5})$	0	1	0	$\frac{1}{4}$	$\frac{1}{4}$	$\frac{1}{4}$	$\frac{1}{4}$	0	0	0	$(\mathbf{1})(\mathbf{12})$
$(0^8)(\frac{1}{2},\frac{1}{2},\underline{-\frac{1}{2}^e,\frac{1}{2}^{6-e}})$	$\frac{1}{2}$	$\frac{1}{2}$	0	0	0	0	0	0	0	0	$(\mathbf{1})(\mathbf{32})$
$(0^8)(\frac{1}{2},-\frac{1}{2},\underline{-\frac{1}{2}^o,\frac{1}{2}^{6-o}})$	$\frac{1}{2}$	$-\frac{1}{2}$	0	0	0	0	0	0	0	0	$(\mathbf{1})(\overline{\mathbf{32}})$
$(0^8)(1,1,0^6)$	1	1	0	$-\frac{1}{2}$	$-\frac{1}{2}$	$\frac{1}{2}$	$-\frac{1}{2}$	0	0	1	$(\mathbf{1})(\mathbf{1})$
$(0^8)(1,-1,0^6)$	1	-1	0	-1	1	0	0	-1	1	0	$(\mathbf{1})(\mathbf{1})$

Table 6.5: The line bundle charges H_i, the triangulation multiplicities N^i, N^S and the difference multiplicities $\Delta\mathsf{N}^i$ are given for all the $E_8\times E_8$ roots charged under the line bundle background defined by (6.52). The underline of some of the entries in these roots denote all possible permutations of them. Notice, that these difference multiplicities, that measure jumps in the spectrum when going through a flop–transition, are always integral.

6.4.4 A "swampland" $SO(10) \times SO(10)$ models

A seemingly closely related model with three independent bundle vectors is given by

$$\mathcal{V}_{1,\beta\gamma} = \mathcal{V}_1 = (0, \tfrac{1}{2}, \tfrac{1}{2}, 0^5)(-1, 0, 0, 0^5) \ , \tag{6.54a}$$

$$\mathcal{V}_{2,\alpha\gamma} = \mathcal{V}_2 = (\tfrac{1}{2}, 0, \tfrac{1}{2}, 0^5)(0, -1, 0, 0^5) \ , \tag{6.54b}$$

$$\mathcal{V}_{3,\alpha\beta} = \mathcal{V}_3 = (\tfrac{1}{2}, \tfrac{1}{2}, 0, 0^5)(0, 0, -1, 0^5) \ . \tag{6.54c}$$

This leads to a gauge group $SO(10)\times SO(10)$. The unbroken roots are given by $(0^3, \underline{\pm 1, \pm 1, 0^3})(0^8)$ and $(0^8)(0^3, \underline{\pm 1, \pm 1, 0^3})$. At first sight this seems to be a valid choice as well, but this model has a number of issues:

First of all, even thought the bundle vectors clearly satisfy the strong conditions (6.39), this model cannot be obtained as the blowup of any orbifold model. The first two bundle vectors are identical to the model discussed in the previous subsection and can be obtained from orbifold gauge shift vectors given there. But the third one does not differ by a lattice vector from $V_1 + V_2$:

$$\mathcal{V}_3 - V_1 - V_2 = (\tfrac{1}{2}, \tfrac{1}{2}, 0, 0^5)(0, 0, -1, 0^5) - (\tfrac{1}{2}, \tfrac{1}{2}, 1, 0^5)(0, 0, 0, 0^5) = (0, 0, -1, 0^5)(0, 0, -1, 0^5) \ . \tag{6.55}$$

(If both -1–entries would have lain in the same E_8, this would be a lattice vector, but they don't.)

Moreover, this choice of line bundle vectors does not satisfy the final flux quantisation condition in (6.45). As a consequence, the spectrum is not integral for a generic choice of triangulation at the 64 $\mathbb{C}^3/\mathbb{Z}_2 \times \mathbb{Z}_2$ resolutions. This can be inferred from the appearance of multiplicities $\pm 1/16$ and $-5/16$ for the $\Delta\mathsf{N}^1$, $\Delta\mathsf{N}^2$ and $\Delta\mathsf{N}^3$ in Table 6.6 when the states are distinguished by their (implicitly given) $U(1)$ charges. Even if one ignores the $U(1)$ charges, the spectrum combined is not necessarily integral:

$$16\,(\overline{\mathbf{16}})(\mathbf{1}) + 48\,(\mathbf{1})(\mathbf{10}) + 4\,(\mathbf{1})(\mathbf{16}) + 36\,(\mathbf{1})(\overline{\mathbf{16}}) + \tfrac{1}{8}N_E\big\{(\mathbf{16})(\mathbf{1}) + (\overline{\mathbf{16}})(\mathbf{1}) + 4\,(\mathbf{1})(\mathbf{16})\big\} + \text{singlets} \ . \tag{6.56}$$

Note, that if the same triangulation is chosen at all 64 resolved $\mathbb{C}^3/\mathbb{Z}_2 \times \mathbb{Z}_2$ singularities, the spectrum would be integral. But any single flop–transition would then lead to an inconsistent spectrum. This demonstrates that satisfying the flux quantisation conditions in any triangulation is essential for the difference multiplicities $\Delta\mathsf{N}^i$ to be always integral.

6.4.5 Blaszczyk's $SU(3) \times SU(2)$ Line Bundle Models

An example with very similar line bundle vectors, but where all their non–trivial entries lie in the observable E_8 can be obtained from the orbifold gauge embeddings $I.a$ of Table 6.4. (But these bundle vectors cannot be obtained from orbifold model $II.a$.) The defining set of three line bundle vectors are given by:

$$\mathcal{V}_1 = V_1 + L_1 = (0, \tfrac{1}{2}, \tfrac{1}{2}, -1, 0, 0, 0^2)(0^8) \ , \qquad L_1 = (0, 0, 1, -1, 0, 0, 0^2)(0^8) \tag{6.57a}$$

$$\mathcal{V}_2 = V_2 + L_2 = (\tfrac{1}{2}, 0, \tfrac{1}{2}, 0, -1, 0, 0^2)(0^8) \ , \qquad L_2 = (0, 1, 0, 0, -1, 0, 0^2)(0^8) \ , \tag{6.57b}$$

$$\mathcal{V}_3 = V_3 + L_3 = (\tfrac{1}{2}, \tfrac{1}{2}, 0, 0, 0, -1, 0^2)(0^8) \ , \qquad L_3 = (1, 0, 0, 0, 0, -1, 0^2)(0^8) \ , \tag{6.57c}$$

weight	H_1	H_2	H_3	N^1	N^2	N^3	N^S	$\Delta\mathsf{N}^1$	$\Delta\mathsf{N}^2$	$\Delta\mathsf{N}^3$	repr.
$(-\frac{1}{2},-\frac{1}{2},-\frac{1}{2},\underline{-\frac{1}{2}^o,\frac{1}{2}^{5-o}})(0^8)$	$\frac{1}{2}$	$\frac{1}{2}$	0	$\frac{1}{8}$	$\frac{1}{8}$	$\frac{1}{8}$	$\frac{1}{16}$	$\frac{1}{16}$	$\frac{1}{16}$	$\frac{1}{16}$	$(\overline{\mathbf{16}})(\mathbf{1})$
$(-\frac{1}{2},\frac{1}{2},\frac{1}{2},\underline{-\frac{1}{2}^o,\frac{1}{2}^{5-o}})(0^8)$	$\frac{1}{2}$	0	0	$\frac{1}{8}$	0	0	$\frac{1}{16}$	$\frac{1}{16}$	$-\frac{1}{16}$	$-\frac{1}{16}$	$(\overline{\mathbf{16}})(\mathbf{1})$
$(\frac{1}{2},-\frac{1}{2},\frac{1}{2},\underline{-\frac{1}{2}^o,\frac{1}{2}^{5-o}})(0^8)$	0	$\frac{1}{2}$	0	0	$\frac{1}{8}$	0	$\frac{1}{16}$	$-\frac{1}{16}$	$\frac{1}{16}$	$-\frac{1}{16}$	$(\overline{\mathbf{16}})(\mathbf{1})$
$(\frac{1}{2},\frac{1}{2},-\frac{1}{2},\underline{-\frac{1}{2}^o,\frac{1}{2}^{5-o}})(0^8)$	0	0	$\frac{1}{2}$	0	0	$\frac{1}{8}$	$\frac{1}{16}$	$-\frac{1}{16}$	$-\frac{1}{16}$	$\frac{1}{16}$	$(\overline{\mathbf{16}})(\mathbf{1})$
$(-1,-1,0,0^5)(0^8)$	$-\frac{1}{2}$	$-\frac{1}{2}$	-1	$\frac{1}{4}$	$\frac{1}{4}$	$\frac{1}{4}$	$\frac{1}{4}$	0	0	0	$(\mathbf{1})(\mathbf{1})$
$(-1,0,-1,0^5)(0^8)$	$-\frac{1}{2}$	-1	$-\frac{1}{2}$	$\frac{1}{4}$	$\frac{1}{4}$	$\frac{1}{4}$	$\frac{1}{4}$	0	0	0	$(\mathbf{1})(\mathbf{1})$
$(0,-1,-1,0^5)(0^8)$	-1	$-\frac{1}{2}$	$-\frac{1}{2}$	$\frac{1}{4}$	$\frac{1}{4}$	$\frac{1}{4}$	$\frac{1}{4}$	0	0	0	$(\mathbf{1})(\mathbf{1})$
$(0^8)(-1,0,0,\underline{\pm1,0^4})$	1	0	0	$\frac{1}{4}$	$\frac{1}{4}$	$\frac{1}{4}$	$\frac{1}{4}$	0	0	0	$(\mathbf{1})(\mathbf{10})$
$(0^8)(0,-1,0,\underline{\pm1,0^4})$	0	1	0	$\frac{1}{4}$	$\frac{1}{4}$	$\frac{1}{4}$	$\frac{1}{4}$	0	0	0	$(\mathbf{1})(\mathbf{10})$
$(0^8)(0,0,-1,\underline{\pm1,0^4})$	0	0	1	$\frac{1}{4}$	$\frac{1}{4}$	$\frac{1}{4}$	$\frac{1}{4}$	0	0	0	$(\mathbf{1})(\mathbf{10})$
$(0^8)(\frac{1}{2},\frac{1}{2},\frac{1}{2},\underline{-\frac{1}{2}^e,\frac{1}{2}^{5-e}})$	$-\frac{1}{2}$	$-\frac{1}{2}$	$-\frac{1}{2}$	$\frac{1}{8}$	$\frac{1}{8}$	$\frac{1}{8}$	$\frac{1}{16}$	$\frac{1}{16}$	$\frac{1}{16}$	$\frac{1}{16}$	$(\mathbf{1})(\mathbf{16})$
$(0^8)(-\frac{1}{2},\frac{1}{2},\frac{1}{2},\underline{-\frac{1}{2}^o,\frac{1}{2}^{5-o}})$	$\frac{1}{2}$	$-\frac{1}{2}$	$-\frac{1}{2}$	$-\frac{1}{8}$	$\frac{1}{8}$	$\frac{1}{8}$	$\frac{3}{16}$	$-\frac{5}{16}$	$-\frac{1}{16}$	$-\frac{1}{16}$	$(\mathbf{1})(\overline{\mathbf{16}})$
$0^8)(\frac{1}{2},-\frac{1}{2},\frac{1}{2},\underline{-\frac{1}{2}^o,\frac{1}{2}^{5-o}})$	$-\frac{1}{2}$	$\frac{1}{2}$	$-\frac{1}{2}$	$\frac{1}{8}$	$-\frac{1}{8}$	$\frac{1}{8}$	$\frac{3}{16}$	$-\frac{1}{16}$	$-\frac{5}{16}$	$-\frac{1}{16}$	$(\mathbf{1})(\overline{\mathbf{16}})$
$0^8)(\frac{1}{2},\frac{1}{2},-\frac{1}{2},\underline{-\frac{1}{2}^o,\frac{1}{2}^{5-o}})$	$\frac{1}{2}$	$-\frac{1}{2}$	$-\frac{1}{2}$	$\frac{1}{8}$	$\frac{1}{8}$	$-\frac{1}{8}$	$\frac{3}{16}$	$-\frac{1}{16}$	$-\frac{1}{16}$	$-\frac{5}{16}$	$(\mathbf{1})(\overline{\mathbf{16}})$
$(0^8)(0,1,1,0^5)$	0	-1	-1	$-\frac{1}{2}$	$\frac{1}{2}$	$\frac{1}{2}$	$\frac{1}{2}$	-1	0	0	$(\mathbf{1})(\mathbf{1})$
$(0^8)(1,0,1,0^5)$	-1	0	-1	$\frac{1}{2}$	$-\frac{1}{2}$	$\frac{1}{2}$	$\frac{1}{2}$	0	-1	0	$(\mathbf{1})(\mathbf{1})$
$(0^8)(1,1,0,0^5)$	-1	-1	0	$\frac{1}{2}$	$\frac{1}{2}$	$-\frac{1}{2}$	$\frac{1}{2}$	0	0	-1	$(\mathbf{1})(\mathbf{1})$
$(0^8)(1,-1,0,0^5)$	-1	1	0	1	-1	0	0	1	-1	0	$(\mathbf{1})(\mathbf{1})$
$(0^8)(-1,0,1,0^5)$	1	0	-1	-1	0	1	0	-1	0	1	$(\mathbf{1})(\mathbf{1})$
$(0^8)(0,1,-1,0^5)$	0	1	-1	0	-1	1	0	0	-1	1	$(\mathbf{1})(\mathbf{1})$

Table 6.6: The line bundle charges H_i and the triangulation multiplicities N^i, N^S are given for all the $E_8 \times E_8$ roots charged under the line bundle background defined by (6.54). Note that for this model many of the triangulation difference multiplicities $\Delta\mathsf{N}^i$ are non–integral signifying that this model is not fully consistent.

These bundle vectors were considered in Section 4.3 of ref. [32] before. In that work the spectra were obtained when at all 64 resolved $\mathbb{C}^3/\mathbb{Z}_2 \times \mathbb{Z}_2$ singularities one of the four possible triangulations were chosen. However, they satisfy the very restrictive conditions (6.39) that ensures that the Bianchi identities are satisfied and the flux quantisation conditions (6.45) for all triangulations simultaneously. Hence, this set of bundle vectors do not suffer from the flaws encountered in the section above.

Besides all the hidden E_8 roots there are six unbroken $SU(3)$ roots $\pm(0^6, 1^2)$ and $\pm(\frac{1}{2}^6, \pm\frac{1}{2}^2)(0^8)$ and two unbroken $SU(2)$ roots $\pm(0^6, 1, -1)$, consequently the unbroken non–Abelian gauge group is $SU(3) \times SU(2) \times E_8$. The Cartan generators of $SU(3)$ are $h_1 = (\frac{1}{2}^6, -\frac{1}{2}^2)$ and $h_2 = (0^6, 1^2)$ and of $SU(2)$ $h = (0^6, 1, -1)$.

The triangulation multiplicities evaluated on all observable E_8 roots are given in Table 6.7. If the same triangulation is used at all resolved singularities then the spectra given in Table 10 of ref. [32] are reproduced. But with the formalism laid out in this chapter an arbitrary triangulation of each of the resolved fixed points can be considered. As the triangulation difference multiplicities $\Delta\mathsf{N}^i$ are all integral and the states come in multiples of 16 if triangulation S is used at all resolved singularities, the spectrum is integral for any choice of local triangulations. Indeed, ignoring all $U(1)$ charges, the full charged $SU(3)\times SU(2)$ spectrum from the observable E_8 can be compactly summarised as

$$48\,(\mathbf{3},\mathbf{2}) + 96\,(\overline{\mathbf{3}},\mathbf{1}) + (96+N_E)\left\{(\overline{\mathbf{3}},\mathbf{1}) + (\mathbf{3},\mathbf{1})\right\} + (176-2\,N_E)\,(\mathbf{1},\mathbf{2}) + (144+N_E)\,(\mathbf{1},\mathbf{1})\ . \tag{6.58}$$

It can be easily confirmed from this spectrum that $SU(3)$ cubed anomaly cancels for any N_E and the $SU(2)$ Witten anomaly is always absent since the number of $SU(2)$ doublets is always even.

weight	H_1	H_2	H_3	N^1	N^2	N^3	N^S	$\Delta\mathsf{N}^1$	$\Delta\mathsf{N}^2$	$\Delta\mathsf{N}^3$	repr.
$(\frac{1}{2},\frac{1}{2},\frac{1}{2},-\frac{1}{2},\frac{1}{2},\frac{1}{2},\underline{-\frac{1}{2},\frac{1}{2}})$	1	0	0	$\frac{1}{4}$	$\frac{1}{4}$	$\frac{1}{4}$	$\frac{1}{4}$	0	0	0	$(\mathbf{3},\mathbf{2})$
$(0,0,0,-1,0,0,\underline{\pm 1,0})$											
$(\frac{1}{2},\frac{1}{2},\frac{1}{2},\frac{1}{2},-\frac{1}{2},\frac{1}{2},\underline{-\frac{1}{2},\frac{1}{2}})$	0	1	0	$\frac{1}{4}$	$\frac{1}{4}$	$\frac{1}{4}$	$\frac{1}{4}$	0	0	0	$(\mathbf{3},\mathbf{2})$
$(0,0,0,0,-1,0,\underline{\pm 1,0})$											
$(\frac{1}{2},\frac{1}{2},\frac{1}{2},\frac{1}{2},\frac{1}{2},-\frac{1}{2},\underline{-\frac{1}{2},\frac{1}{2}})$	0	0	1	$\frac{1}{4}$	$\frac{1}{4}$	$\frac{1}{4}$	$\frac{1}{4}$	0	0	0	$(\mathbf{3},\mathbf{2})$
$(0,0,0,0,0,-1,\underline{\pm 1,0})$											
$(-1,-1,0,0,0,0,0^2)$	$-\frac{1}{2}$	$-\frac{1}{2}$	-1	$\frac{1}{4}$	$\frac{1}{4}$	$\frac{1}{4}$	$\frac{1}{4}$	0	0	0	$(\overline{\mathbf{3}},\mathbf{1})$
$(-\frac{1}{2},-\frac{1}{2},\frac{1}{2},\frac{1}{2},\frac{1}{2},\frac{1}{2},\pm\frac{1}{2}^2)$											
$(-1,0,-1,0,0,0,0^2)$	$-\frac{1}{2}$	-1	$-\frac{1}{2}$	$\frac{1}{4}$	$\frac{1}{4}$	$\frac{1}{4}$	$\frac{1}{4}$	0	0	0	$(\overline{\mathbf{3}},\mathbf{1})$
$(-\frac{1}{2},\frac{1}{2},-\frac{1}{2},\frac{1}{2},\frac{1}{2},\frac{1}{2},\pm\frac{1}{2}^2)$											
$(0,-1,-1,0,0,0,0^2)$	-1	$-\frac{1}{2}$	$-\frac{1}{2}$	$\frac{1}{4}$	$\frac{1}{4}$	$\frac{1}{4}$	$\frac{1}{4}$	0	0	0	$(\overline{\mathbf{3}},\mathbf{1})$
$(\frac{1}{2},-\frac{1}{2},-\frac{1}{2},\frac{1}{2},\frac{1}{2},\frac{1}{2},\pm\frac{1}{2}^2)$											
$(-1,0,0,-1,0,0,0^2)$	1	$-\frac{1}{2}$	$-\frac{1}{2}$	$-\frac{1}{4}$	$\frac{3}{4}$	$\frac{3}{4}$	$\frac{3}{4}$	-1	0	0	$(\overline{\mathbf{3}},\mathbf{1})$
$(-\frac{1}{2},\frac{1}{2},\frac{1}{2},-\frac{1}{2},\frac{1}{2},\frac{1}{2},\pm\frac{1}{2}^2)$											
$(0,-1,0,0,-1,0,0^2)$	$-\frac{1}{2}$	1	$-\frac{1}{2}$	$\frac{3}{4}$	$-\frac{1}{4}$	$\frac{3}{4}$	$\frac{3}{4}$	0	-1	0	$(\overline{\mathbf{3}},\mathbf{1})$
$(\frac{1}{2},-\frac{1}{2},\frac{1}{2},\frac{1}{2},-\frac{1}{2},\frac{1}{2},\pm\frac{1}{2}^2)$											
$(0,0,-1,0,0,-1,0^2)$	$-\frac{1}{2}$	$-\frac{1}{2}$	1	$\frac{3}{4}$	$\frac{3}{4}$	$-\frac{1}{4}$	$\frac{3}{4}$	0	0	-1	$(\overline{\mathbf{3}},\mathbf{1})$
$(\frac{1}{2},\frac{1}{2},-\frac{1}{2},\frac{1}{2},\frac{1}{2},-\frac{1}{2},\pm\frac{1}{2}^2)$											
$(0,0,0,0,1,1,0^2)$	0	-1	-1	$-\frac{1}{2}$	$\frac{1}{2}$	$\frac{1}{2}$	$\frac{1}{2}$	-1	0	0	$(\mathbf{3},\mathbf{1})$
$(-\frac{1}{2},-\frac{1}{2},-\frac{1}{2},-\frac{1}{2},\frac{1}{2},\frac{1}{2},\pm\frac{1}{2}^2)$											
$(0,0,0,1,0,1,0^2)$	-1	0	-1	$\frac{1}{2}$	$-\frac{1}{2}$	$\frac{1}{2}$	$\frac{1}{2}$	0	-1	0	$(\mathbf{3},\mathbf{1})$
$(-\frac{1}{2},-\frac{1}{2},-\frac{1}{2},\frac{1}{2},-\frac{1}{2},\frac{1}{2},\pm\frac{1}{2}^2)$											

weight	H_1	H_2	H_3	N^1	N^2	N^3	N^S	$\Delta\mathsf{N}^1$	$\Delta\mathsf{N}^2$	$\Delta\mathsf{N}^3$	repr.
$(0,0,0,1,1,0,0^2)$	-1	-1	0	$\frac{1}{2}$	$\frac{1}{2}$	$-\frac{1}{2}$	$\frac{1}{2}$	0	0	-1	$(\mathbf{3},\mathbf{1})$
$(-\frac{1}{2},-\frac{1}{2},-\frac{1}{2},\frac{1}{2},\frac{1}{2},-\frac{1}{2},\pm\frac{1}{2}^2)$											
$(-\frac{1}{2},-\frac{1}{2},-\frac{1}{2},\frac{1}{2},\frac{1}{2},\frac{1}{2},\underline{-\frac{1}{2},\frac{1}{2}})$	-1	-1	-1	$\frac{5}{4}$	$\frac{5}{4}$	$\frac{5}{4}$	$\frac{5}{4}$	0	0	0	$(\mathbf{1},\mathbf{2})$
$(-\frac{1}{2},-\frac{1}{2},\frac{1}{2},-\frac{1}{2},\frac{1}{2},\frac{1}{2},\underline{-\frac{1}{2},\frac{1}{2}})$	$\frac{1}{2}$	$-\frac{1}{2}$	-1	$-\frac{3}{4}$	$\frac{1}{4}$	$\frac{1}{4}$	$\frac{1}{4}$	-1	0	0	$(\mathbf{1},\mathbf{2})$
$(-\frac{1}{2},\frac{1}{2},-\frac{1}{2},-\frac{1}{2},\frac{1}{2},\frac{1}{2},\underline{-\frac{1}{2},\frac{1}{2}})$	$\frac{1}{2}$	-1	$-\frac{1}{2}$	$-\frac{3}{4}$	$\frac{1}{4}$	$\frac{1}{4}$	$\frac{1}{4}$	-1	0	0	$(\mathbf{1},\mathbf{2})$
$(-\frac{1}{2},-\frac{1}{2},\frac{1}{2},\frac{1}{2},-\frac{1}{2},\frac{1}{2},\underline{-\frac{1}{2},\frac{1}{2}})$	$-\frac{1}{2}$	$\frac{1}{2}$	-1	$\frac{1}{4}$	$-\frac{3}{4}$	$\frac{1}{4}$	$\frac{1}{4}$	0	-1	0	$(\mathbf{1},\mathbf{2})$
$(\frac{1}{2},-\frac{1}{2},-\frac{1}{2},\frac{1}{2},-\frac{1}{2},\frac{1}{2},\underline{-\frac{1}{2},\frac{1}{2}})$	-1	$\frac{1}{2}$	$-\frac{1}{2}$	$\frac{1}{4}$	$-\frac{3}{4}$	$\frac{1}{4}$	$\frac{1}{4}$	0	-1	0	$(\mathbf{1},\mathbf{2})$
$(-\frac{1}{2},\frac{1}{2},-\frac{1}{2},\frac{1}{2},\frac{1}{2},-\frac{1}{2},\underline{-\frac{1}{2},\frac{1}{2}})$	$-\frac{1}{2}$	-1	$\frac{1}{2}$	$\frac{1}{4}$	$\frac{1}{4}$	$-\frac{3}{4}$	$\frac{1}{4}$	0	0	-1	$(\mathbf{1},\mathbf{2})$
$(\frac{1}{2},-\frac{1}{2},-\frac{1}{2},\frac{1}{2},\frac{1}{2},-\frac{1}{2},\underline{-\frac{1}{2},\frac{1}{2}})$	-1	$-\frac{1}{2}$	$\frac{1}{2}$	$\frac{1}{4}$	$\frac{1}{4}$	$-\frac{3}{4}$	$\frac{1}{4}$	0	0	-1	$(\mathbf{1},\mathbf{2})$
$(-1,0,0,1,0,0,0^2)$	-1	$-\frac{1}{2}$	$-\frac{1}{2}$	$\frac{1}{4}$	$\frac{1}{4}$	$\frac{1}{4}$	$\frac{1}{4}$	0	0	0	$(\mathbf{1},\mathbf{1})$
$(0,-1,0,0,1,0,0^2)$	$-\frac{1}{2}$	-1	$-\frac{1}{2}$	$\frac{1}{4}$	$\frac{1}{4}$	$\frac{1}{4}$	$\frac{1}{4}$	0	0	0	$(\mathbf{1},\mathbf{1})$
$(0,0,-1,0,0,1,0^2)$	$-\frac{1}{2}$	$-\frac{1}{2}$	-1	$\frac{1}{4}$	$\frac{1}{4}$	$\frac{1}{4}$	$\frac{1}{4}$	0	0	0	$(\mathbf{1},\mathbf{1})$
$(1,0,0,0,-1,0,0^2)$	0	$\frac{3}{2}$	$\frac{1}{2}$	1	0	0	0	1	0	0	$(\mathbf{1},\mathbf{1})$
$(1,0,0,0,0,-1,0^2)$	0	$\frac{1}{2}$	$\frac{3}{2}$	1	0	0	0	1	0	0	$(\mathbf{1},\mathbf{1})$
$(0,1,0,-1,0,0,0^2)$	$\frac{3}{2}$	0	$\frac{1}{2}$	0	1	0	0	0	1	0	$(\mathbf{1},\mathbf{1})$
$(0,1,0,0,0,-1,0^2)$	$\frac{1}{2}$	0	$\frac{3}{2}$	0	1	0	0	0	1	0	$(\mathbf{1},\mathbf{1})$
$(0,0,1,-1,0,0,0^2)$	$\frac{3}{2}$	$\frac{1}{2}$	0	0	0	1	0	0	0	1	$(\mathbf{1},\mathbf{1})$
$(0,0,1,0,0,-1,0^2)$	$\frac{1}{2}$	$\frac{3}{2}$	0	0	0	1	0	0	0	1	$(\mathbf{1},\mathbf{1})$
$(0,0,0,0,1,-1,0^2)$	0	-1	-1	$-\frac{1}{2}$	$\frac{1}{2}$	$\frac{1}{2}$	$\frac{1}{2}$	-1	0	0	$(\mathbf{1},\mathbf{1})$
$(0,0,0,1,0,-1,0^2)$	-1	0	-1	$\frac{1}{2}$	$-\frac{1}{2}$	$\frac{1}{2}$	$\frac{1}{2}$	0	-1	0	$(\mathbf{1},\mathbf{1})$
$(0,0,0,1,-1,0,0^2)$	-1	-1	0	$\frac{1}{2}$	$\frac{1}{2}$	$-\frac{1}{2}$	$\frac{1}{2}$	0	0	-1	$(\mathbf{1},\mathbf{1})$

Table 6.7: The line bundle charges H_i, the triangulation multiplicities N^i, N^S and the triangulation difference multiplicities $\Delta\mathsf{N}^i$ are given for the $SU(3)\times SU(2)$ charged and singlet states obtained from the line bundle background defined by (6.57).

Since in this model all the gauge flux is located in a single E_8, the loop–corrected DUY equations in the form (6.30) can be used. Since for this model there are only three bundle vectors $\mathcal{V}_1$, $\mathcal{V}_2$ and $\mathcal{V}_3$ which are clearly independent, the DUY equations reduce to three equations:

$$\begin{aligned}
\sum_{\beta\gamma} e^{-2\phi}\,\mathrm{Vol}(E_{1,\beta\gamma}) &= \frac{1}{16\pi}\big(64 + 2\,N_{E_1} - 2\,N_{E_2} - 2\,N_{E_3}\big)\ , \\
\sum_{\alpha\gamma} e^{-2\phi}\,\mathrm{Vol}(E_{2,\alpha\gamma}) &= \frac{1}{16\pi}\big(64 + 2\,N_{E_2} - 2\,N_{E_1} - 2\,N_{E_3}\big)\ , \\
\sum_{\beta\gamma} e^{-2\phi}\,\mathrm{Vol}(E_{3,\alpha\beta}) &= \frac{1}{16\pi}\big(64 + 2\,N_{E_3} - 2\,N_{E_1} - 2\,N_{E_2}\big)\ .
\end{aligned} \tag{6.59}$$

Since, the sum of volumes all need to be non–negative, the right–hand–sides of these equations all have to be positive. This leads to the conditions on the number of times the exceptional triangulations may be chosen:

$$N_{E_2} + N_{E_3} - N_{E_1} \leq 32\ , \quad N_{E_1} + N_{E_3} - N_{E_2} \leq 32\ , \quad N_{E_1} + N_{E_2} - N_{E_3} \leq 32\ . \tag{6.60}$$

Adding two of these three conditions shows that $N_{E_i} \leq 32$. In addition, (6.6) implies that

$$N_{E_1} + N_{E_2} + N_{E_3} \leq 64\ . \tag{6.61}$$

Thus apparently, one can only choose the S–triangulation at all 64 resolved singularities, but not one of the exceptional triangulations. However, one can choose to use exceptional triangulations at all resolved singularities, but not at all of them the same one. For example, the choice, $N_{E_1} = N_{E_2} = 16$ and $N_{E_3} = 32$, would be allowed by the DUY conditions.

6.5 Jumping Spectra in a Blasczcyk–like GUT model

In ref. [32] a semi–realistic MSSM model line bundle model on a resolution of $T^6/\mathbb{Z}_2 \times \mathbb{Z}_2$ was constructed with gauge group $\mathrm{SU}(5) \times \mathrm{SU}'(3) \times \mathrm{SU}'(2)$. This model possessed an freely acting involution that reduced the gauge symmetry to the standard model gauge group. For this model the E_1–triangulation was chosen at all 64 resolved $\mathbb{C}^3/\mathbb{Z}_2 \times \mathbb{Z}_2$. In this section models similar to the Blasczcyk's GUT model are considered. The emphasis is not so much on finding a phenomenologically satisfactory model but rather on illustrating the effects of flop–transitions on the spectrum.

6.5.1 Generalities of Blasczcyk–like GUT models

Models like the Blaszczyk's GUT model are particular resolution of an orbifold theory with, in addition to two shifts V_1 and V_2 associated to the twists v_1 and v_2, up to five Wilson lines in all torus directions are switched on. The Wilson lines in the second, fourth and sixth torus directions are all taken equal: $W_2 = W_4 = W_6$ and independent of the two remaining Wilson

Bundle vectors	
$\mathcal{V}_{1000} = \mathcal{V}_{1010}$	$(-\frac{1}{2}, -\frac{1}{2}, 1, 0, 0, 0, 0, 0)(0, 0, 0, 0, 0, 0, 0, 0)$
$\mathcal{V}_{1100} = \mathcal{V}_{1110}$	$(0, 1, 0, 0, 0, 0, 0, 0)(0, 0, 0, 0, 0, 0, -\frac{1}{2}, -\frac{1}{2})$
$\mathcal{V}_{1001} = \mathcal{V}_{1011}$	$(\frac{1}{4}, \frac{1}{4}, \frac{3}{4}, -\frac{1}{4}, -\frac{1}{4}, -\frac{1}{4}, -\frac{1}{4}, -\frac{1}{4})(-\frac{1}{4}, -\frac{1}{4}, -\frac{1}{4}, -\frac{1}{4}, -\frac{1}{4}, -\frac{1}{4}, \frac{1}{4}, \frac{1}{4})$
$\mathcal{V}_{1101} = \mathcal{V}_{1111}$	$(\frac{1}{4}, -\frac{3}{4}, \frac{1}{4}, \frac{1}{4}, \frac{1}{4}, \frac{1}{4}, \frac{1}{4}, \frac{1}{4})(-\frac{1}{4}, -\frac{1}{4}, -\frac{1}{4}, -\frac{1}{4}, -\frac{1}{4}, -\frac{1}{4}, -\frac{1}{4}, -\frac{1}{4})$
$\mathcal{V}_{2\_00} = \mathcal{V}_{2\_10}$	$(\frac{1}{4}, -\frac{1}{4}, \frac{1}{4}, -\frac{1}{4}, -\frac{1}{4}, -\frac{1}{4}, -\frac{1}{4}, -\frac{1}{4})(0, 0, 0, 0, 0, 0, 0, -1)$
$\mathcal{V}_{2\_01} = \mathcal{V}_{2\_11}$	$(\frac{1}{2}, 0, \frac{1}{2}, 0, 0, 0, 0, 0)(\frac{1}{4}, \frac{1}{4}, \frac{1}{4}, \frac{1}{4}, -\frac{3}{4}, \frac{1}{4}, -\frac{1}{4}, -\frac{1}{4})$
$\mathcal{V}_{30\_0}$	$(-\frac{1}{4}, \frac{1}{4}, \frac{1}{4}, -\frac{1}{4}, -\frac{1}{4}, -\frac{1}{4}, -\frac{1}{4}, -\frac{1}{4})(0, 0, 0, 0, 0, 0, -1, 0)$
$\mathcal{V}_{31\_0}$	$(-\frac{1}{4}, \frac{1}{4}, \frac{3}{4}, \frac{1}{4}, \frac{1}{4}, \frac{1}{4}, \frac{1}{4}, \frac{1}{4})(0, 0, 0, 0, 0, 0, \frac{1}{2}, -\frac{1}{2})$
$\mathcal{V}_{30\_1}$	$(0, \frac{1}{2}, \frac{1}{2}, 0, 0, 0, 0, 0)(\frac{1}{4}, \frac{1}{4}, \frac{1}{4}, \frac{1}{4}, \frac{1}{4}, -\frac{3}{4}, -\frac{1}{4}, -\frac{1}{4})$
$\mathcal{V}_{31\_1}$	$(-\frac{1}{2}, 0, \frac{1}{2}, 0, 0, 0, 0, 0)(-\frac{1}{4}, -\frac{1}{4}, -\frac{1}{4}, -\frac{1}{4}, -\frac{1}{4}, \frac{3}{4}, -\frac{1}{4}, -\frac{1}{4})$

Table 6.8: A set of bundle vectors associated to two shifts and four Wilson lines that satisfy the flux quantisation conditions and the Bianchi identities in all triangulations.

lines W_3 and W_5. The resulting line bundle vectors are given by

$$\begin{aligned}
\mathcal{V}_{1,\beta\gamma} = \mathcal{V}_{1\beta_3\gamma_5(\beta_4+\gamma_6)} &= V_1 + \beta_3\, W_3 + \gamma_5\, W_5 + (\beta_4+\gamma_6)W_2 + L_{1\beta_3\gamma_5(\beta_4+\gamma_6)} \\
\mathcal{V}_{2,\alpha\gamma} = \mathcal{V}_{2_\gamma_5(\alpha_2+\gamma_6)} &= V_1 + \gamma_5\, W_5 + (\alpha_2+\gamma_6)W_2 + L_{2\gamma_5(\alpha_2+\gamma_6)} \\
\mathcal{V}_{3,\alpha\beta} = \mathcal{V}_{3\beta_3_(\alpha_2+\beta_4)} &= V_3 + \beta_3\, W_3 + (\alpha_2+\beta_4)W_2 + L_{3\gamma_5(\alpha_2+\beta_4)}
\end{aligned} \tag{6.62}$$

using the binary multi–index notation introduced in Subsection 6.2.1. Here $L_{1\beta_3\gamma_5(\beta_4+\gamma_6)}$, $L_{2\gamma_5(\alpha_2+\gamma_6)}$ and $L_{3\gamma_5(\alpha_2+\beta_4)}$ are appropriately chosen $E_8 \times E_8$ lattice vectors. The sum in between brackets is defined modulo two (since two times a Wilson line is a lattice vector which can be absorbed in one of the L's). Thus, in total these kind of blowup models are defined by $8 + 4 + 4 = 16$ line bundle vectors and the 64 resolved fixed points are distinguished in 32 bunches of two fixed points as the index $\alpha_1 = 0, 1$ still parameterises a twofold degeneracy. In addition, there is a freely acting symmetry in such models: if one simultaneously adds 1 to the three indices $\alpha_2, \beta_4, \gamma_6$ modulo two:

$$(\alpha_2, \beta_4, \gamma_6) \mapsto (\alpha_2 + 1, \beta_4 + 1, \gamma_6 + 1)\ , \tag{6.63}$$

all bundle vectors are identical. This isometry was used in ref. [32] introduce a freely acting Wilson line to break the $SU(5)$ GUT to the standard model. This step won't be considered here.

6.5.2 Triangulation independent Blaszczyk–like GUT models

The aim of this section is to engineer a modification of the Blaszczyk's GUT model such that it fulfils the Bianchi identities in an arbitrary triangulation. As this turned out to be a very

Observable E_8				Hidden E_8			
$SU(5)$–adjoint		Singlets		$SU(4)$–adjoint		$\mathbf{1}_4$	$(0^4,0,1,0,1)$
24	$(0^3,\underline{1,-1,0^3})$	$\mathbf{1}_1$	$(1,1,0,0^5)$	**15**	$(\underline{1,-1,0^2},0^4)$	$\mathbf{1}_5$	$(0^4,0,0,1,1)$
5–plets		$\mathbf{1}_2$	$(1,0,1,0^5)$	4–plets		$\mathbf{1}_6$	$(0^4,1,$ -1$,0,0)$
$\mathbf{5}_1$	$(0,1,0,\underline{1,0^4})$	$\mathbf{1}_3$	$(0,1,1,0^5)$	$\mathbf{4}_1$	$(\underline{1,0^3},0,0,1,0)$	$\mathbf{1}_7$	$(0^4,1,0,$ -1$,0)$
$\mathbf{5}_2$	$(0,0,1,\underline{1,0^4})$	$\mathbf{1}_4$	$(1,$ -1$,0,0^5)$	$\mathbf{4}_2$	$(\underline{1,0^3},0,0,0,1)$	$\mathbf{1}_8$	$(0^4,1,0,0,$ -1$)$
$\mathbf{5}_3$	$(0,$ -1$,0,\underline{1,0^4})$	$\mathbf{1}_5$	$(1,0,$ -1$,0^5)$	$\mathbf{4}_3$	$(\underline{1,0^3},$ -1$,0,0,0)$	$\mathbf{1}_8$	$(0^4,1,0,0,$ -1$)$
$\mathbf{5}_4$	$(0,0,$ -1$,\underline{1,0^4})$	$\mathbf{1}_6$	$(0,1,$ -1$,0^5)$	$\mathbf{4}_4$	$(\underline{1,0^3},0,$ -1$,0,0)$	$\mathbf{1}_{10}$	$(0^4,0,1,0,$ -1$)$
$\mathbf{5}_5$	$(-\frac{1}{2},-\frac{1}{2},\frac{1}{2},\underline{\frac{1}{2},-\frac{1}{2}^4})$	$\mathbf{1}_7$	$(-\frac{1}{2},-\frac{1}{2},\frac{1}{2},\frac{1}{2}^5)$	$\mathbf{4}_5$	$(\underline{1,0^3},0,0,$ -1$,0)$	$\mathbf{1}_{11}$	$(0^4,0,0,1,$ -1$)$
$\mathbf{5}_6$	$(-\frac{1}{2},\frac{1}{2},-\frac{1}{2},\underline{\frac{1}{2},-\frac{1}{2}^4})$	$\mathbf{1}_8$	$(-\frac{1}{2},\frac{1}{2},-\frac{1}{2},\frac{1}{2}^5)$	$\mathbf{4}_6$	$(\underline{1,0^3},0,0,0,$ -1$)$	$\mathbf{1}_{12}$	$(\frac{1}{2}^4,\frac{1}{2},\frac{1}{2},\frac{1}{2},\frac{1}{2})$
$\mathbf{5}_7$	$(\frac{1}{2},-\frac{1}{2},-\frac{1}{2},\underline{\frac{1}{2},-\frac{1}{2}^4})$	$\mathbf{1}_9$	$(\frac{1}{2},-\frac{1}{2},-\frac{1}{2},\frac{1}{2}^5)$	$\mathbf{4}_7$	$(\underline{\frac{1}{2},-\frac{1}{2}^3},-\frac{1}{2},\frac{1}{2},-\frac{1}{2},-\frac{1}{2})$	$\mathbf{1}_{13}$	$(\frac{1}{2}^4,-\frac{1}{2},-\frac{1}{2},\frac{1}{2},\frac{1}{2})$
$\mathbf{5}_8$	$(\frac{1}{2},\frac{1}{2},\frac{1}{2},\underline{\frac{1}{2},-\frac{1}{2}^4})$	$\mathbf{1}_{10}$	$(\frac{1}{2},\frac{1}{2},\frac{1}{2},\frac{1}{2}^5)$	$\mathbf{4}_8$	$(\underline{\frac{1}{2},-\frac{1}{2}^3},-\frac{1}{2},\frac{1}{2},\frac{1}{2},\frac{1}{2})$	$\mathbf{1}_{14}$	$(\frac{1}{2}^4,-\frac{1}{2},\frac{1}{2},-\frac{1}{2},\frac{1}{2})$
10–plet		**10**	$(\frac{1}{2},\frac{1}{2},-\frac{1}{2},\underline{\frac{1}{2}^2,-\frac{1}{2}^3})$	$\mathbf{4}_9$	$(\underline{\frac{1}{2},-\frac{1}{2}^3},\frac{1}{2},-\frac{1}{2},\frac{1}{2},\frac{1}{2})$	$\mathbf{1}_{15}$	$(\frac{1}{2}^4,-\frac{1}{2},\frac{1}{2},\frac{1}{2},-\frac{1}{2})$
				Singlets		$\mathbf{1}_{16}$	$(\frac{1}{2}^4,\frac{1}{2},-\frac{1}{2},-\frac{1}{2},\frac{1}{2})$
				$\mathbf{1}_1$	$(0^4,1,0,1,0)$	$\mathbf{1}_{17}$	$(\frac{1}{2}^4,\frac{1}{2},-\frac{1}{2},\frac{1}{2},-\frac{1}{2})$
				$\mathbf{1}_2$	$(0^4,1,0,0,1)$	$\mathbf{1}_{18}$	$(\frac{1}{2}^4,\frac{1}{2},\frac{1}{2},-\frac{1}{2},-\frac{1}{2})$
				$\mathbf{1}_3$	$(0^4,0,1,1,0)$	$\mathbf{1}_{19}$	$(\frac{1}{2}^4,-\frac{1}{2},-\frac{1}{2},-\frac{1}{2},-\frac{1}{2})$

Table 6.9: The identification between the roots and the states in the spectrum in both the observable and hidden sectors. States in the same non–Abelian representation but with different $U(1)$–charges are enumerated.

difficult, here only models are considered in which the Wilson lines $W_2 = W_4 = W_6$ and W_3 are switched on. Concretely the orbifold data of the model under consideration here is given by:

$$\begin{aligned} V_1 &= (-\tfrac{1}{2},-\tfrac{1}{2},1,0^5)(0^8)\ , \qquad V_2 = (\tfrac{1}{4},-\tfrac{1}{4},\tfrac{1}{4},-\tfrac{1}{4}^5)(0^6,0,-1)\ , \\ W_3 &= (0,0,\tfrac{1}{2},\tfrac{1}{2}^5)(0^6,-\tfrac{1}{2},-\tfrac{1}{2})\ , \qquad W_2 = W_4 = W_6 = (\tfrac{1}{4},\tfrac{1}{4},\tfrac{1}{4},\tfrac{1}{4}^5)(-\tfrac{1}{4}^6,\tfrac{1}{4},\tfrac{1}{4})\ . \end{aligned} \tag{6.64}$$

Using the freedom to add lattice vectors in (6.62) it is possible to obtain a set of bundle vectors that satisfy the strong conditions (6.32)and (6.39), which guarantee that the flux quantisation conditions and the Bianchi identities are satisfied in any triangulation. Such a set is given in Table 6.8.

Resolved fixed points	Spectra in S–triangulation $4 \times \mathsf{N}^S$	Spectrum jumps due to flop–transitions $\Delta\mathsf{N}^1$	$\Delta\mathsf{N}^2$	$\Delta\mathsf{N}^3$
$f_{\alpha_1 0\,0\,0\,\gamma_5 0}$,	$\mathbf{5}_2+\mathbf{5}_4+\overline{\mathbf{5}}_5+\overline{\mathbf{10}}+\overline{\mathbf{1}}_1+3\,\mathbf{1}_7+\mathbf{1}_8+\mathbf{1}_9$	$\overline{\mathbf{1}}_7$	$\overline{\mathbf{1}}_5$	$\mathbf{1}_6$
$f_{\alpha_1 1\,0\,1\,\gamma_5 1}$	$\overline{\mathbf{4}}_1+\overline{\mathbf{4}}_2+\mathbf{4}_5+\mathbf{4}_6+\overline{\mathbf{1}}_1+\overline{\mathbf{1}}_2+\overline{\mathbf{1}}_3+\overline{\mathbf{1}}_4+2\,\mathbf{1}_5+\mathbf{1}_7+\mathbf{1}_8+$ $\mathbf{1}_9+\mathbf{1}_{10}$	$\overline{\mathbf{1}}_5$	$\overline{\mathbf{1}}_{11}$	$\mathbf{1}_{11}$
$f_{\alpha_1 0\,1\,0\,\gamma_5 0}$,	$\overline{\mathbf{5}}_1+\mathbf{5}_2+\overline{\mathbf{5}}_3+\mathbf{5}_7+\mathbf{1}_1+2\,\overline{\mathbf{1}}_3+\mathbf{1}_4+\overline{\mathbf{1}}_5+3\,\mathbf{1}_6+3\,\mathbf{1}_7+$ $3\,\overline{\mathbf{1}}_8+\overline{\mathbf{1}}_{10}$	$\overline{\mathbf{1}}_6$	$\mathbf{5}_1+\overline{\mathbf{5}}_7+\mathbf{1}_3+\overline{\mathbf{1}}_4+$ $\mathbf{1}_8+\mathbf{1}_{10}$	$\overline{\mathbf{1}}_7$
$f_{\alpha_1 1\,1\,1\,\gamma_5 1}$	$\mathbf{4}_2+\overline{\mathbf{4}}_6+\mathbf{1}_2+\mathbf{1}_4+2\,\mathbf{1}_5+\overline{\mathbf{1}}_8+\overline{\mathbf{1}}_{10}+2\,\overline{\mathbf{1}}_{11}$	$\mathbf{1}_{11}$		$\overline{\mathbf{1}}_5$
$f_{\alpha_1 1\,0\,0\,\gamma_5 0}$,	$\overline{\mathbf{5}}_2+\mathbf{5}_4+\mathbf{5}_5+\overline{\mathbf{10}}+3\,\overline{\mathbf{1}}_1+\overline{\mathbf{1}}_2+\overline{\mathbf{1}}_3+\mathbf{1}_7$	$\mathbf{1}_1$	$\overline{\mathbf{1}}_5$	$\overline{\mathbf{1}}_6$
$f_{\alpha_1 0\,0\,1\,\gamma_5 1}$	$\mathbf{4}_3+\mathbf{4}_4+\overline{\mathbf{4}}_8+\overline{\mathbf{4}}_9+\overline{\mathbf{1}}_1+\overline{\mathbf{1}}_2+\overline{\mathbf{1}}_3+\overline{\mathbf{1}}_4+\mathbf{1}_{14}+\mathbf{1}_{15}+\mathbf{1}_{16}+$ $\mathbf{1}_{17}+2\,\overline{\mathbf{1}}_{19}$	$\mathbf{1}_{19}$	$\mathbf{1}_6$	$\overline{\mathbf{1}}_6$
$f_{\alpha_1 1\,1\,0\,\gamma_5 0}$,	$\mathbf{5}_1+\overline{\mathbf{5}}_3+\overline{\mathbf{1}}_1+\mathbf{1}_2+\overline{\mathbf{1}}_3+\mathbf{1}_4+\overline{\mathbf{1}}_5+3\,\mathbf{1}_6$	$\overline{\mathbf{1}}_6$	$\overline{\mathbf{1}}_4$	$\mathbf{1}_1$
$f_{\alpha_1 0\,1\,1\,\gamma_5 1}$	$\mathbf{4}_3+\overline{\mathbf{4}}_4+\overline{\mathbf{4}}_7+\mathbf{4}_9+\mathbf{1}_1+\mathbf{1}_2+\mathbf{1}_5+2\,\mathbf{1}_6+\overline{\mathbf{1}}_9+\overline{\mathbf{1}}_{10}+\mathbf{1}_{13}+$ $\mathbf{1}_{14}+\mathbf{1}_{15}+\overline{\mathbf{1}}_{16}+\overline{\mathbf{1}}_{17}+\overline{\mathbf{1}}_{19}$	$\overline{\mathbf{1}}_6$	$\overline{\mathbf{1}}_{13}$	$\mathbf{1}_{19}$
$f_{\alpha_1 0\,0\,1\,\gamma_5 0}$,	$\mathbf{5}_4+\overline{\mathbf{5}}_8+\overline{\mathbf{1}}_2+2\,\overline{\mathbf{1}}_3+2\,\mathbf{1}_8+\mathbf{1}_9$		$\mathbf{1}_3$	$\overline{\mathbf{1}}_8$
$f_{\alpha_1 1\,0\,0\,\gamma_5 1}$	$\overline{\mathbf{4}}_2+\mathbf{4}_4+\overline{\mathbf{4}}_6+\mathbf{4}_8+\overline{\mathbf{1}}_2+\overline{\mathbf{1}}_3+2\,\mathbf{1}_4+\mathbf{1}_5+\mathbf{1}_6+2\,\overline{\mathbf{1}}_8+3\,\mathbf{1}_{10}+$ $\mathbf{1}_{11}+3\,\mathbf{1}_{16}+\overline{\mathbf{1}}_{17}+3\,\overline{\mathbf{1}}_{18}+\overline{\mathbf{1}}_{19}$	$\mathbf{4}_6+\overline{\mathbf{4}}_8+\overline{\mathbf{1}}_4+\overline{\mathbf{1}}_5+$ $\mathbf{1}_8+\mathbf{1}_{17}+\mathbf{1}_{18}+\mathbf{1}_{19}$	$\overline{\mathbf{1}}_{10}$	$\overline{\mathbf{1}}_{16}$
$f_{\alpha_1 0\,1\,1\,\gamma_5 0}$,	$\mathbf{5}_3+\overline{\mathbf{5}}_6+\overline{\mathbf{1}}_4+\overline{\mathbf{1}}_5+\mathbf{1}_6+\overline{\mathbf{1}}_7+\overline{\mathbf{1}}_8+3\,\mathbf{1}_9$	$\overline{\mathbf{1}}_9$	$\mathbf{1}_7$	$\mathbf{1}_4$
$f_{\alpha_1 1\,1\,0\,\gamma_5 1}$	$\mathbf{4}_2+\overline{\mathbf{4}}_4+\mathbf{4}_6+\overline{\mathbf{4}}_7+\mathbf{1}_2+\mathbf{1}_4+\mathbf{1}_5+\overline{\mathbf{1}}_6+\mathbf{1}_8+\mathbf{1}_9+2\,\overline{\mathbf{1}}_{10}+$ $\mathbf{1}_{11}+\mathbf{1}_{12}+\mathbf{1}_{13}+\mathbf{1}_{16}+\mathbf{1}_{17}$	$\mathbf{1}_{10}$	$\overline{\mathbf{1}}_{17}$	$\overline{\mathbf{1}}_4$
$f_{\alpha_1 0\,0\,0\,\gamma_5 1}$,	$\mathbf{5}_4+\overline{\mathbf{5}}_8+2\,\overline{\mathbf{1}}_2+\overline{\mathbf{1}}_3+\mathbf{1}_8+2\,\mathbf{1}_9$		$\overline{\mathbf{1}}_9$	$\mathbf{1}_2$
$f_{\alpha_1 1\,0\,1\,\gamma_5 0}$	$\overline{\mathbf{4}}_1+\mathbf{4}_3+\overline{\mathbf{4}}_5+\mathbf{4}_9+2\,\mathbf{1}_1+\overline{\mathbf{1}}_2+\overline{\mathbf{1}}_3+\mathbf{1}_5+\overline{\mathbf{1}}_6+3\,\mathbf{1}_7+\overline{\mathbf{1}}_9+$ $\overline{\mathbf{1}}_{11}+\overline{\mathbf{1}}_{14}+3\,\mathbf{1}_{15}+3\,\overline{\mathbf{1}}_{18}+\overline{\mathbf{1}}_{19}$	$\mathbf{4}_5+\overline{\mathbf{4}}_9+\overline{\mathbf{1}}_1+\overline{\mathbf{1}}_5+$ $\mathbf{1}_9+\mathbf{1}_{14}+\mathbf{1}_{18}+\mathbf{1}_{19}$	$\overline{\mathbf{1}}_{15}$	$\overline{\mathbf{1}}_7$
$f_{\alpha_1 0\,1\,0\,\gamma_5 1}$,	$\overline{\mathbf{5}}_2+\mathbf{5}_3+\mathbf{5}_6+\overline{\mathbf{5}}_7+\overline{\mathbf{1}}_2+\overline{\mathbf{1}}_3+\overline{\mathbf{1}}_4+\overline{\mathbf{1}}_5+\mathbf{1}_6+2\,\overline{\mathbf{1}}_7+\mathbf{1}_9+\overline{\mathbf{1}}_{10}$	$\mathbf{1}_3$	$\mathbf{1}_7$	$\mathbf{1}_4$
$f_{\alpha_1 1\,1\,1\,\gamma_5 0}$	$\mathbf{4}_3+\overline{\mathbf{4}}_9+\mathbf{1}_1+\mathbf{1}_2+\overline{\mathbf{1}}_6+\mathbf{1}_{11}+\overline{\mathbf{1}}_{12}+3\,\mathbf{1}_{14}+\overline{\mathbf{1}}_{15}+\mathbf{1}_{19}$	$\mathbf{1}_{15}$	$\overline{\mathbf{1}}_{14}$	$\overline{\mathbf{1}}_1$

Table 6.10: Each big row corresponds to two sets of four resolved $\mathbb{C}^3/\mathbb{Z}_2\times\mathbb{Z}_2$ fixed points labelled by $\alpha_1,\gamma_5=0,1$ (because their local bundle vectors are identical and thus so are their local spectra). The lines with the white background give the observable spectra resulting from the first E_8 and the lines with grey background the hidden spectrum from the second E_8. The charge states are labeled in Table 6.9. (Since all singlet are charged it make sense to talk about a singlet state or its conjugate.) The second column gives the contributions at the four local resolved singularities using the S–triangulation combined. The columns $\Delta\mathsf{N}^1$, $\Delta\mathsf{N}^2$ and $\Delta\mathsf{N}^3$ indicate the jumps in the spectra for a single resolved fixed point out of these sets of four singularities.

The resulting spectra are given in Table 6.10. The states used in that table are defined in Table 6.9 from the roots of both E_8–factors. Notice, that not all E_8–roots (up to conjugation) appear here; only the states, that have a non–vanishing multiplicity in the models defined here, are listed. The subscripts are used to distinguish states that have the same non–Abelian representation but different $U(1)$ charges. The second column gives the spectra from the local resolved singularities when the S–triangulation is used at all 64 of them. Since the labels

$\alpha_1, \gamma_5 = 0, 1$ are arbitrary, there will be a fourfold degeneracy in the spectrum, this is already taking into account in the table by multiplying the spectra in the S–triangulation by 4. The additional two–fold degeneracy due to the freely action symmetry is made apparent by giving two sets of four resolved singularities. It is not difficult to see that the full spectrum using the S–triangulation is free of non–Abelian anomalies.

The final three columns of Table 6.10 displays the jumps in the spectra when at a given singularity the S–triangulation is flopped to the triangulation E_1, E_2 or E_3. These are the jumps at a single resolved fixed point. It can be seen that in accordance with our general findings this jumps are always integral. Most jumps that occur in the spectra involve singlets only. At the resolved fixed points $f_{\alpha_1 0\, 10\, \alpha_5 0}$ and $f_{\alpha_1 1\, 11\, \gamma_5 0}$ a $\mathbf{5}$ and $\overline{\mathbf{5}}$ pair appears during a flop from the S to the E_2–triangulation. Similarly, a $\mathbf{4}$ and $\overline{\mathbf{4}}$ pair appears at resolved fixed points $f_{\alpha_1 0\, 01\, \gamma_5 0}$ and $f_{\alpha_1 0\, 00\, \gamma_5 1}$. Thus, at most only non–Abelian vector–like pairs can arise during a flop transition.

6.6 Conclusion

Summary

This chapter has been devoted to a specific problem which occurs in resolutions of certain toroidal orbifolds, namely that the resolutions of the local singularities is not unique at the topological level and therefore leads to an explosion of topologically distinct smooth geometries all associated to one and the same orbifold. As a concrete working example the focus was on the resolutions of a $T^6/\mathbb{Z}_2 \times \mathbb{Z}_2$ orbifold which contains 64 $\mathbb{C}^3/\mathbb{Z}_2 \times \mathbb{Z}_2$ singularities, each of which admits four distinct resolutions encoded by different triangulations of their toric diagram.

The key idea to overcome this complication is to use a parameterisation to keep track of the triangulations chosen at all resolved fixed points simultaneously. It turned out not to be very cumbersome to express the fundamental (self–)intersection numbers of the divisors of the resolution in terms of this data. Once the (self–)intersection numbers were determined, many derived objects can be computed without much more difficulty as determining them within a specific triangulation. In particular, we checked our procedure by computing the integrated third Chern class directly and confirmed that it equals 96 independently of any triangulation choice. We obtained expressions for the volumes of curves, divisors and the manifold as a whole for any possible choice of the triangulation of the 64 $\mathbb{Z}_2 \times \mathbb{Z}_2$ singularities. In addition, we worked out some of the fundamental consistency conditions of line bundle models on the resolutions of the $T^6/\mathbb{Z}_2 \times \mathbb{Z}_2$ like the flux quantisation conditions and the integrated Bianchi identities (which for simplicity were only considered without five branes). Even a tool which is often used to compute the chiral part of the spectrum, the multiplicity operator, could be determined once and for all for any choice of triangulation.

Having written down the fundamental consistency conditions for any possible choice of triangulation, allowed for posing the question what conditions have to be enforced to ensure that they are satisfied for all possible triangulations simultaneously. It turned out that if the flux quantisation conditions are satisfied for a given specific choice of triangulation, they are, in fact, fulfilled for any configuration of triangulations: the flux quantisation conditions turned out to be triangulation independent. The superimposed integrated Bianchi identities reduced to much simpler requirements than those within any particular choice of triangulation. Moreover, they are quite reminiscent of some of the properties of shifted momenta of the blowup modes

Toroidal orbifold	Number of fixed points	Triangulations per fixed point	Naive number of resolutions
$T^6/\mathbb{Z}_{6\text{–II}}$	12	5	$5^{12} \sim 10^8$
$T^6/\mathbb{Z}_2 \times \mathbb{Z}_2$	64	4	$4^{64} \sim 10^{38}$
$T^6/\mathbb{Z}_2 \times \mathbb{Z}_4$	24	16	$16^{24} \sim 10^{28}$
$T^6/\mathbb{Z}_3 \times \mathbb{Z}_3$	27	79	$79^{27} \sim 10^{51}$

Table 6.11: Triangulation dependence and the naive number of resulting resolutions of toroidal orbifolds as can be inferred from the data in ref. [76].

that induce the resolution from the orbifold perspective.

These ideas and results were illustrated by a number of examples in the remainder of the chapter. For simplicity, first line bundle models were considered, where the 48 line bundle vectors were chosen to be determined by three defining vectors. By computing spectra in all triangulations explicitly, it was confirmed that the full chiral spectra are always integral. We take this as a very strong crosscheck of the procedure outlined in this chapter to parameterise all possible triangulations of the resolved singularities of the $T^6/\mathbb{Z}_2 \times \mathbb{Z}_2$ orbifold. This was also checked explicitly in a variant of the Blasczczyk's GUT model with four Wilson lines of which three were set equal. The full spectrum computed in the S–triangulation everywhere is integral and free of non–Abelian anomalies. But also all the local difference multiplicities measuring the jumps in the local spectra at specific resolved singularities are always integral and free of non–Abelian anomalies (as the jumping spectra were all vector–like in this particular example).

Outlook

This chapter focused on one particular $T^6/\mathbb{Z}_2 \times \mathbb{Z}_2$ orbifold, it is to be expected that this procedure can also be applied to the other $T^6/\mathbb{Z}_2 \times \mathbb{Z}_2$ orbifolds. In fact, applications do not stop there, for any orbifold for which the resolution of some of the local singularities is not unique, it may be applied. Table 6.11 gives an overview of some toroidal orbifolds for which the triangulations of their local singularities are not unique and a naive estimate of the number of resolved geometries which therefore can be associated to that orbifold. (The numbers quoted in this table are upper limits: these orbifolds can be defined on different lattices on which the number of fixed points may be lower than the numbers indicated here.) Moreover, triangulation ambiguities do not only show up in toroidal orbifolds resolutions, also in other Calabi–Yau constructions they might be present. For example, some Calabi–Yaus in the Kreuzer–Skarke list obtained as hypersurfaces in toric varieties are not unique due to different triangulation choices [103,104]. One may therefore speculate whether similar methods may also be applied there.

To take these studies further to the resolutions of $\mathbb{Z}_2 \times \mathbb{Z}_2$ orbifolds the present work is likely to be instrumental as it allows to study the required resolutions in general and not be hampered by focusing on a particular triangulation from the very beginning.

Chapter 7

The fate of discrete torsion on resolved heterotic $\mathbb{Z}_2 \times \mathbb{Z}_2$ orbifolds using $(0,2)$ GLSMs

7.1 Introduction

This last chapter aims to shed light on what becomes of discrete torsion within heterotic orbifolds when they are resolved to smooth geometries. Gauged Linear Sigma Models (GLSMs) possessing (0,2) worldsheet supersymmetry are employed as interpolations between them. This question is addressed for resolutions of the non–compact $\mathbb{C}^3/\mathbb{Z}_2 \times \mathbb{Z}_2$ and the compact $T^6/\mathbb{Z}_2 \times \mathbb{Z}_2$ orbifolds to keep track of local and global aspects. The GLSMs associated with the non–compact orbifold with or without torsion are to a large extent equivalent: only when expressed in the same superfield basis, a field redefinition anomaly arises among them, which in the orbifold limit reproduces the discrete torsion phases. Previously unknown, novel resolution GLSMs for $T^6/\mathbb{Z}_2 \times \mathbb{Z}_2$ are constructed. The GLSM associated with the torsional compact orbifold suffers from mixed gauge anomalies, which need to be cancelled by appropriate logarithmic superfield dependent FI–terms on the worldsheet, signaling H–flux due to NS5–branes supported at the exceptional cycles.

The $\mathbb{Z}_2 \times \mathbb{Z}_2$ orbifolds of six dimensional toroidal compactifications are among the most studied string constructions to date. They have been used to derive phenomenological string models and to study how the parameters of the Standard Model may be derived from string theory, using their free fermionic [13–15, 17–19] and orbifold [20–22, 24] realisations, and their smooth resolutions [32]. Other phenomenological interesting smooth compactifications have been investigated in [25–30, 33]. These phenomenological studies encompass supersymmetric and non–supersymmetric string vacua [78, 96, 105–107] with symmetric and asymmetric boundary conditions [108, 109] and the $\mathbb{Z}_2 \times \mathbb{Z}_2$ orbifolding can enable the fixing of all of the untwisted geometrical moduli [110].

The worldsheet constructions of string vacua consist of a perturbative expansion in string amplitudes. They are constrained to preserve the classical symmetries of reparameterisation and Weyl invariance, *i.e.* they are invariant under modular transformations of the worldsheet parameter, and are encoded in the one–loop partition function. The requirement of modular invariance entails that the partition function is a sum over different sectors that combine

to form a modular invariant object. While most of the signs in this sum are dictated by modular invariance, some other may be arbitrary and play a vital role in determining the physical properties of the string models. In particular, the origins of mirror symmetry and spinor–vector dualities may be traced back to (generalised) discrete torsions. Discrete torsions typically arise in the worldsheet constructions as a result of multiple modding out operations. For example, we may mod out by several twists of the internal dimensions; or by identifications by translations of points in the internal compactified space; or we may combine actions of these shifts and twists. Additionally, in the heterotic–string these may be combined with an action on the gauge bundles, which results in a reduction of the gauge symmetry. The spinor–vector duality, for example, arises due to the action of Wilson lines on the gauge bundles.

The interpretation of (generalised) discrete torsions from the geometrical effective field theory point of view is obscured as one does not have an exact partition function description in which these discrete torsion phases are present. It is therefore of interest to elucidate the manifestation of the discrete torsions in the effective field theory limit. If there is a discrete action on the target space, this can be accompanied with discrete torsion in the form of some non–trivial action on the B–field [89, 90, 111]. However, in this chapter we however wondered what happens to the discrete torsion between orbifold twists, if one fully resolves the orbifold so that no discrete symmetries are left on the smooth target space. We aim to investigate this manifestation using the Gauged Linear Sigma Model (GLSM) representation of string vacua. GLSMs provide a particularly appealing framework to explore this question, as they provide a single framework in which one can interpolate between different regimes, like the singular orbifold limit and smooth compactifications.

7.1.1 Main chapter objectives

One of the central objectives of this chapter is to systematically study the discrete torsion phases in smooth string compactifications using the GLSM language to bridge the gap between the orbifold CFT formulations and the effective field theory descriptions for smooth target spaces. Concretely, this program is considered for $\mathbb{Z}_2 \times \mathbb{Z}_2$ orbifolds of free CFTs where the discrete torsion is known as the Vafa–Witten phase.

First resolutions of the non–compact $\mathbb{C}^3/\mathbb{Z}_2 \times \mathbb{Z}_2$ orbifold are considered in the GLSM language. To have a particular simple context the focus is on line bundle resolutions generated by physical blowup modes, twisted string states without oscillator excitations. The precise identification of such resolution GLSMs from this data was worked out in the past [112]. Since only the standard embedding bundles would allow for a $(2, 2)$ worldsheet description, the incorporation of line bundles requires a $(0, 2)$ GLSM language. For both orbifold CFTs without and with torsion the corresponding resolution GLSMs are constructed. In order to compare them at the Lagrangian level on the worldsheet, one has to ensure that one uses the same superfield basis. (In the path integral formulation it only make sense to compare theories using their classical actions when the same integration field variables are employed.) Hence, as the charges of the superfields in the GLSMs of the non–torsion and the torsion orbifolds do not agree, superfield redefinitions are needed before this comparison is possible. As a cross check of the applied methods the GLSMs are considered in the deep orbifold regime to investigate how the torsion phases may be recovered.

The study of compact models with torsion is particularly intriguing since certain fluxes cannot be pushed to infinity and thereby out of the realm of the used description. Hence, the

second part of the chapter focusses on resolutions of compact $T^6/\mathbb{Z}_2 \times \mathbb{Z}_2$ orbifolds without or with discrete torsion switched on. Before, a careful study of the imprints of discrete torsion can be investigated, first GLSMs for resolutions of $T^6/\mathbb{Z}_2 \times \mathbb{Z}_2$ have to be set up. In the past GLSMs for compact orbifold resolutions were worked out in [113]. Even though the necessary techniques were developed there, GLSM resolutions of $T^6/\mathbb{Z}_2 \times \mathbb{Z}_2$ were not considered explicitly. Moreover, that chapter used the $(2,2)$ language throughout. However, to match up with the considerations of the non–compact cases, it is necessary to describe resolutions of $T^6/\mathbb{Z}_2 \times \mathbb{Z}_2$ here using $(0,2)$ GLSM terminology. Having fixed the geometrical aspects in the GLSM description, similar blowups are considered induced by non–oscillator twisted states as in the non–compact context. However, for the compact GLSM resolutions this leads to more complicated bundle constructions which take features of standard embedding bundles on the underlying torus cycles mixed with line bundles on the resolved $\mathbb{Z}_2$–singularities. With all this in place, the resolution GLSMs of the compact orbifolds without and with torsion can be investigated.

7.1.2 Chapter organisation

We begin (Section 7.2) with a motivating introduction of GLSMs and in particular their relation to conformal field theories that describe actual string backgrounds (under renormalisation group flow). After that me move to a short review in Section 7.3 of some features of $\mathbb{Z}_2 \times \mathbb{Z}_2$ orbifolds to provide the necessary foundation for the subsequent investigations. Section 7.4 summarises some essential prerequisites about $(0,2)$ GLSMs without which the remainder of this manuscript might be a bit hard to follow for non–experts. Further technical details on this topic are diverted to Appendix A.1. Next, Section 7.5 focusses on GLSM resolutions of non–compact $\mathbb{C}^3/\mathbb{Z}_2 \times \mathbb{Z}_2$ without and with torsion. Some properties described there rely on charge matrices which are collected in Appendix A.3 not to interrupt the main flow of this section. Section 7.6 repeats these exercises for compact $T^6/\mathbb{Z}_2 \times \mathbb{Z}_2$ GLSM resolutions focusing on the additional features and complications that compactness brings. Appendix A.2 derives gauge anomalies in two dimensions and provide $(0,2)$ superspace expressions for them which are used frequently in Sections 7.5 and 7.6.

7.2 GLSMs and string backgrounds

Even though the technical details of (0,2) GLSM are given in 7.4 and A.1 it is interesting to explain some of the phenomenological motivation of GLSMs and why they can describe conformal field theories needed for a string theory. Recall that a sigma model is a field theory where the fields correspond to maps from a spacetime into some target space. In the case of heterotic string theory, we consider a sigma model which describes the embedding of the string worldsheet into a ten-dimensional target space (the spacetime). For phenomenological reasons, we require the spacetime to be $M^{1,3} \times X$ where we choose X to be a Calabi-Yau threefold.

7.2.1 NLSMs

In principle string theory can be described via a $(2,2)$ non-linear sigma model (NLSM) with the action [136]

$$\begin{aligned} S = \frac{i}{2\pi}\int \frac{1}{2}g_{i\bar{\jmath}}\left(\partial X^i \bar{\partial} X^{\bar{\jmath}} + \partial X^{\bar{\jmath}}\bar{\partial}X^i\right) - \frac{1}{2}b_{i\bar{\jmath}}\left(\partial X^i \bar{\partial} X^{\bar{\jmath}} - \partial X^{\bar{\jmath}}\bar{\partial}X^i\right) \\ + i\left(\psi_{\bar{\imath}} D\psi^{\bar{\imath}} + \lambda_i \bar{D}\lambda^i\right) + R_l^{k\bar{\imath}}{}_{\bar{\jmath}}(X)\lambda_k\lambda^l\psi_{\bar{\imath}}\psi^{\bar{\jmath}} \end{aligned} \tag{7.1}$$

where the left- and right-moving fermions couple to the appropriate pullback connections, $D\psi^{\bar{\imath}} = \partial\psi^{\bar{\imath}} + \partial X^{\bar{\jmath}}\Gamma^{\bar{\imath}}_{\bar{\jmath}\bar{k}}(X)\psi^{\bar{k}}$, etc. The $(0,2)$ generalization of this is to replace the action for the left-moving fermions by

$$S = \frac{i}{2\pi}\int \ldots + i\left(\ldots + \lambda_a \bar{D}\lambda^a\right) + F^a{}_b{}^{\bar{\jmath}}{}_{\bar{\jmath}}(X)\lambda_a\lambda^b\psi_{\bar{\imath}}\psi^{\bar{\jmath}} \tag{7.2}$$

where now the λ^a transform as sections of a holomorphic vector bundle $V \to M$. The data specifying the σ-model now is: the Kähler metric, $g_{i\bar{\jmath}}(X)$, a closed 2 -form $b_{i\bar{\jmath}}(X)$, and the holomorphic connection on V, $A^a_{bi}(X)$, whose curvature is $F^a_{bi\bar{\jmath}}(X)$.
Note that, for a consistent string theory, we are interested in a conformally invariant σ-model. Requiring conformal invariance imposes some conditions on the above data. For instance, demanding that the 1-loop β-function of 7.2.1 vanish requires that $g_{i\bar{\jmath}}$ be Ricci-flat. But these conditions are corrected at higher orders in σ-model perturbation theory, and we do not know what the "all orders" equation necessary for conformal invariance is.

In the face of this obstacle, a better approach is to accept that the σ-model (or, at least any σ-model we can actually write down) is not conformally-invariant per se but *it flows under the Renormalization Group to an infrared fixed point theory which is the desired conformally invariant theory.* The data $g_{i\bar{\jmath}}, b_{i\bar{\jmath}}, A^a_{bi}$ represent an infinite number of coupling constants in the two dimensional quantum field theory. All but a finite number of these are marginally irrelevant and flow to zero in the infrared. Thus the fixed-point theory is characterized by a finite number of parameters which are RG-invariant which are the complex structure of M, the holomorphic structure of the vector bundle V and the cohomology class of the complex Kähler form $\mathcal{J} = B + iJ$, where

$$J = ig_{i\bar{\jmath}}dX^i \wedge dX^{\bar{\jmath}}, \quad B = b_{i\bar{\jmath}}dX^i \wedge dX^{\bar{\jmath}} \tag{7.3}$$

The first two are automatic in this formalism. but the the RG-invariance of the cohomology class of $\mathcal{J}$ is, by contrast, highly nontrivial. Beyond perturbation theory, one needs to worry about σ-model instantons, which are topologically nontrivial maps from the worldsheet into M. Naively, corrections to $g_{i\bar{\jmath}}$ are instanton-antiinstanton effects, and so rather hard to see. There are rather indirect arguments which one might use to try to show that the cohomology class of $\mathcal{J}$ is unrenormalized, even when σ-model instantons are taken into account. But the necessary conditions are very hard to verify, and for a long time this pretty much stymied any progress on $(0,2)$ σ-models. Since nonlinear σ-models are so hard, we can invoke another great principle of the renormalization group, namely universality. There are many QFTs which renormalize to the same IR fixed point. If nonlinear σ-models are too hard, we should look for another, simpler family of QFTs which happen to be in the same universality class. This motivates us to look at linear σ-models.

7.2.2 GLSMs

In this case we also have that as gauge couplings and some kinetic terms are of non-vanishing mass dimension, GLSMs are not conformal. Nevertheless, it is believed that in the infrared limit, where all dimensionful parameters are sent to infinity and massive modes are integrated out, the theory flows to a conformal NLSM model. The demonstrantion of this is non-trivial but is more general than what can be done starting from the NLSM model (which only works for some special cases). There are different analysis to stablish the criteria of the conformal invariance of the $(0,2)$ GLSM [130, 132, 133]. For **perturbatively** conformal cases [130] an elegant argument is to show the absence of space-time superpotential . The main idea there is *the effective spacetime superpotential must vanish because there is no admissible place where it can have a pole*. The steps of the reasoning are:

- If we look at the space-time superpotential as a function of the moduli on which it depends; insofar as the moduli space is compact and the superpotential is not identically zero, the superpotential must have poles somewhere. (The reason for this is that a holomorphic function without poles on a compact complex manifold would have to be constant. The superpotential is not really a holomorphic function but a section of a line bundle of negative curvature, so it cannot even be constant hence if there are no poles, it must vanish).

- Poles can only arise when the parameters are taken to values at which the compactness of the target space is lost because some fields can go to infinity. At large field strength, quantum corrections to the classical theory are small and calculable, so the possible poles can be located. Moreover, the polar parts of the various couplings can be explicitly computed.

- By analyzing the behavior of the linear sigma model as either the Kahler class or the complex structure of the bundle is varied it can be shown that:

  - the linear sigma model gives a natural compact parameter space
  - the places where the sigma model breaks down can be concretely described, and
  - the relevant couplings do not have poles at those places.

Consequently the superpotential must vanish and the GLSM flows in the infrared to conformally invariant solutions of string theory. Even though the analysis is done studying the quintic hypersurface in $\mathbb{P}^4$ the same reasoning can be easily extended to more general GLSM geometries. The easiest way to check if that this extension is valid is by checking that the fields that could potentially go to infinity when the model becomes singular have nonzero $U(1)_R$ charges [130].
Moreover, another reference provided above [132] give also arguments to go **beyond the perturbative** level and show that there is no world-sheet superpotential generated by instantons (this is done there by using calculating the Konishi anomaly for the $(0,2)$ GLSM with no tree level superpotential).

7.3 Properties of $\mathbb{Z}_2 \times \mathbb{Z}_2$ orbifolds

The purpose of the present section is to recall some crucial information about heterotic $\mathbb{Z}_2 \times \mathbb{Z}_2$ orbifolds to understand their resolutions using GLSM methods that are laid out in subsequent sections. Hence, it does not aim to give a complete review of heterotic orbifolds (for more comprehensive discussions see e.g. [8,9,114–116]). In particular, properties of $\mathbb{Z}_2 \times \mathbb{Z}_2$ orbifolds may be found in e.g. [24,46,99,117,118]. A crucial feature of $\mathbb{Z}_2 \times \mathbb{Z}_2$ is that they may posses discrete torsion [64,73]. As is recalled here this feature determines which twisted states survive the orbifold projections.

7.3.1 Orbifold twists and gauge shift vectors

The bosonic description of the $\mathbb{Z}_2 \times \mathbb{Z}_2$ orbifold starts with the introduction of two twist vectors

$$v_1 = \big(0, 0, \tfrac{1}{2}, \text{-}\tfrac{1}{2}\big) \ , \qquad v_2 = \big(0, \text{-}\tfrac{1}{2}, 0, \tfrac{1}{2}\big) \ , \tag{7.4}$$

which act on the complex coordinate fields z_u with $u = 0, 1, 2, 3$. Here z_0 denotes the four dimensional non–compact directions in light–cone gauge. (Since the main interest is on the internal coordinates, u is taken to label the internal coordinates and then runs over $u = 1, 2, 3$ only.) Thus the first entries of the twist vectors indicate that the twists act trivially on the four dimensional Minkowski space. For the non–compact orbifold $\mathbb{C}^3/\mathbb{Z}_2 \times \mathbb{Z}_2$ the coordinates $z_u \in \mathbb{C}$ parametrise three complex planes. While for the compact orbifold $T^6/\mathbb{Z}_2 \times \mathbb{Z}_2$ they parametrise the three underlying two–tori T^2. An arbitrary element g of the $\mathbb{Z}_2 \times \mathbb{Z}_2$ orbifold point group then corresponds to the twist vector

$$v_g = t_1\, v_1 + t_2\, v_2 \ , \tag{7.5}$$

where $t_1, t_2 = 0, 1$ label its four elements.

To complete the definition of the orbifold actions gauge shift vectors have to be given. In the orbifold standard embedding the gauge shift vectors are taken to be equal to these twist vectors augmented with the appropriate number of zero entries:

$$V_1 = \big(0, \tfrac{1}{2}, \text{-}\tfrac{1}{2}, 0^5\big)\big(0^8\big) \ , \qquad V_2 = \big(\text{-}\tfrac{1}{2}, 0, \tfrac{1}{2}, 0^5\big)\big(0^8\big) \ , \tag{7.6}$$

and define the gauge shift embedding

$$V_g = t_1\, V_1 + t_2\, V_2 \ , \tag{7.7}$$

for each of the four orbifold point group elements. As the notation of the shift vectors suggest, this chapter uses the $E_8 \times E_8$ heterotic string for concreteness. In addition a heterotic orbifold might feature a number of discrete Wilson lines. In this chapter the consequences of them are not considered.

7.3.2 Discrete torsion phase

At the one loop level it is conventional to distinguish between constructing elements g, h of the orbifold group, which define the different orbifold sectors of the theory, and the projecting elements g', h', which implement the appropriate orbifold projections. Hence, on the one loop

worldsheet torus a heterotic orbifold model is defined uniquely by the properties introduced above up to a possible discrete torsion phase [64, 73]

$$\Phi^{\times}{}^{t_1,t_2}_{t'_1,t'_2} = e^{\pi i\,\varepsilon^{\times}(t_1 t'_2 - t_2 t'_1)} \tag{7.8}$$

in its one loop partition function [73]. The possible torsion phase leads to a specific interplay between the constructing and projecting orbifold group elements. Clearly, if $\varepsilon^{\times} = 0$ there is no torsion as the torsion phase is equal to unity, but if $\varepsilon^{\times} = 1$ the model possesses discrete torsion as the phase is non–trivial.

An alternative equivalent way that discrete torsion can be introduced is by so–called brother models, i.e. models with gauge shift vectors that differ from the original ones by appropriate lattice vectors [71]. In particular, for the model (7.6) the brother model has gauge shift vectors

$$V_1^{\times} = -V_1 = \big(0, \text{-}\tfrac{1}{2}, \tfrac{1}{2}, 0^5\big)\big(0^8\big)\ , \qquad V_2^{\times} = -V_2 = \big(\tfrac{1}{2}, 0, \text{-}\tfrac{1}{2}, 0^5\big)\big(0^8\big)\ , \tag{7.9}$$

so that their differences are indeed lattice vectors.

7.3.3 Orbifold spectra with(out) torsion

Any state in the orbifold spectrum may be characterised by two shifted momenta

$$p_g = p + v_g\ , \qquad P_g = P + V_g\ , \tag{7.10}$$

where the vector p is an element of the lattice $V_4 \oplus S_4$ and P of $(O_8 \oplus S_8) \otimes (O_8 \oplus S_8)$. The shifted momenta of level matched massless states are subject to the following two conditions

$$\frac{1}{2}\,p_g^2 = \frac{1}{2} - \delta c_g\ , \qquad \frac{1}{2}\,P_g^2 = 1 - \delta c_g - \omega_g \cdot \widetilde{N}_g - \bar{\omega}_g \cdot \overline{\widetilde{N}}_g\ , \tag{7.11}$$

where the orbifold vacuum shift

$$\delta c_g = \frac{1}{2}\sum_u \omega_{g,u}(1 - \omega_{g,u}) \tag{7.12}$$

is defined in terms of $\omega_{g,u} \equiv (v_g)_u$ and $\bar{\omega}_{g,u} \equiv -(v_g)_u$ which satisfy the inequalities: $0 < \omega_{g,u}, \bar{\omega}_{g,u} \leq 1$. Finally, $(\widetilde{N}_g)_u$ and $(\overline{\widetilde{N}}_g)_u$ are the number operators that count the number of right–moving oscillators act on the state. Only the states that survive the orbifold projection conditions,

$$P_g \cdot V_{g'} - p_g \cdot v_{g'} \equiv \frac{1}{2}\big(V_g \cdot V_{g'} - v_g \cdot v_{g'}\big) + \big(\overline{\widetilde{N}}_g - \widetilde{N}_g\big) \cdot v_{g'} + \frac{\varepsilon^{\times}}{2}\big(t_1 t'_2 - t_2 t'_1\big)\ , \tag{7.13}$$

are part of the physical orbifold spectrum. The last term in these projection conditions encodes the consequences of discrete torsion on the massless spectrum. Consequently, the discrete torsion phases only affect the twisted sectors. The resulting orbifold spectrum is conventionally divided in a number of sectors:

Untwisted sector

The untwisted sector is identified by $(t_1, t_2) = (0, 0)$. This sector corresponds to so–called bulk states which live everywhere within the internal geometry. It contains the metric, the anti–symmetric tensor and the dilaton degrees of freedom as well as the target space gauge fields and all their superpartners in ten dimensions. The non–Abelian unbroken gauge group in four dimensions is $E_6 \times E_8$. In addition, there are three copies of charged matter in the $(27) + (\overline{27})$ of E_6 independently of whether torsion is switched on or not.

Sector	Shifted momentum P_g	Repr.	$\varepsilon^{\times}=0$	$\varepsilon^{\times}=1$
$1=$ $(1,0)$	$\big(1,\,\text{-}\frac{1}{2},\,\text{-}\frac{1}{2},0^5\big)\big(0^8\big)$	(1)	in	out
	$\big(\text{-}1,\,\text{-}\frac{1}{2},\,\text{-}\frac{1}{2}0^5\big)\big(0^8\big);\big(0,\,\frac{1}{2},\,\frac{1}{2},\underline{\pm1,0^4}\big)\big(0^8\big);\big(\text{-}\frac{1}{2},0,0,\underline{\text{-}\frac{1}{2}^e,\frac{1}{2}^{5-e}}\big)\big(0^8\big)$	(27)		
	$\big(\text{-}1,\,\frac{1}{2},\,\frac{1}{2},0^5\big)\big(0^8\big)$	$(\overline{1})$	out	in
	$\big(1,\,\frac{1}{2},\,\frac{1}{2},0^5\big)\big(0^8\big);\big(0,\,\text{-}\frac{1}{2},\,\text{-}\frac{1}{2},\underline{\pm1,0^4}\big)\big(0^8\big);\big(\frac{1}{2},0,0,\underline{\text{-}\frac{1}{2}^o,\frac{1}{2}^{5-o}}\big)\big(0^8\big)$	$(\overline{27})$		
$2=$ $(0,1)$	$\big(\text{-}\frac{1}{2},1,\,\text{-}\frac{1}{2},0^5\big)\big(0^8\big)$	(1)	in	out
	$\big(\text{-}\frac{1}{2},\,\text{-}1,\,\text{-}\frac{1}{2},0^5\big)\big(0^8\big);\big(\frac{1}{2},0,\,\frac{1}{2},\underline{\pm1,0^4}\big)\big(0^8\big);\big(0,\,\text{-}\frac{1}{2},0,\underline{\text{-}\frac{1}{2}^e,\frac{1}{2}^{5-e}}\big)\big(0^8\big)$	(27)		
	$\big(\frac{1}{2},\,\text{-}1,\,\frac{1}{2},0^5\big)\big(0^8\big)$	$(\overline{1})$	out	in
	$\big(\frac{1}{2},1,\,\frac{1}{2},0^5\big)\big(0^8\big);\big(\text{-}\frac{1}{2},0,\,\text{-}\frac{1}{2},\underline{\pm1,0^4}\big)\big(0^8\big);\big(0,\,\frac{1}{2},0,\underline{\text{-}\frac{1}{2}^o,\frac{1}{2}^{5-o}}\big)\big(0^8\big)$	$(\overline{27})$		
$3=$ $(1,1)$	$\big(\text{-}\frac{1}{2},\,\text{-}\frac{1}{2},1,0^5\big)\big(0^0\big)$	(1)	in	out
	$\big(\text{-}\frac{1}{2},\,\text{-}\frac{1}{2},\,\text{-}1,0^5\big)\big(0^8\big);\big(\frac{1}{2},\,\frac{1}{2},0,\underline{\pm1,0^4}\big)\big(0^8\big);\big(0,0,\,\text{-}\frac{1}{2},\underline{\text{-}\frac{1}{2}^e,\frac{1}{2}^{5-e}}\big)\big(0^8\big)$	(27)		
	$\big(\frac{1}{2},\,\frac{1}{2},\,\text{-}1,0^5\big)\big(0^8\big)$	$(\overline{1})$	out	in
	$\big(\frac{1}{2},\,\frac{1}{2},1,0^5\big)\big(0^8\big);\big(\text{-}\frac{1}{2},\,\text{-}\frac{1}{2},0,\underline{\pm1,0^4}\big)\big(0^8\big);\big(0,0,\,\frac{1}{2},\underline{\text{-}\frac{1}{2}^o,\frac{1}{2}^{5-o}}\big)\big(0^8\big)$	$(\overline{27})$		

Table 7.1: This table lists the twisted sector spectra obtained from non–oscillator excitation states and indicates whether they are in the physical spectrum without or with torsion, $\epsilon^{\times}=0$ or 1, respectively.

Twisted sectors

There are three twisted sectors with $t=(t_1,t_2):1=(1,0),2=(0,1)$ and $3=(1,1)$ which only posses $\mathcal{N}=1$ supersymmetry in six dimensions[1]: On the non–compact orbifold $\mathbb{C}^3/\mathbb{Z}_2\times\mathbb{Z}_2$ the corresponding twisted states are localised at the three complex codimension two singularities of the three non–trivial orbifold twists. Each twisted sector is supported on 16 fixed two–tori within the compact orbifold $T^6/\mathbb{Z}_2\times\mathbb{Z}_2$. Half of these states are projected out by the orbifold action of the second orbifold element. Which half depends on whether torsion is switched on, see Table 7.1 which gives the twisted states without twisted oscillator excitations.

7.4 Geometries and bundles from (0, 2) gauged (linear) sigma models

7.4.1 (0,2) Superfields

Two dimensional theories with $(0,2)$ supersymmetry admit a number of different types of superfields (or multiplets). Appendix A.1 gives a short review of $(0,2)$ superfields on superspace

[1]Also sometimes referred to as $\mathcal{N}=2$ sectors from the four dimensional point of view.

Superfield	∂	$\bar\partial$	D_+	Φ^a	Λ^m	Ψ^A	Γ^M	V_i	A_i	F_i	Σ_I	$_I$
Phys. Comp.				(z^a, ϕ^a)	(λ^m, h^m)	(y^A, ψ^A)	(γ^M, f^M)	$(A^i_\sigma, A^i_{\bar\sigma}, \varphi^i, D^i)$			(s^I, χ^I)	
#				N_Φ	N_Λ	N_Ψ	N_Γ	N_V			N_Σ	
$\mathcal{L}$	0	1	0	0	$\frac{1}{2}$	0	$\frac{1}{2}$	0	1	1	$\frac{1}{2}$	$\frac{1}{2}$
$\mathcal{R}$	1	0	$\frac{1}{2}$	0	0	0	0	0	0	$\frac{1}{2}$	0	$\frac{1}{2}$
R	0	0	-1	0	0	1	1	0	0	1	0	1
$\mathcal{Q}$	0	0	0	$(q_i)^a$	$(Q_i)^m$	$(\mathsf{q}_i)^A$	$(\mathsf{Q}_i)^M$	n.l.	n.l.	0	0	0

Table 7.2: This table specifies the left– and right–Weyl dimensions, $\mathcal{L}$ and $\mathcal{R}$, the R–charge and the gauge charges $\mathcal{Q}_i$ of the operators $\partial, \bar\partial, D_\pm$ and the superfields which may be used in a (0,2) GLSM. The physical components of these multiplets are indicated as well as the indices that label them; the third line gives the total number of these multiplets.

and sets notations and conventions used in this work. Gauged sigma models are a special class of $(0,2)$ theories with bosonic and possibly also fermionic gaugings. The superfields used in this work are summarised in Table 7.2 and the labels used to enumerate them are indicated there. In addition, their gauge charges, left– and right–Weyl dimensions and R–charges (defined in Appendix A.1.3) are given.

The most important matter superfields are chiral and chiral Fermi multiplets. A chiral multiplet $\Phi = (z, \phi)$ contain a complex scalar z and a right–moving fermion ϕ. A chiral Fermi multiplet $\Lambda = (\lambda, h)$ consists of a left–moving fermion λ and an auxiliary scalar field h. In addition, there are chiral multiplets $\Psi = (y, \psi)$ and chiral Fermi multlplets $\Gamma = (\gamma, f)$. The distinction between these chiral and chiral Fermi superfields is made by their R–symmetry charge: Φ and Λ are neutral while Ψ and Γ carry charge 1. The last line of this table gives the gauge charges and dictates the super gauge transformations of these matter superfields.

For the corresponding bosonic gaugings vector multiplets have to be introduced consisting of two real bosonic superfields V and A from which gauge invariant super field strengths F can be constructed

$$F = -\tfrac{1}{2}\overline{D}_+\big(A - i\bar\partial V\big) \ . \tag{7.14}$$

The physical components of these multiplets are the gauge field A_σ, $A_{\bar\sigma}$ with field strength $F_{\sigma\bar\sigma} = \partial_\sigma A_{\bar\sigma} - \partial_{\bar\sigma} A_\sigma$ and a right–moving fermion φ and a real auxiliary field D.

On the chiral Fermi multiplets fermionic gauge transformations

$$\Lambda \to \Lambda + U(\Phi)\cdot\Xi \ , \qquad \Gamma \to \Gamma + \Psi\, W(\Phi)\cdot\Xi \tag{7.15}$$

may act with chiral Fermi super gauge parameters. To obtain invariant action under these transformation, Fermi gauge multiplets Σ need to be introduced with super field strengths

$$= \overline{D}_+\Sigma \ . \tag{7.16}$$

Their physical components are complex scalars s and left–moving fermions χ.

A few comments are in order. The theories that are studied here do not define proper string theories as their worldsheet actions are not fully conformal. In particular, dynamical gauge fields on the worldsheet are not scale invariant as their gauge coupling is dimensionfull. Nevertheless it is useful to use characterisations, like the left– and right–moving Weyl dimensions, as in the scale invariant limit the corresponding superconformal symmetries are recovered. Moreover, the "linear" in GLSMs signifies that only kinetic terms quadratic in the fields are considered, while in non–linear sigma models this restriction is lifted for chiral superfields.

The main reason why GLSMs are of interest for string theory is that they can provide interesting insights in how geometries and vector bundles on them can arise:

7.4.2 Emergent effective geometry

The scalar part of GLSMs can be associated to target space geometries like weighted projective spaces, complete intersection Calabi–Yaus and many generalisations of these as was realised by the pioneering chapter [119]. The scalar components z of the chiral multiplets Φ can be interpreted as the homogeneous coordinates of projected spaces, where the $\mathbb{C}^*$–scalings are encoded by the scalar part of the super gauge transformations:

$$z \to e^{q_i \cdot \theta}\, z \ , \qquad \theta = \tfrac{1}{2}\, a - i\, \alpha \in \mathbb{C}^{N_V} \ . \tag{7.17}$$

In the Wess–Zumino gauge the sizes of these projective spaces are set by the D–term equations

$$\sum_a (q_i)^a |z^a|^2 = r_i \ , \tag{7.18}$$

for each $i = 1, \ldots, N_V$. (In principle there is a second sum over the scalars y^A here, but they are typically all forced to zero as discussed below.) Here the parameters r are the real parts of the Fayet–Iliopoulos (FI) coefficients $\rho(\Phi)$ which define superpotentials involving the super gauge field strengths

$$W_{\rm FI} = \rho(\Phi) \cdot F \ , \qquad \rho(z) = \tfrac{1}{2}\, r + i\, \beta \in \mathbb{C}^{N_V} \ . \tag{7.19}$$

This is gauge invariant if the functions $\rho(\Phi)$ are neutral. The target space interpretation of r are moduli, that set the radii of certain cycles, and β may be interpreted as axions in the effective geometry.

String backgrounds, like Calabi–Yaus, are often defined as hypersurfaces in such projected spaces. In the GLSM language this can be encoded in a $(0,2)$ superpotential

$$P_{\rm geom} = \Gamma\, P(\Phi) \ . \tag{7.20}$$

In the conformal limit, the scalar components of the algebraic equations of motion of chiral Fermi superfields Γ^M lead to F–term equations:

$$P_M(z) = 0 \ , \tag{7.21}$$

for $M = 1, \ldots, N_\Gamma$, which precisely cut out such hypersurfaces. Consequently, the dimension of the resulting target space manifold $\mathcal{M}$ equals:

$$\dim_{\mathbb{C}}(\mathcal{M}) = \mathrm{N}_\Phi - \mathrm{N}_V - \mathrm{N}_\Gamma \ . \tag{7.22}$$

This should be equal to 2 or 3 if one only considers the internal manifold of complex dimension 2 or 3; or 4 if the complete spacetime in light–cone gauge is described by the GLSM.

In addition, the GLSM description can be used to determine an atlas of coordinate patches: in a given phase one or multiplet set(s) of scalar fields are necessarily non–zero. Hence, by analysing the combined D–term and F–term equations, (7.18) and (7.21), all the coordinate patches within a phase of the GLSM can be determined.

7.4.3 Emergent effective vector bundle

The part of $(0,2)$ GLSMs that involve the chiral Fermi multiplets can be interpreted as vector bundles (or as sheafs if they are not fully regular) [119–121]. The fermionic components λ of the Fermi multiplets Λ are line bundle sections on this manifold as their $\mathbb{C}^*$–scalings read

$$\lambda \to e^{Q_i\cdot\theta}\,\lambda\ . \tag{7.23}$$

If there are no fermionic super gauge transformations and no chiral superfields Ψ in the model, then the target space gauge background is simply a collection of line bundles.

However, in general, they describe a more complicated vector bundle $\mathcal{V}$ which is derived from a complex (generalisation of a monad construction), since they have to satisfy the constraints

$$M(z)\lambda = 0\ , \tag{7.24}$$

due to the lowest components of the algebraic equations of motion of Ψ that follows from the bundle superpotential

$$P_{\text{bundle}} = \Psi\, M(\Phi)\,\Lambda \tag{7.25}$$

and are subject to gauge transformations

$$\lambda \to \lambda + U(z)\cdot\xi\ , \tag{7.26}$$

which are the lowest components of the fermionic super gauge transformations (7.15). Combined the equations (7.24) and (7.26) imply that a vector bundle $\mathcal{V} = \text{Ker}(U)/\text{Im}(M)$ is constructed from the complex

$$0 \to \mathcal{O}^{\text{N}_\Sigma} \xrightarrow{U} \bigoplus_{m=1}^{\widetilde{\text{N}}_\Lambda} \mathcal{O}(Q^m) \xrightarrow{M} \bigoplus_{A=1}^{\text{N}_\Psi} \mathcal{O}(-\mathsf{q}^A) \to 0\ . \tag{7.27}$$

Here $\widetilde{\text{N}}_\Lambda \leq \text{N}_\Lambda$ denotes the number of interacting Fermi multiplets in the GLSM. (The numbers in the $\mathcal{O}$s of such complexes are conventionally integers. But in the normalisations used in this chapter they might be fractional (like 1/2), hence they should then be multiplied by an appropriate common factor. In addition, the charges of the chiral superfields Ψ are negative in the conventions used in this work and they set the degrees of the constraints (7.24) on the fermions.) The dimensionality of the fibers of resulting vector bundle $\mathcal{V}$ is given by

$$\dim_{\mathbb{C}}(\mathcal{V}) = \widetilde{\text{N}}_\Lambda - \text{N}_\Sigma - \text{N}_\Psi\ , \tag{7.28}$$

provided that $M(z)$ and $U(z)$ have maximal ranks $\text{N}_\Psi \leq \text{N}_\Lambda$ and $\text{N}_\Sigma \leq \text{N}_\Lambda$, respectively [120]. (If this is not everywhere the case, this indicates that there are singularities in the bundle

instead.) In order that this bundle can be embedded in the gauge degrees of freedom of the heterotic string $\dim_{\mathbb{C}}(\mathcal{V})$ should less than eight so as to fit within an E_8–factor. (The bundle might also fill up part of both E_8–factors, but then it has to split accordingly.) Since the full rank of $E_8 \times E_8$ is 16, the total number of Fermi multiplets is given by $\mathrm{N}_\Lambda = 16 + \mathrm{N}_\Sigma + \mathrm{N}_\Psi$. Hence, there are a number of spectator (non–interacting and neutral) Fermi multiplets Λ_n, $n = 1, \ldots, \mathrm{N}_\Lambda - \widetilde{\mathrm{N}}_\Lambda$, which lead to the unbroken gauge degrees of freedom in target space.

The superpotential (7.25) has another important consequence: If $M(z)$ has maximal rank, the equations of motion of Λ induced by the bundle superpotential (7.25) imply that all $y^A = 0$. This was implicitly assumed when (7.18) were written down, since, in general, also contributions from the scalars y^A should be present in these equations.

The fermionic gauge transformations (7.15) only leaves the superpotentials (7.20) and (7.25) combined inert when the following compatibility conditions hold

$$W_A{}^{IM}(\Phi) P_M(\Phi) + M_{Am}(\Phi) U^{mI}(\Phi) = 0 \ . \tag{7.29}$$

In general, it is not so straightforward to find functions such that these conditions are fulfilled. However, when the superpotentials and the fermionic gaugings are taken to lie on the $(2,2)$ locus discussed below, these conditions are automatically satisfied.

7.4.4 The (2,2) locus

The interacting part of $(0,2)$ GLSMs (or at least the part that involves fermionic gaugings) might possess a higher amount of supersymmetry. For this to happen the (0,2) multiplets need to be able to pair up. This means in particular, that there are the following relations between the number of interacting multiplets:

$$\widetilde{\mathrm{N}}_\Lambda = \mathrm{N}_\Phi \ , \qquad \mathrm{N}_\Gamma = \mathrm{N}_\Psi \ , \qquad \mathrm{N}_\Sigma = \mathrm{N}_V \ , \tag{7.30}$$

This allows to identify various indices: $m = a$, $M = A$ and $I = i$; we use the latter indices for each type of indices. Furthermore, the gauge charges of chiral and Fermi multiplets need to line up:

$$Q_i = q_i \ , \qquad \mathsf{Q}_i = \mathsf{q}_i \ . \tag{7.31}$$

When some of these relations are not satisfied it is impossible to deform the interactions of the $(0,2)$ GLSM to become $(2,2)$. If this is possible, then the $(0,2)$ theory is said to be on the $(2,2)$ locus.

On the $(2,2)$ locus of the space of $(0,2)$ GLSM, exact $(2,2)$ models possess various interactions encoded in the various functions introduced that need to be of a very specific form. The relations given here are subject to specific normalizations; but the implied proportionalities are essential. First of all, the functions $U(\Phi)$ and $W(\Phi)$ that describe the Fermi gauge transformations now read

$$U^{ai}(\Phi) = (q_i)^a \Phi^a \ , \qquad W_A{}^{iB} = (\mathsf{q}_i)^B \delta_A^B \ . \tag{7.32}$$

They are fully dictated by the index structure and the gauge charges $(q_i)^a$ and $(\mathsf{q}_i)^A$. The functions $M(\Phi)$ are determined as the derivatives of $P(\Phi)$:

$$M_{Aa}(\Phi) = P_{A,a}(\Phi) \ , \tag{7.33}$$

where $F_{,a}(\Phi)$ denotes the partial derivative of $F(\Phi)$ with respect to Φ^a. Consequently, the invariance of the superpotential action under fermionic gauge transformations (7.29) reduces to the gauge invariance of the superpotential:

$$(\mathsf{q}_i)^A P_A(\Phi) + P_{A,a}(\Phi)\Phi^a (q_i)^a = 0 \ . \tag{7.34}$$

7.4.5 Worldsheet instantons and flux quantisation

It is possible that on the worldsheet non–trivial gauge configurations, like instantons, are realised. The involved gauge fluxes need to be properly quantised [122]:

$$\sum_j (q_j)^a \int \frac{F^j_{E_2}}{2\pi} \in \mathbb{Z} \ , \qquad \sum_j (\mathsf{q}_j)^A \int \frac{F^j_{E_2}}{2\pi} \in \mathbb{Z} \tag{7.35}$$

for all charged chiral superfields Φ^a and Ψ^A. Here the subscript E indicates that the gauge fluxes are computed in the Euclidean theory.

7.4.6 Anomaly consistency conditions

On a GLSM there are a number of requirements in order that the theory is both consistent as a quantum theory and that it is likely to have the right properties in the conformal limit.

First of all, like any gauge theory, the GLSM has to be free of gauge anomalies. With the gauge charges given in Table 7.2, this amounts to the following conditions

$$\mathcal{A}_{ij} = -\sum_a (q_i)^a (q_j)^a - \sum_A (\mathsf{q}_i)^A (\mathsf{q}_j)^A + \sum_m (Q_i)^m (Q_j)^m + \sum_M (\mathsf{Q}_i)^M (\mathsf{Q}_j)^M \stackrel{!}{=} 0 \ , \tag{7.36}$$

for all $i, j = 1, \ldots, N_V$. The signs in these equations are determined by whether the fermions in the matter multiplets are right– or left–moving. For $j = i$ this corresponds to pure and for $j \neq i$ to mixed gauge anomalies.

The left–, right–Weyl dimensions and R–charge correspond to bosonic parts of super conformal symmetries in the scale invariant limit of the GLSM. For this limit not to be obstructed the mixed left– and right–Weyl gauge anomalies should vanish. In detail, from Table 7.2 it follows that the left–Weyl – gauge anomalies vanish provided that

$$\sum_m (Q_i)^m + \sum_M (\mathsf{Q}_i)^M \stackrel{!}{=} 0 \ , \tag{7.37}$$

for all i, since the only charged superfields that carry $\mathcal{L}$–charge are Λ and Γ. These conditions can be summarised by the demand that the sum of the charges of all chiral Fermi superfields need to vanish for each gauge symmetry separately.

In addition, the charged right–moving fermions ϕ and γ are obtained by hitting chiral multiplets Φ and Ψ with D_+, hence the right–Weyl – gauge anomalies are absent when

$$\sum_A (\mathsf{q}_i)^a + \sum_A (\mathsf{q}_i)^A \stackrel{!}{=} 0 \ , \tag{7.38}$$

for all i. Thus, these conditions say that the sum of the charges of all chiral superfields need to vanish for each gauge symmetry separately. At the same time these conditions ensure that

the FI–parameters (7.19) do not renormalise. If this isn't the case, it would not be possible to interpret them to set the scales of target space cycles as they would always run off to zero or infinity.

Finally, the R–symmetry survives quantisation provided that

$$\sum_a (q_i)^a + \sum_M (\mathsf{Q}_i)^M \stackrel{!}{=} 0 \ , \tag{7.39}$$

for all i, since the right–moving fermions ϕ and the left–moving fermions γ have R–charges -1 and $+1$, respectively, and opposite chiralities. When these equations are combined with (7.38), they can be stated as the sum of the charges of the chiral Fermi superfields Γ have to be equal to that of the chiral superfields Ψ.

7.4.7 Worldsheet Green–Schwarz mechanism: Torsion and NS5–branes

When the gauge anomalies do not vanish, i.e. not all $\mathcal{A}_{ij}$ in (7.36) vanish, the GLSM is anomalous. It is sometimes possible that certain field dependent none gauge invariant FI–terms (7.19) are precisely able to cancel these gauge anomalies [123,124]. The FI–term coefficients $\rho(\Phi)$ then need to transform as a shift under the anomalous gauge symmetries. This can be viewed as a Green–Schwarz mechanism on the worldsheet and might have some far reaching consequences for the geometry and the interpretation of the theory.

To understand how this comes about, note that in the naive conformal limit, the kinetic terms of the vector multiplets V, A can be set to zero and their equations of motion become non–dynamical. In particular, the superfields A appear linear in the actions of the chiral multiplets (A.26) and the FI–terms (A.30), hence their equation of motion lead to superfield constraints:

$$\overline{\Phi}\, e^{2q\cdot V} q_i\, \Phi = \rho_i(\Phi) + \bar{\rho}_i(\overline{\Phi}) \ . \tag{7.40}$$

Thus after enforcing the equations of motion of A, the vector multiplets V become (implicit) functions of the chiral superfields Φ and their conjugates $\overline{\Phi}$. In the Wess–Zumino gauge the lowest component of these equations are the D–term constraints (7.18). However, in any gauge from (7.40) it can be inferred which (scalars of the) chiral multiplets are necessarily non–zero in a given phase with a certain choice of the FI–parameters. Hence, a unitary gauge can be chosen such that all chiral superfields, that are necessarily non–zero, are set to such values that the solution for the vector superfields V are all zero when all of the remaining chiral superfields are vanishing[2].

Non–constant FI–terms (7.19) modify the target space geometry and generically introduces torsion onto it in the form of non–vanishing H–flux [122, 125, 126]. Indeed, since by (7.40) the vector superfields V become (implicit) functions of the chiral multiplets. Inserting them in the kinetic terms of the chiral multiplets shows that the torsion tensor, the three–form H,

$$H_{ab\underline{c}} \sim \rho_{,[a}\cdot V_{,b]\underline{c}} \ , \tag{7.41}$$

[2]In the remainder of this chapter for presentational simplicity, the D–term equations (7.18) are given in the Wess–Zumino gauge, while for the analysis of the torsional effects (7.40) the unitary gauges, as defined here, are used implicitly.

is non–zero in general, see Appendix A.1.6 or ref. [124] for a derivation. (It reads here in general, because if both ρ_i and V_i only depend on a single chiral superfield this expression still anti–symmetrises to zero.) Since typically, the GLSM only contains chiral superfields Φ, that are linearly charged under the gauge symmetries, the required FI–coefficients can only be made by taking logarithms of combinations of them. As was argued in [123, 124, 127] such logarithmic singularities can be viewed as the imprints of non–perturbative physics in the form of NS5–branes on the worldsheet as the target space exterior derivative of (7.41) lead to delta–function–like sources in the Bianchi identity of the three–form[3].

7.4.8 Orbifold resolution GLSMs

Even though this section so far described properties of GLSMs in general, the main focus of this work is on GLSMs which are associated to (toroidal) orbifold resolutions. The study of resolution of singularities using $(0, 2)$ GLSMs have a long history. Some pioneering works are [120, 121]. A GLSM orbifold resolution construction has the advantage over other methods to match the singular orbifold situations for which exact CFT descriptions exists with smooth compactifications using effective field theory methods. Within a single GLSM framework one has both access to the orbifold phase as well as completely resolved (and potentially many other) phases. The trade off here is that a GLSM is not (yet) a full blown CFT description.

A fully complete correspondence between orbifold CFTs and GLSMs does not exists, but two methods have been uncovered in the past which apply to partially overlapping situations:

A Twisted shifted momenta as (0,2) GLSM charges [112]:

As was recalled in Section 7.3.3, twisted states are uniquely identified by their shifted right– and left–moving momenta (7.10). In particular, the right– and left-moving shifted momenta of non–oscillator massless twisted states automatically satisfy the pure anomaly cancellation conditions when they are interpreted as GLSM gauge charges of chiral and chiral Fermi superfields, respectively. In target space these configurations may have the interpretation of line bundles on the resolved local singularities.

B (2,2) GLSMs for toroidal orbifold resolutions [113]:

Contrary, full global orbifold resolutions in the standard embedding can be obtained in $(2, 2)$ GLSMs. The underlying two–tori are described using (variants of) the Weierstrass models. On some of their homogeneous coordinates additional (exceptional) gaugings are implemented. For certain ranges of their FI–parameters the fixed point structure of toroidal orbifolds, while for others resolved compact Calabi–Yaus emerge.

In the next section method A is employed, while in Section 7.6 method A is combined with a partial (0,2) reduction of method B for the case of $T^6/\mathbb{Z}_2 \times \mathbb{Z}_2$ orbifold resolutions that were not discussed in the literature before explicitly.

7.5 Non–compact $\mathbb{C}^3/\mathbb{Z}_2 \times \mathbb{Z}_2$ resolution GLSMs

This section focus on heterotic resolutions of the non–compact $\mathbb{C}^3/\mathbb{Z}_2 \times \mathbb{Z}_2$ using (0,2) GLSMs. (Some ingredients of the present discussion are inspired by ref. [112].) The three complex

[3] In addition, the inclusion of log–dependent FI–terms may lead to a back reaction to the geometry [124, 127]; in this chapter these consequences are not studied in detail.

Superfield	Φ_1	Φ_2	Φ_3	Φ'_1	Φ'_2	Φ'_3	$\Lambda = (\Lambda^1, \ldots, \Lambda^{16})$	Ω_1	Ω_2	Ω_3
U(1) charge	z_1	z_2	z_3	x_1	x_2	x_3	$\lambda = (\lambda^1, \ldots, \lambda^{16})$	ω_1	ω_2	ω_3
E_1	0	$\frac{1}{2}$	$\frac{1}{2}$	-1	0	0	$Q_1 = (Q_1^1, \ldots, Q_1^{16})$	1	0	0
E_2	$\frac{1}{2}$	0	$\frac{1}{2}$	0	-1	0	$Q_2 = (Q_2^1, \ldots, Q_2^{16})$	0	1	0
E_3	$\frac{1}{2}$	$\frac{1}{2}$	0	0	0	-1	$Q_3 = (Q_3^1, \ldots, Q_3^{16})$	0	0	1

Table 7.3: Superfield charge table for resolutions of the non–compact $\mathbb{C}^3/\mathbb{Z}_2 \times \mathbb{Z}_2$ orbifold.

coordinates z_u, $u = 1, 2, 3$, of $\mathbb{C}^3$ augmented with three exceptional coordinates x_r, $r = 1, 2, 3$, to describe the resolution. These coordinates become part of the chiral superfields Φ_u and Φ'_r on which three $U(1)$ gauge symmetries E_r act according to the charge table 7.3. In this table the unit charged chiral superfields Ω_r are composite, i.e. functions of the fundamental superfields Φ_u and Φ'_r.

7.5.1 Geometrical interpretation

The analysis of the geometrical interpretation of this GLSM starts with writing down the D–term equations

$$\frac{1}{2}|z_2|^2 + \frac{1}{2}|z_3|^2 = b_1 + |x_1|^2 \ , \tag{7.42a}$$

$$\frac{1}{2}|z_1|^2 + \frac{1}{2}|z_3|^2 = b_2 + |x_2|^2 \ , \tag{7.42b}$$

$$\frac{1}{2}|z_1|^2 + \frac{1}{2}|z_2|^2 = b_3 + |x_3|^2 \ . \tag{7.42c}$$

Here the three parameters b_r are the real parts of the three FI–parameters ρ_r associated with the three gaugings E_r which are assumed to be constant. An equivalent but useful representation of these equations are obtained by adding two of them and subtracting the third:

$$|z_1|^2 + |x_1|^2 = b_2 + b_3 - b_1 + |x_2|^2 + |x_3|^2 \ , \tag{7.43a}$$

$$|z_2|^2 + |x_2|^2 = b_1 + b_3 - b_2 + |x_1|^2 + |x_3|^2 \ , \tag{7.43b}$$

$$|z_3|^2 + |x_3|^2 = b_1 + b_2 - b_3 + |x_1|^2 + |x_2|^2 \ . \tag{7.43c}$$

Depending on the relative values of the three FI–parameters the model can be in a number of phases which have different geometrical interpretations [112]. Here not all of them are listed and discussed, instead, the focus is on a number of particular interesting phases: the orbifold phase and the three full resolved phases which are characterised by having all three FI–parameters negative or positive, respectively. Other phases, in which some FI–parameters are positive while others are negative, correspond to partial blowups and are ignored here. (In ref. [112] some aspects of these other phases were investigated.)

Some topological properties of the effective geometries in the various phases can be determined. The divisors in the effective geometry can be identified by setting one of the complex coordinates to zero while satisfying all the D–term equations. The ordinary divisors are defined by $D_u := \{z_u = 0\}$ and the exceptional ones by $E_r := \{x_r = 0\}$. The results of this analysis are summarised in Table 7.4.

For each set of non–vanishing fields $Z_{(P)} = (Z^1_{(P)}, Z^2_{(P)}, Z^3_{(P)})$, that defines a coordinate patch within a phase of the resolution GLSM, the other the complement set of fields $\{\widetilde{Z}^1_{(P)}, \widetilde{Z}^2_{(P)}, \widetilde{Z}^3_{(P)}\} \in \mathbb{R}^3$ then define a coordinate patch. The resulting patches are also given in Table 7.4. A gauge can be chosen such that the phases of these non–zero fields $Z_{(P)}$ are all trivial, i.e. multiplets of $2\pi i$. This only leaves residual discrete gauge transformations in each of these patches:

$$Z^a_{(P)} \to e^{i(\mathcal{Q}_{(P)})^a{}_r\,\alpha^p}\, Z^a_{(P)} \stackrel{!}{=} e^{2\pi i\, m^a}\, Z^a_{(P)}\ , \tag{7.44}$$

where $Z^a_{(P)}$, $a = 1, 2, 3$, are the three scalar fields that do not vanish in patch (P) with charges $(\mathcal{Q}_{(P)})^a{}_r$ and m^a are integers. For the coordinate patches under investigation the charge matrices are given in (A.67). Hence, the gauge parameters of the residual gauge transformations read:

$$\alpha^T = 2\pi\, m^T\, \mathcal{Q}^{-T}_{(P)}\ . \tag{7.45}$$

with $\alpha = \big(\alpha_1, \alpha_2, \alpha_3\big)$ and $m^T = \big(m^1, m^2, m^3\big)$. This induces residual gauge transformation on the coordinates of the coordinate patch (P) transform

$$\widetilde{Z}^a_{(P)} \to e^{i(\widetilde{\mathcal{Q}}_{(P)})^a{}_r\,\alpha^p}\, \widetilde{Z}^a_{(P)} = e^{2\pi i\,(\mathcal{R}m)^a}\, \widetilde{Z}^a_{(P)}\ , \qquad \mathcal{R}_{(P)} = \widetilde{\mathcal{Q}}_{(P)}\mathcal{Q}^{-1}_{(P)} \tag{7.46}$$

where $\widetilde{Q}_{(P)}$ are the charges of the coordinates of the patch which are given in (A.69). Thus if $\mathcal{R}_{(P)}$ is integral, the residual gauge transformations are trivial.

Orbifold phase

In the orbifold regime all three Kähler parameters are negative: $b_1, b_2, b_3 < 0$. The D–term equations (7.42) then imply that all three exceptional coordinates are non–vanishing:

$$|x_1|^2 = -b_1 + |z_2|^2 + |z_3|^2 > 0\ , \tag{7.47a}$$

$$|x_2|^2 = -b_2 + |z_1|^2 + |z_3|^2 > 0\ , \tag{7.47b}$$

$$|x_3|^2 = -b_3 + |z_1|^2 + |z_2|^2 > 0\ , \tag{7.47c}$$

hence there is a single coordinate patch: $\{z_1, z_2, z_3\}$. In particular, the D–term equations allow to set all these three coordinates to zero at the same time. Moreover, it is clear that none of the exceptional divisors E_r exist in this phase. Instead the intersection of $D_1D_2D_3$ exists.

By exploiting the gauge symmetries it is possible to fix the phases of x_1, x_2, x_3 some arbitrary values (which are typically taken to be zero for simplicity). However, these gauge fixings do

Phase	Non–zero fields	Patches	Curves	Intersection
Orbifold	$x_1, x_2, x_3 \neq 0$	$(O) := \{z_1, z_2, z_3\}$	$D_1D_2,\ D_2D_3,\ D_3D_1$	$D_1D_2D_3$
S–triangulation	$z_1, z_2, z_3 \neq 0$	$(S) := \{x_1, x_2, x_3\}$	$E_1E_2,\ E_2E_3,\ E_3E_1$	$E_1E_2E_3$
	$z_1, z_2, x_3 \neq 0$	$(33) := \{x_1, x_2, z_3\}$	$E_1E_2,\ E_2D_3,\ D_3E_1$	$E_1E_2D_3$
	$z_1, x_2, z_3 \neq 0$	$(22) := \{x_1, x_3, z_2\}$	$E_1E_3,\ E_1D_2,\ D_2E_3$	$E_1E_3D_2$
	$x_1, z_2, z_3 \neq 0$	$(11) := \{x_2, x_3, z_1\}$	$E_2E_3,\ E_2D_1,\ D_1E_3$	$E_2E_3D_1$
E_1–triangulation	$z_2, z_3, x_3 \neq 0$	$(31) := \{x_1, x_2, z_1\}$	$E_1E_2,\ E_2D_1,\ D_1E_1$	$E_1E_2D_1$
	$z_1, z_2, x_3 \neq 0$	$(33) := \{x_1, x_2, z_3\}$	$E_1E_2,\ E_2D_3,\ D_3E_1$	$E_1E_2D_3$
	$z_2, z_3, x_2 \neq 0$	$(21) := \{x_1, x_3, z_1\}$	$E_1E_3,\ E_3D_1,\ D_1E_1$	$E_1E_3D_1$
	$z_1, z_3, x_2 \neq 0$	$(22) := \{x_1, x_3, z_2\}$	$E_1E_3,\ E_3D_2,\ D_2E_1$	$E_1E_3D_2$
E_2–triangulation	$z_1, z_3, x_3 \neq 0$	$(32) := \{x_1, x_2, z_2\}$	$E_1E_2,\ E_2D_2,\ D_2E_1$	$E_1E_2D_2$
	$z_1, z_2, x_3 \neq 0$	$(33) := \{x_1, x_2, z_3\}$	$E_1E_2,\ E_2D_3,\ D_3E_1$	$E_1E_2D_3$
	$z_2, z_3, x_1 \neq 0$	$(11) := \{x_2, x_3, z_1\}$	$E_2E_3,\ E_3D_1,\ D_1E_2$	$E_2E_3D_1$
	$z_1, z_3, x_1 \neq 0$	$(12) := \{x_2, x_3, z_2\}$	$E_2E_3,\ E_3D_2,\ D_2E_2$	$E_2E_3D_2$
E_3–triangulation	$z_2, z_3, x_1 \neq 0$	$(11) := \{x_2, x_3, z_1\}$	$E_2E_3,\ E_3D_1,\ D_1E_2$	$E_2E_3D_1$
	$z_1, z_2, x_1 \neq 0$	$(13) := \{x_2, x_3, z_3\}$	$E_2E_3,\ E_3D_3,\ D_3E_2$	$E_2E_3D_3$
	$z_1, z_2, x_2 \neq 0$	$(23) := \{x_1, x_3, z_3\}$	$E_1E_3,\ E_3D_3,\ D_3E_1$	$E_1E_3D_3$
	$z_1, z_3, x_2 \neq 0$	$(22) := \{x_1, x_3, z_2\}$	$E_1E_3,\ E_3D_2,\ D_2E_1$	$E_1E_3D_2$

Table 7.4: This table indicates which combination of fields are necessarily non–vanishing in the orbifold and the three full resolution phases. This in turn determines the coordinate patches of the phases and hence the curves and intersections that exist within the patches. The notation (ru) of the patches of the fully resolved geometries signify that the coordinates x_r and $z_{v\neq u}$ are non–zero.

not fix the gauges completely, since the matrix (7.46) in this case,

$$\mathcal{R}_{(O)} = \widetilde{\mathcal{Q}}_{(O)}\mathcal{Q}_{(O)}^{-1} = -\widetilde{\mathcal{Q}}_{(O)} = \begin{pmatrix} 0 & \frac{1}{2} & \frac{1}{2} \\ \frac{1}{2} & 0 & \frac{1}{2} \\ \frac{1}{2} & \frac{1}{2} & 0 \end{pmatrix} , \tag{7.48}$$

is non–integer, therefore, there are non–trivial residual $\mathbb{Z}_2$ gauge transformations which act as

$$E_1 \ : \ (z_1, z_2, z_3) \to (z_1, -z_2, -z_3) \ , \tag{7.49a}$$

$$E_2 \ : \ (z_1, z_2, z_3) \to (-z_1, z_2, -z_3) \ , \tag{7.49b}$$

$$E_3 \ : \ (z_1, z_2, z_3) \to (-z_1, -z_2, z_3) \tag{7.49c}$$

on the remaining coordinates. The first two are precisely the transformations that defined the $\mathbb{C}^3/\mathbb{Z}_2 \times \mathbb{Z}_2$ orbifold and the third one is simply the combination of the first two and hence redundant in the orbifold phase.

S–triangulation full resolution phase

In the S–triangulation the Kähler parameters satisfy the following inequalities:

$$0 < b_3 < b_1 + b_2 \ , \quad 0 < b_2 < b_1 + b_3 \ , \quad 0 < b_1 < b_2 + b_3 \ . \tag{7.50}$$

From (7.42) it follows that at least two of the three z_u are non–zero. Hence, there is one coordinate patch $\{x_1, x_2, x_3\}$ when all three z_u are non–vanishing. Taking (7.43) into account, there are, in addition, three coordinate patches $\{z_u, x_{p\neq u}\}$ for $u = 1, 2, 3$ when x_u and $z_{p\neq u}$ are non–zero.

There is no non–trivial residual gauge transformation on the coordinate patch $(S) := \{x_1, x_2, x_3\}$, since fixing the phases of all three z_u fixes all gauge parameters θ_r up to multiples of $2\pi i$, hence the actions on the coordinates x_r are trivial. For the coordinate patch $(33) := \{z_1, x_2, x_3\}$ the non–vanishing coordinates of which the phases can be set to unity are x_1, z_2, z_3, consequently, the gauge parameters $\theta_{2,3}$ are fixed modulo multiples of $4\pi i$ and θ_1 modulo multiplets of $2\pi i$. But the residual gauge transformations on coordinates

$$z_1 \to e^{\frac{1}{2}\,\theta_2 + \frac{1}{2}\,\theta_3} z_1 \ , \quad x_2 \to e^{-\theta_2} x_2 \ , \quad x_3 \to e^{-\theta_3} x_3 \tag{7.51}$$

in the patch (33) only involve the gauge parameters $\theta_{2,3}$, and hence these phase transformations are trivial. Similar arguments can be provided for the other patches $(22) := \{x_1, x_3, z_2\}$ and $(11) := \{x_2, x_3, z_1\}$. The fact that all the coordinate patches of this triangulation are regular can also be verified by showing that the matrices $\mathcal{R}_{(P)}$ defined in (7.46) are all integral.

It follows that in the S–triangulation all the divisors D_u and E_r exist, though not in all coordinate patches. Aside from the curves $E_r D_{u\neq r}$, all three exceptional curves E_1E_2, E_2E_3 and E_3E_1 exist. In particular, the intersections

$$E_1E_2E_3 = E_2E_3D_1 = E_1E_3D_2 = E_1E_2D_3 = 1 \tag{7.52}$$

are all equal to unity as there is just a single solution to the D–term equations and there is no residual gauge transformation acting on the coordinates in any given coordinate patch. All this information is encoded in the toric diagram for the S–triangulation:

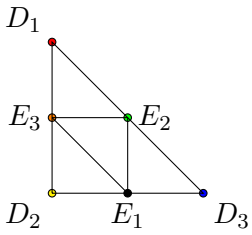

Indeed, all the divisors are indicated as dots. The existing curves are represented as lines between two adjacent dots and the unit intersections are the smallest triangles in the diagram. At the same time these smallest triangles also indicate the four coordinate patches.

E_1–triangulation full resolution phase

In the E_1–triangulation the Kähler parameters satisfy the conditions

$$0 < b_2 + b_3 < b_1 \ , \quad 0 < b_3 < b_1 + b_2 \ , \quad 0 < b_2 < b_1 + b_3 \ . \tag{7.53}$$

Again at least two of the three z_u are non–zero. In light of the first inequality above, it is convenient to write the equation (7.43a) as

$$|x_2|^2 + |x_3|^2 = b_1 - b_2 - b_3 + |z_1|^2 + |x_1|^2 \ . \tag{7.54}$$

Hence either x_2 or x_3 is non–zero. If $x_2 \neq 0$ then (7.43c) implies that z_3 is non–vanish as there needs to at least two $z_u \neq 0$. Similarly, if $x_3 \neq 0$ then (7.43b) says that z_2 is non–vanishing. Therefore, in total there are four coordinate patches: $\{x_1, x_2, z_1\}$, $\{x_1, x_2, z_3\}$, $\{x_1, x_3, z_1\}$, $\{x_1, x_3, z_2\}$. Again all these patches are regular; there is no residual orbifold action on them.

In this phase the exceptional curves E_1E_2 and E_1E_3 exist but E_2E_3 does not. Instead the curve D_1E_1 is allowed by the D–term equations. The following intersections

$$E_1E_2D_3 = E_1E_3D_2 = E_1E_2D_1 = E_1E_3D_1 = 1 \tag{7.55}$$

are all equal to unity. All this information is encoded in the toric diagram for the E_1–triangulation:

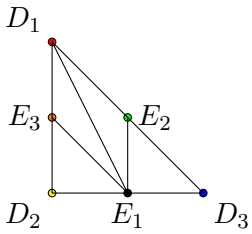

A similar analysis can be performed for the other two full resolution phases corresponding to the triangulations E_2 and E_3. A summary of the results are given in table 7.4.

7.5.2 Pairs of GLSMs associated to torsion related orbifolds

The charges of the Fermi superfields are kept arbitrary in table 7.3. In order that the GLSM is free of gauge anomalies these charge vectors are subject to the conditions [112]

$$Q_1^2 = Q_2^2 = Q_3^2 = \frac{3}{2} \ , \qquad Q_1 \cdot Q_2 = Q_2 \cdot Q_3 = Q_3 \cdot Q_1 = \frac{1}{4} \tag{7.56}$$

and the sum of charges for each of the three gaugings vanishes, see Subsection 7.4.6. The first three equations indicates that consistent choices for the charge vectors are given by the shifted momenta of the three twisted sectors without oscillators, see table 7.1, since they all square to 3/2. The latter three equations can be satisfied by taking the shifted momenta

$$Q_1 = \big(0, \tfrac{1}{2}, \tfrac{1}{2}, \text{-}1, 0, 0, 0^2\big)\big(0^8\big) \ ; \quad Q_2 = \big(\tfrac{1}{2}, 0, \tfrac{1}{2}, 0, \text{-}1, 0, 0^2\big)\big(0^8\big) \ ; \quad Q_3 = \big(\tfrac{1}{2}, \tfrac{1}{2}, 0, 0, 0, \text{-}1, 0^2\big)\big(0^8\big) \tag{7.57}$$

out of the three twisted sectors of the orbifold model without discrete torsion or by

$$Q_1^{\times} = \text{-}\big(0, \tfrac{1}{2}, \tfrac{1}{2}, \text{-}1, 0, 0, 0^2\big)\big(0^8\big); \ Q_2^{\times} = \text{-}\big(\tfrac{1}{2}, 0, \tfrac{1}{2}, 0, \text{-}1, 0, 0^2\big)\big(0^8\big); \ Q_3^{\times} = \text{-}\big(\tfrac{1}{2}, \tfrac{1}{2}, 0, 0, 0, \text{-}1, 0^2\big)\big(0^8\big) \tag{7.58}$$

of the orbifold model with torsion. Notice that this is precisely how the brother gauge shift vectors were related to the original ones as discussed in Subsection 7.3.2.

These certainly do not represent unique choices, but for any choice of anomaly free charge vectors from shifted momenta of the physical twisted states without oscillators in the orbifold model without torsion, the choice of the same charge vectors but all with the opposite sign, is an anomaly free choice with torsion. Hence, switching torsion on or off corresponds to the mapping

$$Q_1 \leftrightarrow Q_1^{\times} = -Q_1 \ , \qquad Q_2 \leftrightarrow Q_2^{\times} = -Q_2 \ , \qquad Q_3 \leftrightarrow Q_3^{\times} = -Q_3 \tag{7.59}$$

of all the charges in the two associated resolution GLSMs simultaneous. This suggests that there is a field redefinition from the Fermi superfields Λ in the non–torsion model to the Fermi superfields $\Lambda^{\times}$ in the torsion model. Formally, in terms of the chiral superfields Ω_r defined in table 7.3 this superfield redefinition can be stated as

$$\Lambda \to \Lambda^{\times} = e^{-2\log\Omega\cdot Q}\,\Lambda \ , \tag{7.60}$$

since this precisely reverses all the charges of Λ. In order that this field redefinition is well–defined Ω_r should be non–singular. Given that in various coordinate patches within the phases of the theory, there are always three superfields non–vanishing they can be used in this field redefinition. Table 7.5 summarises the choices for Ω_r in the patches under investigation here.

Notice that (7.60) precisely looks like a super gauge transformation (A.28) but with the super gauge parameters Θ replaced by $-2\log\Omega$. Since only the Fermi multiplet are involved in this superfield redefinition, it is anomalous. Because this superfield redefinition is of the same form as a super gauge transformation, the form of the anomaly is known to be

$$W_{\text{sf redef anom}} = -\frac{1}{2\pi}\sum_{r,s}\mathcal{A}_{rs}\,\log\Omega^r F^s = -\frac{1}{2\pi}\Big\{\frac{3}{2}\sum_r \log\Omega_r\,F^r + \frac{1}{4}\sum_{s\neq r}\log\Omega_s\,F^r\Big\} \ , \tag{7.61}$$

Phase	Patch	Non–singular superfield representation of		
	(P)	Ω_1	Ω_2	Ω_3
Orbifold	(O)	$\Phi_1'^{-1}$	$\Phi_2'^{-1}$	$\Phi_3'^{-1}$
S–triangulation	(S)	$\Phi_2\Phi_3\Phi_1^{-1}$	$\Phi_1\Phi_3\Phi_2^{-1}$	$\Phi_1\Phi_2\Phi_3^{-1}$
	(33)	$\Phi_2^2\Phi_3'$	$\Phi_1^2\Phi_3'$	$\Phi_3'^{-1}$
	(22)	$\Phi_3^2\Phi_2'$	$\Phi_2'^{-1}$	$\Phi_1^2\Phi_2'$
	(11)	$\Phi_1'^{-1}$	$\Phi_3^2\Phi_1'$	$\Phi_2^2\Phi_1'$
E_1–triangulation	(31)	$\Phi_2^2\Phi_3'$	$\Phi_3^2\Phi_2^{-2}\Phi_3'^{-1}$	$\Phi_3'^{-1}$
	(33)	$\Phi_2^2\Phi_3'$	$\Phi_1^2\Phi_3'$	$\Phi_3'^{-1}$
	(21)	$\Phi_3^2\Phi_2'$	$\Phi_2'^{-1}$	$\Phi_2^2\Phi_3^{-2}\Phi_2'^{-1}$
	(22)	$\Phi_3^2\Phi_2'$	$\Phi_2'^{-1}$	$\Phi_1^2\Phi_2'$
E_2–triangulation	(32)	$\Phi_1^{-2}\Phi_3^2\Phi_3'^{-1}$	$\Phi_1^2\Phi_3'$	$\Phi_3'^{-1}$
	(33)	$\Phi_2^2\Phi_3'$	$\Phi_1^2\Phi_3'$	$\Phi_3'^{-1}$
	(11)	$\Phi_1'^{-1}$	$\Phi_3^2\Phi_1'$	$\Phi_2^2\Phi_1'$
	(12)	$\Phi_1'^{-1}$	$\Phi_3^2\Phi_1'$	$\Phi_1^2\Phi_3^{-2}\Phi_1'^{-1}$
E_3–triangulation	(11)	$\Phi_1'^{-1}$	$\Phi_3^2\Phi_1'$	$\Phi_2^2\Phi_1'$
	(13)	$\Phi_1'^{-1}$	$\Phi_2^2\Phi_3^{-2}\Phi_1'^{-1}$	$\Phi_3^2\Phi_1'$
	(23)	$\Phi_1^{-2}\Phi_2^2\Phi_2'^{-1}$	$\Phi_2'^{-1}$	$\Phi_1^2\Phi_2'$
	(22)	$\Phi_3^2\Phi_2'$	$\Phi_2'^{-1}$	$\Phi_1^2\Phi_2'$

Table 7.5: This table gives the explicite non–singular forms of Ω_r the orbifold and the full resolution patches in the three triangulations.

using the general form of the super gauge anomaly (A.66). The latter form is obtained by using the explicit expression (7.56) of the anomaly matrix $\mathcal{A}_{rs} = Q_r \cdot Q_s$ given by

$$\mathcal{A} = \begin{pmatrix} \frac{3}{2} & \frac{1}{4} & \frac{1}{4} \\ \frac{1}{4} & \frac{3}{2} & \frac{1}{4} \\ \frac{1}{4} & \frac{1}{4} & \frac{3}{2} \end{pmatrix} \ . \tag{7.62}$$

The superfield anomaly (7.61) is of the form of superfield dependent FI–actions (A.30) but with the FI–parameters ρ_r replaced by

$$\rho^T \to \rho^{\times\, T} = \rho^T - \frac{1}{2\pi}\, \log\Omega^T\, \mathcal{A}\ . \tag{7.63}$$

where $\rho^T = \big(\rho_1, \rho_2, \rho_3\big)$ and $\log\Omega^T = \big(\log\Omega_1, \log\Omega_2, \log\Omega_3\big)$.

The field redefinition anomaly (7.61) is not gauge invariant: it gives a phase in the Euclidean path integral

$$\delta_\Theta S_{\text{sf redef anom}} \supset -i \int \alpha_r\, \mathcal{A}_{rs}\ \frac{F^s_{E2}}{2\pi}\ . \tag{7.64}$$

However, since it is only obtained under the assumption that the field redefinition (7.60) is non–singular, it only receives discrete phase contributions from the scalar fields in Table 7.4 that do not vanish.

The flux quantisation conditions (7.35) for the present GLSM read

$$\int \frac{F^1_{E_2}}{2\pi} \in \mathbb{Z}, \qquad \int \frac{F^2_{E_2}}{2\pi} \in \mathbb{Z}, \qquad \int \frac{F^3_{E_2}}{2\pi} \in \mathbb{Z}\ , \tag{7.65a}$$

$$\frac{1}{2}\int \frac{F^2_{E_2}}{2\pi} + \frac{1}{2}\int \frac{F^3_{E_2}}{2\pi} \in \mathbb{Z}, \quad \frac{1}{2}\int \frac{F^1_{E_2}}{2\pi} + \frac{1}{2}\int \frac{F^3_{E_2}}{2\pi} \in \mathbb{Z}, \quad \frac{1}{2}\int \frac{F^1_{E_2}}{2\pi} + \frac{1}{2}\int \frac{F^2_{E_2}}{2\pi} \in \mathbb{Z}\ . \tag{7.65b}$$

The first three conditions follow from the charges of the chiral superfields Φ'_r and the latter three from those of Φ_u. Thus all gauge fluxes are integers and the sums of two gauge fluxes are even integers. The latter quantisation conditions are solved by adding two equations and subtracting the third:

$$\frac{1}{2\pi}\int \begin{pmatrix} F^1_{E2} \\ F^2_{E2} \\ F^3_{E2} \end{pmatrix} = \mathcal{F}\, n\ , \qquad \mathcal{F} = \mathcal{Q}^{-1}_{(S)}\ , \tag{7.66}$$

in terms of three integers $n^T = \big(n_1, n_2, n_3\big)$. Here, $\mathcal{Q}_{(S)}$ is one of the charge matrices defined in (A.67) of Appendix A.3 and their inverse transposed forms in (A.68). As can be seen from there, $\mathcal{F}$ is an integral matrix, the first three quantisation conditions are fulfilled as well. As was argued in [122] possible vacuum phases in (orbifold) partition functions may be recovered in the GLSM as non–invariances of the path integral encoded in

$$\delta_\Theta S_{\text{sf redef anom}} \supset -2\pi i\, m^T \mathcal{M}_{(P)}\, n\ \ , \qquad \mathcal{M}_{(P)} = \mathcal{Q}_r^{-T}\mathcal{A}\mathcal{F} = \mathcal{Q}^{-T}_{(P)}\mathcal{A}\mathcal{Q}^{-1}_{(S)}\ . \tag{7.67}$$

Hence, the path integral is invariant if $\mathcal{M}_{(P)}$ is an integral matrix. By explicit matrix multiplications it may be confirmed that $\mathcal{M}_{(P)}$ is indeed integral for all charge matrices (A.67) that correspond to any of the patches of the three fully resolved phases. On the contrary in the orbifold phase one finds:

$$\mathcal{M}_{(O)} = \begin{pmatrix} 1 & -\frac{3}{2} & -\frac{3}{2} \\ -\frac{3}{2} & 1 & -\frac{3}{2} \\ -\frac{3}{2} & -\frac{3}{2} & 1 \end{pmatrix} \equiv \begin{pmatrix} 0 & \frac{1}{2} & \frac{1}{2} \\ \frac{1}{2} & 0 & \frac{1}{2} \\ \frac{1}{2} & \frac{1}{2} & 0 \end{pmatrix} . \tag{7.68}$$

The final expression is obtained modulo integral matrices. This shows that in the orbifold phase the discrete torsion phases are reproduced by the residual gauge transformations of the field redefinition anomaly.

To summarise, the two non–compact resolution GLSMs associated to the orbifold theories with and without torsions are both free of gauge anomalies and hence consistent models. The effect of discrete torsion between the two models is recovered in their orbifold phases, if both models are expressed in the same field basis (i.e. with chiral Fermi multiplets with the same gauge charges in both models) because of a field redefinition anomaly (7.61). Even though in this expression there are logs of chiral superfields, these are non–singular, because the superfields which appear in the field redefinition (7.60) do not vanish in the patch where the particular field redefinition is defined (see Table 7.5). In particular this does not signify that the geometry has torsion or should be augmented with NS5–branes, since in the unitary gauge the FI–terms are constants in each patch, hence the three–form flux (7.41) vanishes.

7.6 GLSMs for resolutions of $T^6/\mathbb{Z}_2 \times \mathbb{Z}_2$

The study of $(0,2)$ resolution GLSMs of the toroidal orbifold $T^6/\mathbb{Z}_2 \times \mathbb{Z}_2$ is more involved than those for the non–compact orbifold $\mathbb{C}^3/\mathbb{Z}_2 \times \mathbb{Z}_2$ considered in the previous section. First of all, additional ingredients are needed to describe the geometry as the orbifold is compact. And partially because of this also the description of possible gauge backgrounds is more complicated. Only with these aspects understood, the consequences of discrete torsion in the underlying orbifold model can be properly investigated. Therefore, first Subsections 7.6.1 to 7.6.4 are used to develop a both accurate and manageable description of resolution GLSMs associated with the singular $T^6/\mathbb{Z}_2 \times \mathbb{Z}_2$ geometry dubbed a minimal full resolution model. Subsection 7.6.5 then gives the GLSM for a particular gauge background using the same blowup modes as in the non–compact model studied in the previous section. Finally, Subsection 7.6.6 the GLSM for the compact orbifold model with discrete torsion is studied.

7.6.1 Construction of resolution GLSMs for compact $\mathbb{Z}_2 \times \mathbb{Z}_2$ orbifolds

To construct GLSMs that describe resolutions of toroidal orbifold geometries, the following steps need to be taken [113]:

1. Give GLSM descriptions for each of the three underlying two–tori compatible with the orbifold symmetries.

2. Add so–called exceptional gaugings to introduce the orbifold actions and define the exceptional cycles.
3. Confirm that there is a regime where the GLSM description can be interpreted as the orbifold geometry under consideration.
4. Determine the regimes in which the GLSM description can be interpreted as resolved geometries.

This program was discussed in [113] for $(2,2)$ models, but these steps can equally well be executed in the $(0,2)$ language, which is used throughout this work.

It is important to realise that there are a number of different $T^6/\mathbb{Z}_2\times\mathbb{Z}_2$ orbifolds depending on their underlying six–torus lattice, see e.g. [50, 99, 128]. The construction here is aimed to resolve the particular one with Hodge numbers $(51,3)$. Moreover, one single orbifold geometry may be associated to many different GLSMs, even if the target space gauge configurations are not considered. The descriptions differ in the number of exceptional gaugings. Descriptions in which for all exceptional cycles of the resolved geometry there are exceptional gaugings, were dubbed maximal full resolution GLSMs in ref. [113]. On the other end there are GLSMs descriptions with the least number of exceptional gaugings such that still the effective geometry in appropriate regimes corresponds to fully resolved orbifold resolutions. Such models were called minimal full resolution GLSMs. Between these two extremes there is a whole variety of GLSMs. Some of these models cannot describe fully resolved geometries; while others do [113]. The focus in this chapter is on full resolution GLSMs only. Such resolution GLSMs might possess many different phases. Only the orbifold phase and fully smooth resolution phases are investigated in this work in detail, while all kinds of interesting other phases will be ignored.

Maximal full resolution GLSMs are the most complete in the sense that all the Kähler parameters associated to the volumes of the exceptional cycles are made explicit. On the down side, this means that such models typically contain a large number of $U(1)$ gauge symmetries. As is discussed below the maximal full resolution GLSM for the toroidal orbifold $T^6/\mathbb{Z}_2\times\mathbb{Z}_2$ contains 51 $U(1)$ gaugings: for each of the 51 Kähler parameters there is a dedicated gauging available. The minimal full resolution GLSM for this orbifold only requires six $U(1)$ gaugings: The radii of the three two–tori and collective volumes of the three types of exceptional cycles are explicit in that description.

Below, first the GLSMs description of a two–torus with $\mathbb{Z}_2$ symmetries is recalled. After that the basic ingredients of the maximal full resolution GLSM are laid out. Details of the resulting geometry and the consequences of the discrete torsion of the orbifold model are investigated in the minimal full resolution GLSM only for simplicity.

7.6.2 Two–tori GLSM with $\mathbb{Z}_2$ symmetries

In ref. [113] it was argued that a convenient description of two–tori that admit $\mathbb{Z}_2$ involutions are given by the superfields given in Table 7.6 with the superpotential

$$P_{\text{three two–tori}} = \sum_u \Big(\kappa_u\,\Phi_{u\,1}^2 + \Phi_{u\,2}^2 + \Phi_{u\,3}^2\Big)\Gamma_u + \Big(\Phi_{u\,1}^2 + \Phi_{u\,2}^2 + \Phi_{u\,4}^2\Big)\Gamma'_u\ , \tag{7.69}$$

where

$$\kappa_u = \frac{\mathcal{P}_{\tau_u}(\frac{\tau_u}{2}) - \mathcal{P}_{\tau_u}(\frac{1}{2})}{\mathcal{P}_{\tau_u}(\frac{1+\tau_u}{2}) - \mathcal{P}_{\tau_u}(\frac{1}{2})} \tag{7.70}$$

Superfield	$\Phi_{u\,1}$	$\Phi_{u\,2}$	$\Phi_{u\,3}$	$\Phi_{u\,4}$	Γ_u	Γ'_u
U(1) charges	$z_{u\,1}$	$z_{u\,2}$	$z_{u\,3}$	$z_{u\,4}$	γ_u	γ'_u
$R_{u'}$	$\frac{1}{2}\delta_{u'u}$	$\frac{1}{2}\delta_{u'u}$	$\frac{1}{2}\delta_{u'u}$	$\frac{1}{2}\delta_{u'u}$	$-\delta_{u'u}$	$-\delta_{u'u}$

Table 7.6: Superfield charge table for the GLSM for three two–tori admiting $\mathbb{Z}_2$ symmetries.

Superfield	$\Phi_{1\,x}$	$\Phi_{2\,y}$	$\Phi_{3\,z}$	Γ_1	Γ'_1	Γ_2	Γ'_2	Γ_3	Γ'_3	$\Phi'_{1\,yz}$	$\Phi'_{2\,xz}$	$\Phi'_{3\,xy}$
U(1) charge	$z_{1\,x}$	$z_{2\,y}$	$z_{3\,z}$	γ_1	γ'_1	γ_2	γ'_2	γ_3	γ'_3	$x_{1\,yz}$	$x_{2\,xz}$	$x_{3\,xy}$
R_1	$\frac{1}{2}$	0	0	-1	-1	0	0	0	0	0	0	0
R_2	0	$\frac{1}{2}$	0	0	0	-1	-1	0	0	0	0	0
R_3	0	0	$\frac{1}{2}$	0	0	0	0	-1	-1	0	0	0
$E_{1\,y'z'}$	0	$\frac{1}{2}\delta_{y'y}$	$\frac{1}{2}\delta_{z'z}$	0	0	0	0	0	0	$-\delta_{y'y}\delta_{z'z}$	0	0
$E_{2\,x'z'}$	$\frac{1}{2}\delta_{x'x}$	0	$\frac{1}{2}\delta_{z'z}$	0	0	0	0	0	0	0	$-\delta_{x'x}\delta_{z'z}$	0
$E_{3\,x'y'}$	$\frac{1}{2}\delta_{z'z}$	$\frac{1}{2}\delta_{y'y}$	0	0	0	0	0	0	0	0	0	$-\delta_{x'x}\delta_{y'y}$

Table 7.7: Superfield charge table that determines the geometry of maximal full resolution of $T^6/\mathbb{Z}_2 \times \mathbb{Z}_2$.

parameterise the complex structures τ_u of the three two–tori in terms of the Weierstrass $\mathcal{P}$ function. This description was obtained as a rewriting of the well–known Weierstrass model of an eliptic curve. On each of the four chiral superfields $\Phi_{u\,x}$ of two–torus T^2_u a separate $\mathbb{Z}_2$ reflection symmetry $\Phi_{u\,x} \to -\Phi_{u\,x}$ can act leaving the superpotential invariant. In addition, there are two involutions per two–torus which can be identified with $\mathbb{Z}_2$ translation on the two–torus lattice [113]. The Kähler structures of the two–tori are encoded in the GLSM description as the FI–parameter a_u associated with the gauging R_u. The resulting D– and F–term equations in the conformal limit read:

$$|z_{u\,1}|^2 + |z_{u\,2}|^2 + |z_{u\,3}|^2 + |z_{u\,4}|^2 = a_u \ , \tag{7.71a}$$

$$\kappa_u\, z^2_{u\,1} + z^2_{u\,2} + z^2_{u\,3} = 0 \ , \quad z^2_{u\,1} + z^2_{u\,2} + z^2_{u\,4} = 0 \ . \tag{7.71b}$$

Because $\kappa_u \neq 1$ the two F–term conditions can never combined to an equation with just two terms. Together with the $U(1)$ gaugings, which can remove a phase per u, shows that each set of $z_{u\,1}, \ldots, z_{u\,4}$ coordinates for a given u describes a geometry of real dimension two.

7.6.3 Maximal full resolution GLSM

The maximal full resolution GLSM for the toroidal orbifold $T^6/\mathbb{Z}_2 \times \mathbb{Z}_2$ has three ordinary gaugings R_1, R_2 and R_3 to define three two–tori and $3 \cdot 16 = 48$ exceptional gaugings $E_{1,yz}$,

Superfield	Φ_{1x}	Φ_{2y}	Φ_{3z}	Γ_1	Γ'_1	Γ_2	Γ'_2	Γ_3	Γ'_3	Φ'_1	Φ'_2	Φ'_3
U(1) charge	z_{1x}	z_{2y}	z_{3z}	γ_1	γ'_1	γ_2	γ'_2	γ_3	γ'_3	x_1	x_2	x_3
R_1	$\frac{1}{2}$	0	0	-1	-1	0	0	0	0	0	0	0
R_2	0	$\frac{1}{2}$	0	0	0	-1	-1	0	0	0	0	0
R_3	0	0	$\frac{1}{2}$	0	0	0	0	-1	-1	0	0	0
E_1	0	$\frac{1}{2}\delta_{y1}$	$\frac{1}{2}\delta_{z1}$	0	0	0	0	0	0	-1	0	0
E_2	$\frac{1}{2}\delta_{x1}$	0	$\frac{1}{2}\delta_{z1}$	0	0	0	0	0	0	0	-1	0
E_3	$\frac{1}{2}\delta_{x1}$	$\frac{1}{2}\delta_{y1}$	0	0	0	0	0	0	0	0	0	-1

Table 7.8: A choice for a superfield charge table that determines the geometry of a minimal full resolution of $T^6/\mathbb{Z}_2 \times \mathbb{Z}_2$.

$E_{2,xz}$ and $E_{3,xy}$ associated to the exceptional cycles. The full charge table is given in Table 7.7. The fermi superfields Γ_1, Γ'_1, Γ_2, Γ'_2 and Γ_3, Γ'_3 feature in the superpotential to define the three underlying two–tori, see (7.69). Because the exceptional gaugings the superpotential has to be extended to

$$\begin{aligned} P_{\text{max res}} &= \Big(\kappa_1\, \Phi^2_{1\,1} \prod_z \Phi'_{2\,1z} \prod_y \Phi'_{3\,1y} + \Phi^2_{1\,2} \prod_z \Phi'_{2\,2z} \prod_y \Phi'_{3\,2y} + \Phi^2_{1\,3} \prod_z \Phi'_{2\,3z} \prod_y \Phi'_{3\,3y}\Big)\Gamma_1 \\ &\quad + \Big(\Phi^2_{1\,1} \prod_z \Phi'_{2\,1z} \prod_y \Phi'_{3\,1y} + \Phi^2_{1\,2} \prod_z \Phi'_{2\,2z} \prod_y \Phi'_{3\,2y} + \Phi^2_{1\,4} \prod_z \Phi'_{2\,4z} \prod_y \Phi'_{3\,4y}\Big)\Gamma'_1 \\ &+ \Big(\kappa_2\, \Phi^2_{2\,1} \prod_x \Phi'_{1\,1x} \prod_z \Phi'_{3\,1z} + \Phi^2_{2\,2} \prod_x \Phi'_{1\,2x} \prod_z \Phi'_{3\,2z} + \Phi^2_{2\,3} \prod_x \Phi'_{1\,3x} \prod_z \Phi'_{3\,3z}\Big)\Gamma_2 \\ &\quad + \Big(\Phi^2_{2\,1} \prod_x \Phi'_{1\,1x} \prod_z \Phi'_{3\,1z} + \Phi^2_{2\,2} \prod_x \Phi'_{1\,2x} \prod_z \Phi'_{3\,2z} + \Phi^2_{2\,4} \prod_x \Phi'_{1\,4x} \prod_z \Phi'_{3\,4z}\Big)\Gamma'_2 \\ &+ \Big(\kappa_3\, \Phi^2_{3\,1} \prod_x \Phi'_{1\,1x} \prod_y \Phi'_{2\,1y} + \Phi^2_{3\,2} \prod_x \Phi'_{1\,2x} \prod_y \Phi'_{2\,2y} + \Phi^2_{3\,3} \prod_x \Phi'_{1\,3x} \prod_y \Phi'_{2\,3y}\Big)\Gamma_3 \\ &\quad + \Big(\Phi^2_{3\,1} \prod_x \Phi'_{1\,1x} \prod_y \Phi'_{2\,1y} + \Phi^2_{3\,2} \prod_x \Phi'_{1\,2x} \prod_y \Phi'_{2\,2y} + \Phi^2_{3\,4} \prod_x \Phi'_{1\,4x} \prod_y \Phi'_{2\,4y}\Big)\Gamma'_3 \end{aligned} \tag{7.72}$$

in order to make it gauge invariant under all exceptional gaugings. The resulting D– and F–term conditions are rather involved and not particularly illuminating. For this reason we refrain from giving them here and turn to the more transparant minimal full resolution model.

7.6.4 Minimal full resolution GLSM

The minimal full resolution GLSM has three ordinary and three exceptional gaugings. Contrary to the maximal full resolution GLSM, the charge assignments of minimal full resolution models are not unique as for each of the three exceptional gaugings there are $4 \cdot 4 = 16$ choices, which of the homogeneous coordinate superfields to be gauged.

Here only gaugings of the superfields $\Phi_{1\,1}$, $\Phi_{2\,1}$ and $\Phi_{3\,1}$ are considered[4], as can be seen in Table 7.8. Consequently, the superpotential for the geometry reduces to

$$P_{\text{min res}} = \sum_{u=1}^{3} \Gamma_u \Big(\kappa_u \, \Phi_{u\,1}^2 \prod_{r\neq u} \Phi'_r + \Phi_{u\,2}^2 + \Phi_{u\,3}^2 \Big) \; + \sum_{u=1}^{3} \Gamma'_u \Big(\Phi_{u\,1}^2 \prod_{r\neq u} \Phi'_2 \Phi'_3 + \Phi_{u\,2}^2 + \Phi_{u\,4}^2 \Big) \; . \tag{7.73}$$

The effective target space geometries are determined by six D– and six F–term equations. The six resulting D–term conditions read

$$\begin{aligned}
&|z_{1\,1}|^2 + |z_{1\,2}|^2 + |z_{1\,3}|^2 + |z_{1\,4}|^2 = a_1 \; , \qquad && |z_{2\,1}|^2 + |z_{3\,1}|^2 - 2\,|x_1|^2 = 2\,b_1 \; , \\
&|z_{2\,1}|^2 + |z_{2\,2}|^2 + |z_{2\,3}|^2 + |z_{2\,4}|^2 = a_2 \; , \qquad && |z_{1\,1}|^2 + |z_{3\,1}|^2 - 2\,|x_2|^2 = 2\,b_2 \; , \\
&|z_{3\,1}|^2 + |z_{3\,2}|^2 + |z_{3\,3}|^2 + |z_{3\,4}|^2 = a_3 \; , \qquad && |z_{1\,1}|^2 + |z_{2\,1}|^2 - 2\,|x_3|^2 = 2\,b_3
\end{aligned} \tag{7.74}$$

and the six F–term conditions

$$\begin{aligned}
&\kappa_1 \, z_{1\,1}^2 \, x_2 x_3 + z_{1\,2}^2 + z_{1\,3}^2 = 0 \; , \qquad && z_{1\,1}^2 \, x_2 x_3 + z_{1\,2}^2 + z_{1\,4}^2 = 0 \; , \\
&\kappa_2 \, z_{2\,1}^2 \, x_1 x_3 + z_{2\,2}^2 + z_{2\,3}^2 = 0 \; , \qquad && z_{2\,1}^2 \, x_1 x_3 + z_{2\,2}^2 + z_{2\,4}^2 = 0 \; , \\
&\kappa_3 \, z_{3\,1}^2 \, x_1 x_2 + z_{3\,2}^2 + z_{3\,3}^2 = 0 \; , \qquad && z_{3\,1}^2 \, x_1 x_2 + z_{3\,2}^2 + z_{3\,4}^2 = 0 \; .
\end{aligned} \tag{7.75}$$

The properties of the resulting geometries depend crucially on the values of the Kähler parameters. As can be seen from the three D–term conditions on the left in (7.74) the parameters a_1, a_2, a_3 all need to be positive (since we have assumed that all $y^A = 0$). The other Kähler parameters b_1, b_2, b_3 may in principle have either sign.

Orbifold phase

Consider the phase in which all three parameters b_1, b_2, b_3 are negative while the parameters a_1, a_2, a_3 all positive. It follows that all three coordinates x_1, x_2, x_3 are necessarily non–zero so that their phases can be fixed to some preset values. This does not fix the gauge symmetries completely, as there are residual $\mathbb{Z}_2$ actions left over:

$$\begin{aligned}
&\mathbb{Z}_2 : \quad z_{2\,1} \to -z_{2\,1} \; , \quad z_{3\,1} \to -z_{3\,1} \; , \\
&\mathbb{Z}_2 : \quad z_{1\,1} \to -z_{1\,1} \; , \quad z_{3\,1} \to -z_{3\,1} \; , \\
&\mathbb{Z}_2 : \quad z_{1\,1} \to -z_{1\,1} \; , \quad z_{2\,1} \to -z_{2\,1} \; .
\end{aligned} \tag{7.76}$$

For concreteness, focus on the first of these three $\mathbb{Z}_2$ actions. The fixed set of this action is given by $z_{2\,1} = z_{3\,1} = 0$. In the target space geometry this does not correspond to a single

[4]Other choices would be equally well justified, however we expect that the physical understanding does not depend much on this, even though the detailed description will.

fixed set, but a collection of disjoint fixed sets. Indeed, inserting this in the second and third equations in (7.75) gives the equations:

$$z_{2\,2}^2 + z_{2\,3}^2 = z_{2\,2}^2 + z_{2\,4}^2 = 0 \ , \qquad z_{3\,2}^2 + z_{3\,3}^2 = z_{3\,2}^2 + z_{3\,4}^2 = 0 \ . \tag{7.77}$$

Each of these equations are quadratic with two roots:

$$z_{2\,3} = \pm i\, z_{2\,2} \ , \quad z_{2\,4} = \pm i\, z_{2\,2} \ , \qquad z_{3\,3} = \pm i\, z_{3\,2} \ , \quad z_{3\,4} = \pm i\, z_{3\,2} \ , \tag{7.78}$$

where all the signs are independent, hence there are $2^4 = 16$ solutions in total. Each of these fixed sets have the topology of a two–torus: The equations for the homogeneous coordinates $z_{1\,x}$ are those of the deformed two–torus used in Subsection 7.6.2 since the absolute values of the coordinates x_2 and x_3 are determined by the second and third equation on the right hand side in (7.74). This argumentation may be repeated for the second and third $\mathbb{Z}_2$ actions in (7.76). Hence one has in total $3 \cdot 16 = 48$ fixed two–tori; precisely the number of fixed two–tori to be expected in the $T^6/\mathbb{Z}_2 \times \mathbb{Z}_2$ orbifold.

The coordinate patches suggested by the minimal full resolution model for the orbifold geometry can be extracted from the D– and F–term equations (7.74) and (7.75). Since all blowup parameters b_1, b_2, b_3 are negative, the three D–term equations on the right–hand–side of (7.74) imply that $x_1, x_2, x_3 \neq 0$. Each of the other three D–term equations imply that at least one coordinate in each is non–zero. But then the F–term equations (7.75) imply that two other coordinates are non–zero. Hence, three out of four z_{1x}, z_{2y} and z_{3z} coordinates are non–zero. This leads to $4^3 = 64$ coordinate patches; the same number of coordinate patches as the $(T^2)^3$ torus GLSM would have.

Full resolution phases

In the full resolution phases all parameters b_1, b_2, b_3 are positive but parametrically much smaller than the parameters a_1, a_2, a_3. (If this is not the case, the GLSM might develop more exotic phases, like critical– and over–blowup phases [113].) In the full resolution phases it is useful to reshuffle the three D–term equations on the right hand side of (7.74) in the following fashion:

$$\begin{aligned} |z_{1\,1}|^2 + |x_1|^2 &= b_2 + b_3 - b_1 + |x_2|^2 + |x_3|^2 \ . \\ |z_{2\,1}|^2 + |x_2|^2 &= b_1 + b_3 - b_2 + |x_1|^2 + |x_3|^2 \ , \\ |z_{3\,1}|^2 + |x_3|^2 &= b_1 + b_2 - b_3 + |x_1|^2 + |x_2|^2 \ . \end{aligned} \tag{7.79}$$

These equations contain important information as they decide which coordinate fields are necessarily non–zero. For example, if the sign of the combination $b_2 + b_3 - b_1$ is positive either $z_{1\,1}$ or x_1 is necessarily non–zero, while if this combination is negative either x_2 or x_3 is necessarily non–zero.

The following divisors can be easily defined by setting one of the homogeneous coordinates to zero: the exceptional divisors $E_r := \{x_r = 0\}$ and the ordinary divisors $D_u := \{z_{u\,1} = 0\}$. The exceptional divisors consists of $2^4 = 16$ disjoint components and the ordinary divisors of $2^2 = 4$ disjoint components. As was observed in [113] the inherited torus divisors R_u and R'_u can be identified with the polynomials multiplying the chiral Fermi superfields Γ_u and Γ'_u in the superpotential (7.73).

S–triangulation full resolution phase

In the S–triangulation phase of the GLSM the three Kähler parameters are of similar size in the sense that each one is smaller than the sum of the other two, e.g. the following three inequalities

$$0 < b_1 < b_2 + b_3 \ , \quad 0 < b_2 < b_1 + b_3 \ , \quad 0 < b_3 < b_1 + b_2 \ , \tag{7.80}$$

hold simultaneously. In this phase the intersection $E_1E_2E_3$ exists because it is possible to satisfy all the D– and F–term equations while setting $x_1 = x_2 = x_3 = 0$. In fact, in this case the F–term equations have $2^6 = 64$ solutions. This number comes as no surprise, since the $T^6/\mathbb{Z}_2 \times \mathbb{Z}_2$ has 64 $\mathbb{Z}_2 \times \mathbb{Z}_2$ fixed points. When all resolved using the S–triangulation, one 64 times the intersection of these three exceptional divisors. Note that the first equation in (7.79) implies that not both z_{11} and x_1 can be zero at the same time, hence, in particular, the curve D_1E_1 does not exist. All this is in accordance with the topological properties of the S–triangulation of the resolved $T^6/\mathbb{Z}_2 \times \mathbb{Z}_2$ orbifold.

E_1–triangulation full resolution phase

In the E_1–triangulation phase of the GLSM the Kähler parameter b_1 is much larger than the sum of the other two:

$$0 < b_2 < b_1 + b_3 \ , \quad 0 < b_3 < b_1 + b_2 \ , \quad b_2 + b_3 < b_1 \ . \tag{7.81}$$

Then (7.79) implies that not both x_2 and x_3 can be zero at the same time, hence, in particular, the curve E_2E_3 and the intersection $E_1E_2E_3$ do not exist in this phase. Contrary, in this phase the curve D_1E_1 does exist. All this is, again, in accordance with the topological properties of the E_1–triangulation of the resolved $T^6/\mathbb{Z}_2 \times \mathbb{Z}_2$ orbifold. The transition from the S– to the E_1–triangulation phase thus provides the GLSM description of the flop transition. Note that in the GLSM there is nothing singular at the transition $b_1 = b_2 + b_3$ even though the target space geometry is singular there.

The other two full resolutions phases, the E_2– and E_3–triangulations may be defined in an analogous fashion.

Full resolution coordinate patches

To understand the coordinate patches in the full resolution phases, first observe that the three D–term equations on the right–hand–side of (7.74) lead to the same options for non–vanishing coordinates $z_{11}, z_{21}, z_{31}, x_1, x_2, x_3$ as obtained in the non–compact case summarised in Table 7.4. Hence, in the S–, E_1–, E_2– or E_3–triangulation the following coordinate combinations

$$S: \quad z_{11}z_{21}z_{31} \neq 0 \ , \quad z_{11}z_{21}x_3 \neq 0 \ , \quad z_{11}z_{31}x_2 \neq 0 \ \text{ or } \ z_{21}z_{31}x_1 \neq 0 \ , \tag{7.82a}$$

$$E_1: \quad z_{21}z_{31}x_3 \neq 0 \ , \quad z_{11}z_{21}x_3 \neq 0 \ , \quad z_{21}z_{31}x_2 \neq 0 \ \text{ or } \ z_{11}z_{31}x_2 \neq 0 \ , \tag{7.82b}$$

$$E_2: \quad z_{11}z_{31}x_3 \neq 0 \ , \quad z_{11}z_{21}x_3 \neq 0 \ , \quad z_{21}z_{31}x_1 \neq 0 \ \text{ or } \ z_{11}z_{31}x_1 \neq 0 \ , \tag{7.82c}$$

$$E_3: \quad z_{21}z_{31}x_1 \neq 0 \ , \quad z_{11}z_{21}x_1 \neq 0 \ , \quad z_{11}z_{21}x_2 \neq 0 \ \text{ or } \ z_{11}z_{31}x_2 \neq 0 \ . \tag{7.82d}$$

are non–zero, respectively. Next, observe that the first D–term equation on the left–hand–side of (7.74) implies that at least $z_{1\,x}$ is non–zero. If this happens to be $z_{1\,1}$ then the latter two D–term equations on the right–hand–side of (7.74) imply that x_2 and x_3 are also non–zero because a_1 is parametrically larger than the parameters b_1, b_2, b_3 so that cancellations are never possible. But the the two top F–term equations (7.75) imply that two other z_{1x}, $x \neq 1$ are non–zero. There are three options for this to happen. Finally, it is possible that all three $z_{1\,x}$, $x \neq 1$ are non–zero. In total this gives four non–vanishing coordinate combinations for the first lines of the D– and F–term equations. A similar analysis can be performed for the second and third lines of these equations, leading to the following combinations of non–vanishing coordinates

$$z_{1\,2}z_{1\,3}z_{1\,4} \neq 0\ ,\quad z_{1\,1}z_{1\,3}z_{1\,4}x_2x_3 \neq 0\ ,\quad z_{1\,1}z_{1\,2}z_{1\,4}x_2x_3 \neq 0\ \text{ or }\ z_{1\,1}z_{1\,2}z_{1\,3}x_2x_3 \neq 0\ , \tag{7.83a}$$

$$z_{2\,2}z_{2\,3}z_{2\,4} \neq 0\ ,\quad z_{2\,1}z_{2\,3}z_{2\,4}x_1x_3 \neq 0\ ,\quad z_{2\,1}z_{2\,2}z_{2\,4}x_1x_3 \neq 0\ \text{ or }\ z_{2\,1}z_{2\,2}z_{2\,3}x_1x_3 \neq 0\ , \tag{7.83b}$$

$$z_{3\,2}z_{3\,3}z_{3\,4} \neq 0\ ,\quad z_{3\,1}z_{3\,3}z_{3\,4}x_1x_2 \neq 0\ ,\quad z_{3\,1}z_{3\,2}z_{3\,4}x_1x_2 \neq 0\ \text{ or }\ z_{3\,1}z_{3\,2}z_{3\,3}x_1x_2 \neq 0\ . \tag{7.83c}$$

Coordinate patches can now be composed by taking one out of four equations on each line of (7.83) combined with one out of the four equations from the line in (7.82) corresponding to the chosen triangulation. Not all combinations are valid however, in total there should be 12 non–vanishing coordinates out of the 15 original ones, so that the coordinate patch has complex dimension three.

The results of this analysis are summarised in Table 7.9. The GLSM description leads to 76 coordinate patches for each of the full resolution phases. There are 72 universal coordinate patches which exist independently of which triangulation is chosen: for each triangulation choice in (7.82) there is at least one combination of non–vanishing fields which is contained in the non–vanishing set coordinates of that patch to the extent that precisely 12 coordinates are non–zero. 54 of those patches do not involve any of the exceptional coordinates and therefore coincide with the coordinate patches of the orbifold discussed above. These coordinate patches are indicated above the line that splits the universal patches in Table 7.9. In addition, to the 72 universal coordinate patches there are four patches that depend on the triangulation. The GLSM therefore dictates a gluing procedure in which ten of the coordinate patches of the orbifold are replaced by 22 patches for the full resolutions.

7.6.5 Gauge background on the minimal full resolution of the non–torsional orbifold

The gauge charges of the Fermi and chiral multiplets that define a simple gauge bundle on the minimal full resolution model is given in Table 7.10. This gauge bundle is quite closely related to the standard embedding on the two–tori. The exceptional E–gauge charges are identical to those indicated in (7.56) of the non–compact resolution model. In order to avoid any of the four types of anomalies mentioned in Subsection 7.4.6, additional chiral multiplets Ψ_u, Ψ'_u are introduced with identical charges as Γ_u, Γ'_u and the sum of charges of all chiral superfields and all chiral Fermi superfields vanish separately.

In total there are $3 \cdot 4 + 3 = 15$ Fermi multiplets involved in the gauge bundle subject to $3 \cdot 2 = 6$ constraints enforced by the chiral multiplets Ψ_u, Ψ'_u. This leave nine Fermi multiplets part of the gauge background which cannot be fitted into a single E_8 factor. Hence a number of fermionic gaugings are needed. If all six gaugings in the minimal resolution model are accompanied by fermionic gaugings, (a deformation of) the standard embedding is obtained. To

Phase	#	Non–zero fields	Patches	Conditions
Universal	54	$z_{1\,x'\neq x}\, z_{2\,y'\neq y}\, z_{z'\neq z}\, x_1\, x_2\, x_3 \neq 0$	$\{z_{1\,x}, z_{2\,y}, z_{3\,z}\}$	$x, y, z \neq 1$
		$z_{1\,x'\neq 1}\, z_{2\,y'\neq y}\, z_{z'\neq z}\, x_1\, x_2\, x_3 \neq 0$	$\{z_{1\,1}, z_{2\,y}, z_{3\,z}\}$	$y, z \neq 1$
		$z_{1\,x'\neq x}\, z_{2\,y'\neq 1}\, z_{z'\neq z}\, x_1\, x_2\, x_3 \neq 0$	$\{z_{1\,x}, z_{2\,1}, z_{3\,z}\}$	$x, z \neq 1$
		$z_{1\,x'\neq x}\, z_{2\,y'\neq y}\, z_{z'\neq 1}\, x_1\, x_2\, x_3 \neq 0$	$\{z_{1\,x}, z_{2\,y}, z_{3\,1}\}$	$x, y \neq 1$
	18	$z_{u'\neq u\,1} z_{1\,x'\neq 1}\, z_{2\,y'\neq 1}\, z_{z'\neq z}\, x_1\, x_2 \neq 0$	$\{z_{u\,1}, z_{3\,z}, x_3\}$	$u', u = 1, 2; z \neq 1$
		$z_{u'\neq u\,1} z_{1\,x'\neq 1}\, z_{2\,y'\neq y}\, z_{z'\neq 1}\, x_1\, x_3 \neq 0$	$\{z_{u\,1}, z_{2\,y}, x_2\}$	$u', u \neq 1, 3; y \neq 1$
		$z_{u'\neq u\,1} z_{1\,x'\neq x}\, z_{2\,y'\neq 1}\, z_{z'\neq 1}\, x_2\, x_3 \neq 0$	$\{z_{u\,1}, z_{1\,x}, x_1\}$	$u', u = 2, 3; x \neq 1$
S–triang.	4	$z_{u\,x} \neq 0$	$\{x_1, x_2, x_3\}$	$u = 1, 2, 3; x = 1, .., 4$
		$z_{u\,x\neq 3\,1} x_3 \neq 0$	$\{z_{3\,1}, x_1, x_2\}$	$u = 1, 2, 3; x = 1, .., 4$
		$z_{u\,x\neq 2\,1} x_2 \neq 0$	$\{z_{2\,1}, x_1, x_3\}$	$u = 1, 2, 3; x = 1, .., 4$
		$z_{u\,x\neq 1\,1} x_1 \neq 0$	$\{z_{1\,1}, x_2, x_3\}$	$u = 1, 2, 3; x = 1, .., 4$
E_1–triang.	4	$z_{u\,x\neq 1\,1} x_3 \neq 0$	$\{z_{1\,1}, x_1, x_2\}$	$u = 1, 2, 3; x = 1, .., 4$
		$z_{u\,x\neq 3\,1} x_3 \neq 0$	$\{z_{3\,1}, x_1, x_2\}$	$u = 1, 2, 3; x = 1, .., 4$
		$z_{u\,x\neq 1\,1} x_2 \neq 0$	$\{z_{1\,1}, x_1, x_3\}$	$u = 1, 2, 3; x = 1, .., 4$
		$z_{u\,x\neq 2\,1} x_2 \neq 0$	$\{z_{2\,1}, x_1, x_3\}$	$u = 1, 2, 3; x = 1, .., 4$
E_2–triang.	4	$z_{u\,x\neq 2\,1} x_3 \neq 0$	$\{z_{2\,1}, x_1, x_2\}$	$u = 1, 2, 3; x = 1, .., 4$
		$z_{u\,x\neq 3\,1} x_3 \neq 0$	$\{z_{3\,1}, x_1, x_2\}$	$u = 1, 2, 3; x = 1, .., 4$
		$z_{u\,x\neq 1\,1} x_1 \neq 0$	$\{z_{1\,1}, x_2, x_3\}$	$u = 1, 2, 3; x = 1, .., 4$
		$z_{u\,x\neq 2\,1} x_1 \neq 0$	$\{z_{2\,1}, x_2, x_3\}$	$u = 1, 2, 3; x = 1, .., 4$
E_3–triang.	4	$z_{u\,x\neq 1\,1} x_1 \neq 0$	$\{z_{1\,1}, x_2, x_3\}$	$u = 1, 2, 3; x = 1, .., 4$
		$z_{u\,x\neq 3\,1} x_1 \neq 0$	$\{z_{3\,1}, x_2, x_3\}$	$u = 1, 2, 3; x = 1, .., 4$
		$z_{u\,x\neq 3\,1} x_2 \neq 0$	$\{z_{3\,1}, x_1, x_3\}$	$u = 1, 2, 3; x = 1, .., 4$
		$z_{u\,x\neq 2\,1} x_2 \neq 0$	$\{z_{2\,1}, x_1, x_3\}$	$u = 1, 2, 3; x = 1, .., 4$

Table 7.9: The 76 coordinate patches of the full resolution phases of the minimal full resolution GLSM. There are 72 universal coordinate patches which are the same for each of the full resolution phases. In addition, there are four coordinate patches which are specific for the triangulation chosen.

Superfield	Λ_{1x}	Λ_{2y}	Λ_{3z}	Ψ_1	Ψ'_1	Ψ_2	Ψ'_2	Ψ_3	Ψ'_3	Λ'_1	Λ'_2	Λ'_3	Λ_n
U(1) charge	λ_{1x}	λ_{2y}	λ_{3z}	ψ_1	ψ'_1	ψ_2	ψ'_2	ψ_3	ψ'_3	λ'_1	λ'_2	λ'_3	λ_n
R_1	$\frac{1}{2}$	0	0	-1	-1	0	0	0	0	0	0	0	0
R_2	0	$\frac{1}{2}$	0	0	0	-1	-1	0	0	0	0	0	0
R_3	0	0	$\frac{1}{2}$	0	0	0	0	-1	-1	0	0	0	0
E_1	0	$\frac{1}{2}\delta_{y1}$	$\frac{1}{2}\delta_{z1}$	0	0	0	0	0	0	-1	0	0	0
E_2	$\frac{1}{2}\delta_{x1}$	0	$\frac{1}{2}\delta_{z1}$	0	0	0	0	0	0	0	-1	0	0
E_3	$\frac{1}{2}\delta_{x1}$	$\frac{1}{2}\delta_{y1}$	0	0	0	0	0	0	0	0	0	-1	0

Table 7.10: A choice for a charge table of the superfields that determine a gauge bundle on the minimal full resolution of $T^6/\mathbb{Z}_2 \times \mathbb{Z}_2$. The Fermi multiplets Λ_n, $n = 1, \ldots, 18$, are spectators and generate the broken gauge group.

make contact with the non–torsion line bundle model that was discussed in Section 7.5.2, only the inherited R_u–gaugings are accompanied with fermionic gaugings with parameters Ξ_u, while the exceptional E_r–gaugings are not. With this choice of Fermionic gaugings $9 - 3 = 6$ gauge bundle directions are left over, exactly matching the number in the non–compact resolution of the non–torsion orbifold model.

In target space this gauge background does not correspond to the standard embedding as there are no fermionic gaugings associated to the exceptional E_r–gaugings. Neither can this background be interpreted as line bundles only because of the presence of the chiral multiplets Ψ_u, Ψ'_u that enforce constraints on the bundle degrees of freedom as well as the fermionic gaugings Ξ_u.

Given the charges of Table 7.10 the following superpotential can be written down:

$$\begin{aligned} P_{\text{min res bundle}} &= \sum_{u=1}^{3} \Psi_u \Big(2\kappa_u \, \Phi_{u\,1} \prod_{r\neq u} \Phi'_r \, \Lambda_{u\,1} + \kappa_u \, \Phi^2_{u\,1} \prod_{r\neq s\neq u} \Phi'_r \Lambda'_s + 2\,\Phi_{u\,2}\Lambda_{u\,2} + 2\,\Phi_{u\,3}\Lambda_{u\,3} \Big) \\ &\quad + \sum_{u=1}^{3} \Psi'_u \Big(2\,\Phi_{u\,1} \prod_{r\neq u} \Phi'_r \, \Lambda_{u\,1} + \Phi^2_{u\,1} \prod_{r\neq s\neq u} \Phi'_r \Lambda'_s + 2\,\Phi_{u\,2}\Lambda_{u\,2} + 2\,\Phi_{u\,4}\Lambda_{u\,4} \Big) \ . \end{aligned} \tag{7.84}$$

This specific form of a general expression for this superpotential is inspired by the standard embedding following (7.33).

In the model under investigation only the R_u–gaugings are associated to fermionic gauge transformations, hence the only non–zero fermionic gauge transformations are:

$$\delta\Lambda_{u\,x} = \tfrac{1}{2}\,\Phi_{u\,x}\,\Xi_u \ , \qquad \delta\Gamma_u = -\Psi_u\,\Xi_u \ , \qquad \delta\Gamma'_u = -\Psi'_u\,\Xi_u \ . \tag{7.85}$$

The specific form, given here, is obtained by requiring that the fermionic gauges are on the (2,2)–locus. In this case is follows automatically that (7.73) and (7.84) combined are inert under these fermionic transformations.

Superfield	$\Lambda^{\times}_{1x}$	$\Lambda^{\times}_{2y}$	$\Lambda^{\times}_{3z}$	Ψ_1	Ψ'_1	Ψ_2	Ψ'_2	Ψ_3	Ψ'_3	${\Lambda^{\times}_1}'$	${\Lambda^{\times}_2}'$	${\Lambda^{\times}_3}'$	Λ_n
U(1) charge	λ_{1x}	λ_{2y}	λ_{3z}	ψ_1	ψ'_1	ψ_2	ψ'_2	ψ_3	ψ'_3	λ'_1	λ'_2	λ'_3	λ_n
R_1	$\frac{1}{2}$	0	0	-1	-1	0	0	0	0	0	0	0	0
R_2	0	$\frac{1}{2}$	0	0	0	-1	-1	0	0	0	0	0	0
R_3	0	0	$\frac{1}{2}$	0	0	0	0	-1	-1	0	0	0	0
E_1	0	$-\frac{1}{2}\delta_{y1}$	$-\frac{1}{2}\delta_{z1}$	0	0	0	0	0	0	$+1$	0	0	0
E_2	$-\frac{1}{2}\delta_{x1}$	0	$-\frac{1}{2}\delta_{z1}$	0	0	0	0	0	0	0	$+1$	0	0
E_3	$-\frac{1}{2}\delta_{x1}$	$-\frac{1}{2}\delta_{y1}$	0	0	0	0	0	0	0	0	0	$+1$	0

Table 7.11: A choice for a charge table of the superfields that determine a gauge bundle on the minimal full resolution of $T^6/\mathbb{Z}_2 \times \mathbb{Z}_2$ with torsion.

This construction leads to a regular bundle as for each of the three fermionic gaugings in (7.85) not all coefficients vanish simultaneously. The same goes for the six constraints coming from (7.84). It is straightforward to check this for all coordinate patches given in Table 7.9 for all four fully resolved phases of this GLSM. This should not come as a surprise as the fermionic gaugings (7.85) and the bundle superpotential (7.84) are precisely those that are dictated by the (2,2) locus, see Subsection 7.4.4.

7.6.6 Gauge background on the minimal full resolution of the torsional orbifold

In section 7.3.3 it was explained that the twisted states that survive the orbifold projections are precisely opposite when torsion is switched on to when it is absent. Since the shifted momenta of the twisted states without oscillators dictated the exceptional E_1, E_2, E_3–charges in the GLSM of the Fermi multiplet Λ. Hence the charge Table 7.8, which determines the geometry, remains unchanged when torsion is switched on, but the charge table for the vector bundle is modified to Table 7.11: the R_i–charges remain the same while the E_r–charges are all sign–flipped as compared to those in Table 7.10.

The flipping of the E_r–gauge charges has various consequences. First of all, the fermionic gauge transformations (7.85) are not gauge covariant any more. This is easily alleviated by inserting appropriate factors of Φ'_r in the first column of fermionic gauge transformations of Λ_{u1}:

$$\delta\Lambda^{\times}_{u\,1} = \tfrac{1}{2}\prod_{r\neq u}\Phi'_r\,\Phi_{u\,1}\,\Xi_u\ , \qquad \delta\Lambda^{\times}_{u\,x} = \tfrac{1}{2}\,\Phi_{u\,x}\,\Xi_u\ , \qquad \delta\Gamma_u = -\Psi_u\,\Xi_u\ , \qquad \delta\Gamma'_u = -\Psi'_u\,\Xi_u\ , \tag{7.86}$$

for $x \neq 1$. Secondly, the bundle superpotential (7.84) has to be modified to

$$\begin{aligned} P_{\text{min res bundle}} &= \sum_{u=1}^{3} \Psi_u \Big(2\kappa_u \, \Phi_{u\,1} \, \Lambda^{\times}_{u\,1} + \kappa_u \, \Phi^2_{u\,1} \prod_{r\neq s\neq u} \Phi'_r \Phi'^2_s \Lambda^{\times\,\prime}_s + 2\,\Phi_{u\,2} \Lambda^{\times}_{u\,2} + 2\,\Phi_{u\,3} \Lambda^{\times}_{u\,3} \Big) \\ &+ \sum_{u=1}^{3} \Psi'_u \Big(2\,\Phi_{u\,1}\,\Lambda^{\times}_{u\,1} + \Phi^2_{u\,1} \prod_{r\neq s\neq u} \Phi'_r \Phi'^2_s \Lambda^{\times\,\prime}_s + 2\,\Phi_{u\,2} \Lambda^{\times}_{u\,2} + 2\,\Phi_{u\,4} \Lambda^{\times}_{u\,4} \Big) \end{aligned} \tag{7.87}$$

by making the following replacements

$$\Lambda_{u1} \to \Phi'^{-1}_r \Phi'^{-1}_s \Lambda^{\times}_{u1} \ , \quad \Lambda_{ux} \to \Lambda^{\times}_{ux} \ , \quad \Lambda'_r \to \Phi'^2_r \Lambda^{\times\,\prime}_r \ , \tag{7.88}$$

with $x \neq 1$ and $r \neq s \neq u$, to ensure that it is gauge invariant again. With these modifications of the fermionic gauge transformations and the bundle superpotential, it is not difficult to see that the full superpotential including the part for the geometry (7.72) is invariant under the fermionic gauge transformations.

The replacements (7.88) are the same as the field redefinitions (7.60) in the non–compact case with the chiral superfields Ω_r given by the ones in the orbifold case (O) of Table 7.5. It should be stressed that in the present case the replacements (7.88) in the bundle superpotential apply to the GLSM theory as a whole globally, not just to a particular (coordinate patch within a) phase of the theory. Moreover, it is unique in the sense that other factors, that would have the same charges (like the other combinations in Table 7.5), would always involve some powers of Ψ_u or Ψ'_u, but that is forbidden because they are only allowed to appear linearly in the superpotential because of the R–symmetry, as was emphasised below (7.29).

Mixed anomalies and worldsheet Green–Schwarz mechanism

The flipped E_r–gauge charges in Table 7.11 is irrelevant for most anomalies which still vanish identically as can be verified using (7.36) through (7.38). Only mixed $R_u E_{r\neq u}$–anomalies are now non–zero:

$$\mathcal{A}_{ur} = \mathcal{A}_{ru} = \tfrac{1}{2} \cdot \tfrac{1}{2} - \tfrac{1}{2} \cdot (-\tfrac{1}{2}) = \tfrac{1}{2} \ , \tag{7.89}$$

$u \neq r$. Hence, contrary to the GLSMs associated to the non–compact orbifold models, the GLSMs associated to the compact orbifold models without or with torsion are genuinely physically distinct.

These mixed anomalies need to be cancelled by field dependent FI–terms of the form

$$W_{\text{FI anom}} = \frac{1}{4\pi} \sum_{u,r} \frac{c_{ru}}{2} \, \log(N^r) \, F^u + \frac{1}{4\pi} \sum_{u,r} \frac{1 - c_{ru}}{2} \, \log(N^u) \, F^r \ , \tag{7.90}$$

where the composite N^r and N^u have negative unit charge under the R_u– and E_r–gaugings, respectively, and all other gauge charges zero. The arbitrary coefficients c_{ru} arise as it is possible by counter terms to shift two dimensional mixed anomalies around. The choice $c_{ru} = 1/2$ would treat all mixed anomalies symmetrically. (See e.g. ref. [123] for a more extensive discussion.) The composite chiral superfields N^u and N^r can be realised as rational functions of (fractional)

powers of the chiral superfields. They may be expressed as

$$N^r = \Phi'_r \ , \quad N^u = \sum_{x,y\neq 1} n_{uxy}\, \Phi_{ux}^{-1}\Phi_{uy}^{-1} + n_{u11}\Phi_{u1}^{-2}\prod_{r\neq u}\Phi_r'^{-1} + \sum_{x\neq 1} n_{u1x}\, \Phi_{u1}^{-1}\Phi_{ux}^{-1}\prod_{r\neq u}\Phi_r'^{-\frac{1}{2}} \ , \tag{7.91}$$

with some generically non–zero parameters n_{uxy}, n_{u11} and n_{u1x}. Since the chiral superfields Ψ_u and Ψ'_u cannot appear here as they would break R–symmetry, the possible forms in these expressions are restricted.

The superfield dependent FI–terms (7.90) are defined on the level of the definition of the model and are singular independently of how the coefficients c_{ru} and n_{uxy}, n_{u11} and n_{u1x} are chosen, hence they signify the presence of NS5–branes [123, 124]. The interpretation of the coefficients c_{ru} is not so clear. However, if they are all set to zero: $c_{ru} = 1$, then the expressions of N^u become irrelevant. The NS5–branes are then located on the resolved exceptional cycles E_r and they would disappear inside the orbifold singularities in the blow down limit. Maybe other values of c_{ru} could be interpreted that the NS5–branes are moved around the resolved orbifold geometry and for $c_{ru} = 0$ they are pushed fully off the resolved singularities onto the two–torus cycles. This seems to signify that the NS5–branes can move around on the resolved geometry without losing their influx effects on the worldsheet. This interpretation may be more transparent in another parameterisation

$$W_{\text{FI anom}} = \frac{1}{8\pi}\sum_{u,r} c_{ru}\log\Phi'_r F^u - \frac{1}{4\pi}\sum_{u,r}\left[\sum_{x\neq 1} c_{uxr}\log\Phi_{u\,x} + c_{u1r}\Big(\log\Phi_{u\,1} - \sum_{r'\neq u}\tfrac{1}{2}\log\Phi'_{r'}\Big)\right]F^r \tag{7.92}$$

of (7.90), since the coefficients determining the position of the NS5–branes are subject to the constraint $c_{ru} + \sum_x c_{uxr} = 1$.

Comparing the pair of torsion related GLSMs

Just like in the non–compact case, it is instructive to compare the resoluton GLSMs of the orbifold theories without and with torsion with each other by working in the same superfield basis. By interpreting (7.88) as a superfield redefinition (7.61), but now both R_u– and E_u–transformations are involved, the anomaly matrix $\mathcal{A}$ extends to

$$\mathcal{A} = \begin{pmatrix} \frac{1}{4} & 0 & 0 & 0 & \frac{1}{4} & \frac{1}{4} \\ 0 & \frac{1}{4} & 0 & \frac{1}{4} & 0 & \frac{1}{4} \\ 0 & 0 & \frac{1}{4} & \frac{1}{4} & \frac{1}{4} & 0 \\ 0 & \frac{1}{4} & \frac{1}{4} & \frac{3}{2} & \frac{1}{4} & \frac{1}{4} \\ \frac{1}{4} & 0 & \frac{1}{4} & \frac{1}{4} & \frac{3}{2} & \frac{1}{4} \\ \frac{1}{4} & \frac{1}{4} & 0 & \frac{1}{4} & \frac{1}{4} & \frac{3}{2} \end{pmatrix} . \tag{7.93}$$

Notice that the lower 3×3–block is identical to (7.62). Since in the replacements (7.88) only the superfields Φ'_r feature, the superfield redefintion anomalies reads

$$W_{\text{field redef anom}} = -\frac{1}{2\pi}\left\{\frac{1}{4}\sum_{u\neq r}\log\Phi'_r\,F^u + \frac{3}{2}\sum_r \log\Phi'_r\,F^r + \frac{1}{4}\sum_{r'\neq r}\log\Phi'_r\,F^{r'}\right\}. \tag{7.94}$$

The first contributions coincides with the general expression (7.90) provided that $c_{ur} = 0$ and $N^r = \Phi'_r$, hence they cancel each other exactly. The latter two contributions were also obtained in the non–compact situation (7.61). Hence, the analysis performed in Subsection (7.5.2) can be repeated here as well. In particular in the orbifold phase, that analysis recovers the discrete torsion phases.

7.7 Conclusions

Discrete torsion within the $\mathbb{Z}_2\times\mathbb{Z}_2$ orbifolds correspond to particular additional phases between the sum of partition functions of different sectors corresponding to different boundary conditions on the worldsheet torus. Smooth geometries are typically described by NLSMs which cannot be exactly quantised and the path integral cannot be represented as a sum over similar sectors as the orbifold theory. It is therefore unclear how to include effects of discrete torsion for smooth geometries. The main aim of this chapter was to understand where discrete torsion goes when orbifolds have been resolved to fully smooth geometries. This question was addressed both for resolutions of the non–compact orbifold $\mathbb{C}^3/\mathbb{Z}_2\times\mathbb{Z}_2$ as well as the compact $T^6/\mathbb{Z}_2\times\mathbb{Z}_2$ orbifold with Hodge numbers $(51,3)$ to understand both local and global aspects.

GLSMs were chosen as the framework for this investigation, as they can both make contact with the orbifolds as well as with fully resolved smooth geometries within the same description. From an effective field theory point of view orbifold resolutions correspond to giving VEVs to twisted states defining the blowup modes. Unless very particular blowup modes are selected, this leads to $(0,2)$ compactifications in which the gauge backgrounds are not dictated by the standard embedding. Therefore, in this work $(0,2)$ GLSMs were used for the interpolation between singular orbifolds and smooth compactifications.

The non–compact resolution GLSM of the $\mathbb{C}^3/\mathbb{Z}_2\times\mathbb{Z}_2$ geometry had already given in the literature, the same goes for the resulting line bundle backgrounds obtained by using non–oscillator blowup modes on the three $\mathbb{C}^2/\mathbb{Z}_2$ singularities. The GLSM gauge charges of the chiral Fermi multiplets under the resulting three exceptional gauge symmetries are given as the shifted left–moving momenta of these blowup modes. The effect of discrete torsion on the orbifold is that the twisted states with the opposite left–moving shifted momenta survive the orbifold projections. Consequently, the chiral Fermi multiplets in resolution GLSM for the torsional orbifold has the opposite worldsheet gauge charges as the non–torsional case. The GLSM associated to the torsional orbifold is equally well defined as the non–torsional model in the sense that all (gauge) anomalies vanish. In many respects the two models look identical. However, if one wants to express the physics of the GLSM associated with the torsional orbifold in terms of the superfield basis of the non–torsional GLSM, one has to perform anomalous superfield redefinitions. Since, these superfield redefinitions have to be well defined in each patch where they are performed, the expression of the anomaly is harmless within the smooth resolution phases. But in the orbifold phase this anomaly turns out not to be invariant under

residual discrete $\mathbb{Z}_2 \times \mathbb{Z}_2$ gauge transformations, precisely reproducing the torsion phases of the orbifold theory.

The story for the compact case is more involved. GLSMs for resolutions of the $T^6/\mathbb{Z}_2 \times \mathbb{Z}_2$ orbifold have not explicitly appeared in the literature. Moreover, GLSMs for other compact orbifold resolutions have only been studied in the $(2,2)$ context. Therefore, before the question about discrete torsion on compact orbifold resolutions could be addressed, first resolution GLSMs for $T^6/\mathbb{Z}_2 \times \mathbb{Z}_2$ had to be constructed. Contrary to the existing literature on compact orbifold resolutions, this was done immediately in the $(0,2)$ language. The simplest version of such a GLSM involves six gaugings on the worldsheet: three to define modified Weierstrass models to describe the underlying two–tori of the T^6 and three exceptional gaugings associated with the blowup process. In order to make comparisons with the non–compact situations most transparant, the same blowup modes were chosen as in the non–compact case, i.e. non–oscillatory twisted states. To pass all consistency conditions this resulted in a more complicated bundle that shares both features of line bundles on the resolved fixed two–tori as well as the standard embedding on the underlying two–tori of the T^6.

The resolution GLSM of the $T^6/\mathbb{Z}_2 \times \mathbb{Z}_2$ with discrete torsion was obtained in a similar fashion as its non–compact analog: the exceptional gauge charges were flipped, while the other three gauge charges remained unchanged. As a consequence the resolution GLSM associated with the torsional orbifold suffers from mixed gauge anomalies. These anomalies can be cancelled by superfield dependent FI–terms in the GLSM globally. This signifies that the target space geometry has torsion in the sense that the three–form H–flux is non–zero. Moreover, given the GLSM chiral superfield content, the field dependent FI–terms need to involve logs of chiral superfields. As argued in the past, this signals that there are NS5–branes in the system. The structure of these logs can be taken such that these NS5–branes are located at the resolved exceptional cycles. In the orbifold limit they would disappear inside these singularities.

It is striking to see the differences of the effect of discrete torsion in the resolution process for non–compact and compact orbifolds. In the non–compact case apart from a physically irrelevant flip of charge conjugated states the non–torsional and torsional orbifold resolutions are to a large extent indistinguishable: only the relative signs of the gauge charges of the chiral and chiral Fermi multiplets distinguish them. In the compact case the GLSM associated to the torsional orbifold is really physically different from the non–torsional one as the mixed gauge anomalies and the related NS5–branes signify. These differences may be explained by realising that in the non–compact case the effect of flux can be pushed off to infinity while in the compact case this is impossible.

Outlook

The work presented here can be extended in a number of ways.

First of all, it would be interesting if it is possible by other means to show that the emerged picture that NS5–branes are located at the resolved singularities of the resolved torsional orbifold can be corroborate. And it would be interesting to confirm the interpretation of the coefficients that allow to shift mixed gauge anomalies around as moving around the NS5–branes of the resolved geometry. In addition, it would be interesting to investigate what the geometrical consequences are of the back reaction induced by the log–dependent FI–terms.

In this chapter the focus was on only very simple bundles (line bundles combined with bundles that are on the (2,2) locus, hence closely related to the standard embedding). However,

the procedures used here could be applied to other gauge backgrounds as well. In particular, by choosing other blowup modes, for example, those with oscillator excitations, see e.g. [112].

Moreover, in this work only the discrete torsion between two orbifold twists was considered. For possible applications of the spinor–vector duality on smooth geometries other generalised discrete torsion phases would be of interest. First attempts in this direction were performed using effective field theory techniques in [2]. Such phases are between orbifold twists and torus translations and associated Wilson lines or among two different torus translations. This requires that within the GLSM distinctions between the various (resolved) fixed tori can be made. Clearly, this is possible in the maximal full resolution model, which treats all 48 (resolved) fixed tori independently, or in certain full resolution GLSM that have a certain number of additional gauging so that at least some fixed two–tori in certain directions can be distinguished. The effect of the Wilson lines would then be that the exceptional GLSM charges (dictated by the shifted twisted state momenta) are not the same at the different fixed tori. Then, just like in the models considered here, the effect of generalised discrete torsion is that particular states are projected out or in, leading to different charge assignments for the Fermi multiplets. Presumably, the consequences of these differences could then be analysed in much the same fashion as done in the current work.

Chapter 8

Conclusion and Outlook

We think that the work of the previous Chapters show promising results for the extension of SVD to smooth compactifications. The program is yet to be completed and extended to the four dimensional case. This fact is (to some extent) not totally surprising due to the great difference among the formalisms it should deal with, i.e. free fermions, orbifolds, line bundle resolutions and GLSMs.
However this can be also interpreted as an advantage of the program; as some direction tangent to it can produce new results which are interesting by themselves. This is what is shown in Chapters 6 and 7 which constitute some progress in the study of the resolutions and GLSMs of the $T^6/\mathbb{Z}_2 \times \mathbb{Z}_2$ and especially for one possible implementation of discrete torsion in smooth compactifications. In fact some subtleties of the models discussed can lead to even further connections and applications. In the end of the GLSM Chapter it was already pointed out that it would be interesting to have further confirmation of our interpretation of the coefficients in equation (7.90) as moving around the NS5-branes of the resolved geometry or the consequences of the back reaction induced by the log–dependent FI–terms.
However, the main connection to SVD duality, also noted at the end of Chapter 7 is the possibility of develop a GLSM torsional model which includes a torsion between the orbifold twist and a suitable Wilson line.
The implementation of this should follow a similar logic that the process explained in Chapter 7, with a concrete superfield redefinition whose effects were unavoidable in the compact case. A possible complication is that, as we need a Wilson line (in some of the (orbifolded) tori), the model will be more complicated than the minimal full resolution one as some singularity should be trated distinctly than the others.
In any case we can always try to implement the line bundle resolved model to the $4D$ case as we did in Chapter 5 for the $5D$ case. We will have the same issue (i.e. different vector bundle at least in the appropriate singularities) but in principle it can be done. However, there are some theoretical reasons why the GLSM formalism is preferable to the "line bundle" one in some situations, which probably include the implementation of SVD in 4D (once whe have successfully implemented a discrete torsion phase (Chapter 7)). The main one is that GLSM models are in some sense closer to a real string theory (rather than an "mere" effective theory lying in the Swampland) than line bundle resolutions, as they are formulated as proper worldsheet theories and subject to a more robust consistency "stringy" conditions. There are also some non-perturbative effects coming from the GLSM (see the discussion about $NS5$

branes) to which the line bundle models can be blind at some situations.
In any case, the promising results from the previous Chapter and the ongoing work make us expect new insight about spinor-vector duality in the short time.

Appendix A

Appendix

A.1 Elements of (0, 2) sigma models

A.1.1 (0, 2) superspace

The $(0,2)$ superspace is spanned by a complex fermionic variable θ^+ and its conjugate $\bar{\theta}^+$ of positive chiralilty in two dimensions and worldsheet coordinates $\sigma = \frac{1}{\sqrt{2}}(\sigma_1 + \sigma_0)$ and $\bar{\sigma} = \frac{1}{\sqrt{2}}(\sigma_1 - \sigma_0)$. Using their derivatives denoted by $\partial_+, \bar{\partial}_+, \partial = \frac{1}{\sqrt{2}}(\partial_1 + \partial_0)$ and $\bar{\partial} = \frac{1}{\sqrt{2}}(\partial_1 - \partial_0)$, respectively, super covariant derivates D_+ and $\overline{D}_+ = -(D_+)^\dagger$ can be defined as

$$D_+ = \partial_+ - i\bar{\theta}^+ \partial \ , \qquad \overline{D}_+ = \bar{\partial}_+ - i\theta^+ \partial \ , \qquad \left\{\overline{D}_+, D_+\right\} = -2i\,\partial \ . \tag{A.1}$$

These super covariant derivatives anti–commute with the supercharges

$$Q_+ = \partial_+ + i\bar{\theta}^+ \partial \ , \qquad \overline{Q}_+ = \bar{\partial}_+ + i\theta^+ \partial \ . \tag{A.2}$$

The supercharges generate the $(0,2)$ super algebra

$$\left\{\overline{Q}_+, Q_+\right\} = 2\,P \ , \tag{A.3}$$

where $P = i\,\partial$ is the right moving momentum generator.

A.1.2 (0, 2) superfields

A general $(0,2)$ superfield G is a complex function of $(0,2)$ superspace on which supersymmetry act as

$$\delta_\epsilon G = (\epsilon^+ Q_+ + \bar{\epsilon}^+ \overline{Q}_+) G \ . \tag{A.4}$$

Consequently sums, products and super covariant derivatives of superfields are again superfields.

The components of a superfield are defined by taking a number of super covariant derivates and then set all θ^+ and $\bar{\theta}^+$ to zero which is denoted as $|_+$. A superfield G is called bosonic (fermionic) if its lowest component $G|_+$ is bosonic (fermionic).

There are four fundamental multiplets of $(0,2)$ supersymmetry: the chiral multiplet, the chiral Fermi multiplet, the vector multiplet and the Fermi gauge multiplet:

Chiral multiplet

A chiral multiplet Φ and its conjugate $\overline{\Phi}$ are bosonic superfields defined by the chirality constraints:

$$\overline{D}_+\Phi = 0 \ , \qquad D_+\overline{\Phi} = 0 \ . \tag{A.5}$$

Their components,

$$z = \Phi|_+ \ , \quad \phi = \tfrac{1}{\sqrt{2}} D_+\Phi|_+ \ , \qquad \bar{z} = \overline{\Phi}|_+ \ , \quad \bar{\phi} = -\tfrac{1}{\sqrt{2}} D_+\overline{\Phi}|_+ \ , \tag{A.6}$$

are a complex scalar z, a negative chiral (right–moving) complex spinor ϕ and their conjugates $\bar{z}$ and $\bar{\phi}$.

Chiral Fermi multiplet

A chiral Fermi multiplet Λ and its conjugate $\overline{\Lambda}$ are fermionic superfields defined by the chirality constraints:

$$\overline{D}_+\Lambda = 0 \ , \qquad D_+\overline{\Lambda} = 0 \ . \tag{A.7}$$

Their components,

$$\lambda = \Lambda|_+ \ , \quad h = \tfrac{1}{\sqrt{2}} D_+\Lambda|_+ \ , \qquad \bar{\lambda} = -\overline{\Lambda}|_+ \ , \quad \bar{h} = \tfrac{1}{\sqrt{2}} \overline{D}_+\overline{\Lambda}|_+ \ , \tag{A.8}$$

are a positive chiral (left–moving) complex spinor λ, a complex scalar h and their conjugates $\bar{\lambda}$ and $\bar{h}$.

Vector multiplet

The vector multiplet (V, A) consists of two real bosonic superfields V and A subject to a bosonic super gauge transformation

$$V \to V - \tfrac{1}{2}\big(\Theta + \overline{\Theta}\big) \ , \qquad A \to A + \tfrac{i}{2}\bar{\partial}\big(\Theta - \overline{\Theta}\big) \ , \tag{A.9}$$

with a chiral superfield Θ gauge parameter and its conjugate $\overline{\Theta}$. (Non–Abelian gauge superfields are not considered in this work.) Their components are

$$\Theta|_+ = \theta = \tfrac{1}{2}\, a + i\, \alpha \ , \qquad \tfrac{1}{\sqrt{2}} D_+\Theta|_+ = \zeta \ , \qquad \overline{\Theta}|_+ = \theta = \tfrac{1}{2}\, a - i\, \alpha \ , \qquad -\tfrac{1}{\sqrt{2}} D_+\overline{\Theta}|_+ = \bar{\zeta} \ , \tag{A.10}$$

where a and α are real fields. The two dimensional gauge field components are identified as

$$A_\sigma = \tfrac{1}{2}\big[\,\overline{D}_+, D_+\big]V|_+ \ , \quad A_{\bar{\sigma}} = A|_+ \ , \tag{A.11}$$

which transform as

$$A_\sigma \to A_\sigma - \partial\alpha \ , \qquad A_{\bar{\sigma}} \to A_{\bar{\sigma}} - \bar{\partial}\alpha \ . \tag{A.12}$$

The super field strengths

$$F = -\tfrac{1}{2}\overline{D}_+\big(A - i\bar\partial V\big)\ , \qquad \overline{F} = \tfrac{1}{2}D_+\big(A + i\bar\partial V\big)\ , \tag{A.13}$$

are super gauge invariant chiral Fermi multiplets, since by construction $\overline{D}_+F = D_+\overline{F} = 0$. Consequently, their components

$$F|_+ = \tfrac{1}{\sqrt{2}}\varphi\ , \quad \overline{F}|_+ = \tfrac{1}{\sqrt{2}}\bar\varphi\ , \quad D_+F|_+ = \tfrac{1}{2}\big(D + i\,F_{\sigma\bar\sigma}\big)\ , \quad \overline{D}_+\overline{F}|_+ = \tfrac{1}{2}\big(D - i\,F_{\sigma\bar\sigma}\big)\ , \tag{A.14}$$

are identical in any gauge. In particular, $D = \frac{1}{2}\,[\overline{D}_+, D_+]A|_+ - \partial\bar\partial V|_+$ and $F_{\sigma\bar\sigma} = F_{01}$.

The super gauge transformation can be used to set some of the components of the vector multiplet to zero: $V|_+ = D_+V|_+ = \overline{D}_+V|_+ = 0$. In this so–called Wess–Zumino (WZ) gauge all quadratic and higher powers of V vanish. Since V is a real superfield the WZ gauge does not fix the super gauge transformations completely, there is a residual gauge transformation with $\Theta = i\alpha$.

Fermi gauge multiplet

A Fermi gauge multiplet Σ and its conjugate $\overline{\Sigma}$ are complex fermionic superfields subject to fermionic super gauge transformations

$$\Sigma \to \Sigma - \Xi\ , \qquad \overline{\Sigma} \to \overline{\Sigma} - \overline{\Xi}\ , \tag{A.15}$$

where Ξ is a Fermi multiplet and $\overline{\Xi}$ its conjugate. The associated super field strength and its conjugate

$$= \overline{D}_+\Sigma\ , \qquad = D_+\overline{\Sigma}\ , \tag{A.16}$$

are inert under the fermionic gauge transformations. Their components are

$$s = \tfrac{1}{\sqrt{2}}|_+\ , \qquad \bar s = \tfrac{1}{\sqrt{2}}|_+\ , \qquad \chi = \tfrac{1}{2}D_+|_+\ , \qquad \bar\chi = \tfrac{1}{2}\overline{D}_+|_+\ . \tag{A.17}$$

Using the fermionic gauge transformations, the following components of the Fermi gauge multiplet Σ are set to zero in the WZ–gauge: $\Sigma|_+ = D_+\Sigma|_+ = 0$.

A.1.3 Super conformal transformations and scaling dimensions

Real conformal transformations of the worldsheet coordinates

$$\sigma \to f(\sigma)\ , \qquad \bar\sigma \to \bar f(\bar\sigma)\ , \tag{A.18}$$

are characterized by two real functions $f(\sigma)$ of σ only and $\bar f(\bar\sigma)$ of $\bar\sigma$ only. Consequently, their differential and derivatives transform

$$\mathrm{d}\sigma \to \omega^{-1}\,\mathrm{d}\sigma \qquad \mathrm{d}\bar\sigma \to \bar\omega^{-1}\,\mathrm{d}\bar\sigma\ , \qquad \partial \to \omega\,\partial\ , \qquad \bar\partial \to \bar\omega\,\bar\partial\ , \tag{A.19}$$

where $\omega = (\partial f)^{-1}$ and $\bar\omega = (\bar\partial \bar f)^{-1}$. Moreover, since θ^+ is a complex parameter, there is a phase transformation, often dubbed R–symmetry,

$$\theta^+ \to e^{i\kappa}\,\theta^+\ , \qquad \bar\theta^+ \to e^{-i\kappa}\,\bar\theta^+\ , \tag{A.20}$$

with $\kappa \in \mathbb{R}$. Requiring that the algebra of the super covariant derivatives transforms consistently with this implies:

$$D_+ \to \omega^{\frac{1}{2}} e^{-i\kappa} D_+ \ , \qquad \overline{D}_+ \to \omega^{\frac{1}{2}} e^{+i\kappa} \overline{D}_+ \ . \tag{A.21}$$

The left– and right–Weyl dimensions and the R–charge $(\mathcal{L}, \mathcal{R}, \mathrm{R})$ (often collectively referred to as Weyl charges) of a general complex superfield G, defined as

$$G \to \bar{\omega}^{\mathcal{L}} \, \omega^{\mathcal{R}} \, e^{i\mathrm{R}\kappa} \, G \tag{A.22}$$

identify how it responds to these conformal transformations. Real superfields are necessarily inert under the R–symmetry. The Weyl and R–charges of the superfields used in this work can be found in Table 7.2.

A.1.4 Scale invariant matter actions

Scale invariant superspace integrals

Any real bosonic superfield R can be used to form a supersymmetric invariant by an integral over the full superspace:

$$S_{\text{full superspace}} = \int \mathrm{d}^2\sigma \mathrm{d}^2\theta^+ \, R = \int \mathrm{d}^2\sigma \, \overline{D}_+ D_+ R|_+ \ . \tag{A.23}$$

This action is gauge invariant if R caries no gauge charges and scale invariant if it has Weyl and R–charges $(+1, 0, 0)$.

Any chiral Fermi superfield Ω can be used to form a supersymmetric invariant by an integral over the chiral superspace:

$$S_{\text{chiral superspace}} = \int \mathrm{d}^2\sigma \mathrm{d}\theta^+ \, \Omega + \int \mathrm{d}^2\sigma \mathrm{d}\bar{\theta}^+ \, \overline{\Omega} = \int \mathrm{d}^2\sigma \, \big[D_+\Omega + \overline{D}_+\overline{\Omega} \big]|_+ \ . \tag{A.24}$$

This is gauge invariant if Ω carries no gauge charges and conformally invariant if it has Weyl and R–charges $(+1, +\frac{1}{2}, +1)$.

Chiral superfield action

The gauge interactions of chiral superfields Φ^a and their conjugates $\overline{\Phi}^{\underline{a}}$ with Abelian vector multiplets $(V, A)_i$ are parameterized by the gauge charges $(q^i)_a$. In order to reduce the abundance of indices, interpret $q \cdot V$ as the diagonal matrix with on the diagonal $\sum_i (q^i)_a V_i$ and interpret Φ as standing and $\overline{\Phi}$ as lying vectors of N_Φ chiral superfields and their conjugates, respectively. Their super gauge transformations read

$$\overline{\Phi} \to \overline{\Phi} \, e^{q \cdot \overline{\Theta}} \ , \qquad \Phi \to e^{q \cdot \Theta} \, \Phi \ . \tag{A.25}$$

Their super gauge invariant kinetic action is given by

$$S_{\text{chiral}} = \frac{i}{4} \int \mathrm{d}^2\sigma \mathrm{d}^2\theta^+ \left[\overline{\Phi} \, e^{2q \cdot V} \overline{\mathcal{D}} \Phi - \overline{\mathcal{D}} \, \overline{\Phi} \, e^{2q \cdot V} \Phi \right] \ , \tag{A.26}$$

in terms of the super gauge covariant derivatives of the chiral superfields and their conjugates

$$\overline{\mathcal{D}} \Phi = \bar{\partial} \Phi + q \cdot \big(\bar{\partial} V + iA \big) \Phi \ , \qquad \overline{\mathcal{D}} \overline{\Phi} = \bar{\partial} \, \overline{\Phi} + \overline{\Phi} \, q \cdot \big(\bar{\partial} V - iA \big) \ . \tag{A.27}$$

Chiral Fermi superfield action

The gauge and Fermi gauge interactions of the chiral Fermi superfields Λ^m and their conjugates $\overline{\Lambda^m}$ with the Fermi gauge multiplets are parameterised by the gauge charges $(Q^i)_m$ and holomorphic functions $U^{mI}(\Phi)$. The super gauge and super fermionic gauge transformations of them read

$$\overline{\Lambda} \to \left(\overline{\Lambda} + \overline{\Xi}\cdot\overline{U}(\overline{\Phi})\right) e^{Q\cdot\overline{\Theta}} \ , \qquad \Lambda \to e^{Q\cdot\Theta}\left(\Lambda + U(\Phi)\cdot\Xi\right) \ . \tag{A.28}$$

Here the notation $\big(U(\Phi)\cdot\Xi\big)^m = U^{mI}(\Phi)\,\Xi_I$ is employed. The gauge charges of the holomorphic functions $U^{mI}(\Phi)$ are $(Q^I)_m$ as well. Their super gauge invariant kinetic action is given by

$$S_{\text{Fermi}} = -\frac{1}{2}\int \mathrm{d}^2\sigma\mathrm{d}^2\theta^+ \left(\overline{\Lambda} + \overline{\Sigma}\cdot\overline{U}(\overline{\Phi})\right) e^{2Q\cdot V}\left(\Lambda + U(\Phi)\cdot\Sigma\right) \ . \tag{A.29}$$

FI actions

The Fayet–Ililopoulos (FI) action is given by the chiral superspace integral

$$S_{\text{FI}} = \int \mathrm{d}^2\sigma\mathrm{d}\theta^+ \, W_{\text{FI}} + \text{c.c.} \ , \quad W_{\text{FI}} = \rho(\Phi)\cdot F + (\kappa(\Phi)\cdot)\Lambda \ , \tag{A.30}$$

where $(\kappa(\Phi)\cdot)\Lambda = \kappa_{Im}(\Phi)_I\Lambda^m$ employing holomorphic functions $\rho_i(\Phi)$ and $\kappa_{Im}(\Phi)$ of the chiral superfields Φ^a. The lowest components of $\rho(\Phi)$,

$$\rho_i|_+ = \tfrac{1}{2}\, r_i + i\,\beta_i \ , \qquad \bar{\rho}_i|_+ = \tfrac{1}{2}\, r_i - i\,\beta_i \ , \tag{A.31}$$

couple to the auxiliary field D^i and the gauge field strength F^i_{01}, respectively:

$$\int \mathrm{d}\theta^+ \, \rho(\Phi)\cdot F + \int \mathrm{d}\bar{\theta}^+ \, \bar{\rho}(\overline{\Phi})\cdot\overline{F} \supset \tfrac{1}{2}\, r\cdot D - \beta\cdot F_{01} \ , \tag{A.32}$$

where $\supset$ indicates that the expression on the left includes terms given on the right.

Only when $\rho_i(\Phi)$ are super gauge invariant and $\kappa_{IA}(\Phi)$ carry the opposite charges as Λ^a, the FI action is gauge invariant. This action is only invariant under fermionic gauge transformation if

$$\kappa_{Im}(\Phi)U^{mJ} = 0 \ , \tag{A.33}$$

for all I, J. A worldsheet variant of the Green–Schwarz mechanism involves chiral superfield functions $\rho_i(\Phi)$ that transforms as shifts under super gauge transformations.

A.1.5 None scale invariant actions

In GLSMs also actions are used that are not scale invariant. They involve parameters of mass dimension one or two in two dimensions. For simplicity all these parameters are assumed to be equal to m or $|m|^2$, depending on whether these action are chiral or full superspace integrals. Consequently, conformal invariance is broken by these actions unless these parameters are send to either 0 or ∞. Here, the conformal limit is taken to be the strong coupling limit $|m| \to \infty$. In a more precise analysis one should study the renormalisation of the theory to understand if a conformal limit exists [129, 130].

Gauge multiplet actions

Abelian vector multiplets $(V, A)_i$ have kinetic actions

$$S_{\text{gauge}} = \frac{1}{2|m|^2} \int \mathrm{d}^2\sigma \mathrm{d}^2\theta^+ \, \overline{F} F \ . \tag{A.34}$$

The kinetic terms for Fermi gauge multiplets Σ_I are given by

$$S_{\text{Fermi gauge}} = \frac{1}{2|m|^2} \int \mathrm{d}^2\sigma \mathrm{d}^2\theta^+ \, \bar{\partial} \ . \tag{A.35}$$

Superpotentials

To introduce gauge invariant superpotential actions, chiral superfields Ψ^A and Fermi superfields Γ^M are needed. They are given in Table 7.2. The super gauge transformations of Ψ read

$$\overline{\Psi} \to \overline{\Psi}\, e^{\mathsf{q}\cdot\overline{\Theta}} \ , \qquad \Psi \to e^{\mathsf{q}\cdot\Theta}\, \Psi \ . \tag{A.36}$$

The super gauge and super fermionic gauge transformations of Γ are given by

$$\overline{\Gamma} \to \left(\overline{\Gamma} + (\overline{\Xi}\cdot\overline{W}(\overline{\Phi}))\, \overline{\Psi}\right) e^{\mathsf{Q}\cdot\overline{\Theta}} \ , \qquad \Gamma \to e^{\mathsf{Q}\cdot\Theta} \left(\Gamma + (\Psi\, W(\Phi)\cdot\Xi)\right) \ . \tag{A.37}$$

Here $\left[\Psi\, (W(\Phi)\Xi)\right]^M = \Psi^A W_A{}^{IM}(\Phi)\Xi_I$ is parameterised by chiral superfield functions $W_{AI}{}^M(\Phi)$.

The superpotential action contains two pieces associated to the target space geometry and the gauge bundle that supports it:

$$S_{SP} = m \int \mathrm{d}^2\sigma \mathrm{d}\theta^+ \left(P_{\text{geom}} + P_{\text{bundle}}\right) + \text{c.c.} \ , \quad P_{\text{geom}} = \Gamma\, P(\Phi) \ , \quad P_{\text{bundle}} = \Psi\, M(\Phi)\, \Lambda \ . \tag{A.38}$$

Here, Γ and Ψ are interpreted as lying vectors of Fermi multiplets Γ^M and chiral multiplets Ψ^A, respectively; $P(\Phi)$ as a standing vector of chiral superfield functions $P_M(\Phi)$ and $M(\Phi)$ as a matrix of chiral superfield functions $M_{Am}(\Phi)$. This is gauge invariant if the functions $P_M(\Phi)$ carry the opposite gauge charges as Γ^M and $M_{Am}(\Phi)$ the opposite gauge charges as $\Psi^A\Lambda^m$. The superpotential action is only invariant under fermionic gauge transformations if (7.29) holds.

The structure of the superpotential is dictated by a large extend by the Weyl charges: The R–charge implies that Ψ^A and Γ^M can only appear linearly in this expression. However, the superpotential is not conformal invariant, hence the mass parameter m sits out front. This implies that in the conformal limit the superpotential has to vanish strictly.

To complete the description also kinetic terms need to be added for the field Ψ and Γ. The super gauge invariant kinetic action for Ψ is given by

$$S_{\text{chiral}} = \frac{i}{4} \int \mathrm{d}^2\sigma \mathrm{d}^2\theta^+ \left[\overline{\Psi}\, e^{2\mathsf{q}\cdot V} \overline{\mathcal{D}} \Psi - \overline{\mathcal{D}}\, \overline{\Psi}\, e^{2\mathsf{q}\cdot V} \Psi\right] \ . \tag{A.39}$$

The super gauge invariant kinetic action for Γ is given by

$$S_{\text{Fermi}} = -\frac{1}{2} \int \mathrm{d}^2\sigma \mathrm{d}^2\theta^+ \left(\overline{\Gamma} + \overline{\Sigma}\cdot\overline{W}(\overline{\Phi})\overline{\Psi}\right) e^{2\mathsf{Q}\cdot V} \left(\Gamma + \Psi W(\Phi)\cdot\Sigma\right) \ . \tag{A.40}$$

The are both scale invariant.

A.1.6 (0,2) non–linear sigma models

The general action of a $(0,2)$ non–linear sigma model consists of two parts: an action for the chiral superfields $\mathbf{\Phi}^{\alpha}$, $\alpha = 0,\ldots,3$, and Fermi multiplets $\mathbf{\Lambda}^{\mu}$, $\mu = 1,\ldots,16$. Here the scalar components of the chiral multiplets are interpreted as the local coordinates of the target space manifold $\mathcal{M}$ and the fermionic components of the Fermi multiplets as the local coordinates in a section of the bundle $\mathcal{V}$ in the same coordinate patch.

Torsional non–linear sigma models

The most general conformal $(0,2)$ action of the chiral multiplets

$$S_{\text{n.l. chiral}} = \frac{i}{4}\int \mathrm{d}^2\sigma\mathrm{d}^2\theta^+ \left[K(\mathbf{\Phi},)\,\bar\partial\mathbf{\Phi} - \bar\partial\,\overline{K}(\mathbf{\Phi},)\right] , \tag{A.41}$$

are parameterised in terms of a lying complex vector function $K(\mathbf{\Phi},)$ with entries $K_\alpha(\mathbf{\Phi},)$ and its conjugate, a standing vector $\overline{K}(\mathbf{\Phi},)$ with entries $\overline{K}_{\underline{\alpha}}(\mathbf{\Phi},)$. These functions are defined modulo additions

$$\overline{K}(\mathbf{\Phi},) \to \overline{K}(\mathbf{\Phi},) + \bar k() \ , \qquad K(\mathbf{\Phi},) \to K(\mathbf{\Phi},) + k(\mathbf{\Phi}) \tag{A.42}$$

of holomorphic vector functions $k(\mathbf{\Phi})$ and $\bar k()$, as this would modify the full superspace integrant by a sum of a chiral superfield and its conjugate which vanishes. The superfield functions $K(\mathbf{\Phi},)$ and $\overline{K}(\mathbf{\Phi},)$ can be thought of as prepotentials for the metric

$$G_{\underline{\alpha}\alpha} = \tfrac{1}{2}\Big(\overline{K}_{\underline{\alpha},\alpha} + K_{\alpha,\underline{\alpha}}\Big) \tag{A.43}$$

and the Kalb–Ramond two–form B_2

$$B_{\underline{\alpha}\alpha} = \tfrac{1}{2}\Big(\overline{K}_{\underline{\alpha},\alpha} - K_{\alpha,\underline{\alpha}}\Big) \ , \qquad B_{\alpha\beta} = \tfrac{1}{2}\Big(K_{\alpha,\beta} - K_{\beta,\alpha}\Big) \ , \qquad B_{\underline{\alpha}\underline{\beta}} = \tfrac{1}{2}\Big(\overline{K}_{\underline{\alpha},\underline{\beta}} - \overline{K}_{\beta,\underline{\alpha}}\Big) \ , \tag{A.44}$$

combined, as can be seen by working out the kinetic action for the scalar components of the chiral superfields. The representation of the action for the scalar components is not unique due to B_2-field gauge transformations. A gauge can be chosen such that the components of the B_2–field with purely (anti–)holomorphic indices are absent. The non–vanishing components of the gauge invariant three–form field strength $H_3 = \mathrm{d}B_2$ can also be expressed in terms of these prepotential functions:

$$H_{\alpha\beta\underline{\gamma}} = H_{\beta\underline{\gamma}\alpha} = H_{\underline{\gamma}\alpha\beta} = K_{\alpha,\beta\underline{\gamma}} - K_{\beta,\alpha\underline{\gamma}} \ , \qquad H_{\underline{\alpha}\underline{\beta}\gamma} = H_{\underline{\beta}\gamma\underline{\alpha}} = H_{\gamma\underline{\alpha}\underline{\beta}} = \overline{K}_{\underline{\alpha},\underline{\beta}\gamma} - \overline{K}_{\underline{\beta},\underline{\alpha}\gamma} \ . \tag{A.45}$$

if some of these components are non–zero the manifold possesses torsion.

Chiral superfield interactions with Fermi multiplets

The most general Weyl invariant action of Fermi multiplets is given by

$$S_{\text{n.l. Fermi}} = -\frac{1}{2}\int \mathrm{d}^2\sigma\mathrm{d}^2\theta^+ \Big\{ N(\mathbf{\Phi},)\,\mathbf{\Lambda} + \frac{1}{2}\,\mathbf{\Lambda}^T\, n(\mathbf{\Phi},)\,\mathbf{\Lambda} + \frac{1}{2}\ \bar n(\mathbf{\Phi},)^{\,T}\ , \Big\} \tag{A.46}$$

parameterised by an Hermitean matrix $N(\mathbf{\Phi},)$ with entries $N_{\underline{\mu}\nu}(\mathbf{\Phi},)$ assumed to be invertible and a complex anti–symmetric matrix $n(\mathbf{\Phi},)$ with holomorphic indices $n_{\mu\nu}(\mathbf{\Phi},)$ and its conjugate $\bar{n}(\mathbf{\Phi},)$ with entries $\bar{n}_{\underline{\mu}\underline{\nu}}(\mathbf{\Phi},)$. They can be thought of as the prepotentials for the target space gauge fields

$$A_\alpha(N) = N^{-1}N_{,\alpha} \ , \qquad A_{\underline{\alpha}}(N) = N^{-1}N_{,\underline{\alpha}} \ , \qquad A_{\underline{\alpha}}(n) = n_{,\underline{\alpha}} \qquad A_\alpha(\bar{n}) = \bar{n}_{,\alpha} \ . \tag{A.47}$$

From (0,2) GLSMs to (0,2) NLSMs

By integrating out the gauge superfields $(0,2)$ GLSMs can be related to $(0,2)$ NLSMs. In particular, the equations of motion of A lead to the constraints (7.40) in the conformal limit. Then, by applying partial integrations on the derivative $\bar{\partial}$ in the remaining (A independent) terms in the FI–interaction (A.30) and combining them with the remaining kinetic terms of the chiral multiplets (A.26), these actions can be cast in the form of the NLSM action (A.41) with the prepotentials

$$K_a = \left(\overline{\Phi}\, e^{2q\cdot V}\right)_a + 2\,\rho_{,a}\cdot V \ , \qquad \overline{K}_{\underline{a}} = \left(e^{2q\cdot V}\Phi\right)_{\underline{a}} + 2\,\bar{\rho}_{,\underline{a}}\cdot V \ . \tag{A.48}$$

To see if these prepotentials for the metric and the B–field possess torsion, we compute the anti–symmetrised derivative

$$K_{[a,b]} = K_{a,b} - K_{b,a} = \left(\overline{\Phi}\, e^{2q\cdot V} q\cdot V_{,[b}\right)_{a]} + 2\,\rho_{,[a}\cdot V_{,b]} \ . \tag{A.49}$$

This expression can be simplified by taking the partial derivative w.r.t. Φ^a of equation (7.40) and after that contracting it with $V_{i,b}$. This gives

$$\left(\overline{\Phi}\, e^{2q\cdot V} q\cdot V_{,b}\right)_a + 2\overline{\Phi}\, e^{2q\cdot V}(q\cdot V_{,a})(q\cdot V_{,b})\Phi = \rho_{,a}\cdot V_{,b} \ , \tag{A.50}$$

hence anti–symmetrised:

$$\left(\overline{\Phi}\, e^{q\cdot V} q\cdot V_{,[b}\right)_{a]} = \rho_{,[a}\cdot V_{,b]} \ . \tag{A.51}$$

From which in general it may be concluded, that there will be torsion if the FI–functions $\rho_i(\Phi)$ are not constant

$$K_{[a,b]} = 3\,\rho_{,[a}\cdot V_{,b]} \ . \tag{A.52}$$

From this the three–form H expression (7.41) follows immediately.

A.2 Anomalies in two dimensional GLSMs

A.2.1 Chiral anomaly

Let ψ be a Dirac fermion in two dimensions and $\bar{\psi}$ its conjugate. Consider the chiral transformation

$$\psi \to e^{i\alpha\frac{\mathbb{1}+\tilde{\gamma}}{2}}\,\psi \ , \qquad \bar{\psi} \to \bar{\psi}\, e^{-i\alpha\frac{\mathbb{1}+\tilde{\gamma}}{2}} \ . \tag{A.53}$$

Here $\tilde{\gamma} = \gamma^0\gamma^1$ is the chirality operator in two dimensions satisfying $\tilde{\gamma}^2 = \mathbb{1}$. The anti–symmetrised product product of two gamma matrices is proportion to this operator:

$$\gamma^{\mu\nu} = \tfrac{1}{2}\,[\gamma^\mu, \gamma^\nu] = \epsilon^{\mu\nu}\,\tilde{\gamma}\ , \tag{A.54}$$

where $\epsilon^{\mu\nu} = -\epsilon^{\nu\mu}$ is the anti–symmetric epsilon tensor in two with the normalisation $\epsilon^{01} = 1$. The Dirac operator of this fermion is assumed to couple chirally to a gauge field A_μ:

$$\not{D} = \not{\partial} + i\,\not{A}\,\frac{\mathbb{1} + \tilde{\gamma}}{2}\ , \tag{A.55}$$

where $\not{A} = \gamma^\mu A_\mu$ as usual. Note that

$$\not{D}^2 = D^2 + \frac{i}{2}\,\tilde{\gamma}\,\epsilon^{\mu\nu}F_{\mu\nu}\ , \tag{A.56}$$

where $iF_{\mu\nu} = [D_\mu, D_\nu]$ is the invariant gauge field strength or expressed as a two form

$$F_2 = \tfrac{1}{2}\,F_{\mu\nu}\mathrm{d}\sigma^\mu\mathrm{d}\sigma^\nu = \tfrac{1}{2}\,\epsilon^{\mu\nu}F_{\mu\nu}\,\mathrm{d}^2\sigma = F_{01}\,\mathrm{d}^2\sigma\ . \tag{A.57}$$

If the path integral measure

$$\mathcal{D}\psi\mathcal{D}\bar{\psi} \to \mathcal{D}\psi\mathcal{D}\bar{\psi}\,e^{i\mathcal{A}_{\mathrm{chiral}}} \tag{A.58}$$

is not invariant under this transformation, the chiral transformation is said to be anomalous. The anomaly can be expressed as the trace

$$\mathcal{A}_{\mathrm{chiral}} = \mathrm{Tr}[\alpha\,\tilde{\gamma}] \tag{A.59}$$

over both the full Hilbert and spinor space. This trace needs to be regularised. In case of anomalies a standard procedure is to use Fujikawa's regularisation

$$\mathcal{A}_{\mathrm{chiral}} = \int \mathrm{d}^2\sigma\,\alpha\,\mathrm{tr}\langle x|\tilde{\gamma}\,e^{\not{D}^2/M^2}|x\rangle\ , \tag{A.60}$$

where M is a regulator mass taken to be infinitely large. Using a plane wave expansion with a momentum variable p, scaling it as $p \to M\,p$ and keeping only the leading terms this expression can be evaluated to

$$\mathcal{A}_{\mathrm{chiral}} = \int \mathrm{d}^2\sigma\,\alpha \int \frac{\mathrm{d}^2p}{(2\pi)^2} e^{-p^2}\,\mathrm{tr}\Big[\tilde{\gamma}\,\tfrac{i}{2}\,\tilde{\gamma}\,\epsilon^{\mu\nu}F_{\mu\nu}\Big] \tag{A.61}$$

where all the M dependence dropped out (after taking the limit $M \to \infty$). Using the Gaussian integral

$$\int \mathrm{d}^2p\,e^{-p^2} = \pi\ , \tag{A.62}$$

the chiral anomaly can be expressed as

$$\mathcal{A}_{\mathrm{chiral}} = \int \tfrac{i}{2}\,\alpha\,\frac{F_2}{2\pi}\ . \tag{A.63}$$

A.2.2 Super gauge anomalies

The result for the chiral anomaly above can be used for chiral gauge theories as well where then the parameter α is interpreted as the gauge parameter of a $U(1)$ symmetry. For left–moving charged fermion the result can immediately be taken over, while for a right–moving fermion the expression will have an additional minus sign. If we have a set of left– and right–moving fermions with charges Q_i and q_i under a number of $U(1)$ gauge symmetries, the result generalises to

$$\mathcal{A}_{\text{gauge}} = \int \tfrac{i}{2}\, \alpha^i\, \mathcal{A}_{ij}\, \frac{F_2^j}{2\pi} \ , \tag{A.64}$$

where the anomaly matrix is given by

$$\mathcal{A}_{ij} = Q_i \cdot Q_j - q_i \cdot q_j \ . \tag{A.65}$$

Here the dot product indicates the sum over all charged left and right fermions present in the theory. Assuming the existence of a supersymmetric regulator, the general form of super gauge anomalies in two dimensions can be written as

$$S_{\text{anom}} = \int \mathrm{d}^2\sigma \mathrm{d}\theta^+ \, \frac{1}{4\pi} \sum_{i,j} \mathcal{A}_{ij}\, \Theta^i F^j + \int \mathrm{d}^2\sigma \mathrm{d}\bar{\theta}^+ \, \frac{1}{4\pi} \sum_{i,j} \mathcal{A}_{ij}\, \overline{\Theta}^i \overline{F}^j \ . \tag{A.66}$$

A.3 Charge matrices

In Section 7.5 a number of so–called charge matrices are used to perform certain computations. In a given patch of a given phase of the GLSM a number of charged superfields are necessarily

non–zero. Their charge matrices are given by:

$$\mathcal{Q}_{(O)} = \begin{pmatrix} -1 & 0 & 0 \\ 0 & -1 & 0 \\ 0 & 0 & -1 \end{pmatrix}, \qquad \mathcal{Q}_{(S)} = \begin{pmatrix} 0 & \frac{1}{2} & \frac{1}{2} \\ \frac{1}{2} & 0 & \frac{1}{2} \\ \frac{1}{2} & \frac{1}{2} & 0 \end{pmatrix}, \tag{A.67a}$$

$$\mathcal{Q}_{(11)} = \begin{pmatrix} -1 & 0 & 0 \\ \frac{1}{2} & 0 & \frac{1}{2} \\ \frac{1}{2} & \frac{1}{2} & 0 \end{pmatrix}, \quad \mathcal{Q}_{(12)} = \begin{pmatrix} -1 & 0 & 0 \\ 0 & \frac{1}{2} & \frac{1}{2} \\ \frac{1}{2} & \frac{1}{2} & 0 \end{pmatrix}, \quad \mathcal{Q}_{(13)} = \begin{pmatrix} -1 & 0 & 0 \\ 0 & \frac{1}{2} & \frac{1}{2} \\ \frac{1}{2} & 0 & \frac{1}{2} \end{pmatrix}, \tag{A.67b}$$

$$\mathcal{Q}_{(21)} = \begin{pmatrix} \frac{1}{2} & 0 & \frac{1}{2} \\ 0 & -1 & 0 \\ \frac{1}{2} & \frac{1}{2} & 0 \end{pmatrix}, \quad \mathcal{Q}_{(22)} = \begin{pmatrix} 0 & \frac{1}{2} & \frac{1}{2} \\ 0 & -1 & 0 \\ \frac{1}{2} & \frac{1}{2} & 0 \end{pmatrix}, \quad \mathcal{Q}_{(23)} = \begin{pmatrix} 0 & \frac{1}{2} & \frac{1}{2} \\ 0 & -1 & 0 \\ \frac{1}{2} & 0 & \frac{1}{2} \end{pmatrix}, \tag{A.67c}$$

$$\mathcal{Q}_{(31)} = \begin{pmatrix} \frac{1}{2} & 0 & \frac{1}{2} \\ \frac{1}{2} & \frac{1}{2} & 0 \\ 0 & 0 & -1 \end{pmatrix}, \quad \mathcal{Q}_{(32)} = \begin{pmatrix} 0 & \frac{1}{2} & \frac{1}{2} \\ \frac{1}{2} & \frac{1}{2} & 0 \\ 0 & 0 & -1 \end{pmatrix}, \quad \mathcal{Q}_{(33)} = \begin{pmatrix} 0 & \frac{1}{2} & \frac{1}{2} \\ \frac{1}{2} & 0 & \frac{1}{2} \\ 0 & 0 & -1 \end{pmatrix}. \tag{A.67d}$$

Their transposed inverse are:

$$\mathcal{Q}^{-T}_{(O)} = \begin{pmatrix} -1 & 0 & 0 \\ 0 & -1 & 0 \\ 0 & 0 & -1 \end{pmatrix}, \qquad \mathcal{Q}^{-T}_{(S)} = \begin{pmatrix} -1 & 1 & 1 \\ 1 & -1 & 1 \\ 1 & 1 & -1 \end{pmatrix}, \tag{A.68a}$$

$$\mathcal{Q}^{-T}_{(11)} = \begin{pmatrix} -1 & 1 & 1 \\ 0 & 0 & 2 \\ 0 & 2 & 0 \end{pmatrix}, \quad \mathcal{Q}^{-T}_{(12)} = \begin{pmatrix} -1 & 1 & -1 \\ 0 & 0 & 2 \\ 0 & 2 & -2 \end{pmatrix}, \quad \mathcal{Q}^{-T}_{(13)} = \begin{pmatrix} -1 & -1 & 1 \\ 0 & 2 & 0 \\ 0 & -2 & 2 \end{pmatrix}, \tag{A.68b}$$

$$\mathcal{Q}^{-T}_{(21)} = \begin{pmatrix} 0 & 0 & 2 \\ 1 & -1 & -1 \\ 2 & 0 & -2 \end{pmatrix}, \quad \mathcal{Q}^{-T}_{(22)} = \begin{pmatrix} 0 & 0 & 2 \\ 1 & -1 & 1 \\ 2 & 0 & 0 \end{pmatrix}, \quad \mathcal{Q}^{-T}_{(23)} = \begin{pmatrix} -2 & 0 & 2 \\ -1 & -1 & 1 \\ 2 & 0 & 0 \end{pmatrix}, \tag{A.68c}$$

$$\mathcal{Q}^{-T}_{(31)} = \begin{pmatrix} 2 & -2 & 0 \\ 0 & 2 & 0 \\ 1 & -1 & -1 \end{pmatrix}, \quad \mathcal{Q}^{-T}_{(32)} = \begin{pmatrix} -2 & 2 & 0 \\ 2 & 0 & 0 \\ -1 & 1 & -1 \end{pmatrix}, \quad \mathcal{Q}^{-T}_{(33)} = \begin{pmatrix} 0 & 2 & 0 \\ 2 & 0 & 0 \\ 1 & 1 & -1 \end{pmatrix}. \tag{A.68d}$$

The charge matrices associated to the superfields that define a given patch read:

$$\widetilde{\mathcal{Q}}_{(O)} = \begin{pmatrix} 0 & \frac{1}{2} & \frac{1}{2} \\ \frac{1}{2} & 0 & \frac{1}{2} \\ \frac{1}{2} & \frac{1}{2} & 0 \end{pmatrix}, \qquad \widetilde{\mathcal{Q}}_{(S)} = \begin{pmatrix} -1 & 0 & 0 \\ 0 & -1 & 0 \\ 0 & 0 & -1 \end{pmatrix}, \tag{A.69a}$$

$$\widetilde{\mathcal{Q}}_{(11)} = \begin{pmatrix} 0 & \frac{1}{2} & \frac{1}{2} \\ 0 & -1 & 0 \\ 0 & 0 & -1 \end{pmatrix}, \quad \widetilde{\mathcal{Q}}_{(12)} = \begin{pmatrix} \frac{1}{2} & 0 & \frac{1}{2} \\ 0 & -1 & 0 \\ 0 & 0 & -1 \end{pmatrix}, \quad \widetilde{\mathcal{Q}}_{(13)} = \begin{pmatrix} \frac{1}{2} & \frac{1}{2} & 0 \\ 0 & -1 & 0 \\ 0 & 0 & -1 \end{pmatrix}, \tag{A.69b}$$

$$\widetilde{\mathcal{Q}}_{(21)} = \begin{pmatrix} -1 & 0 & 0 \\ 0 & \frac{1}{2} & \frac{1}{2} \\ 0 & 0 & -1 \end{pmatrix}, \quad \widetilde{\mathcal{Q}}_{(22)} = \begin{pmatrix} -1 & 0 & 0 \\ \frac{1}{2} & 0 & \frac{1}{2} \\ 0 & 0 & -1 \end{pmatrix}, \quad \widetilde{\mathcal{Q}}_{(22)} = \begin{pmatrix} -1 & 0 & 0 \\ \frac{1}{2} & \frac{1}{2} & 0 \\ 0 & 0 & -1 \end{pmatrix}, \tag{A.69c}$$

$$\widetilde{\mathcal{Q}}_{(31)} = \begin{pmatrix} -1 & 0 & 0 \\ 0 & -1 & 0 \\ 0 & \frac{1}{2} & \frac{1}{2} \end{pmatrix}, \quad \widetilde{\mathcal{Q}}_{(32)} = \begin{pmatrix} -1 & 0 & 0 \\ 0 & -1 & 0 \\ \frac{1}{2} & 0 & \frac{1}{2} \end{pmatrix}, \widetilde{\mathcal{Q}}_{(33)} = \begin{pmatrix} -1 & 0 & 0 \\ 0 & -1 & 0 \\ \frac{1}{2} & \frac{1}{2} & 0 \end{pmatrix}. \tag{A.69d}$$

Bibliography

[1] A. E. Faraggi, S. Groot Nibbelink, and M. Hurtado Heredia "Constraint on spinor-vector dualities in six dimensions" Phys. Rev. D **103** (2021) no. 12, 126016 [arXiv:2103.14684].

[2] A. E. Faraggi, S. Groot Nibbelink, and M. Hurtado-Heredia "Uncovering a spinor–vector duality on a resolved orbifold" Nucl. Phys. B **969** (2021) 115473 [arXiv:2103.13442].

[3] A. E. Faraggi, S. Groot Nibbelink and M. Hurtado Heredia, JHEP **01** (2022), 169 doi:10.1007/JHEP01(2022)169 [arXiv:2111.10407 [hep-th]].

[4] A. E. Faraggi, S. G. Nibbelink and M. H. Heredia, Nucl. Phys. B **988** (2023), 116111 doi:10.1016/j.nuclphysb.2023.116111 [arXiv:2211.01397 [hep-th]].

[5] E. Palti "The Swampland: Introduction and review" Fortsch. Phys. **67** (2019) no. 6, 1900037 [arXiv:1903.06239].

[6] I. Antoniadis, C. Bachas, and C. Kounnas "Four-dimensional superstrings" Nucl. Phys. **B289** (1987) 87–108.

[7] I. Antoniadis and C. Bachas "4d fermionic superstrings with arbitrary twists" Nucl. Phys. **B298** (1988) no. 3, 586–612.

[8] L. J. Dixon, J. A. Harvey, C. Vafa, and E. Witten "Strings on orbifolds" Nucl. Phys. **B261** (1985) 678–686.

[9] L. J. Dixon, J. A. Harvey, C. Vafa, and E. Witten "Strings on orbifolds. 2" Nucl. Phys. **B274** (1986) 285–314.

[10] A. E. Faraggi "$Z_2 \times Z_2$ orbifold compactification as the origin of realistic free fermionic models" Phys. Lett. **B326** (1994) 62–68 [arXiv:hep-ph/9311312].

[11] P. Athanasopoulos, A. E. Faraggi, S. Groot Nibbelink, and V. M. Mehta "Heterotic free fermionic and symmetric toroidal orbifold models" JHEP **04** (2016) 038 [arXiv:1602.03082].

[12] P. Candelas, G. T. Horowitz, A. Strominger, and E. Witten "Vacuum configurations for superstrings" Nucl. Phys. **B258** (1985) 46–74.

[13] A. E. Faraggi, D. V. Nanopoulos, and K.-j. Yuan "A Standard like model in the 4D free fermionic string formulation" Nucl. Phys. **B335** (1990) 347.

[14] A. E. Faraggi "A new standard - like model in the four-dimensional free fermionic string formulation" Phys. Lett. **B278** (1992) 131–139.

[15] A. E. Faraggi "Construction of realistic standard - like models in the free fermionic superstring formulation" Nucl. Phys. B **387** (1992) 239–262 [arXiv:hep-th/9208024].

[16] P. K. S. Vaudrevange, [arXiv:0812.3503 [hep-th]].

[17] G. Cleaver, A. Faraggi, and D. Nanopoulos "String derived MSSM and M-theory unification" Phys. Lett. **B455** (May, 1999) 135–146 [arXiv:hep-th/9811427].

[18] A. E. Faraggi, E. Manno, and C. Timirgaziu "Minimal Standard Heterotic String Models" Eur. Phys. J. C **50** (2007) 701–710 [arXiv:hep-th/0610118].

[19] A. E. Faraggi, J. Rizos, and H. Sonmez "Classification of standard-like heterotic-string vacua" Nucl. Phys. B **927** (2018) 1–34 [arXiv:1709.08229].

[20] O. Lebedev et al. "A mini-landscape of exact MSSM spectra in heterotic orbifolds" Phys. Lett. **B645** (2007) 88–94 [arXiv:hep-th/0611095].

[21] O. Lebedev, H. Nilles, S. Raby, S. Ramos-Sánchez, M. Ratz, P. Vaudrevange, and A. Wingerter "Heterotic road to the MSSM with R parity" Phys. Rev. **D77** (2008) no. 4, 046013 [arXiv:0708.2691].

[22] O. Lebedev, H. P. Nilles, S. Ramos-Sánchez, M. Ratz, and P. K. Vaudrevange "Heterotic mini-landscape. (II). Completing the search for MSSM vacua in a Z(6) orbifold" Phys. Lett. **B668** (2008) 331–335 [arXiv:0807.4384].

[23] R. Friedman, J. W. Morgan and E. Witten, [arXiv:alg-geom/9709029 [math.AG]].

[24] M. Blaszczyk et al. "A Z2xZ2 standard model" Phys. Lett. **B683** (2010) 340–348 [arXiv:0911.4905].

[25] R. Donagi, B. A. Ovrut, T. Pantev, and D. Waldram "Standard models from heterotic M-theory" Adv. Theor. Math. Phys. **5** (2002) 93–137 [arXiv:hep-th/9912208].

[26] R. Donagi, B. A. Ovrut, T. Pantev, and D. Waldram "Standard-model bundles" Adv. Theor. Math. Phys. **5** (2002) 563–615 [arXiv:math/0008010].

[27] V. Braun, Y. H. He, B. A. Ovrut, and T. Pantev "A heterotic Standard Model" Physics Letters B **618** (2005) no. 1, 252–258 [arXiv:0501070].

[28] V. Braun, Y.-H. He, B. A. Ovrut, and T. Pantev "The exact MSSM spectrum from string theory" JHEP **05** (2006) 043 [arXiv:hep-th/0512177].

[29] V. Bouchard and R. Donagi "An SU(5) heterotic standard model" Phys. Lett. **B633** (2006) 783–791 [arXiv:hep-th/0512149].

[30] L. B. Anderson, J. Gray, Y.-H. He, and A. Lukas "Exploring positive monad bundles and a new heterotic Standard Model" JHEP **02** (2010) 054 [arXiv:0911.1569].

[31] S. Groot Nibbelin and F. Ruehle, JHEP **04** (2016), 186 doi:10.1007/JHEP04(2016)186 [arXiv:1601.00676 [hep-th]].

[32] M. Blaszczyk, S. Groot Nibbelink, F. Ruehle, M. Trapletti, and P. K. S. Vaudrevange "Heterotic MSSM on a resolved orbifold" JHEP **09** (2010) 065 [arXiv:1007.0203].

[33] L. B. Anderson, J. Gray, A. Lukas, and E. Palti "Two hundred heterotic Standard Models on smooth Calabi-Yau threefolds" [arXiv:1106.4804].

[34] K. Becker, M. Becker and J. H. Schwarz, Cambridge University Press, 2006, ISBN 978-0-511-25486-4, 978-0-521-86069-7, 978-0-511-81608-6 doi:10.1017/CBO9780511816086

[35] M. F. Fischer,"Heterotic orbifolds"

[36] S. Groot Nibbelink, O. Loukas, and F. Ruehle "(MS)SM-like models on smooth Calabi-Yau manifolds from all three heterotic string theories" Fortsch. Phys. **63** (2015) 609–632 [arXiv:1507.07559].

[37] B. R. Greene and M. R. Plesser "Duality in Calabi-Yau moduli space" Nucl. Phys. **B338** (1990) 15–37.

[38] P. Candelas, M. Lynker, and R. Schimmrigk "Calabi-Yau manifolds in weighted P(4)" Nucl. Phys. **B341** (1990) 383–402.

[39] P. Candelas, X. C. De La Ossa, P. S. Green, and L. Parkes "A pair of Calabi-Yau manifolds as an exactly soluble superconformal theory" Nucl. Phys. **B359** (1991) 21–74.

[40] A. Strominger, S.-T. Yau, and E. Zaslow "Mirror symmetry is T duality" Nucl. Phys. B **479** (1996) 243–259 [arXiv:hep-th/9606040].

[41] A. Giveon, M. Porrati, and E. Rabinovici "Target space duality in string theory" Phys. Rept. **244** (1994) 77–202 [arXiv:hep-th/9401139].

[42] A. E. Faraggi, C. Kounnas, and J. Rizos "Chiral family classification of fermionic heterotic orbifold models" Physics Letters B **648** (Apr., 2007) 84–89 [arXiv:hep-th/0606144].

[43] A. E. Faraggi, C. Kounnas, and J. Rizos "symm–Vector Duality in fermionic $Z_2 \times Z_2$ heterotic orbifold models" Nuclear Physics B **774** (Nov., 2006) 29 [arXiv:0611251].

[44] A. E. Faraggi, C. Kounnas, and J. Rizos "symm-vector duality in N=2 heterotic string vacua" Nucl. Phys. B **799** (2008) 19–33 [arXiv:0712.0747].

[45] T. Catelin-Jullien, A. E. Faraggi, C. Kounnas, and J. Rizos "symm–vector duality in heterotic SUSY vacua" Nuclear Physics B **812** (May, 2009) 103–127 [arXiv:0807.4084].

[46] A. E. Faraggi, C. Kounnas, S. E. M. Nooij, and J. Rizos "Classification of the chiral Z(2) x Z(2) fermionic models in the heterotic superstring" Nucl. Phys. **B695** (2004) 41–72 [arXiv:hep-th/0403058].

[47] C. Angelantonj, A. E. Faraggi, and M. Tsulaia "symme-vector duality in heterotic string orbifolds" JHEP **07** (2010) 004 [arXiv:1003.5801].

[48] A. E. Faraggi, I. Florakis, T. Mohaupt, and M. Tsulaia "Conformal aspects of spinor-vector duality" Nucl. Phys. B **848** (2011) 332–371 [arXiv:1101.4194].

[49] S. D. Avramis, [arXiv:hep-th/0611133 [hep-th]].

[50] P. Athanasopoulos, A. E. Faraggi, S. Groot Nibbelink and V. M. Mehta, JHEP **04** (2016), 038 doi:10.1007/JHEP04(2016)038 [arXiv:1602.03082 [hep-th]].

[51] P. Athanasopoulos, A. E. Faraggi, and D. Gepner "Spectral flow as a map between N = (2, 0)-models" Phys. Lett. B **735** (2014) 357–363 [arXiv:1403.3404].

[52] G. Aldazabal, A. Font, L. E. Ibáñez, A. M. Uranga, and G. Violero "Non-perturbative heterotic D = 6,4, N = 1 orbifold vacua" Nucl. Phys. **B519** (1998) 239–281 [arXiv:hep-th/9706158].

[53] G. Honecker and M. Trapletti "Merging heterotic orbifolds and K3 compactifications with line bundles" JHEP **01** (2007) 051 [arXiv:hep-th/0612030].

[54] M. B. Green, J. H. Schwarz, and P. C. West "Anomaly free chiral theories in six-dimensions" Nucl. Phys. **B254** (1985) 327–348.

[55] J. Erler "Anomaly cancellation in six-dimensions" J. Math. Phys. **35** (1994) 1819–1833 [arXiv:hep-th/9304104].

[56] M. B. Green and J. H. Schwarz "Anomaly cancellation in supersymmetric d=10 gauge theory and superstring theory" Phys. Lett. **B149** (1984) 117–122.

[57] H. Kawai, D. C. Lewellen, and S.-H. Henry Tye "Construction of fermionic string models in four dimensions" Nucl. Phys. **B288** (1987) 1–76.

[58] A. E. Faraggi "Generation mass hierarchy in superstring derived models" Nuclear Physics B **407** (Oct., 1993) 57–72 [arXiv:9210256].

[59] W. Nahm and K. Wendland "A hiker's guide to K3: Aspects of N = (4,4) superconformal field theory with central charge c = 6" Commun. Math. Phys. **216** (2001) 85–138 [arXiv:hep-th/9912067].

[60] S. Groot Nibbelink, M. Trapletti, and M. Walter "Resolutions of C^n/Z_n orbifolds, their U(1) bundles, and applications to string model building" JHEP **03** (2007) 035 [arXiv:hep-th/0701227].

[61] S. Groot Nibbelink, T.-W. Ha, and M. Trapletti "Toric Resolutions of heterotic orbifolds" Phys. Rev. **D77** (2008) 026002 [arXiv:0707.1597].

[62] C. Closset, "Toric geometry and local Calabi-Yau varieties: An Introduction to toric geometry (for physicists)," [arXiv:0901.3695 [hep-th]].

[63] F. Rühle, "Exploring the Web of Heterotic String Theories using Anomalies,

[64] C. Vafa and E. Witten "On orbifolds with discrete torsion" J. Geom. Phys. **15** (1995) 189–214 [arXiv:hep-th/9409188].

[65] A. N. Schellekens and N. P. Warner "Anomalies, characters and strings" Nucl. Phys. **B287** (1987) 317.

[66] T. van Ritbergen, A. N. Schellekens, and J. A. M. Vermaseren "Group theory factors for feynman diagrams" Int. J. Mod. Phys. **A14** (1999) 41–96 [arXiv:hep-ph/9802376].

[67] M. B. Green, J. H. Schwarz, and E. Witten Superstring theory vol. 2: Loop amplitudes, anomalies and phenomenology. Cambridge, Uk: Univ. Pr. 596 P. (Cambridge Monographs On Mathematical Physics) 1987.

[68] J. Polchinski String theory vol. 2: Superstring theory and beyond. Cambridge, Uk: Univ. Pr. 531 P. (Cambridge Monographs On Mathematical Physics) 1998.

[69] D. Gepner "Exactly solvable string compactifications on manifolds of SU(N) holonomy" Phys. Lett. **B199** (1987) 380–388.

[70] A. Gregori, C. Kounnas, and J. Rizos "Classification of the N=2, Z(2) x Z(2) symmetric type II orbifolds and their type II asymmetric duals" Nucl. Phys. B **549** (1999) 16–62 [arXiv:hep-th/9901123].

[71] F. Plöger, S. Ramos-Sánchez, M. Ratz, and P. K. S. Vaudrevange "Mirage torsion" JHEP **04** (2007) 063 [arXiv:hep-th/0702176].

[72] L. E. Ibáñez and A. M. Uranga "D = 6, N = 1 string vacua and duality" [arXiv:hep-th/9707075].

[73] C. Vafa "Modular invariance and discrete torsion on orbifolds" Nucl. Phys. **B273** (1986) 592.

[74] K. Wendland "Orbifold constructions of K3: A link between conformal field theory and geometry" [arXiv:hep-th/0112006].

[75] F. Denef, M. R. Douglas, and B. Florea "Building a better racetrack" JHEP **06** (2004) 034 [arXiv:hep-th/0404257].

[76] D. Lüst, S. Reffert, E. Scheidegger, and S. Stieberger "Resolved toroidal orbifolds and their orientifolds" Adv. Theor. Math. Phys. **12** (2008) 67–183 [arXiv:hep-th/0609014].

[77] S. Groot Nibbelink, J. Held, F. Ruehle, M. Trapletti, and P. K. S. Vaudrevange "Heterotic Z6-II MSSM orbifolds in blowup" JHEP **03** (2009) 005 [arXiv:0901.3059].

[78] S. Groot Nibbelink, O. Loukas, F. Ruehle, and P. K. S. Vaudrevange "Infinite number of MSSMs from heterotic line bundles?" Phys. Rev. D **92** (2015) no. 4, 046002 [arXiv:1506.00879].

[79] S. Groot Nibbelink, H. P. Nilles, and M. Trapletti "Multiple anomalous U(1)s in heterotic blow-ups" Phys. Lett. **B652** (2007) 124–127 [arXiv:hep-th/0703211].

[80] S. Groot Nibbelink, D. Klevers, F. Plöger, M. Trapletti, and P. K. S. Vaudrevange "Compact heterotic orbifolds in blow-up" JHEP **04** (2008) 060 [arXiv:0802.2809].

[81] I. Antoniadis, J. R. Ellis, J. S. Hagelin, and D. V. Nanopoulos "The flipped SU(5) x U(1) string model revamped" Phys. Lett. **B231** (1989) 65.

[82] I. Antoniadis, G. Leontaris, and J. Rizos "A three-generation $SU(4) \times O(4)$ string model" Phys. Lett. **B245** (1990) 161–168.

[83] A. E. Faraggi "Construction of realistic standard-like models in the free fermionic superstring formulation" Nucl. Phys. **B387** (1992) 239–262.

[84] A. E. Faraggi, V. G. Matyas, and B. Percival "Stable three generation standard–like model from a tachyonic ten dimensional heterotic–string vacuum" Eur. Phys. J. C **80** (2020) no. 4, 337 [arXiv:1912.00061].

[85] A. E. Faraggi and J. Rizos "A light Z' heterotic-string derived model" Nucl. Phys. **B895** (2015) 233–247 [arXiv:1412.6432].

[86] A. E. Faraggi "Sterile Neutrinos in String Derived Models" Eur. Phys. J. C **78** (2018) no. 10, 867 [arXiv:1807.08031].

[87] E. R. Sharpe "Discrete torsion and gerbes. 1." [arXiv:hep-th/9909108].

[88] E. R. Sharpe "Discrete torsion and gerbes (2)" [arXiv:hep-th/9909120].

[89] E. R. Sharpe "Discrete torsion" Phys. Rev. D **68** (2003) 126003 [arXiv:hep-th/0008154].

[90] E. R. Sharpe "Discrete torsion in perturbative heterotic string theory" Phys. Rev. D **68** (2003) 126005 [arXiv:hep-th/0008184].

[91] R. Donagi, A. Lukas, B. A. Ovrut, and D. Waldram "Non-perturbative vacua and particle physics in m-theory" JHEP **05** (1999) 018 [arXiv:hep-th/9811168].

[92] V. Braun, Y.-H. He, B. A. Ovrut, and T. Pantev "A heterotic standard model" Phys. Lett. **B618** (2005) 252–258 [arXiv:hep-th/0501070].

[93] R. Blumenhagen, G. Honecker, and T. Weigand "Loop-corrected compactifications of the heterotic string with line bundles" JHEP **06** (2005) 020 [arXiv:hep-th/0504232].

[94] L. B. Anderson, Y.-H. He, and A. Lukas "Heterotic Compactification, An Algorithmic Approach" JHEP **0707** (2007) 049 [arXiv:hep-th/0702210].

[95] L. B. Anderson, Y.-H. He, and A. Lukas "Monad Bundles in Heterotic String Compactifications" JHEP **0807** (2008) 104 [arXiv:0805.2875].

[96] S. Groot Nibbelink, O. Loukas, and F. Ruehle "(MS)SM-like models on smooth Calabi-Yau manifolds from all three heterotic string theories" Fortsch. Phys. **63** (2015) 609–632 [arXiv:1507.07559].

[97] S. Reffert "Toroidal orbifolds: Resolutions, orientifolds and applications in string phenomenology" [arXiv:hep-th/0609040].

[98] S. Groot Nibbelink "Blowups of heterotic orbifolds using toric geometry" [arXiv:0708.1875].

[99] R. Donagi and K. Wendland "On orbifolds and free fermion constructions" Journal of Geometry and Physics **59** (Sept., 2008) 46 [arXiv:0809.0330].

[100] G. Honecker "Massive U(1)s and heterotic five-branes on K3" Nucl.Phys. **B748** (2006) 126–148 [arXiv:hep-th/0602101].

[101] S. Donalson "Anti-self-dual Yang–Mills connections over complex algebraic surfaces and stable vector bundles" Proc. Londan Math. Soc. **50** (1985) 1–26.

[102] K. Uhlenbeck and S. Yau "On the existence of Hermitian-Yang-Mills connections in stable vector bundles" Comm. Pure and Appl. Math. **19** (1986) 257–293.

[103] M. Kreuzer and H. Skarke "Complete classification of reflexive polyhedra in four-dimensions" Adv.Theor.Math.Phys. **4** (2002) 1209–1230 [arXiv:hep-th/0002240].

[104] R. Altman, J. Gray, Y.-H. He, V. Jejjala, and B. D. Nelson "A Calabi-Yau database: threefolds constructed from the Kreuzer-Skarke List" JHEP **02** (2015) 158 [arXiv:1411.1418].

[105] M. Blaszczyk, S. Groot Nibbelink, O. Loukas, and S. Ramos-Sanchez "Non-supersymmetric heterotic model building" JHEP **10** (2014) 119 [arXiv:1407.6362].

[106] S. Abel, K. R. Dienes, and E. Mavroudi "Towards a nonsupersymmetric string phenomenology" Phys. Rev. **D91** (2015) 126014 [arXiv:1502.03087].

[107] A. E. Faraggi, V. G. Matyas, and B. Percival "Classification of nonsupersymmetric Pati-Salam heterotic string models" Phys. Rev. D **104** (2021) no. 4, 046002 [arXiv:2011.04113].

[108] S. Groot Nibbelink and P. K. S. Vaudrevange "T-duality orbifolds of heterotic Narain compactifications" JHEP **04** (2017) 030 [arXiv:1703.05323].

[109] S. Groot Nibbelink "A worldsheet perspective on heterotic T-duality orbifolds" JHEP **04** (2021) 190 [arXiv:2012.02778].

[110] A. E. Faraggi "Moduli fixing in realistic string vacua" Nucl. Phys. B **728** (2005) 83–108 [arXiv:hep-th/0504016].

[111] E. R. Sharpe "Recent developments in discrete torsion" Phys. Lett. B **498** (2001) 104–110 [arXiv:hep-th/0008191].

[112] S. Groot Nibbelink "Heterotic orbifold resolutions as (2,0) gauged linear sigma models" Fortsch. Phys. **59** (2011) 454–493 [arXiv:1012.3350].

[113] M. Blaszczyk, S. Groot Nibbelink, and F. Ruehle "Gauged Linear Sigma Models for toroidal orbifold resolutions" JHEP **05** (2012) 053 [arXiv:1111.5852].

[114] L. E. Ibáñez, J. Mas, H. P. Nilles, and F. Quevedo "Heterotic strings in symmetric and asymmetric orbifold backgrounds" Nucl. Phys. **B301** (1988) 157.

[115] L. E. Ibáñez, H. P. Nilles, and F. Quevedo "Orbifolds and Wilson lines" Phys. Lett. **B187** (1987) 25–32.

[116] H. P. Nilles, S. Ramos-Sanchez, P. K. S. Vaudrevange, and A. Wingerter "The Orbifolder: A Tool to study the low energy effective theory of heterotic orbifolds" Comput. Phys. Commun. **183** (2012) 1363–1380 [arXiv:1110.5229].

[117] S. Förste, H. P. Nilles, P. K. S. Vaudrevange, and A. Wingerter "Heterotic brane world" Phys. Rev. **D70** (2004) 106008 [arXiv:hep-th/0406208].

[118] R. Donagi and A. E. Faraggi "On the number of chiral generations in $Z_2 \times Z_2$ orbifolds" Nucl. Phys. **B694** (2004) 187–205 [arXiv:0403272].

[119] E. Witten "Phases of N = 2 theories in two dimensions" Nucl. Phys. **B403** (1993) 159–222 [arXiv:hep-th/9301042].

[120] J. Distler, B. R. Greene, and D. R. Morrison "Resolving singularities in (0,2) models" Nucl. Phys. **B481** (1996) 289–312 [arXiv:hep-th/9605222].

[121] T.-M. Chiang, J. Distler, and B. R. Greene "Some features of (0,2) moduli space" Nucl. Phys. **B496** (1997) 590–616 [arXiv:hep-th/9702030].

[122] A. Adams "Orbifold phases of heterotic flux vacua" [arXiv:0908.2994].

[123] M. Blaszczyk, S. Groot Nibbelink, and F. Ruehle "Green-Schwarz Mechanism in Heterotic (2,0) Gauged Linear Sigma Models: Torsion and NS5 Branes" JHEP **1108** (2011) 083 [arXiv:1107.0320].

[124] C. Quigley and S. Sethi "Linear Sigma Models with Torsion" JHEP **1111** (2011) 034 [arXiv:1107.0714].

[125] A. Adams, M. Ernebjerg, and J. M. Lapan "Linear models for flux vacua" Adv. Theor. Math. Phys. **12** (2008) 817–851 [arXiv:hep-th/0611084].

[126] A. Adams, E. Dyer, and J. Lee "GLSMs for non-Kahler Geometries" JHEP **01** (2013) 044 [arXiv:1206.5815].

[127] I. V. Melnikov, C. Quigley, S. Sethi, and M. Stern "Target Spaces from Chiral Gauge Theories" JHEP **02** (2013) 111 [arXiv:1212.1212].

[128] M. Fischer, M. Ratz, J. Torrado, and P. K. S. Vaudrevange "Classification of symmetric toroidal orbifolds" JHEP **01** (2013) 084 [arXiv:1209.3906].

[129] E. Silverstein and E. Witten "Global U(1) R symmetry and conformal invariance of (0,2) models" Phys. Lett. **B328** (1994) 307–311 [arXiv:hep-th/9403054].

[130] E. Silverstein and E. Witten "Criteria for conformal invariance of (0,2) models" Nucl. Phys. **B444** (1995) 161–190 [arXiv:hep-th/9503212].

[131] A. Basu and S. Sethi, Phys. Rev. D **68** (2003), 025003 doi:10.1103/PhysRevD.68.025003 [arXiv:hep-th/0303066 [hep-th]].

[132] A. Basu and S. Sethi, Phys. Rev. D **68** (2003), 025003 doi:10.1103/PhysRevD.68.025003 [arXiv:hep-th/0303066 [hep-th]].

[133] C. Beasley and E. Witten, JHEP **10** (2003), 065 doi:10.1088/1126-6708/2003/10/065 [arXiv:hep-th/0304115 [hep-th]].

[134] A. Font, L. E. Ibanez and F. Quevedo, Phys. Lett. B **217** (1989), 272-276 doi:10.1016/0370-2693(89)90864-2

[135] E. Manno, [arXiv:0908.3164 [hep-th]].

[136] J. Distler, [arXiv:hep-th/9502012 [hep-th]].

[137] J. Distler, Phys. Lett. B **188** (1987), 431-436 doi:10.1016/0370-2693(87)91643-1